LITHIC RESIDUE ANALYSIS AT STAR CARR

Volume 2 of 2

Shannon Charmaine Klassen Croft

Doctor of Philosophy

University of York

Archaeology

September 2017

LIST OF CONTENTS

VOLUME 2

CHAPTER 10 RESULTS: SHINY DEPOSITS

10.1 Introduction

In 1983, Holmes (1987), first used the term 'post-depositional surface modification' (PDSM), followed by Levi Sala (1986), to describe a large and diverse class of phenomena which represent non-archaeological surface alterations on flint artefacts. One of these natural PDSM phenomena appears as a shiny polished or glossy surface on the flint, and has been called natural surface polishing, soil sheen (Levi Sala, 1986), or soil polish (Kooyman, 1985, p. 138). Similarly, shiny deposits with a smooth, reflective surface covering all or part of an archaeological flint have been described as a 'gloss patina' (Glauberman and Thorson, 2012, p. 24), with some researchers suggesting it originates in peat conditions rich in humic acid (Howard, 2002, 1999; Rottländer, 1975; van Gijn, 2010, p. 44, 1990, p. 53). It is apparent that a variety of terms have been used to describe natural shiny deposits on stone tools: natural surface polishing, soil sheen, soil polish, gloss patina, and glossy wear traces. Sometimes it seems usewear analysts themselves are unclear in their descriptions of natural PDSM. For instance, Van Gijn (1990, p. 53) states: "It [gloss patina] concerns a *more or less uniform* sheen over the surface of the flint", and then three sentences later directly contradicts this with: "Because gloss patina *does not develop uniformly* over the tool, depending as it does on very localized groundwater circulation..." (italics added). Adding to the confusion, it is difficult to determine if all microwear/usewear analysts have indeed reported the same phenomenon, even when the same terminology is used because it is recorded and described in subjective terms and the micrographs of what appears as polish are not specifically diagnostic.

The mechanism(s) of the formation of natural shiny deposits such as gloss patina on flint are unclear, and this has been a long-standing critique in usewear studies

(Juel Jensen, 1988, p. 81). Both additive deposition and subtractive dissolution have been proposed. Slow chemical dissolution of the flint seems to be the favoured explanation to account for gloss patina. However, biogenic amorphous silica from plants is known to be an important component of soils (Drees et al., 1989, p. 947), and is also present as dissolved silica in soils (McKeague and Cline, 1963a). Thus, it has also been suggested that infilling of the microscopic depressions of the flint with dissolved silica in the groundwater or mechanical abrasive forces may also be responsible or contributing to gloss patina formation (Stapert, 1976, p. 12).

As will be shown in this chapter, using visual clues to differentiate between a real anthropogenic usewear polish and a shiny deposit that has formed due to natural soil processes and/or post-excavation curation practices can be misleading and uncertain.

10.2 Methods

Shiny deposits were observed with reflected VLM, documented with z-stacked images, and their chemical composition investigated in a preliminary way with confocal Micro-Raman spectroscopy.

10.3 Results

10.3.1 Introduction

During microscopic analysis of lithics, a shiny deposit was defined as a reflective, transparent and texturally smooth layer on the flint surface. Shiny deposits were observed on many tools, and at the beginning of analysis were initially interpreted

as usewear polishes. There were two major types of shiny deposits observed on the Star Carr lithic sample, which have been termed 'tideline' and 'dull lustre'. The morphology of the tideline deposit was indicative of a non-archaeological deposit, primarily because it was associated with the washing process in the lab, and secondly because it left a trace similar to the natural process of evaporites forming at the edge of a salt lake. The dull-lustre type of shiny deposit was more complex to interpret, sometimes clearly associated with washing (polish from lab processing), but in other cases appearing to be confined to working edges of the tool. Shiny deposits were often found to contain gypsum crystals (identified with confocal Micro-Raman in Chapter 9). Any potential relationship between shiny deposits and burial context was not examined in this chapter because the difference between natural and anthropogenic polishes was not always clear.

10.3.2 Microscopic description

10.3.2.1 Tideline

The tideline shiny deposit can be described as lines which have transparent and reflective surfaces, taking one of two sub-forms: 1) a wavy curvilinear line resembling the trail left behind by a slug, sometimes extending several millimeters (see Figure 10.1), or 2) a circular outline of a water pool or droplet (Figure 10.2). Tideline deposits were often found in conjunction with red-orange iron oxide deposits (as identified in Chapter 8), typically as small 'granules' within the tideline. The co-occurrence of the red-orange deposits with shiny deposits may be expected, as natural iron oxides are usually associated with variable amounts of other minerals (Cavallo et al., 2015). The tideline morphology was always interpreted as a naturally-formed shiny deposit, since it appeared as a crust formed at the edge of a salt lake, similar to a line of evaporites.

Figure 10.1. Example of wavy line tideline on blade tool 94066, ventral left mid edge. Approximate length of this tideline is 6600 μm (6.6 mm).
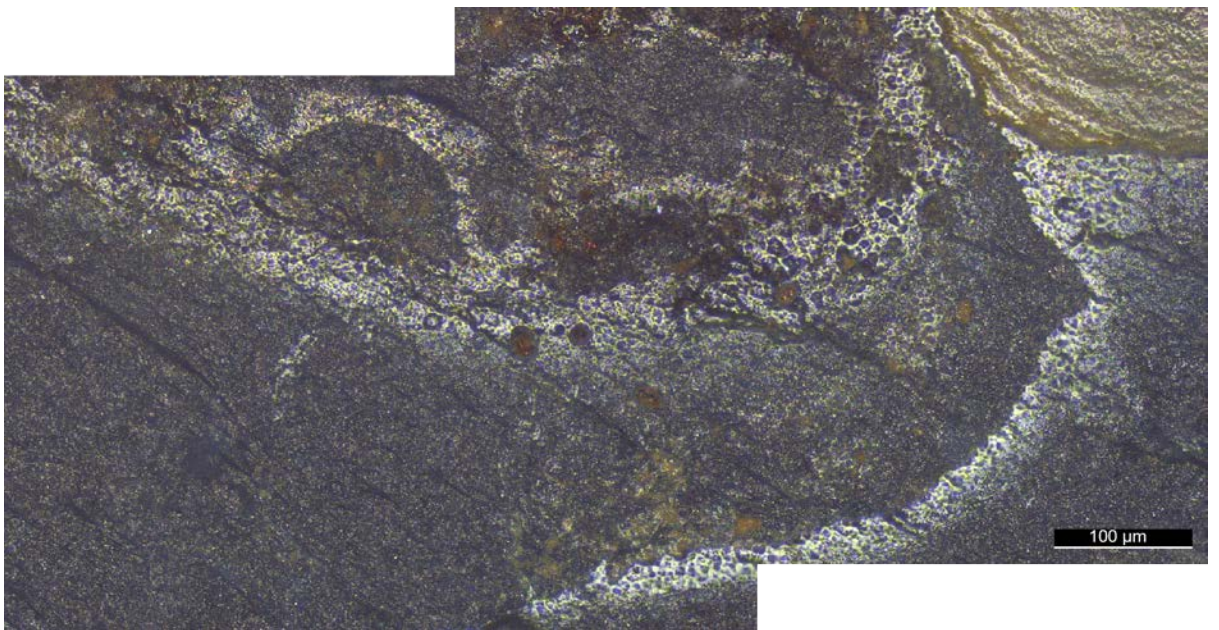
Figure 10.2. Example of tideline on blade tool 94066, ventral left mid edge. Note pool-like edges.

10.3.2.2 Dull lustre

Some stone tools in the sample displayed shiny deposits macroscopically, which appeared greasy or waxy with a dull lustre (Figure 10.3 and 10.4). Unfortunately, this deposit was not consistently recognised throughout the assemblage during microscopic analysis, since it was first interpreted as a polish, sometimes called 'dull polish', but usually termed generally as 'polish'. However, the dull lustre deposit was noted to contain gypsum crystals (Figures 10.4). It is important to note that these crystals are not phytoliths and shiny deposits with such inclusions should not be interpreted as evidence of plant-working. Rather, it was found that the crystals contained in the dull lustre deposits were identical in shape to crystals previously identified as gypsum with Micro-Raman.
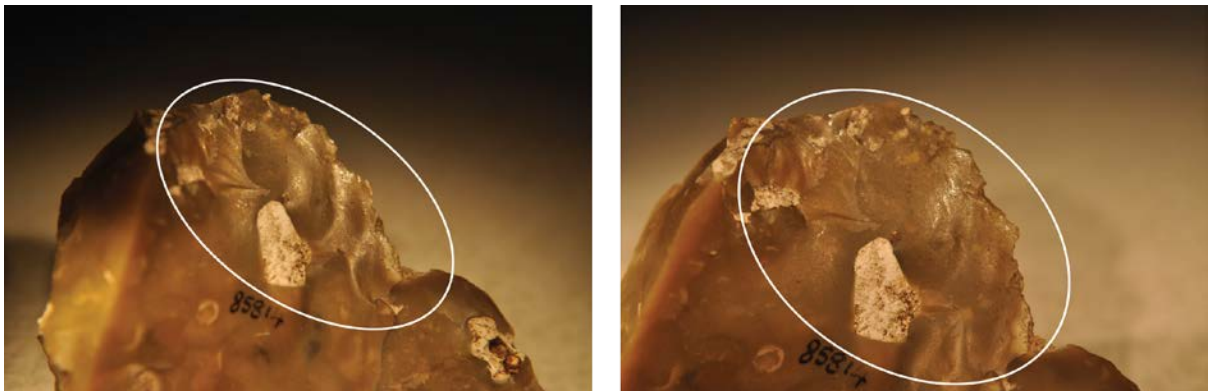
Figure 10.3. Core preparation flake 85814 with dull lustre deposit (circled). This deposit is likely silicon dioxide, originating either as a precipitate of dissolved amorphous silica from the soil from or from dissolution of the flint (quartz) itself.
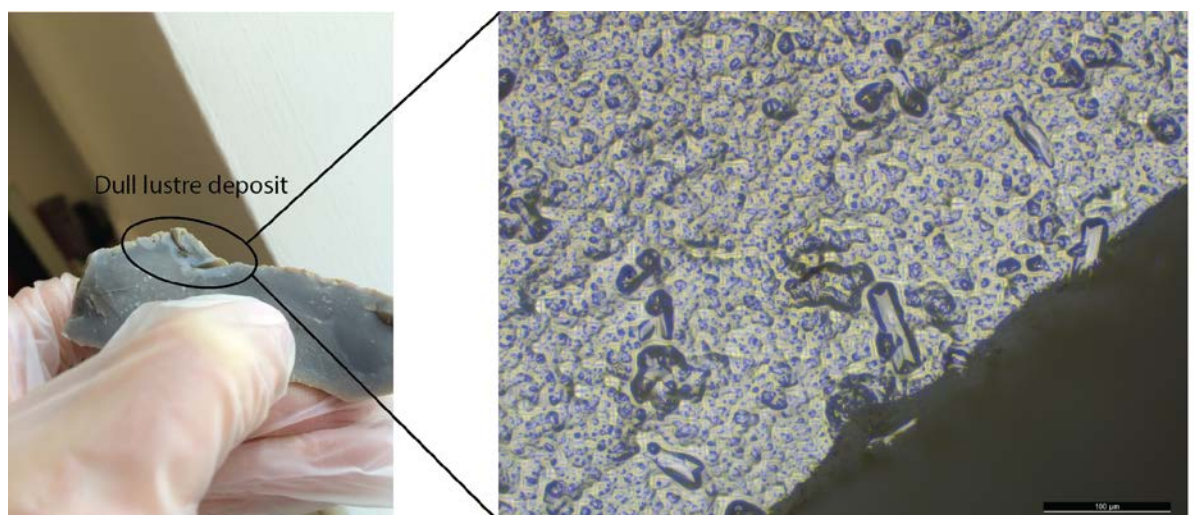
Figure 10.4. Left: Blade 109720 showing macroscopically visible deposit which appears greasy with a dull lustre. Right: Twinned swallowtail gypsum crystals within the dull lustre deposit.

10.3.2.3 Shiny deposits related to the lithic washing process

Some shiny deposits observed were connected with the normal wash process for lithics (see examples in Figures 10.5-10.12). These shiny deposits were highly reflective and contained gypsum crystals. Their borders were often distinct like 'islands' appearing to have some height, suggesting an additive deposit, but clear borders were not always present. Shiny deposits were seen on areas of the tool that were in direct contact with the cling film drying surface, sometimes with the deposit clearly mirroring the folds present in the underlying cling film (Figure 10.8), which were macroscopically visible.
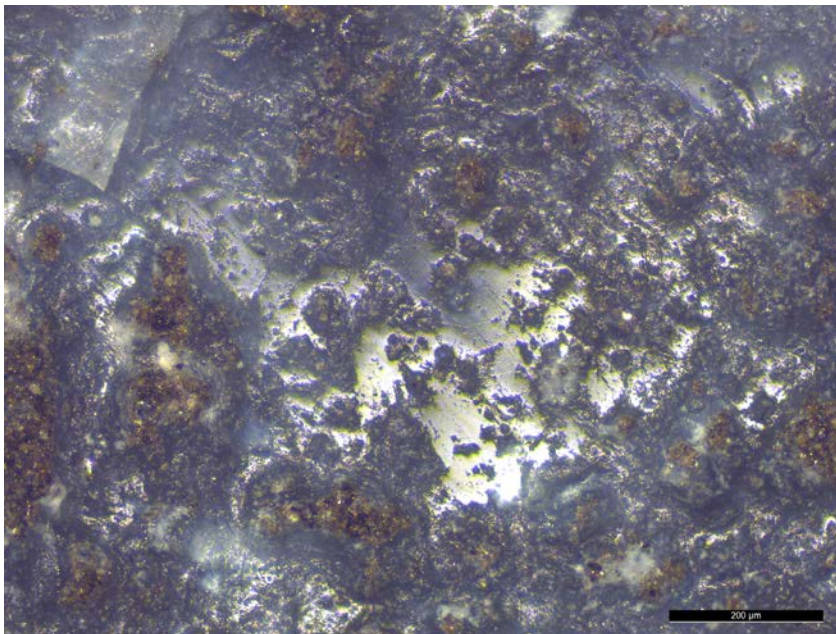
Figure 10.5. This shiny deposit was found on chamfered fragment piece 109735. As with all lithics, the tool was washed with water and left to air dry on a cling film-lined tray. The deposit is located on the dorsal centre surface – this part of the tool was in contact and adhered to the cling film whilst drying and is considered a shiny deposit formed by curation procedures.
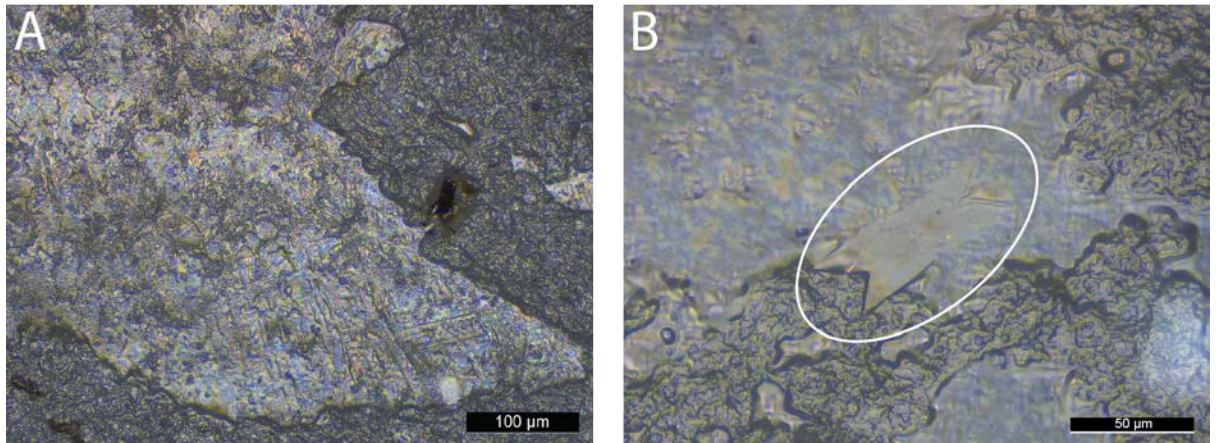
Figure 10.6. Shiny deposits related to the washing process on blade 99765. A) Fibrous sheet formation suggestive of gypsum. Steep edges of this shiny deposit suggests its origin is additive, not due to dissolution of the flint. B) A twinned swallowtail crystal embedded in the shiny deposit.
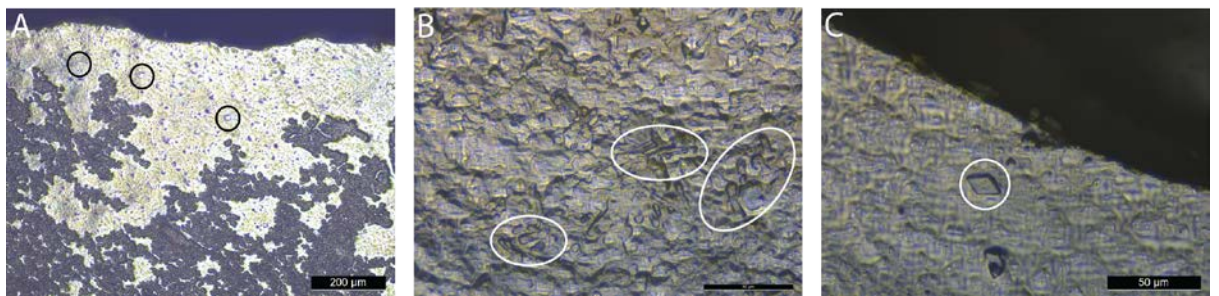
Figure 10.7. Examples of shiny deposits documented in relation to the wash process, containing different types of gypsum crystal shapes. All images show areas on blade 98855 which were in contact with cling film during drying. A) Shiny deposit, exhibiting 'islands' with raised edges, and containing twinned swallowtail gypsum crystals, dorsal left mid edge. B) Lath and rosette crystals embedded within shiny deposit, dorsal left mid edge. C) Rhombus crystal within shiny deposit, ventral right mid edge.
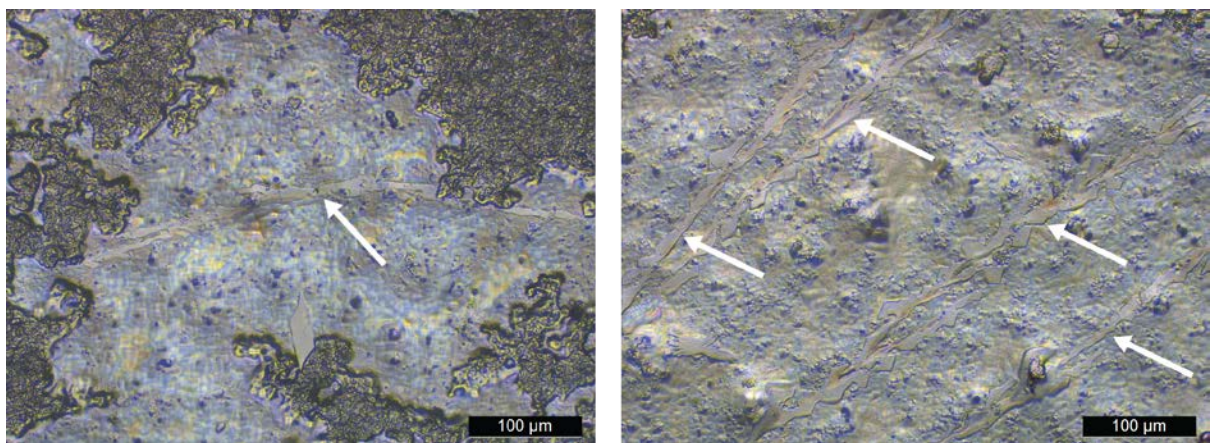
Figure 10.8. Shiny deposits with lines mirroring the folds present in the cling film drying surface. Blade 99765.

313

After washing and drying blade 99516, the lithic was lifted from the cling film-lined tray and it was discovered that the cling film underneath the tool adhered strongly to the blade. A shiny deposit was observed macroscopically on the tool. This deposit was found on the cling film as well, underneath the contact point between the tool and the cling film, and the same deposit was seen underneath the artefact plastic label (Figure 10.9). The plastic tag was washed in the same way as the tool to remove sediment. The shiny deposits on the cling film appeared translucent and highly reflective and sparkly, just as the shiny deposit appears on the blade. The deposit on the blade and the deposits on the cling film were both examined. Micrographs of the deposit on the cling film (Figure 10.10) reveal it contains the same shapes of gypsum crystals that were found on the tool (Figure 10.11). This shows that the deposit on the tool and the cling film were the same, and suggests the sediment is the origin.
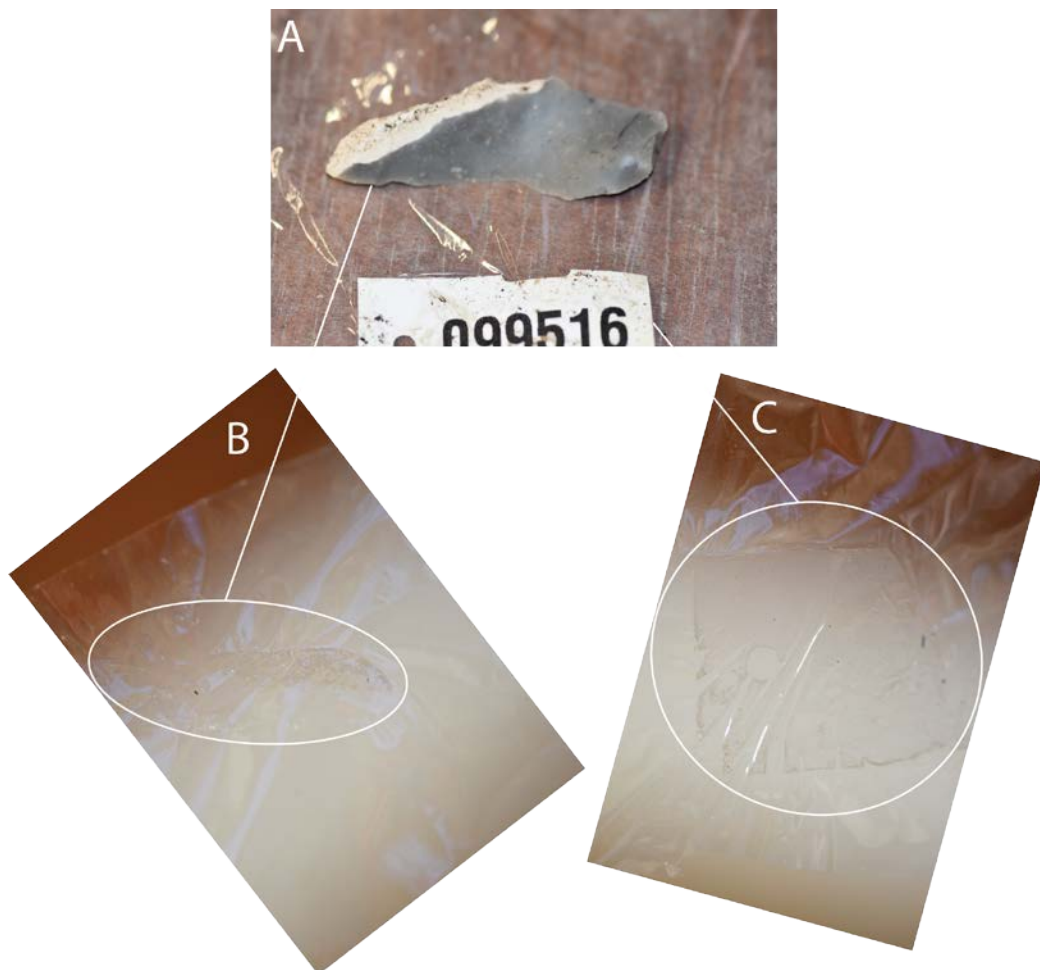
Figure 10.9. Blade 99516 and shiny deposits on the cling film. A) Blade 99516 and associated label drying on cling film after first wash with ultrapure water. B) Shiny deposit imprint left on cling

film matching the outline of the blade. C) Shiny deposit imprint left on cling film matching the outline of the plastic tag.
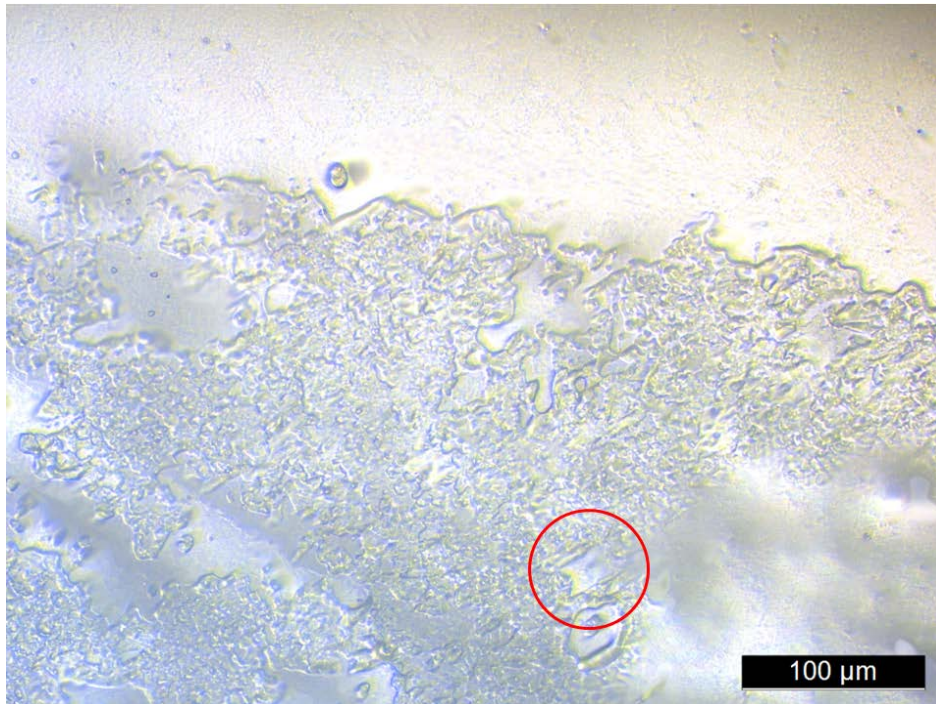
Figure 10.10. Shiny deposit on the cling film left after air drying blade 99516. Circled is the formation of a twinned swallowtail gypsum crystal.
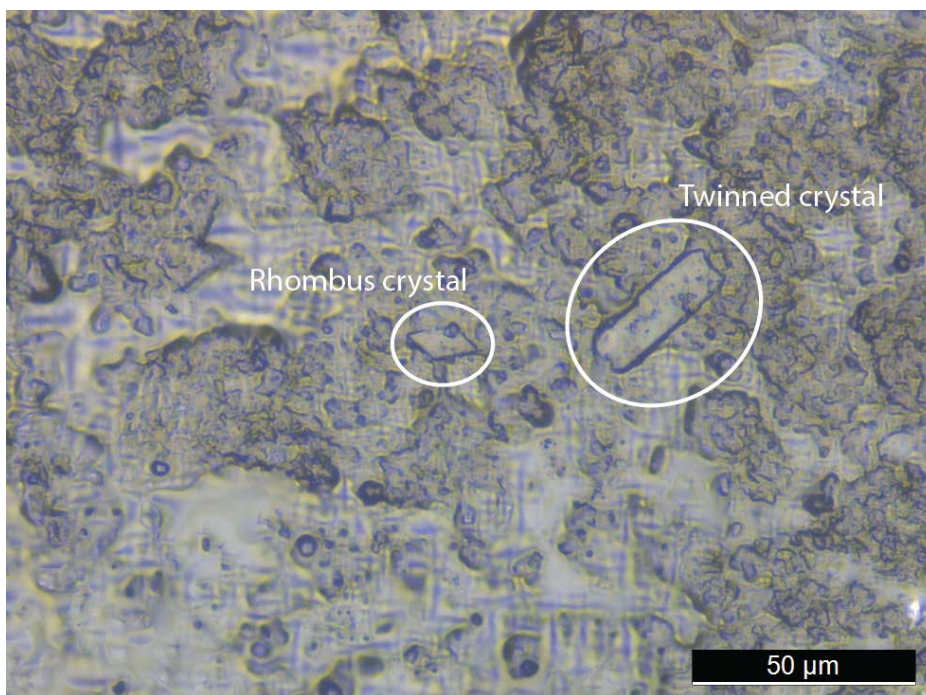
Figure 10.11. Shiny deposit on blade tool 99516 observed after first wash. Deposit contains rhombus and twinned swallowtail gypsum crystals. The deposit was located ventral centre interior part of the blade, slightly distal.

It was thought likely that the shiny deposit formed after the wash process was water soluble. To test this hypothesis, blade 99516 was subject to a second wash involving gentle stream of ultrapure water. Drying after the second wash and microscopic analysis of the blade showed the deposit was still present, albeit fainter, reduced in size, and containing no gypsum crystals (Figure 10.12). No shiny deposit imprints were found remaining on the cling film after the second wash. These observations show that this type of shiny deposit on lithics is water soluble and washing does affect its formation.
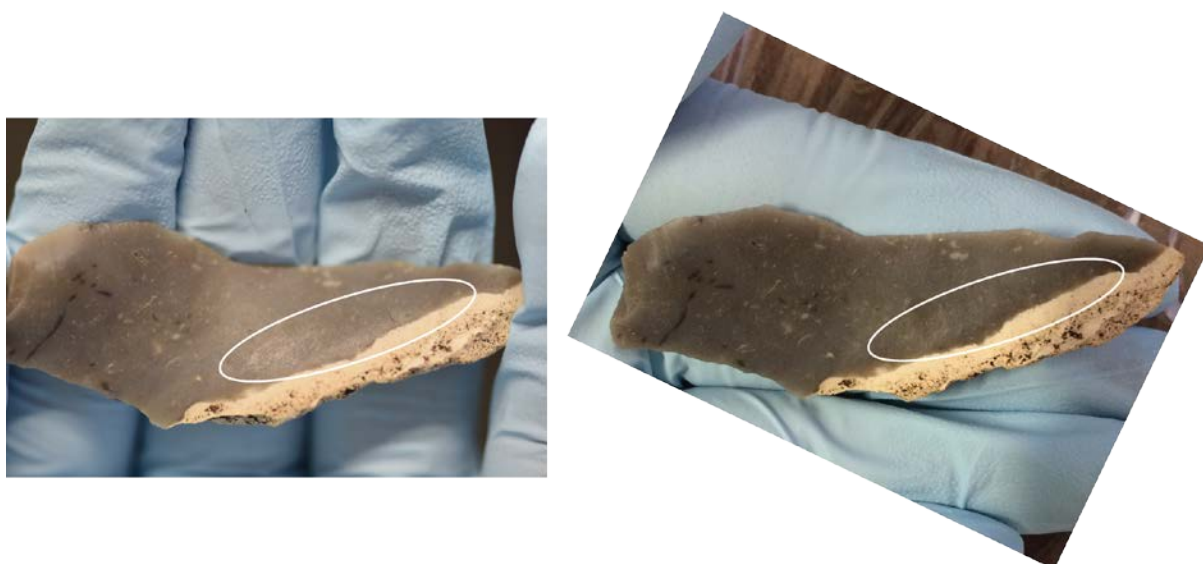
Figure 10.12. Left: Macroscopically visible shiny deposit on blade 99516 after first wash. Right: After the second wash with water, the shiny deposit is still present, but appears to be fainter and less shiny. No gypsum crystals were found in the shiny deposit on the tool after the second wash.

The origin of these shiny deposits related to washing, which look like usewear polish, was discovered part-way through the reflected VLM analysis. The shiny wash deposits might be proposed as originating from the polyvinyl chloride (PVC, $(C_2H_3Cl)_n$) cling film. Another PVC product containing plasticiser bis-(2-ethylhexyl)phthalate (brand name Mipofolie), was shown to emit damaging hydrochloric acid after 29 years in contact with skin parchment (Wouters 1992, p.68). The long contact period between the PVC product and the artefact of several decades is not, however, comparable to the short contact period of several days between the lithics drying on cling film and the microscopic analysis. Additionally, a cling film origin of the shiny deposits seem unlikely, since 1)

gypsum crystals were found within the shiny deposits on the tool, and 2) PVC cling film does not contain the minerals that would form gypsum.

It is unclear exactly how the formation of shiny deposits related to washing occur, but it was hypothesised that dissolved amorphous silica in the sediment adhering to the tools was mobilised by the wash water, then deposited as precipitate on the flint surfaces. It also appears likely that gypsum present in the sediment dissolves during artefact washing, followed by recrystallization on the flint surface. The pH of the water used to wash lithics was 6.5 to 7, so acidic wash water did not influence the dissolution/precipitation of materials on the tool. However, many soils at Star Carr are highly acidic, with readings from the peats often around pH 2.

10.3.3 Micro-Raman

10.3.3.1 Blade 99765

Spots of ~1 µm diameter within a shiny tideline deposit found on blade 99765 were tested with confocal Micro-Raman to chemically characterise the deposit (Figure 10.13). The closest identification for the tideline deposit was α-quartz and moganite (Figure 10.14), both polymorphs of silicon dioxide, but further work is required to better resolve this tideline type of shiny deposit.

317
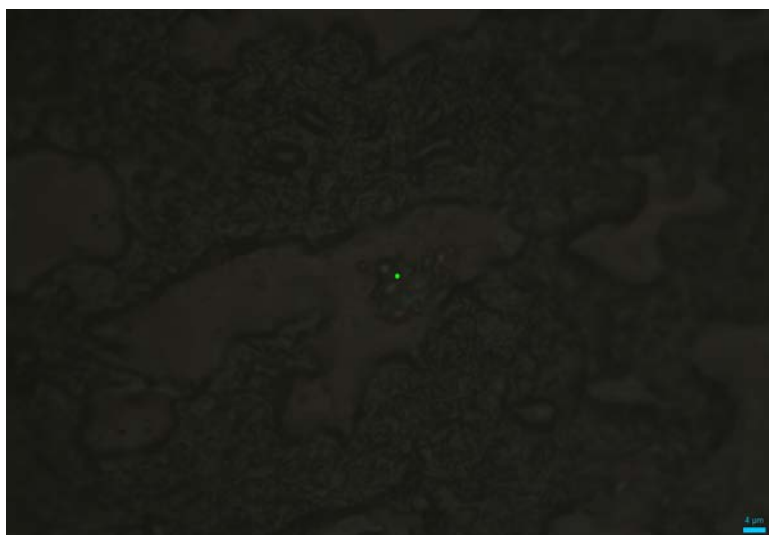
Figure 10.13. The spot on blade 99765 where the spectrum in Figure X was collected. The spot was within a tideline deposit.
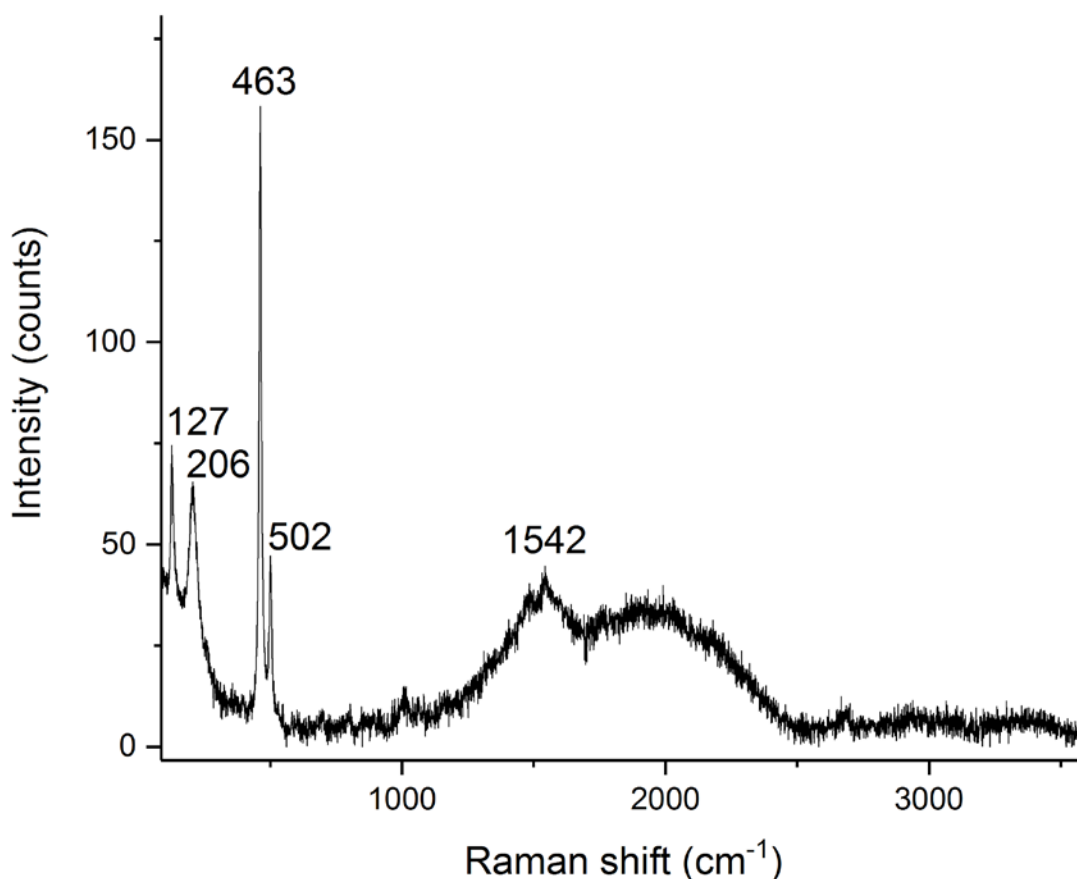
Figure 10.14. Raman spectrum of a tideline deposit from blade 99765, showing two polymorphs of silicon dioxide are present: α-quartz and moganite.

10.3.3.2 Comparison of shiny tideline deposits on archaeological flint with α-quartz reference values

The Raman spectra collected on the shiny tideline deposits were compared to silicon dioxide reference values. Silicon dioxide (SiO_2) exists in several polymorphs, which have different Raman features due to differences in the crystal lattice structure. The crystalline polymorphs include quartz (trigonal α-quartz, and hexagonal β-quartz), tridymite (orthorhombic α-tridymite and hexagonal β-tridymite), cristobalite (tetragonal α-cristobalite and cubic β-cristobalite), monoclinic moganite, monoclinic coesite, tetragonal stishovite (Götze and

Möckel, 2012, p. 3; Wenk and Bulakh, 2016, p. 296). The amorphous polymorphs of silicon dioxide are lechatelierite (silica glass), and opal silica (Drees et al., 1989, p. 913). At surface temperature and pressures, the most crystalline and stable polymorph is α-quartz. α-quartz is also the most common of these silicon dioxide polymorphs. Opal silica is the least stable polymorph – it has a disordered structure that incorporates hydroxyl and water (Weiner, 2010, p. 88).

It was thought that the tideline deposits might be composed of amorphous silica, since the subtraction of silicon dioxide within the flint (SiO_2) by chemical erosion and the addition of dissolved silica from the soil solution have both been proposed as mechanisms of natural polish formation (discussed in section 10.4.1).

However, the Raman spectrum presented in Figure 10.14 and the other spectra of the tideline deposit do not support an interpretation of amorphous silica. Amorphous (noncrystalline) silica contains a strong broad band at ~57-68 cm^{-1}, a strong broad band at ~435-440 cm^{-1}, a strong and characteristic band at ~490-500 cm^{-1} (Si–O bending, referred to as 'defect' D_1), and a weaker band at ~604-608 cm^{-1} (referred to as D_2) (Alessi et al., 2013; Bates et al., 1974; Brinker et al., 1988; Colomban et al., 2006; Galeener, 1982; Hibino et al., 1985; Matson et al., 1983; Sharma et al., 1981).

The closest match with the tideline deposit is mainly α-quartz (SiO_2), with evidence for inclusion of moganite (SiO_2). As can be seen in Figure 10.14, the main features of the tideline residue deposit are at 127, 206, 463, and 502 cm^{-1}, which generally correspond to α-quartz reference values (see Table 10.1). The sharp peak at ~465 cm^{-1} is the most intense Raman feature in both the tideline residue and the α-quartz references (Asell and Nicol, 1968, p. 5396; Gillet et al., 1990, p. 21640; Kingma and Hemley, 1994, p. 271; Krishnan, 1953, p. 382; Nedungadi, 1940, p. 88; Shapiro et al., 1967, p. 362; Sharma et al., 1981; Tekippe et al., 1973, p. 711). This strong peak at ~465 cm^{-1} is attributed to symmetric stretching-bending vibrations of SiO_2 A_1 mode of α-quartz (Olivares et al., 2009, p. 494).

Table 10.1. Correspondence between Raman wavenumbers (cm^{-1}) seen in the tideline shiny deposit and quartz.

Tideline residue on tool 99765	crystalline quartz Nedungadi 1940	crystalline quartz Krishnan 1953	α-quartz Shapiro et al. 1967	α-quartz Asell and Nicol 1968	α-quartz Tekippe et al. 1973	α-quartz Sharma et al. 1981	α-quartz Gillet and Le Cléac'h 1990	α-quartz Kingma and Hemley 1994	quartz powder (SiO2) ENS Lyon	Assignment (Götze et al. 1998; Kingma and Hemley 1994)
127	127	128		128	128	128	128	128	128	
			147		~145					
206	207	207	207	207	205	207	206	206	206	
	263	266		265	263	264	265	265	264	
357	354	356	355		354	356	355	355	354	
	397	394			393	395	394	394	390	
424		403			400		401	401		
	453				450		450	450	450	
463	**465**	**466**	**466**	**464**	**464**	**465**	**464**	**464**	**464**	symmetric stretching-bending SiO2 (A1 mode)
502	**501**									symmetric stretching-bending SiO2 (A1 mode) in moganite
							511	511		
					537					
	694	695		697	695	696	696	696	697	
	794	796		795	796	795	796	796	796	
805	805	809		807	805	807	808	808	808	
	1064	1063			1064	1066	1069	1069	1069	
	1082	1082	1081		1081	1083	1085	1085		
	1158	1160			1160	1161	1162	1162	1162	
	1228	1227			1231	1231	1230	1230		
1483										
1542										

Mineral quartz is classified into two major groups: macrocrystalline quartz and microcrystalline quartz (also known as cryptocrystalline quartz). Microcrystalline quartz is further split into two structural types of fine-grained microcrystalline quartz: fibrous quartz (e.g. agate and chalcedony) and nonfibrous quartz (e.g. chert and flint) (Heaney and Post, 1992). The fibrous quartz varieties are aggregates of microscopic parallely grown quartz crystals that can appear 'feathery', and the nonfibrous quartz varieties are composed of fine 'grainy' crystals that are roughly equant (Nesse, 1986, p. 253). Both the fibrous and nonfibrous quartz subgroups can contain variable amounts of moganite, one of the polymorphs of silicon dioxide (Flörke et al., 1976; Heaney and Post, 1992; Kingma and Hemley, 1994). Moganite has the same chemical composition as α-quartz (SiO_2), but forms a different crystal structure – in this case a monoclinic crystal system (Miehe and Graetsch, 1992, p. 693; Polyakova, 2014, p. 214). Moganite has not been found to exist as a pure mineral in nature, but rather is found associated with quartz in a densely interwoven mixture (Gíslason et al., 1997, p. 1193).

The peak seen at 502 cm^{-1} in Figure 10.14 of the tideline shiny deposit spectrum is consistent with moganite (Götze et al., 1998; Kingma and Hemley, 1994). Since the tideline spectrum contains both the peak found in pure α-quartz (~465 cm^{-1}, attributed to symmetric stretching-bending vibrations of SiO_2 A_1 mode) and the peak found in moganite (~503 cm^{-1}, attributed to symmetric stretching-bending vibrations of SiO_2 A_1 mode), it is possible to say that the sample contains both of these polymorphs of silicon dioxide (cf. Götze et al., 1998, p. 99; Rodgers and Hampton, 2003 Fig. 1c).

The ratio of moganite to quartz has been proposed as a way to distinguish between different sources of microcrystalline quartz (Götze et al., 1998; Schmidt et al., 2012), but quantification of the amount of moganite present in varieties of microcrystalline quartz using Raman spectra to allow their classification is still a developing area of research (Olivares et al., 2009; e.g. Schmidt et al., 2013). The finding of both quartz and moganite together in the Raman spectrum of the tideline shiny deposit does not allow a specific identification of the material

beyond 'microcrystalline silicon dioxide containing both α-quartz and moganite polymorphs'. This is because it is possible to find moganite existing with quartz in fibrous quartz varieties (chalcedony and agate), as well as nonfibrous quartz varieties (chert and flint) from all over the world (Heaney and Post, 1992, p. 442).

The Raman features seen in Figure 10.14 at 1483 cm^{-1} and 1542 cm^{-1} in the tideline residue spectrum are carbon related contaminants, perhaps remnants of the original adhering soil that was washed away with water. One of the major bands in carbon (graphite) is located around ~1575 to 1582 cm^{-1} (Cesare and Maineri, 1999, p. 47; Cuesta et al., 1994, p. 1523; Dresselhaus et al., 2010, p. 752; Kingma and Hemley, 1994, p. 1521; Tuinstra and Koenig, 1970, p. 1127), and this is consistent with the wide band present in the spectrum around 1542 cm^{-1}.

If we assume that all tideline shiny deposits in the Star Carr lithic assemblage are chemically similar based on their similar microscopic appearance, the evidence supports an interpretation of tideline deposits as composed of two silicon dioxide polymorphs, α-quartz and moganite. The silicon dioxide tideline shiny deposits identified in this study are interpreted as natural phenomena, based on their irregularly curved line morphology, their presence at random locations on the flint surfaces away from edges, and their common association with red-orange iron oxide deposits.

10.4 Discussion

10.4.2 The confusion between natural and cultural shiny deposits

Vaughan (1985, p. 42) stated that a general soil sheen is present "...on *every archaeological flint* that has resided in a sedimentary or aqueous matrix" (italics added). If this is true, all the flint tools from waterlogged Star Carr should be

expected to contain a soil sheen polish, which complicates the interpretation of all genuine anthropogenic usewear traces. Further regarding soil sheen, Vaughan (1985, p. 43) states: "Meat and fresh hide polish can be *identical* to the lesser developed end of soil sheen, just as the polish resulting from very limited plant cutting can resemble the generic weak polish of lesser developed soil sheen" (italics added). Thus, it would seem that soil polish can be mistakenly identified as any one of a variety of types of usewear traces. Even though Vaughan's book (1985) is considered a classic text for the identification of lithic usewear, his above statements highlight the inherent subjectivity that characterises the interpretations made in lithic usewear analysis.

The gloss patinas which form on flint due to natural soil processes in peat can easily be mistaken as polishes resulting from human actions, and Van Gijn (2010, p. 44), noted the difficulty in distinguishing natural gloss patina from anthropogenic usewear polish. Van Gijn believes the problem of differentiating gloss patina from usewear polish can be overcome by viewing the deposit with SEM. Van Gijn (2010, p. 44) describes gloss patinas as easy to identify with SEM because they are completely 'recrystallised', and that gloss patina contains none of the original granularity of the underlying flint. The evidence Van Gijn (2010, p. 44) uses to support this assertion is an SEM image of an archaeological, not experimental, stone tool (1990, p. 53 Fig. 35), so it cannot be said whether the formation of the shiny gloss on the tool originated from human-working or a natural cause. It is also not clear by what criteria one would tell the difference between a deposit which has crystallised versus one which has recrystallised. Additionally, since Van Gijin states that a lack of granularity is a key factor for identifying gloss patina, following this logic the assumptions made are: 1) all anthropogenic usewear polishes show some of the underlying granularity of the stone (doubtful), and 2) gloss patina presents itself only in the well-developed state whereby the granular stone surface microtopography is completely obliterated (i.e. the progressive stages of gloss patina development ignored). From the evidence presented above regarding stone tool polish, it is considered most likely that neither a 'recrystallised' appearance or an absence of granularity provide a sufficient means to identify with certainty whether the origin of a shiny deposit is a natural gloss patina or an anthropogenic polish.

10.4.2 Formation mechanisms of shiny deposits

The formation mechanisms responsible for the natural shiny deposits observed in the Star Car lithic assemblage merits discussion since their presence can confound interpretation of residues and usewear. Firstly, it must be remembered that flint weathering and alteration occur continuously – archaeologists do not dig up flint tools in the same condition as the moment they were deposited. Thus, we should always expect some natural wear and/or natural deposits on prehistoric flint artefacts due to general taphonomic and pedogenic processes in the burial environment.

That the Raman signature of the tideline is likely similar to the flint substrate is fascinating, suggestive of the dissolution of the flint itself. However, dissolution does not appear to be the formation mechanism for all shiny deposits, and shiny deposit formation processes require further investigation. Preliminarily, it appears shiny deposits are forming by both dissolution and additive precipitation. Additive shiny deposits were observed with raised edges (Figure 10.5) and containing cling film folds after washing (Figure 10.7). The slow dissolution of quartz (i.e. flint) is known to occur in water (Kendrick, 2006, p. 1251; McKeague and Cline, 1963a, 1963b), yielding silicic acid (also called monosilicic acid), according to the following hydrolysis equation:

$$SiO_2 + 2\ H_2O \rightarrow H_4SiO_4$$

Perhaps problematically, silicic acid (H_4SiO_4) is also the form in which silicon (Si) is transported in solution in the soil (Kendrick, 2006, p. 1251; Thiry et al., 2014/9, p. 142). Whether there are structural differences in silicic acid originating from the flint versus the soil that are detectable with Micro-Raman remains to be explored. It can be said that the spectra collected from the tideline deposit are not consistent with Raman spectra for silicic acid. The presence and concentration of

moganite might prove a useful specific marker that could help determine if a shiny deposit originates from the dissolution of the flint.

According to weathering experiments by Burroni et al. (2002, p. 1279), natural disturbances in the forms of chemical processes and friction from movement (tribological processes), produce polished or glossy surfaces on flint and chert artefacts. These chemical and physical weathering processes which cause the dissolution and precipitation of silica in the soil are typically slow, low intensity, and cumulative (Thiry et al., 2014). There are arguments for natural shiny deposit generation as an additive deposit (adsorption) to the flint surface from the soil, as well as a subtractive process (by physical abrasion or chemical dissolution) of the flint surface. The debate about the additive and/or subtractive origins of polish is not a new one in usewear studies (Christensen et al., 1998; Evans and Donahue, 2005; Fullagar, 1991; Juel Jensen, 1988; Šmit et al., 1999; see Tringham et al., 1974; Unger-Hamilton, 1984) and is still ongoing.

This unresolved debate is well-illustrated in the specific case of the natural formation of gloss patina. Howard (1994, p. 324), drawing on pedological literature, suggested that gloss patina formation is an additive process which is the result of dissolved silica in the soil precipitating first as an amorphous silica gel (a hydrogel), that then solidifies into a dried and hardened xerogel. This transformation process has been modelled as soluble silicic acid → hydrosols (colloids) → hydrogels (nonrigid gels) → xerogels (rigid gels), with the amorphous silica in the sequence progressively losing water (Drees et al., 1989, p. 943). In a later publication, Howard (2002) suggested that both additive and subtractive processes could to contribute to the formation of gloss patina. Recently, Thiry et al. (2014) reviewed the mineralogical and micromorphological literature and high resolution petrographic and SEM investigations concerning silica behaviour. According to this review, both additive and subtractive processes are at work contributing to the formation of silica deposits on flint.

Drees et al. (1989, p. 949), Kendrick (2006), and Thiry et al. (2014) note the following factors control silica dissolution/precipitation: particle size, soil pH (e.g. presence of acids like humic acid), the presence of organic matter, presence of a disrupted surface layer, composition of the silica components (types of silica polymorphs and their crystallinity), amount of water in soil, flow rate of water (including percolation), temperature, and the saturation level of silica in soil (high silica content in soil means limited dissolution of flint). The crystallinity of the silicon dioxide is an important factor in particular, with experiments by Siffert (1967) showing that amorphous silica easily dissolves with water into solution at room temperature within a matter of a days, whereas quartz dissolves much more slowly due to higher crystallinity.

The general consensus among soil researchers is that silicon (Si) content is positively correlated with soil organic matter content (Liang et al., 2015, p. 59), and soils that are high in organic matter also have high amounts of soluble silica (Jones and Handreck, 1967, p. 113). It has also been shown that experimental solutions containing the organic acids (such as citrates and oxalate) accelerate quartz dissolution (Bennett, 1991; Evans, 1964). Not only does organic matter enhance the dissolution of silicon dioxide, including crystalline quartz and noncrystalline amorphous forms, Kendrick (2006, p. 1251) notes organic matter also impedes precipitation of silicon dioxide. Thus, the acidic organic-rich sediments at Star Carr may be contributing to the dissolution of quartz (flint lithics) and also contain high levels of amorphous silicon dioxide. Within the soil, it appears precipitation of any silicon dioxide present may be prevented in organic-rich burial environments. Once an artefact is removed from the sediment and organics are washed away however, this may trigger silicon dioxide precipitation onto artefact surfaces.

The natural formation of what has been referred to as gloss patina is thought to require low energy chemical alteration of the flint interacting with weakly acting acidic solvents over long periods of time. However, an experiment by Rottländer (1975, p. 108), showed a glossy surface could be produced on flint flakes by treatment of the flakes in peat with water (pH 4) at 50°C after only 3 weeks. It was

326

suggested that the flakes were being dissolved in the peat/water solution, since the flakes lost 0.3% of their original weight. Also, Rottländer reported that the water contained twice the amount of silica expected for water at pH 4. Unfortunately, it was not clear if the amount of silica present in the water/peat solution was measured prior to the experiment for comparison. Also, it was not considered that a source for the high levels of dissolved silica present in the water at the end of the experiment might be accounted for by the contribution of amorphous silica from plant tissues (such as phytoliths) in the peat.

The development of gloss patina has been described as the formation of a complex containing one silicon atom from the flint (quartz) combined with the organic compound catechol (also referred to pyrocatechol, $C_6H_4(OH)_2$) (Hahn et al., 1995; Rottländer, 1975, p. 108; Weiss et al., 1961). Crook (1968) also hypothesised the formation of a silica-organic complex to account for the rounding and embayments observed in thin sections of quartz grains from several organic rich soils, proposing in situ chemical weathering was responsible for their eroded appearance. Extensive experiments by Bennett (1991), and Bennett et al. (1988) tested the dissolution of pure quartz in a variety of solutions and at variable concentrations and pH; they also suggested dissolved silica from quartz forms a silica-organic acid complex.

The activity of microbial communities likely also play a part in the chemical breakdown of flint (i.e. cryptocrystalline quartz). It is known that heterotrophic bacteria, cyanobacteria, and diatoms all cause biological dissolution of three types of silica (quartz sand, crystalline (scepter) quartz, and commercial glass), as demonstrated experimentally by Brehm et al. (2005).

10.4.3 The relationship between shiny deposits and iron oxide

It was noted during microscopic analysis that tideline deposits were often associated with red-orange deposits identified as iron (III) oxide (see Chapter 8). It is known that silica is attracted to adsorb to the surfaces of aluminium and iron oxides, and these compounds act as a sink in the soil for the precipitation of silica (Carlson and Schwertmann, 1981; Drees et al., 1989; Kendrick, 2006, p. 1251; Taylor, 1995). Aluminium and iron oxides have also been shown to lower the concentration of silica present in soil solutions experimentally (Jones and Handreck, 1967, p. 109). A relationship between iron oxide and silica appears to be illustrated at the microscopic scale in Figure 10.2. Iron oxides on flint tools at Star Carr might act as a magnet for the adsorption of soluble silica onto flint tools.

10.4.4 The relationship between shiny deposits and gypsum

It appears that the formation processes of gypsum crystals and shiny deposits may be related, as they are often found occurring together in direct spatial association on the stone tool surface. Furthermore, gypsum crystals were observed in various states of partial crystal formation within dull lustre shiny deposits and shiny deposits associated with the washing process, suggesting that the crystals formed in situ. However, shiny deposits were not always found to contain gypsum crystals, and as seen in the previous chapter, gypsum crystals also occurred in isolation on stone tool surfaces. The process or mechanism to explain if/how gypsum crystals and shiny deposits consisting of silicon dioxide are related is not known. However, both gypsum ($CaSO_4 \cdot 2H_2O$) and amorphous silica are known to easily dissolve in water, and their formation may be greatly influenced by water in the sediment, and post-excavation washing of lithic tools.

10.4.5 Dull lustre shiny deposits are probably not fat or protein residues

The dull lustre shiny deposits on lithics might be visually interpreted as evidence of 'fatty meat polish' from tool contact with animal flesh during hunting and butchering activities in the Mesolithic. There have been reports of visually identified 'dull greasy meat polish' on lithics, such as Clovis bifaces from the USA (Bebber et al., 2017, p. 548 Fig. 6), Mousterian bifaces from France (Soressi and Hays, 2003, p. 134), Magdalenian backed bladelets from France (Symens, 1986, p. 217 Fig. 3), Pleistocene (1.5 Myr ago) implements from Kenya (Keeley and Toth, 1981, p. 464), and Upper Paleolithic blades and bladelets from Sinai, Egypt (Phillips, 1988, p. 186). Experimentally used stone tools have also been described as containing meat polish with a dull greasy lustre (Keeley and Newcomer, 1977, p. 42), a bright rough polish, sometimes with a greasy lustre from meat cutting (Keeley, 1980, p. 66), and as a dull generic weak polish from fresh hide and meat (Vaughan, 1985, p. 38).

However, these 'dull meat polishes' are problematic. Butchering experiments by Smallwood (2015, p. 23) found that no microscopic usewear was produced after using two chert replica Clovis fluted points to cut meat 1,000 times, and this is consistent with the findings of previous butchery experiments by Newcomer et al. (Newcomer et al., 1986, p. 210) and Levi Sala (1996). Similarly, in Juel Jensen's (1988, p. 55) review of high power usewear analysis, she also found meat polish to be an issue because no polish was formed even after 90 min of meat cutting with experimental tools. Levi Sala (1996, p. 29) critiqued 'meat polish' as impossible to identify: "Even **if** this stage of polish development were to survive thousands and millions of years of burial and even **if** one could distinguish this brightness from the subsequent soil sheen, it would be impossible to identify it as "meat polish" since, as mentioned earlier, all used material produce this generalised brightness in the early stages of use". Instead, she suggested that lithics with 'meat polish' are actually evidencing the development of 'soil sheen',

also known as the gloss patina arising from chemical interactions with the soil discussed previously.

The dull lustre shiny deposits are interpreted as a result of soil processes. The dull lustre shiny deposits described here were found not only on tools, but also on flint pieces which are not tools (see example of core illustrated in Figure 10.15 from excavations at Star Carr in 2007). The arbitrary locations of these deposits are often macroscopically apparent across flint surfaces. The fact that there are many lithics in the Star Carr assemblage which contain randomly distributed dull lustre shiny deposits, and on pieces which are not tools, questions the utility of 'meat polish' as an identifiable phenomenon.
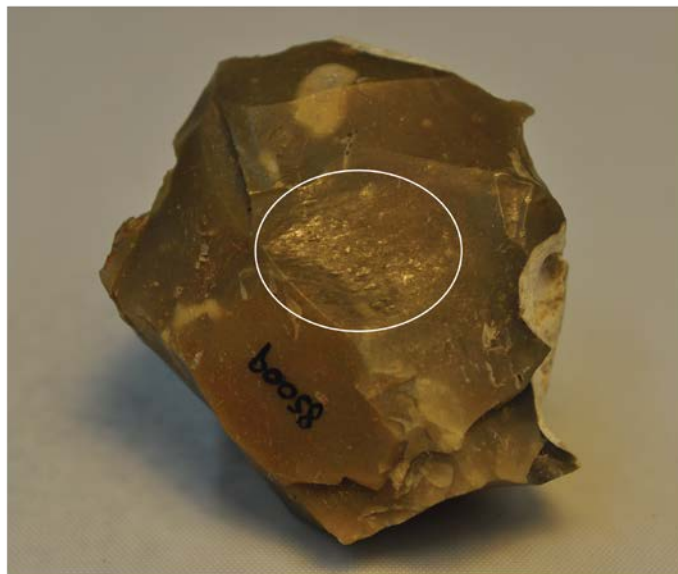
Figure 10.15. Dull lustre deposits (circled) present on core 85009. Flint 85009 is a core piece of knapping waste with cortex that contains a dull lustre shiny deposit in the centre of the flint surface. This piece is unlikely to have been used.

Since biological tissues have been investigated with Micro-Raman and contain characteristic peak frequencies attributable to functional groups (De Gelder et al., 2007; Motoyama, 2012; Movasaghi et al., 2007), it was possible to search for protein and fats within the Raman spectra presented in this thesis. The spectra obtained on the tideline shiny deposits contained no Raman features that could be assigned to protein amide groups or fatty acid groups that are found in lithic residues resulting from contact with meat.

De Gelder et al. (2007, p. 136) found that proteins can quickly be identified in a Raman spectrum by the presence of amide III ($\sim$1300 cm^{-1}) and amide I bands ($\sim$1655 cm^{-1}). Similarly, in a review of Raman bands relevant to biological tissues, Movasaghi et al. (2007) show amide III bands occurring between 1302-1337 cm^{-1} and amide I bands 1600-1697 cm^{-1}. Raman features representing amide III and amide I were not present in the spectrum of the tideline shiny deposit, nor any other Raman spectrum collected on a residue presented in this thesis. Thus, there is currently no evidence for the presence of protein residues on the stone tools from Star Carr. This is unsurprising, since it is contested that archaeologically significant proteins are able to preserve on the exposed surfaces of stone tools where they are accessible to microorganisms (Gernaey et al., 2001). Micro-Raman analysis is also a surficial analysis technique, so any proteins trapped and potentially preserved in microcracks or microtopography (Shanks et al., 2004, 2001) are unlikely to be detected.

The tideline deposit does not contain plant or animal lipids (saturated/unsaturated fatty acids, triacylglycerols, cholesterol, cholesteryl esters, and phospholipids). Triacylglycerols (TAGs) in particular are an important group to consider, since they are present in animals as the major stores of fat (within adipose tissue), as milk fats, and are the major dietary lipid for humans (Garrett and Grisham, 2012, p. 762; Hames and Hooper, 2000, p. 328; Pollard and Heron, 2008, p. 390). TAGs also occur in plants (Evershed, 1993) and are the main store of energy as seed oils for growing embryos. In terms of molecular structure, TAGs are composed of three fatty acid chains attached to a glycerol backbone. However, free fatty acids (FAs) which have broken away from the backbone as degradation products are commonly found in archaeological samples and can evidence the

enzymatic hydrolysis of the original TAG molecule (Pollard and Heron, 2008, p. 394). FAs (as the degradation products of TAGs) are expected to be the lipid type in greatest abundance in archaeological samples, since TAGs are the major storage fats in living plants and animals. Despite the tendency for TAGs to break down, in tact TAGs have been recovered from early Neolithic pottery from sites in Anatolia and the northern Mediterranean, dated to the seventh millennium BC (Evershed et al., 2008, p. 529; Spiteri et al., 2016, p. 13594), and from early Neolithic pottery from sites in northern Europe dated to the sixth millennium BC (Salque et al., 2013, p. 523).

For solid fatty acids, the most important band for identification is located at ~1400 cm^{-1} to 1440 cm^{-1} (represents CH_2 bending vibrations) (Czamara et al., 2015, p. 18; De Gelder et al., 2007, p. 1144; Wu et al., 2011, p. 3810). Another strong band found in solid fatty acids is located at ~1300 cm^{-1} (CH_2 twisting) (De Gelder et al., 2007, p. 1144; Wu et al., 2011, p. 3810). For solid triacylglycerols, the doublet band at ~1720 cm^{-1} to 1750 cm^{-1} (represents $v(C=O)$ carbonyl stretch), is the main marker for TAGs (Czamara et al., 2015, p. 18; Weng et al., 2003, p. 414). Based on the absence of the above bands, the tideline does not contain TAG or FA lipid residues.

10.5 Conclusion

Shiny deposits were observed on many tools during microscopic analysis and were originally misinterpreted as usewear polishes. It was also discovered that there is a relationship between the washing process and the formation of some shiny deposits. Two morphologies were documented within the lithic sample: tideline and dull lustre.

The shiny tideline deposit was identified as two polymorphs of silicon dioxide (α-quartz and moganite) that did not contain proteins or fats. Since only one tideline shiny deposit from one tool was chemically characterised, it is difficult to say whether the results are representative of the rest of the shiny deposits observed

in the lithic assemblage. However, the Raman data makes it possible to preliminarily suggest a dissolution origin of silicon dioxide from the flint, since the highly crystalline α-quartz was the main polymorph represented in the tideline shiny deposit. Although not specifically characterised with Micro-Raman, the dull lustre deposits can be suggested to be of natural origin, since they often contained gypsum crystals (identified previously in Chapter 9) from the sediment and were randomly distributed on both tools and non-tools.

Shiny deposits on lithics related to washing with ultrapure water were also found. These contained gypsum crystals on both tools and in the precipitated shiny residue left on the cling film drying surface. Many of these shiny deposits had contained imprints mirroring the folds of the cling film drying surface, indicating that their formation was directly attributable to interaction with water from washing. Further support for the idea that these shiny deposits are additive and originate from the sediment and not from the tool was supported by the fact that these deposits were also found underneath washed plastic artefact tags.

There are numerous types of reflective surface alterations that are possible to find on lithics and there are a multitude of complex chemical, physical, and biological taphonomic variables that can contribute to their formation. Some shiny deposits are natural surface modifications resulting from interactions between artefacts and burial environment, some are due to post-excavation curation practices, and some are probably genuine traces of usewear. The results of the analyses here have drawn attention to the need to carefully interpret any shiny deposits or 'polish' encountered on lithic tools, from Star Carr and elsewhere.

CHAPTER 11 RESULTS: WHITE ANGULAR CRYSTALS

11.1 Introduction

White, cream, and light brown angular crystalline residues were observed adhering to 17% of the Star Carr assemblage analysed (Figures 11.1 and 11.2). It was thought that these residues could potentially be bone and/or antler flakes, especially considering their locations on the edges of the flint. The general appearance of this residue type matched the characteristics used for the visual identification of bone residues outlined by Lombard (2005, p. 287), Lombard (2008, p. 36 Figs. 13, 14) Langejans (2012, p. 1697), and Langejans and Lombard (2015, p. 207): amorphous, angular and rigid, opaque, white to light yellow. The posited bone/antler residues discovered also appeared similar to experimental examples of bone residues in Jahren et al. (1997, p. 248 Fig. 5), Rots et al. (2017 Fig. 10), and bone and antler residues in Monnier et al. (2012, p. 3289 Fig. 5, Fig. 6), and archaeological bone residues illustrated by Babot and Apella (2003, p. 125 Fig. 4). Not only were the potential archaeological bone residues seen on tools consistent with the descriptions and images present in the literature, but were also consistent with the bone and antler residues observed in the reference collection.
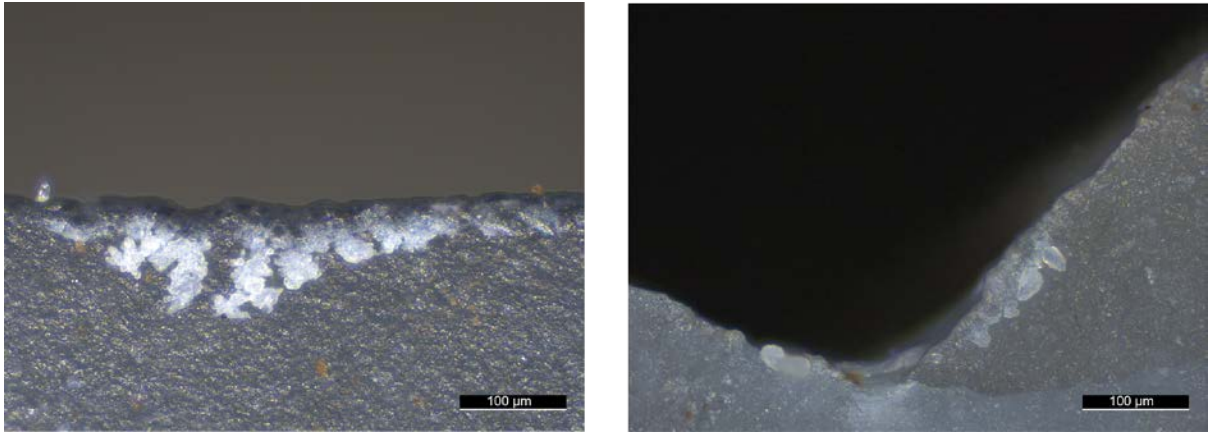
Figure 11.1. Examples of opaque angular crystalline material. Left: white angular crystalline residue on the ventral right proximal edge of blade 93327. Right: crystalline residue found around a microchip on blade 93312, dorsal right mid edge. From microscopic examination, both traces were originally interpreted as possible tool attrition or bone residue.

The published literature and observations of the reference bone residues led to the hypothesis that the white angular crystals were the remnants of Mesolithic bone-working and/or antler-working activities. However, the experimental study (see Chapter 6; Croft et al., 2016) showed that even modern bone residues on stone tools are not distinct enough morphologically to be identified with reflected VLM alone. Further investigation of the potential bone residues by chemical characterisation was required for identification, since no osteons (Haversian systems), which are diagnostic structures present in bone and antler, were visible with VLM examination. The anatomical structures of the osteon unit – concentric lamellae, Haversian canals, and osteocytes with branched canaliculi – are invisible within crushed bone fragments that are positioned in multiple directions on the stone surface. Thus, this residue type was chemically investigated with confocal Micro-Raman spectroscopy.

11.2 Methods

White angular residues were first identified in situ with reflected VLM and residue maps and composite z-stacked micrographs were taken. Potential bone/antler residues found on awl 109731 and bladelet 110656 were investigated with

confocal Micro-Raman spectroscopy to determine the chemical nature of these residues.

11.3 Results

11.3.1 Presence of white angular crystals in relation to burial context

White angular crystal were observed on 24 of 138 stone tools examined (17%). These crystals were detected on artefacts from contexts (301), (308), (310), (312), and (317) (Table 11.1).

Table 11.1. Contexts containing artefacts with white angular crystals.

Context	Number of tools with white angular crystals/total number of artefacts examined from context	Percentage %
301	2/3	67
308	10/27	37
310	9/46	20
312	2/38	5
317	1/11	9
Total	24/138	17

11.3.2 Microscopic description

It was noted during microscopic observations (Accompanying Material 3) that these residues appeared lighter than the flint and thus stood out. Unlike other residue deposits described in previous chapters 8-10, this residue had a consistent morphology, always appearing as groups of crystalline angular

fragments (Figure 11.2). However, this residue did vary from white to cream to light brown in colour, but was usually white.
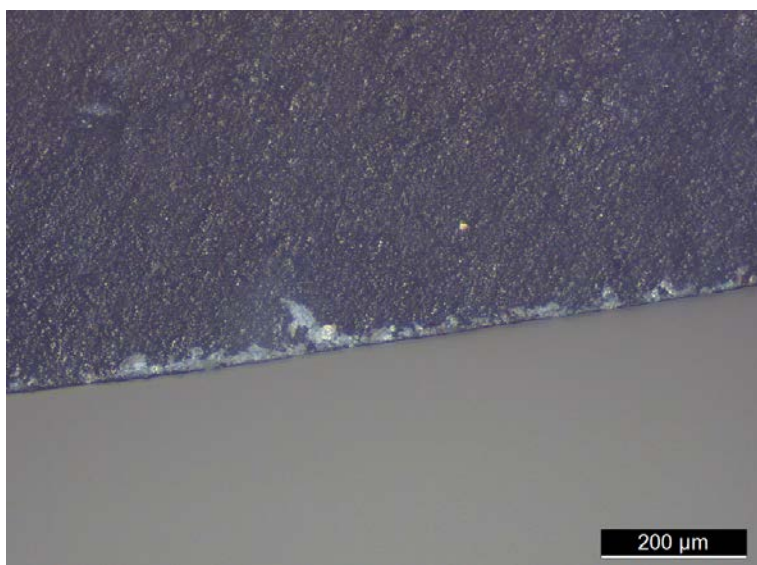
Figure 11.2. Residue identified as possible bone or stone attrition from bladelet 98859.

11.3.3 Micro-Raman

White angular crystals on two flint tools were investigated using confocal Micro-Raman spectroscopy. If bone and/or antler is present on the artefacts, it is expected that the Raman spectra collected will contain the same major peaks as found in published reference spectra for bone. Raman reference spectra of bone show that it contains a characteristic sharp peak at ~958-965 cm^{-1}, representing the symmetric stretch between phosphorus and oxygen of apatite v_1 PO$_4^{3-}$ in bone mineral (Awonusi et al., 2007, p. 47; Chatzipanagis et al., 2016, p. 2; Crane et al., 2006, p. 436; Delgado-López et al., 2012, p. 3497; Gamsjaeger et al., 2010, p. 395; Mandair and Morris, 2015, p. 2; Penel et al., 2005, p. 896; Tarnowski et al., 2002, p. 1119). This sharp peak is also found in archaeological bone (Edwards et al., 2001, p. 21, 1999, p. 2695; Kerns et al., 2015, p. 518). Bone also exhibits strong bands at 430-450 cm^{-1} (v_2 PO$_4^{3-}$), 584-590 cm^{-1} (v_4 PO$_4^{3-}$),1070-1076 cm^{-1} (v_1 CO$_3^{2-}$, v_3 PO$_4^{3-}$), 1242-1340 cm^{-1} (Amide III), 1446 cm^{-1} (CH$_2$ deformation), and 1660-1690 cm^{-1} (Amide I) (Antonakos et al., 2007, p. 3045; Awonusi et al., 2007, p. 47; Bart et al., 2014, p. 5; Makowski et al., 2013, p.

337

515; Mandair and Morris, 2015, p. 2; Movasaghi et al., 2007, p. 5; Penel et al., 2005, p. 896; Raghavan et al., 2012, p. 944; Takahata et al., 2012, p. 3650).

11.3.3.1 Awl tool 109731

Several small negative flake scars or microchips along the ventral right middle edge of awl 109731 contained white to cream angular material within microchips (Figure 11.3). Usewear in the form of a discrete polish along the edge of the tool was found in association with the white residue, which seemed to strengthen the hypothesis that these residues were bone or antler.
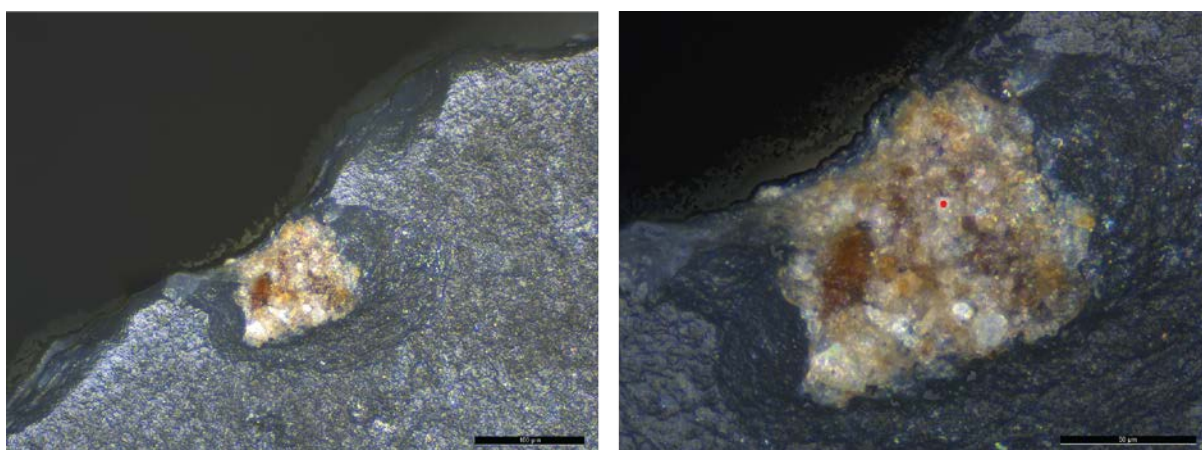
Figure 11.3. Left: Non-bone deposit located within microchip scar on awl 109731, ventral right mid edge. Right: Spot shows the location investigated with the Micro-Raman laser, corresponding to the spectrum below.

The Micro-Raman spectra collected (see example spectrum in Figure 11.4) show this residue is not bone, as it lacks the sharp peak at ~960-963 cm^{-1} (symmetric P-O stretching) expected of bone apatite. The spectra collected from this residue suggests the residue (or perhaps contaminants from soil organics) contains carbon, as indicated by the band at 1570 cm^{-1}, similar to the peak at 1575 cm^{-1} originally reported by Tuinstra and Koenig (1970, p. 1126) for single crystal graphite (crystalline carbon). This band at ~1575 cm^{-1} is now referred to as G band (after graphite) (Cuesta et al., 1994, p. 1523).
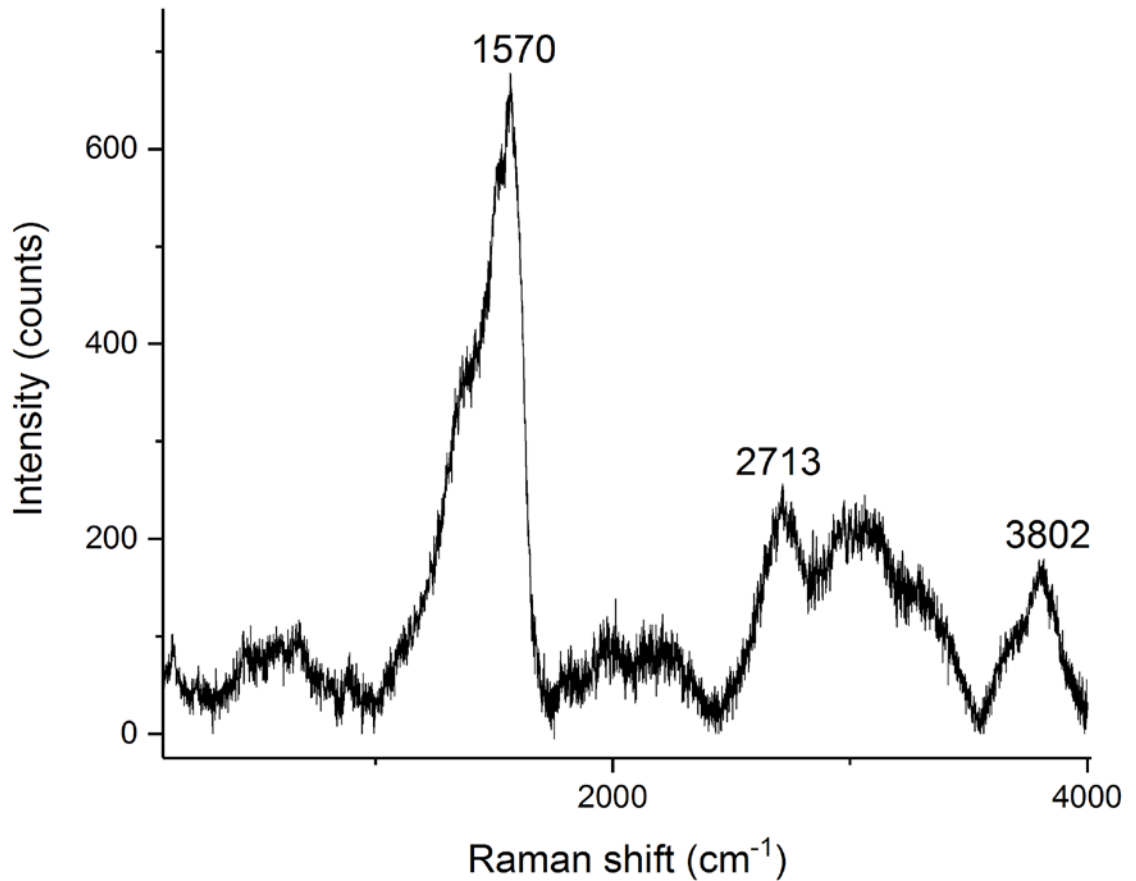
Figure 11.4. Raman spectrum of a white crystalline deposit within microchip on awl tool 10973 (image above). The spectrum illustrates that this residue is not bone.

11.3.3.2 Bladelet 110656

Bladelet 110565 was excavated as part of a spatial clustering of four bladelets, all possibly part of a multi-component tool. White angular crystals were located on the dorsal tip of this bladelet, slightly to the right (Figure 11.5). These residues were also proposed to be anthropogenic residues from contact with animal bone.
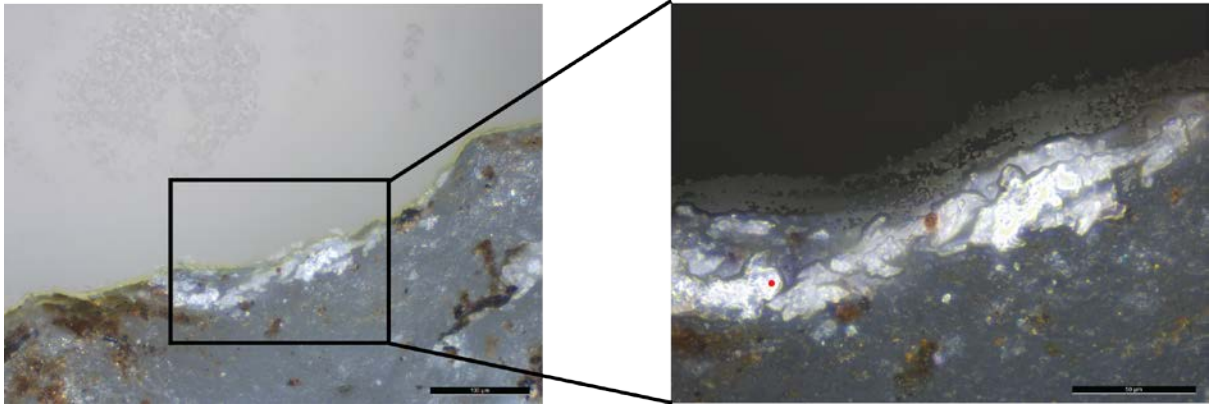
Figure 11.5. Bladelet 110656 with potential bone residue present on edge of tool, just right of dorsal tip. The red dot in the right image shows the location investigated with the Micro-Raman laser, corresponding to the spectrum below.

The Raman spectra collected indicate that the residue is not consistent with bone (Figure 11.6). Although the origin of the white angular crystals on tool 110565 was not completely resolved, this residue is most likely a mineral. The sample is related to α-quartz, but this requires further investigation to resolve. The most pronounced peak in α-quartz is major peak at 464 cm^{-1} (Ciupiński et al., 2010, p. 4943; Kingma and Hemley, 1994, p. 270), which was found in the spectra collected. The spectra for this residue also contained a peak at 1570 cm^{-1}, consistent with the presence of carbon (see carbon in residue on awl 109731).
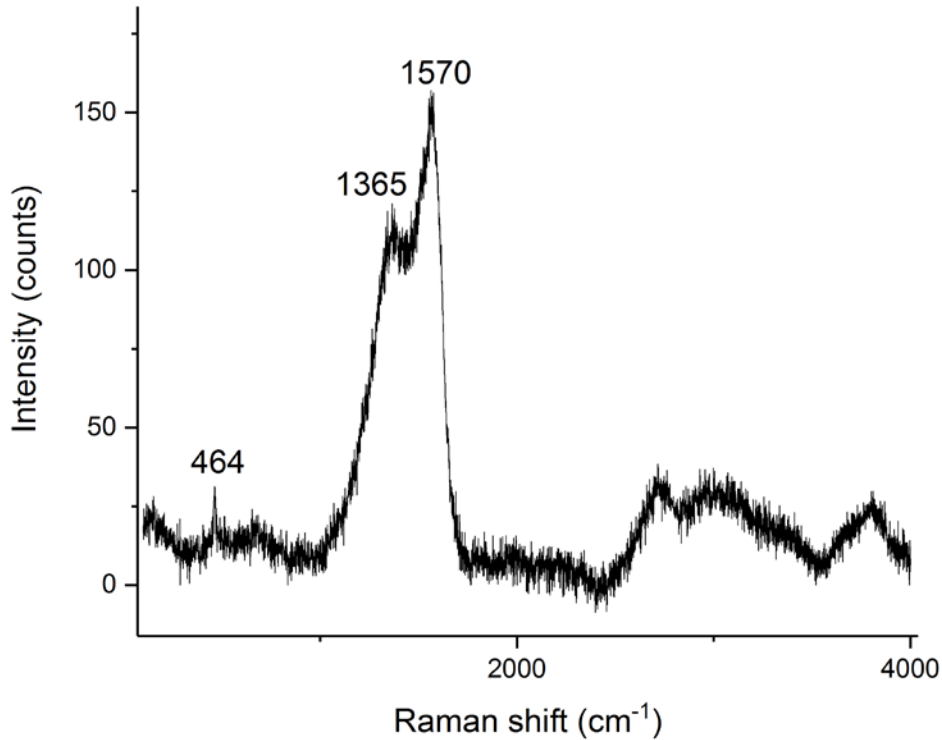
Figure 11.6. The spectrum illustrates that this white crystalline residue on bladelet 110656 (image above) is not bone, but possibly a mineral related to α-quartz, based on the peak present at 464 cm^{-1}.

11.4 Discussion

This study has shown that the visual microscopic strategy for identification of residues, when used as the only method of investigation, can be misleading. If the identification of the white angular crystalline residues in question was based solely on microscopic appearance, the residue would have been identified incorrectly as bone/antler. The Raman spectra collected show that the white angular residues investigated on the awl and bladelet are not consistent with reference values for bone.

Two explanations have been proposed to account for the presence of white angular crystals on the flint tools examined from Star Carr: 1) flint attrition in the form of angular pieces of flint dust from tool use by Mesolithic people, or 2) natural sediment contaminant that was not removed during gentle washing with water. The white crystal residues tested on the bladelet contained a peak

associated with quartz, providing tentative support for the attrition explanation. Experiments with the use of flint on hard surfaces suggest that attrition of the flint may occur and form a fine white powder or dust as a result (Needham 2017, pers. comm.). Although the attrition explanation requires further testing within a framework that incorporates chemical characterisation techniques such as Micro-Raman, it appears to be consistent with microscopic observations of thin pieces of crystalline dust seen standing out against grey flint. The second plausible explanation is the white angular crystals represent the remnants of minerals in the sediment, and thus are a form of natural contamination. Perhaps natural quartz crystals remained firmly attached to the flint substrate. However, what is striking about the white angular deposits is that their distribution is usually focused on the edges, not randomly over tool surfaces as would be expected if this residue originated from natural contamination.

The diagenesis results of bone and antler from the residue burial experiment (Chapter 6; Croft et al., 2016) also make the point that it is unlikely that any bone or antler residues would survive in the first place at Star Carr. No microscopic traces of bone or antler preserved on flint flakes buried in the dryland or the wetland at Star Carr after 11 months of burial.

11.5 Conclusion

White angular crystalline residues resembling bone and/or antler, similar to identifications of bone described and illustrated in the literature, were found on 24 flint implements during microscopic scanning of lithic residue specimens. The hypothesis that the white angular deposits were bone and/or antler was falsified. The Micro-Raman spectra collected on the posited bone and/or antler residues from two stone tools were not consistent with reference values for bone. Rather, these crystalline deposits as were of another, likely mineral, origin. In particular, the white angular crystalline traces found on the bladelet appear to be related to α-quartz, but more work on this residue type may be able to define it more precisely.

CHAPTER 12 RESULTS: ENGRAVED PENDANT AND BEADS

12.1 Introduction

This chapter will showcase residue analysis conducted on an engraved shale pendant (finds number 115527), and three shale beads from Star Carr. The pendant, and two beads (113830, 110671) were excavated in context at Star Carr, and one bead was analysed from Clark's backfill. To date, 30 shale and amber beads and at least two perforated animal teeth have been recovered from Star Carr (Clark, 1954; Milner et al., 2013a) (see examples of shale beads Figure 12.1).

Figure 12.1. The shale beads from Star Carr (Museum of Archaeology and Anthropology, Cambridge, accession number: 1953.72). Image from Milner et al. (2016).

Some Mesolithic amber pendants from Denmark (which particular pendants and sites unclear) have been suggested to contain black resin as a filling to enhance the contrast of the incised decorations against the surrounding surface (Toft and

Brinch Petersen, 2013, p. 205). Additionally, Late Mesolithic cyprinid tooth ornaments from Vlasac, Serbia, have been reported to contain red ochre and calcite residues used as red and white pigments (Cristiani et al., 2014b, p. 300). Thus, the beads recovered at Star Carr were investigated for any residues of colourants or pigments, such as ochre, charcoal, or resin were used. Overall, the pendant and beads were investigated for any trace microscopic residues that might indicate how they were made and used by Mesolithic people.

12.2 Pendant

The engraved Star Carr pendant is special because it represents the oldest example of British Mesolithic art (Figure 12.2): the artefact is an incredibly rare finding and was examined in detail by Milner et al. (2016). The pendant was found in context (317), which is described as a brown-green moist fine detrital mud containing a lower component of reeds but still a high proportion of organic material within the matrix, very close to the original trenches excavated by Clark in 1949-1950, containing a rich array of material including faunal remains, artefacts and flint.

Figure 12.2. Left: The engraved side of the pendant. Right: The back of the pendant.

The shale pendant is extremely fragile. Laminar cracks were seen forming between the sheets of the stone material on the bottom and right edges of the pendant. Trowel lines were the same colour as the stone microscopically, unlike the dark incisions. The shale must have been reasonably easy to shape into beads and engrave because the stone material itself is soft.

The line designs on the pendant are very faint and elaborate and cannot be seen clearly with the naked eye or traditional photography. Upon microscopic inspection, short lines were seen emanating from several of the long lines, like the legs of a centipede (Figure 12.3). A needle-sharp implement, likely made from flint, was used to make the incisions, as the lines are about .25 mm or less in width. The person or people who engraved the fine geometric designs on the pendant must have had good eyesight and steady hands, and therefore perhaps they were young.
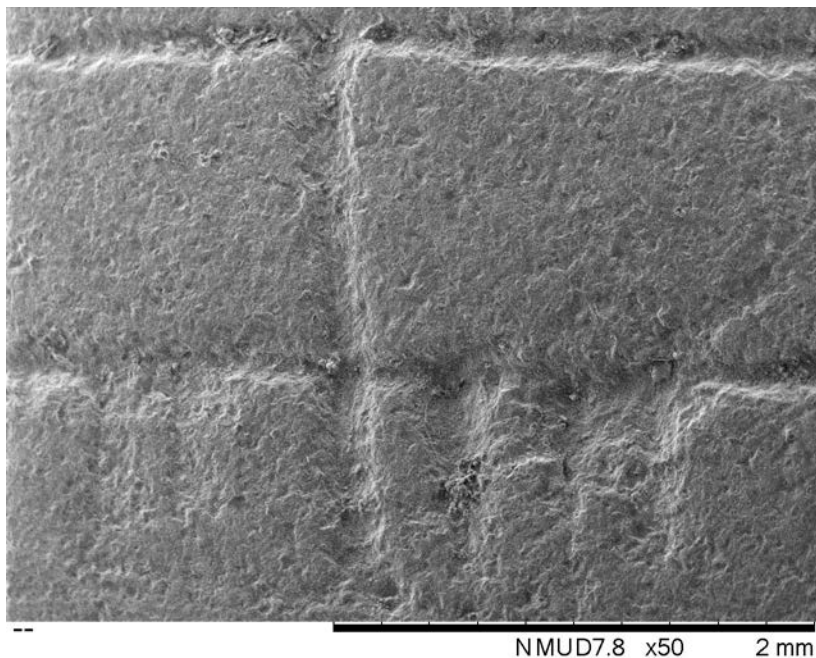
Figure 12.3. Finely engraved sub lines, branching from a long main line. SEM, secondary electron mode, 50 x.

12.2.1 Questions

The pendant was investigated for any microscopic trace residues which might indicate how it had been made and used, with a particular focus on whether coloured materials, such as ochre, charcoal, or resin had been used to emphasise the lines. Four residues were identified: brown staining, gold-coloured crystals, biological structures, and white crystals within the perforation hole. In addition, two soil samples from the same context as the pendant were tested as controls for contamination from the surrounding burial environment.

12.2.2 Methods

The pendant was first analysed using reflected light microscopy A series of z-stacked micrographs were taken for each microscopic residue. Each engraved line on the pendant was systematically examined and the locations of microscopic residues were mapped. Soil sample controls were prepared by direct mounting on glass slides with double sided tape and examined with reflected light microscopy. Located residues and the engraved lines were investigated with a VP-SEM (Hitachi TM3030Plus). SEM images were collected in secondary electron mode and backscattered electron mode and from 25x to 3000x magnification.

Residues were further analysed with Micro-Raman (HORIBA Jobin Yvon Xplora confocal Raman microscope). The 100x objective was used to record images of the exact locations of laser penetration on each residue. LabSpec 6 software was used to collect spectra and conduct peak analysis and OriginPro 2016 was used to plot data.

12.2.3 Results: brown stains

The depressed area within the engraved lines contained brown deposits (Figure 12.4). Micro-Raman analysis was conducted to identify the possible presence of crystalline phases in these areas that could be associated with the presence of pigments. However, the respective spectra showed no evidence for this. Rather, spectra collected from the brown deposit within the lines shows that the brown material is organic in nature (see sample spectrum in Figure 12.5) and it is very likely that this is peat from the burial environment which has become trapped within the grooves.
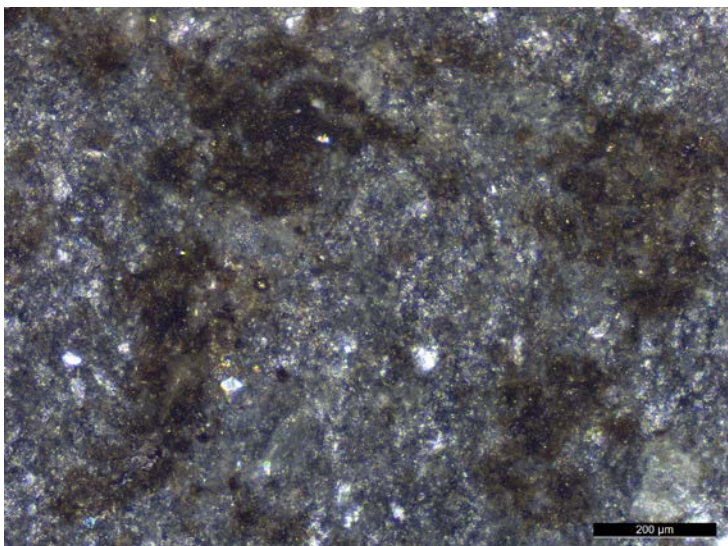
Figure 12.4. The engraved lines on the pendant can be seen microscopically as depressed grooves with brown infilling.
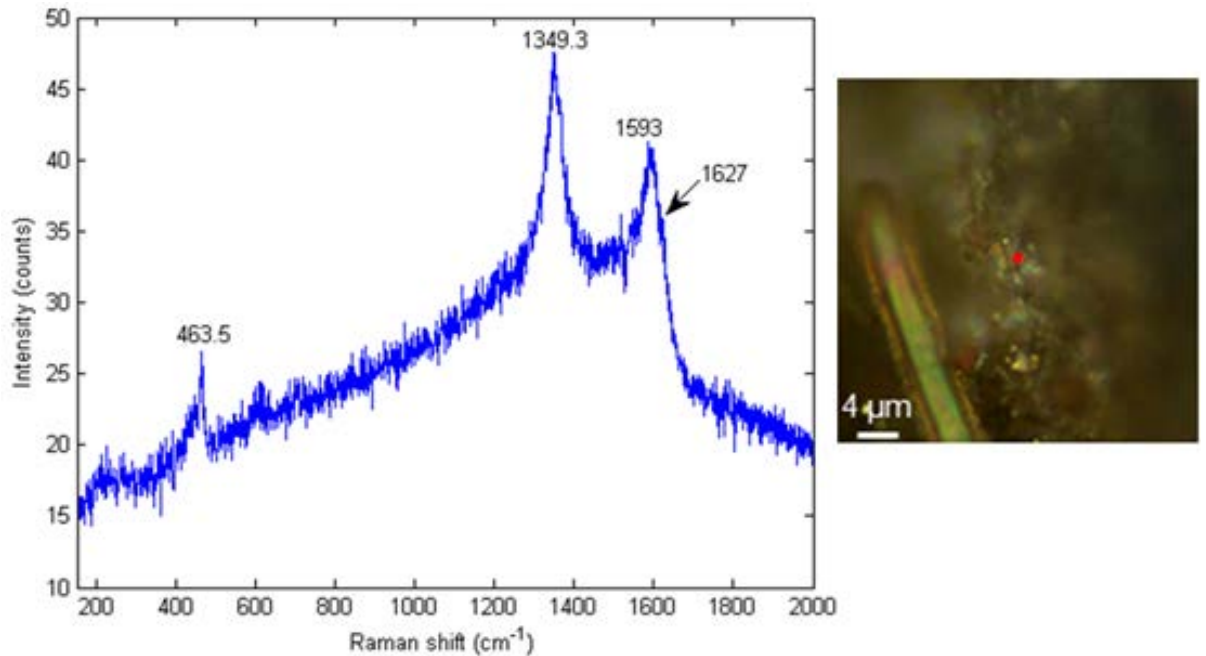
Figure 12.5. Micro-Raman spectra taken of brown deposit from within engraved line 11. Clear presence of organic material is indicated, likely peat. Image by Konstantinos Chatzipanagis.

12.2.4 Results: gold structures

A large number of gold structures were seen on the pendant during inspection with light microscopy. These structures were located on the surface of the stone, in the engraved lines, in the perforated hole, and also within a nick on the back of the pendant. Two types of gold structures were found: equilateral triangles (max diameter approximately 5.6 μm), and granular spherical crystals (max diameter approximately 40 μm) which were located on the non-engraved side of the pendant within the nick mark (Figures 12.6 and 12.7).
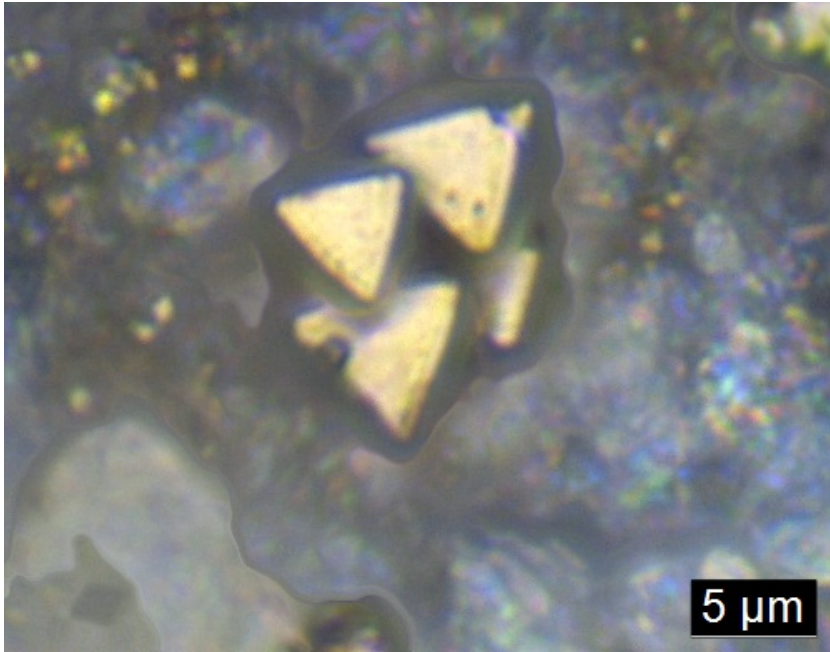
Figure 12.6. Gold structures with triangular faces.
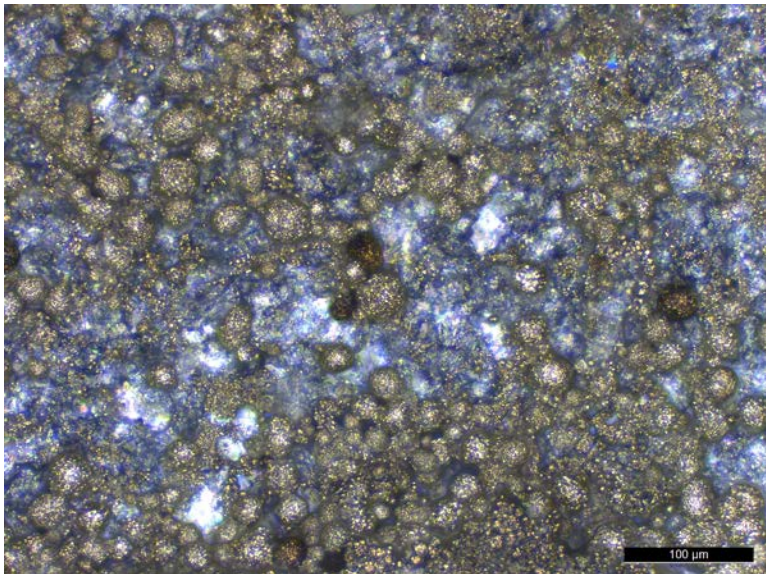
Figure 12.7. High density of gold granular spherical crystals located within the nick mark on the non-engraved side of the pendant.

It was noted that pyrite had previously been found at Star Carr, possibly used as firelighters (Clark 1954, p. 20) though none have been found within the museum archives (Milner et al., 2013a) for comparison. One hypothesis on discovering the pyrite on the shale pendant was that it might have been struck with iron pyrite. A reference piece from the nearby coast was pounded on a hard surface and the

resulting residue mounted on a slide for observation. It was clear that this produced angular pieces as opposed to the forms found on the pendant (Figure 12.8).
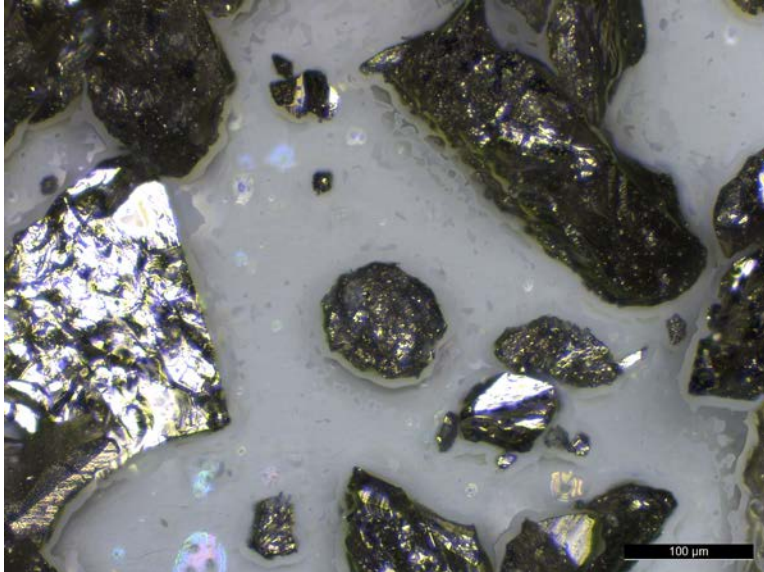
Figure 12.8. Gold angular pyrite from the reference collection.

The framboidal structures seen under the light microscope were confirmed under SEM as overall spheroid shapes with individual cubo-octahedral microcrystals (Figure 12.9) (Butler and Rickard, 2000; Popa et al., 2004), a typical crystal habit of pyrite. The Raman data obtained support the suggestion that the crystal structures with triangular faces are also pyrite. Figure 12.10 shows an example spectrum obtained from these samples.
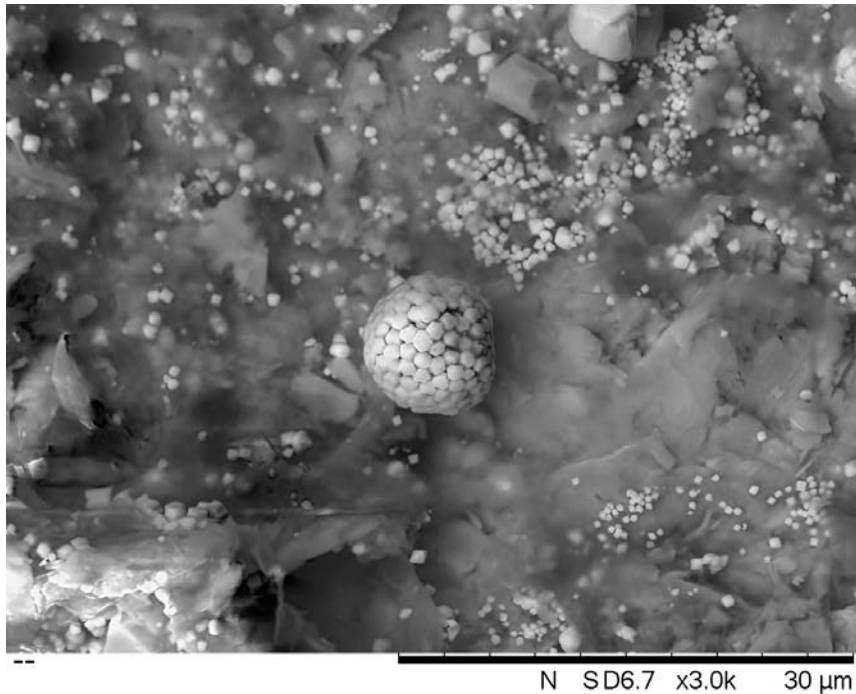
Figure 12.9. Close up of a pyrite framboid with cubo-octahedral microcrystals. SEM, backscattered electron mode.
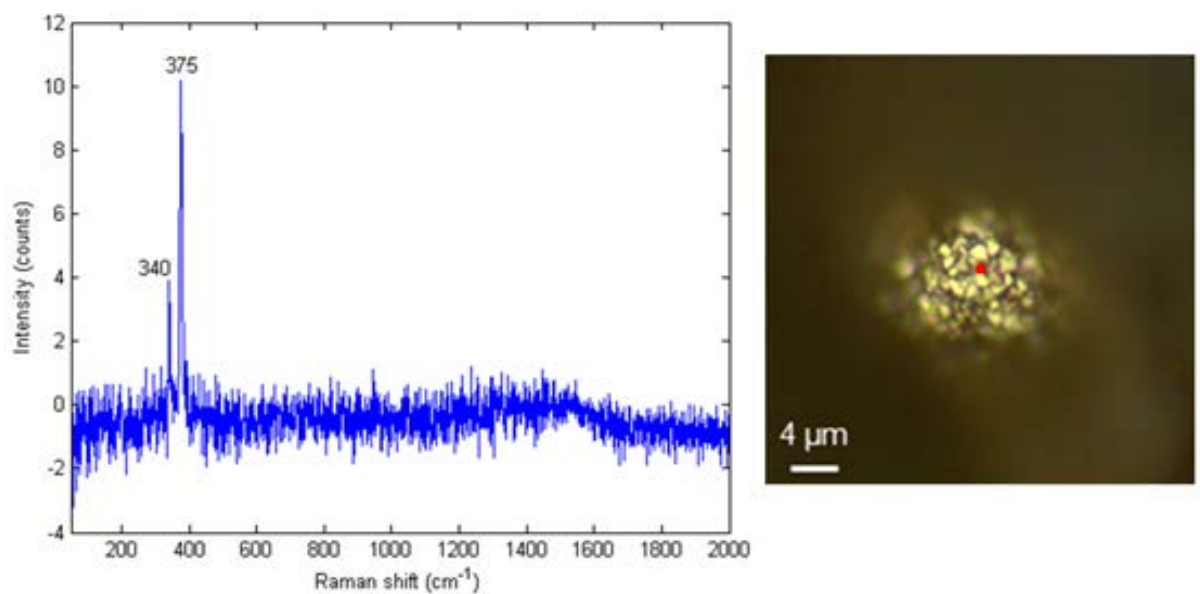
Figure 12.10. Micro-Raman spectrum collected from the red spot on the framboidal structure. Image by Konstantinos Chatzipanagis.

Anisotropic pyrite contains two intense peaks at ~342 cm^{-1} and 377 cm^{-1}, and one minor peak at 428 cm^{-1} (Mernagh and Trudu, 1993, p. 118). The ENS de Lyon Handbook of Minerals Raman Spectra ("ENS de Lyon Handbook of Minerals

351

Raman Spectra," 2000) quotes three Raman frequencies in anisotropic pyrite: two strong peaks at 340-342 and 375-377, as well as a minor peak at 428 cm^{-1} (Handbook of mineral spectra, ENS de Lyon). According to Demoisson (2008, p. 345), pure pyrite shows scattering signals at 340 and 377 cm^{-1}. Both Raman spectra from the triangular crystals and framboids are consistent with reference spectra for anisotropic pyrite. As can be seen in the spectrum (Figure 12.10), the first two prominent bands are present. The third low-intensity peak at 428 cm^{-1} noted by Mernagh and Trudu (1993) and ENS de Lyon ("ENS de Lyon Handbook of Minerals Raman Spectra," 2000) is not completely clear. The third peak may be present, but it is difficult to resolve due to signal to noise distortion in the spectrum.

It is clear that the gold-coloured crystals found on the pendant are natural pyrite, not an anthropogenic addition of pigment to the pendant. Pyrite (FeS_2) is known to form naturally in reducing environments which are rich in decomposing organic materials, such as peat bogs and wetlands (Jacobs and Vance, 2014, p. 25; López-Buendía et al., 2007). Recently, an analysis of macrobotanical remains across Star Carr found that pyrite formed within some of the charcoal, causing fragmentation (Radini et al., in press). Examples of pyrite framboids have also been found in several sites containing Holocene peat soils in England (Brown et al., 2010), and the Netherlands (Miedema et al., 1974). Triangular and framboid pyrite crystal formations were also observed within two soil samples taken from the context in which the pendant was found, demonstrating pyrite occurs in situ within deposits at Star Carr.

12.2.5 Results: biological structures

Several unidentified fragments of what appear to be lacustrine zooplanktonic microfauna such as fairy shrimp, copepods, cladocerans, ostracods, or insects, were identified within the engraved lines of the pendant (Figures 12.11-12.15). One of these fragments, mapped to location 1 within line 1 on the pendant surface (Figures 12.11 and 12.12) is probably the remains of a copepod, a very

small crustacean. No microfauna were found within the soil samples analysed, although specimens may have been bound up in soil aggregates and thus obscured.

Figure 12.11. Fragmentary microfaunal remains, likely part of a copepod. Location 1, line 1.
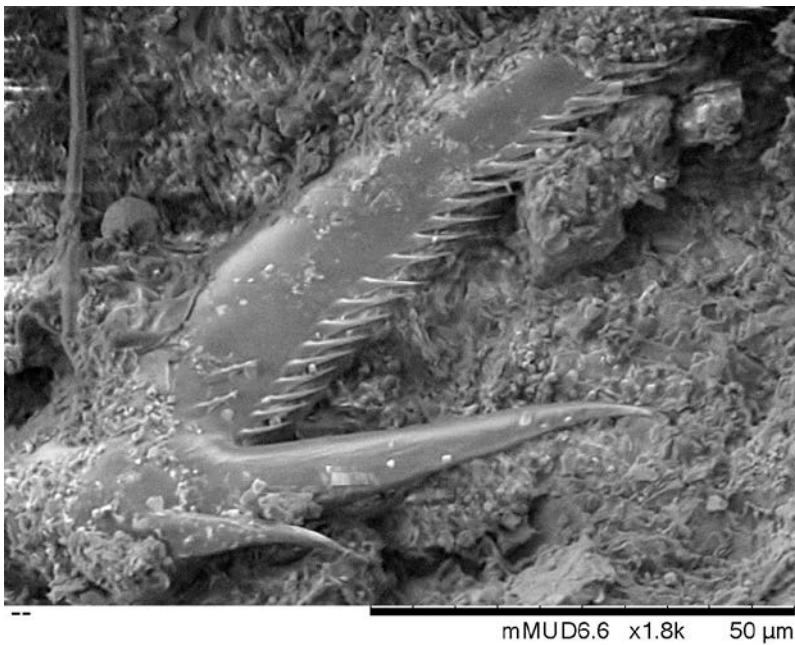
Figure 12.12. Fragmentary microfaunal remains, likely part of a copepod. Location 1, Line 1. SEM, secondary electron mode.
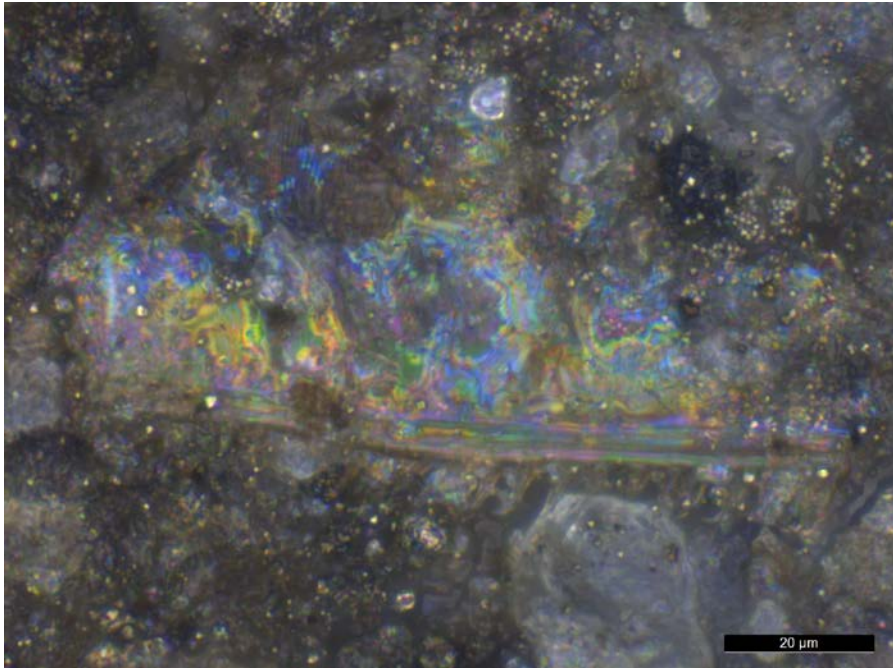
Figure 12.13. Unidentified biological structure, likely microfaunal remains. Loc 17, Line 1.
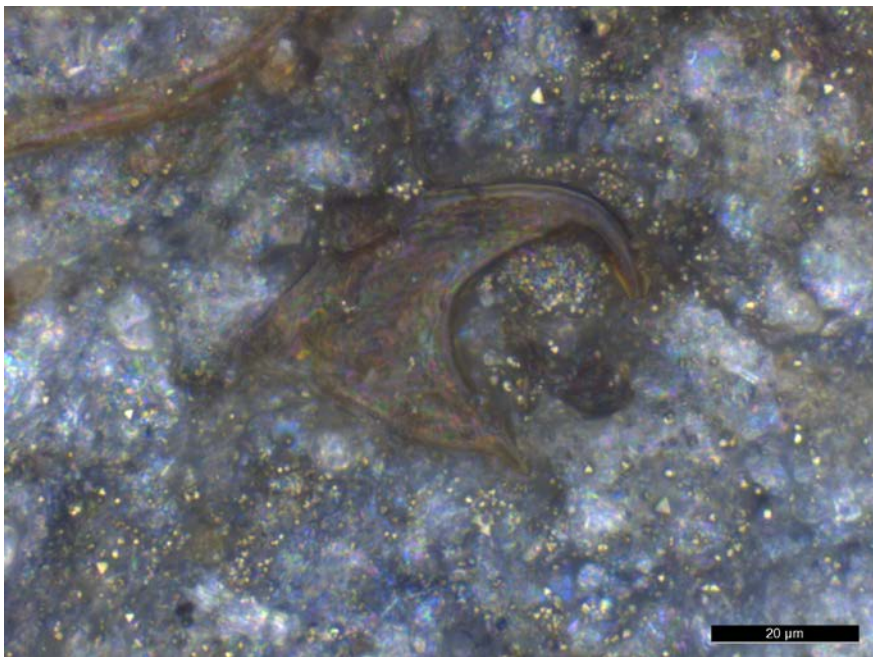
Figure 12.14. Perhaps a chitinous insect structure. Loc 32, Line 26.

There was some question as to whether the putative biological structures were perhaps mineral in origin. Thus, one of these structures (at location 9 on the pendant, see Figure 12.15) was investigated with Micro-Raman, taking spectra in three locations. The presence of carbon in all spectra confirmed the structure was organic (Figure 12.16).
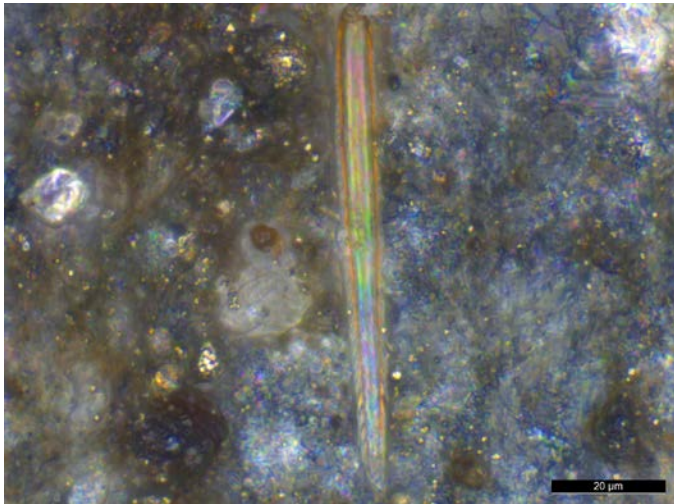
Figure 12.15. Loc 9. Biological structure, possibly a diatom. Micro-Raman analysis has showed the structure is carbon-rich, and thus likely organic. Loc 9, Line 11.
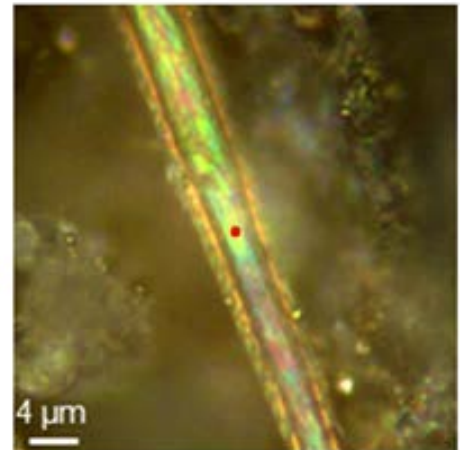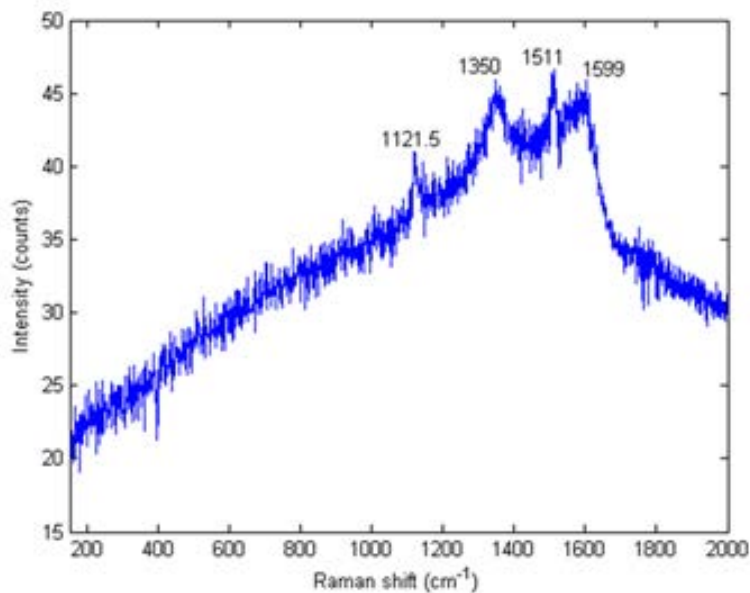
Figure 12.16. Raman spectrum collected on suspected microfaunal remain in one of three locations demonstrating that this is organic. Image by Konstantinos Chatzipanagis.

The conclusion from the Micro-Raman analysis is that these are biological structures but a number of specialists have been unable to identify what they are specifically. They are not related to the use or manufacture of the artefact and might have adhered within the engravings due to the pendant being placed within the lake edge deposits where such microfauna naturally occur.

12.2.6 Results: white crystals within the perforation

Clear and white translucent globular crystals were located within the perforation of the pendant. These crystals were not angular, but show what appears to be weathering as their edges are somewhat rounded (Figures 12.17 and 12.18).
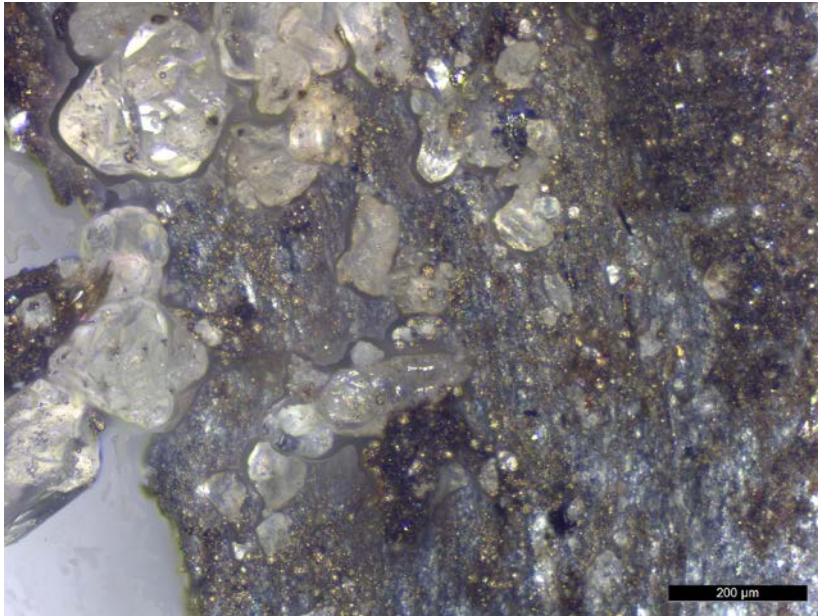
Figure 12.17. White crystals within the perforation of the pendant.

Figure 12.18. SEM image of the perforation and crystals within it (right), 200x magnification. Image by Andy Needham.

These crystals were investigated with Micro-Raman. Good quality spectra with minimal noise and fluorescence were able to be obtained on the smooth surface of one of these crystals (Figure 12.19). According to several sources, (Kingma and Hemley, 1994, p. 270; Krishnan, 1953, p. 382; Tekippe et al., 1973, p. 711), the most prominent Raman band in crystalline α-quartz (SiO_2) is located at 464-466 cm^{-1}, which is detected in spectrum at 464 cm^{-1}. Less intense bands related to the Raman assignment of α-quartz were also detected in our spectrum as indicated.
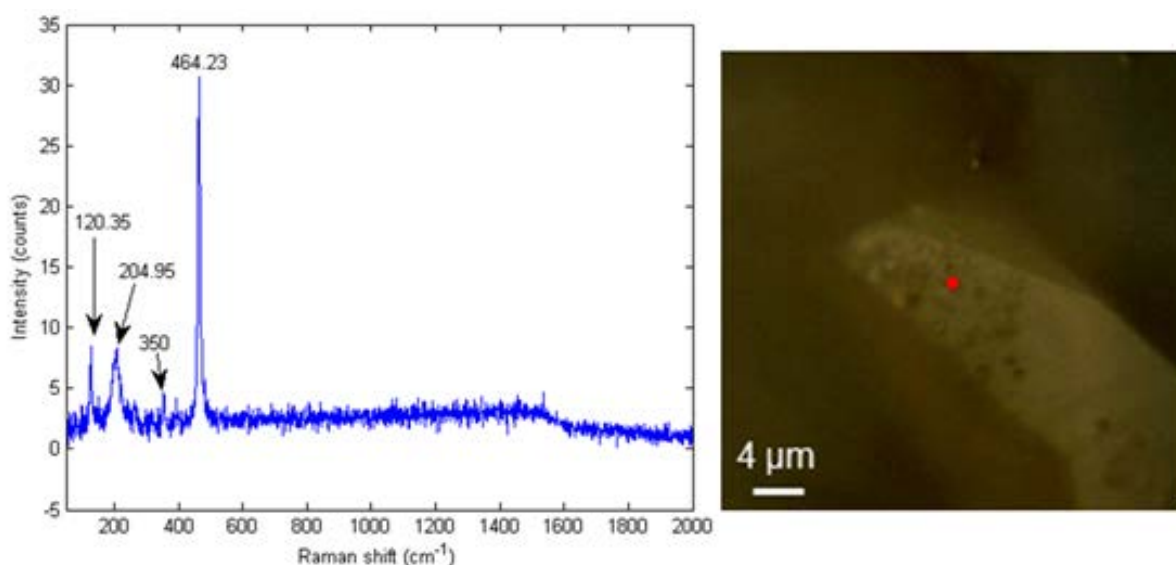
Figure 12.19. Micro-Raman spectrum collected from a crystal grain located within the perforation of the pendant. Image by Konstantinos Chatzipanagis.

The Raman spectra collected match closely with reference spectra for α-quartz. Clear crystals which were hexagonal in two dimensional outline were also noted in one of the soil samples, although no suggestion can be made as to their chemical nature. No quartz crystals similar in appearance to those found within the hole of the pendant were able to be located in the soil samples. However, it should be noted that only two soil samples from the context were analysed. Also, no soil samples that were in direct contact with the pendant were taken at the time of excavation, and thus it is possible that this surrounding area may have contained the same quartz sand as found within the hole.

The reason for the quartz in the perforation is not clear. One possibility is that the sand had been used in the manufacture of the hole; however, recent experiments on shale have shown that because shale is a soft stone it is very easy to create a hole with a flint tool, such as a with a stone drill and that sand would not be necessary.

The origin of this sand remains an enigma: quartz crystals were not found anywhere else on the pendant and not within the soil samples analysed. However, sand is present on the site associated with the lake marls, and in some cases within areas of the peat because it has washed down from the dry land. Therefore, it may be that fine sand has settled within the hole as part of the deposition process, perhaps even because the lake water has filtered through this hole.

12.3 Shale beads

12.3.1 Questions

The questions about the other shale beads examined were similar to those posed for the pendant. The beads were examined with high and low power reflected visible light microscopes to see if any engraved lines could be located on their surfaces, and if any pigments or suspension wear traces were preserved and could be detected.

12.3.2 Methods

Three shale beads were washed, handled and analysed in the same fashion as lithics for residue analysis, involving a rinse with a fine stream of ultrapure water, and handling with non-powdered nitrile gloves. Thereafter they were air dried and examined with low and high power reflected light microscopes and residues mapped on their surfaces, but no further chemical analyses were carried out.

For the four shale artefacts examined in this chapter, the 'front' face of the bead is designated as the side which exhibits the wider opening of the perforation – the dominantly worked side (Figure 12.20).
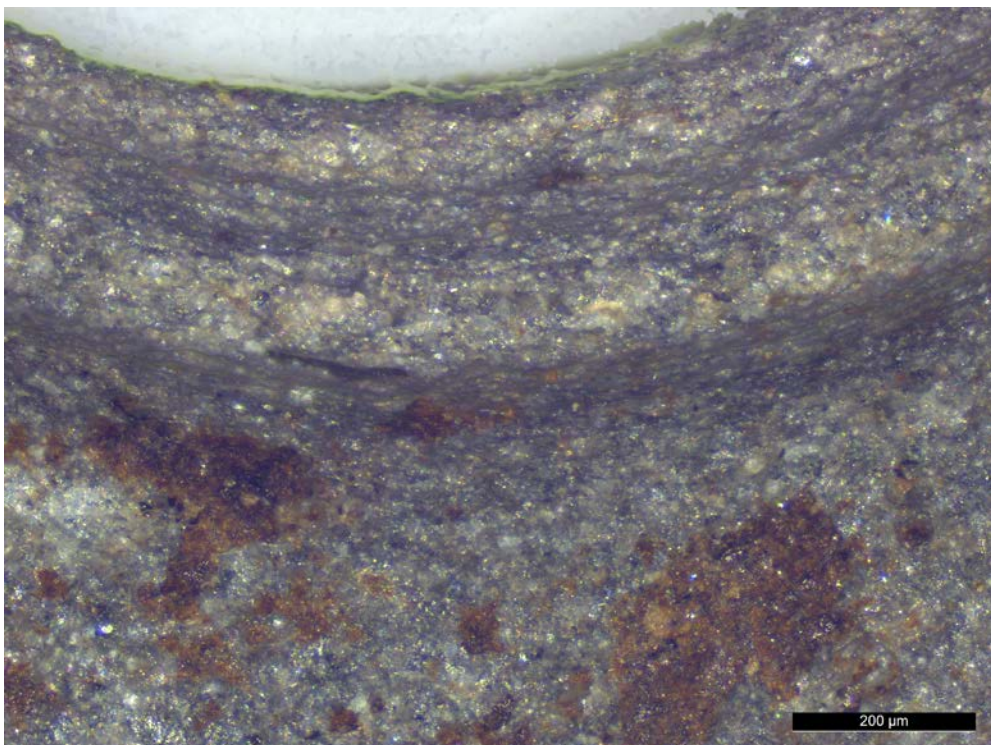
Figure 12.20. Detail of the perforation of bead 110671. Designation of the 'front' face of the bead is based on the gradual widening of the hole and the presence of grooves.

12.3.3 Results

Table 12.1 provides a summary of the findings from the pendant and three shale beads. Only the lines on the pendant could confidently be assigned to anthropogenic origin. The microscopically investigated lines on the beads were interpreted natural parts of the shale, for instance as a selectively weathered

area, or as white mineral inclusions in the shale. None of the lines on the beads displayed the same appearance as those engraved on the pendant, which exhibited fine grooves containing a mixed composition of organics infilling the grooves. The lack of engraving on the shale beads examined further emphasises the importance of the artwork documented on the pendant (Milner et al., 2016); it seems the pendant was a particularly special item to the person or people who made and used it at Star Carr.

Table 12.1. Comparison of microscopic finds on shale beads and pendant. The 'very small' designation means the iron oxide pieces encountered were less than 20µm in maximum diameter, and also found in very low abundance, with less than ten grains found per artefact.

Artefact	Context	Anthropogenic lines	Microfauna	Plant remains	Gypsum	Iron oxide	Pyrite
Pendant 115527	317	✓	✓	✓	✗	very small	✓
Bead 110671	310	✗	✗	✓	✗	✓	✗
Bead 113830	310	✗	✗	✓	✓	✓	✓
Bead Clark's	Backfill	✗	✗	✓	✓	very small	✓

12.3.3.1 Bead 110671

The author excavated this small oblong shale bead 110671 in situ, and collected it for residue analysis (Figure 12.21). During cleaning, sand was noted as part of the sediment within the perforation of the bead. White lines and two circles on the back face of the bead were observed. Microscopically, these white lines and circles were flush with the stone, not depressed as would be expected of grooves, and not displaying height above the stone, as would be expected of residue deposits (Figures 12.22 and 12.23). Thus, the white lines and circles were interpreted as part of the natural shale. No pyrite framboids or triangular crystals were found during microscopic observation. No evidence for suspension wear around the perforation and no anthropogenic residues were found. Plant

matter that appears to be infiltrated with orange/red iron oxide was located on the back of the bead. This plant matter is possibly the remains of reed leaves, based on the similarity of its cell wall structure with modern reedmace (*Typha latifolia*) and common reed (*Phragmites australis*) leaf residues in the microscopic reference collection, and originated from the peat deposits surrounding the artefact.

Figure 12.21. Shale bead 110671 found in situ at Star Carr.
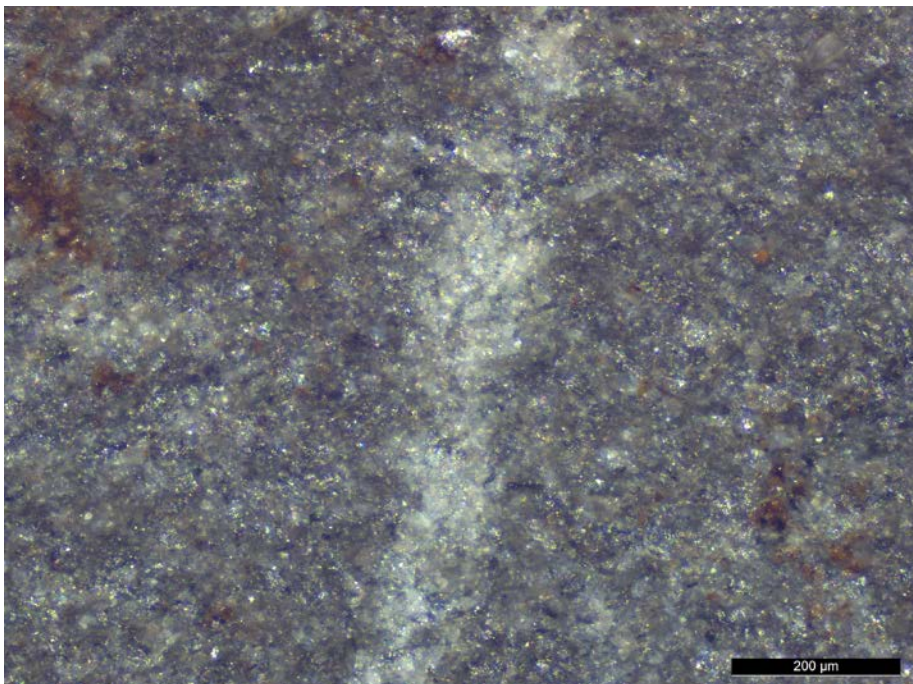
Figure 12.22. White line 2 within the shale on the front of the bead. This is part of the natural stone material.
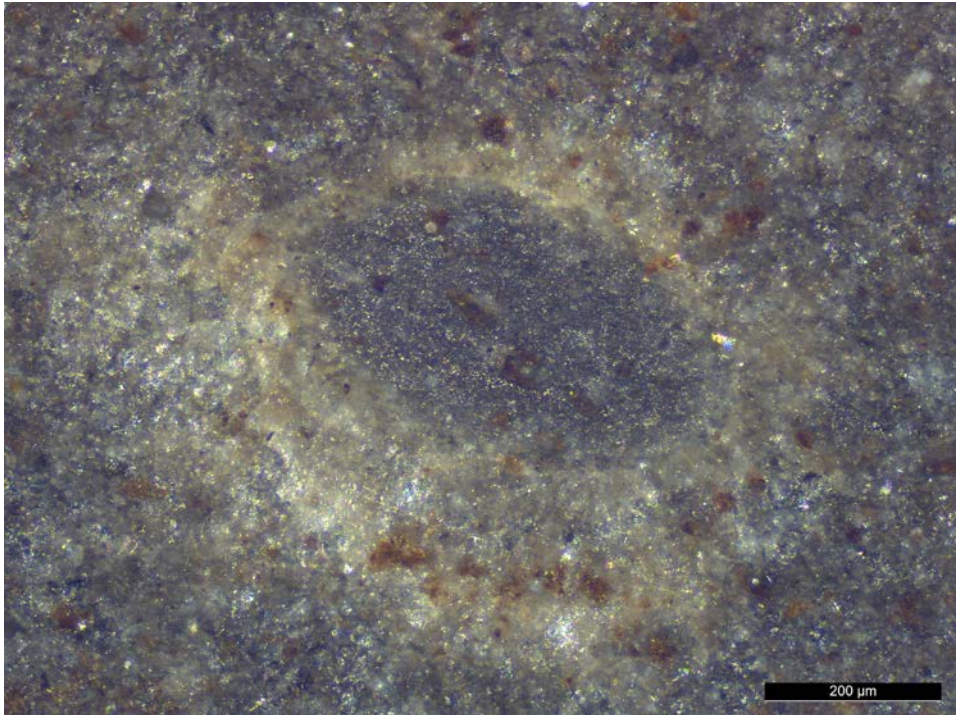
Figure 12.23. White material within the natural shale in a circular formation on the back of the bead.

12.3.3.2 Bead 113830

This small bead 113830 had a relatively wide groove on its front and back surfaces (Figure 12.24). When the bead was turned over and examined with a low-power stereoscope, it was apparent that the groove was continuous and encircling both sides of the bead and the groove was a natural weathering of material within the shale. No suspension wear could be located around the perforation.
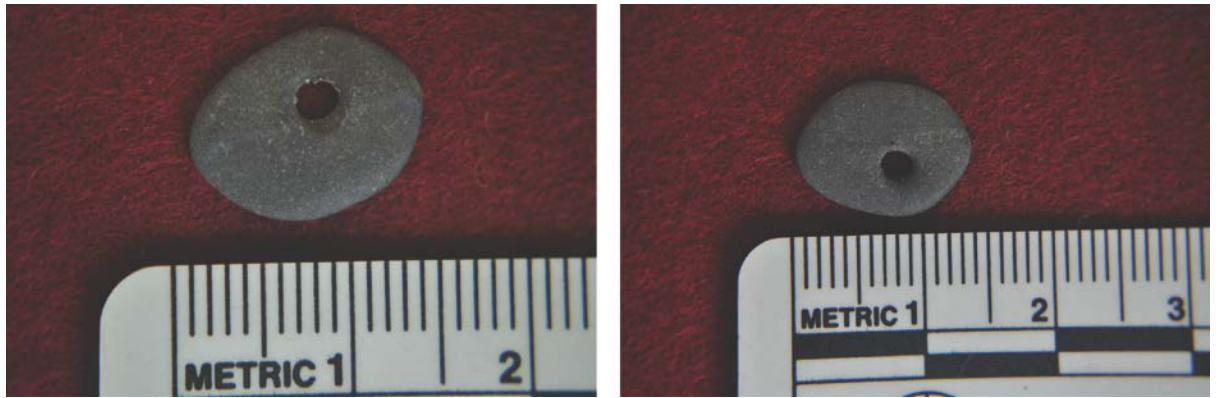
Figure 12.24. Bead 113830. Left image shows the front surface. Right image shows the back surface. Note groove visible on both sides of the bead.

Crystals suspected to be gypsum were visible macroscopically on both sides of the bead. During microscopic analysis, these crystals were clear and present in rosette shapes, a crystal habit expected of gypsum. At location 1, iron oxide deposits (Figure 12.25) were found and faint traces of what appeared to be elongate plant cell walls were also documented at this location. Framboidal and triangular pyrite microcrystals (Figure 12.26) were documented at location 3.
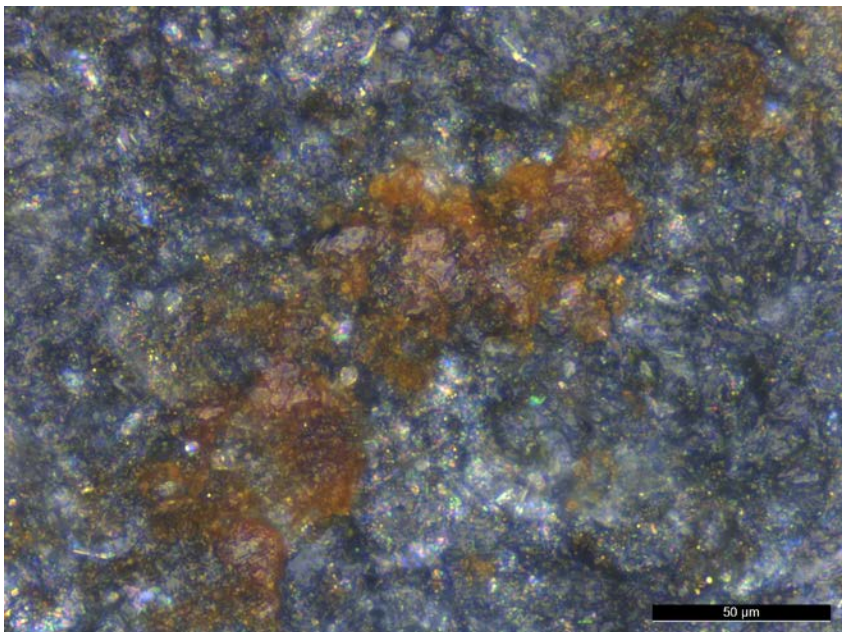
Figure 12.25. Iron oxide deposit, location 1, front of bead 113830.
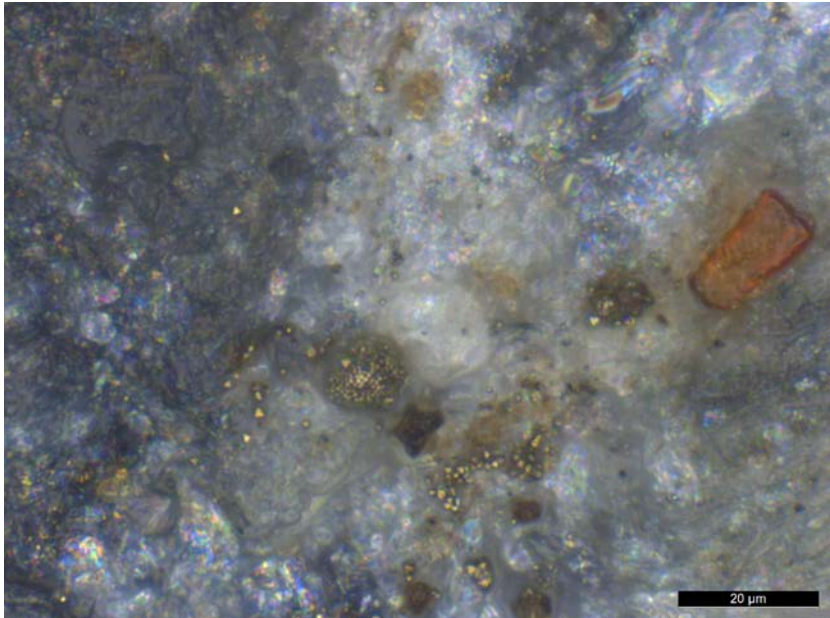
Figure 12.26. Pyrite framboids and triangular microcrystals, location 3, front of bead 113830.

12.3.3.3 Bead from Clark's backfill

This bead was discovered in the 2015 excavation season within the backfill from excavations by Grahame Clark in trench 34. Macroscopically, this bead appeared to have several parallel lines on the front side (Figure 12.27).

Figure 12.27. Clark's backfill bead. Left: the front surface. Right: the back surface.

Fine striations were seen on the front and back of Clark's backfill bead during microscopic investigation. Since the bead was previously excavated and mistakenly redeposited in the backfill of a trench, some scratches are expected on the surfaces of the bead due to physical disturbance. Another view, proposed by a usewear analyst (see Needham et al., in press), is that the fine lines on the

back surface of the bead are evidence of deliberate geometric cross hatching marks made during Mesolithic. However, the fine overlapping criss-cross striations observed on the back of the bead are only ~ 20 μm wide, contrasting with the width of anthropogenic engraved lines on the pendant that are ~ 300 μm. This author believes that since this bead comes from a secondary disturbed context, the most parsimonious explanation for the 'cross hatch' marks is that they are incidental, not anthropogenic, scratches (Figure 12.28).
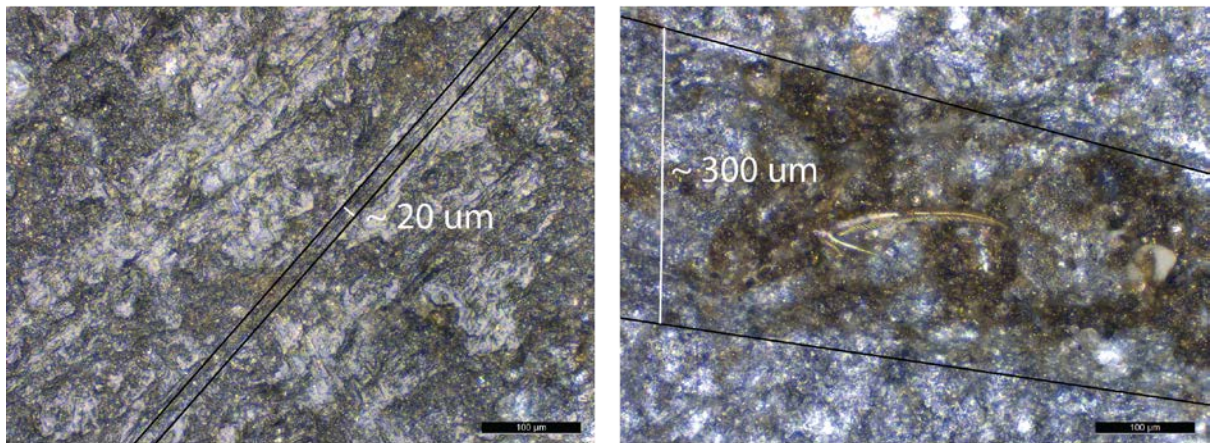
Figure 12.28. Comparison of lines on Clark's Backfill bead with lines on the pendant at the same magnification. Left: criss-cross striations on the back of Clark's backfill bead (location 10). Right: wide anthropogenic engraved line with brown sediment infilling (location 1).

Plant material residue, evidenced by the presence of rectangular cell walls (see Figure 12.29), was found at location 11 on the back of this bead. Plant cells of this morphology are likely to originate from epidermal tissue. Gypsum crystals in rosette 1 and lath habits (described in Chapter 9) were also found on the both the front and back of the bead (Figure 12.30). Pyrite framboids were also encountered on both sides of the bead.
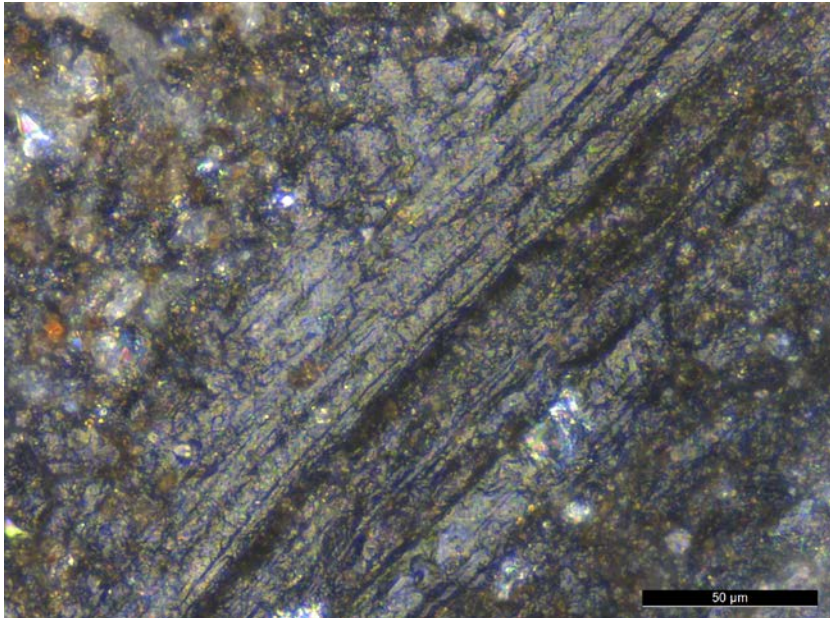
Figure 12.29. Elongate rectangular plant cell walls on the back of Clark's backfill bead (location 11).
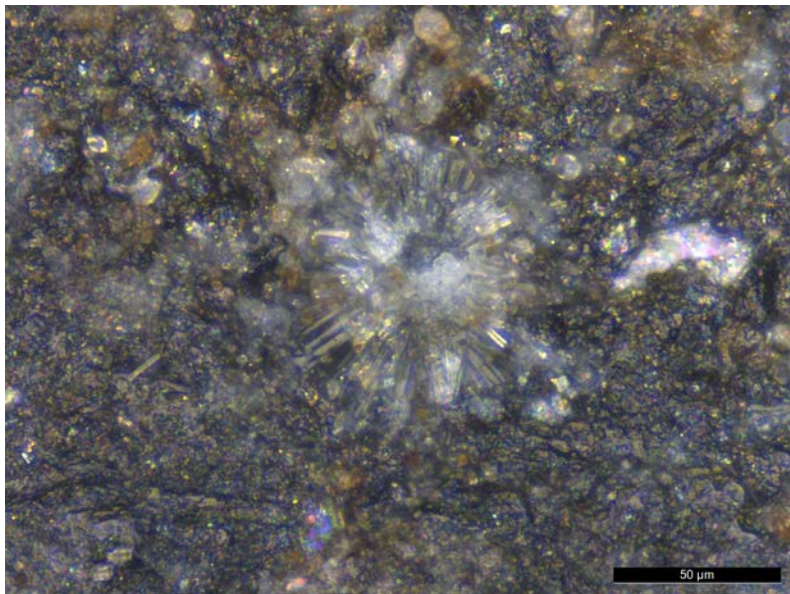
Figure 12.30. Gypsum rosette 1 and lath crystals on the back of Clark's backfill bead (location 12).

12.4 Discussion

None of the shale beads or the pendant examined showed clear wear traces around the perforation or elsewhere on their surfaces. Clark's backfill bead did exhibit some shiny areas, however, these were interpreted as plant remains from

the depositional environment, since elongate cell walls were embedded in the residues. Nevertheless, it is possible that people strung and wore the beads for short durations but too short to allow wear traces to develop.

The pendant and three beads collectively seem to display a patterned way of making the perforations, with preference for uniconical working of the shale. It was observed that one side of each bead exhibited a wider opening of the perforation that gradually flares out at an angle to the hole. The opposite face of each bead showed a smaller opening of the perforation that did not exhibit pronounced signs of circular groove production around the hole. This suggests that people manufacturing beads predominantly worked the shale from one side to create the hole.

12.5 Conclusion

The addition of the shale pendant and three more shale beads to the existing bead assemblage offer us a fascinating glimpse at life beyond simple subsistence at Star Carr. Beads can be used for personal ornamentation, talismans, ceremonies, special occasions, and as currency and grave goods. It has been suggested that fish teeth beads from Late Mesolithic burials at the site of Vlasac, Serbia (Cristiani et al., 2014b), and shell beads from Mesolithic El Mazo and El Toral III, Spain (Rigaud and Gutiérrez-Zugasti, 2016), were used for personal ornamentation and decoration, and it seems likely that the beads from Star Carr were also probably decorative items meant to be displayed and seen.

The residue analysis of the pendant showed that there were no discernable pigments present on any of the beads or the pendant. Only the lines on the pendant can be attributed with certainty to deliberate human actions and not natural taphonomic processes or inclusions within the shale. The lacustrine microfauna found within the engraved lines of the pendant supports the interpretation that people purposefully deposited the artefact into Paleolake Flixton.

CHAPTER 13 RESULTS: POTENTIAL RESINOUS RESIDUES

13.1 Introduction

Several dark-coloured potentially resinous deposits were identified during microscopic residue analysis of lithics from Star Carr. Because these deposits were amorphous and lacked visually diagnostic characteristics, their chemical compositions were investigated.

It was hypothesised that these residues were resinous, thus organic, and GC-MS offered a prospective method to test the microscopic observations. More specifically, it was thought likely that the residues would be birch bark tar, since previous GC-MS results on a lump of resin from a microlith and five 'resin cakes' from Star Carr (Chapter 3) clearly demonstrate the presence of manufactured birch bark tar (Aveling and Heron, 1998). Aveling and Heron's (1998) chromatograms show large and well-defined peaks to which compound identity was ascribed based on similarity with modern reference birch bark tar samples and ancient bark samples. The findings are also compelling because a suite of compounds unique to birch bark were identified together. In addition to Aveling and Heron's (1998) study, birch bark tar has been identified at other Mesolithic sites in Northern Europe by simple visual inspection (Bang-Andersen, 1989; Bokelmann et al., 1981; Gramsch and Kloss, 1989), and by GC-MS and direct temperature resolved mass spectrometry (DTMS) (Aveling, 1998; 2000, 1999; Roberts et al., 1998; Van Gijn and Boon, 2006). Thus, the use of birch bark tar appears to be a relatively common phenomenon during the Mesolithic in Northern Europe.

Solvent extraction and gas chromatography-mass spectrometry (GC-MS) was conducted since this technique provides good resolution of individual compounds present in a sample and has been successfully employed to identify archaeological resins (see review in Chapter 2).

13.2 Methods

Twelve stone tools of the microscopically analysed assemblage (n=138) that contained amorphous black residues were selected for further examination with GC-MS. The GC-MS procedure used to chemically characterise residues present on the flint tools is detailed in Accompanying Material 4.

All tool samples, sediment samples, and reference resins were solvent extracted with dichloromethane/methanol (DCM:MeOH, 2:1 v/v) in an ultrasonic bath and then analysed with GC-MS. Compounds represented by mass spectra were identified by comparison with the NIST Library, published literature, and reference resins. Each tool extract total gas chromatogram was analysed first to see if it contained any potentially resinous residues. If it did, the sediment sample associated with the tool was tested as well and compared to the tool extract. Table 13.1 lists all samples from which extracts were obtained and GC-MS performed.

Table 13.1. Sampled archaeological stone tools, negative controls, and sediment samples.

Number	Type	Sample type	Context	Context description
94554	Microlith fragment	Tool with residues	308	Dryland clay grey and orange mottled till
95828	Burin	Tool with residues	310	Wood peat
94362	Flake	Tool with residues	310	Wood peat
108205	Burin	Tool with residues	312	Reed peat with roundwood
108373	Blade	Tool with residues	337	Fill of [336]
108397	Microlith	Tool with residues	325	Darker siltier feature/not structure, Upper Fill of [330]
109649	Blade	Tool with residues	317	Detrital muds underneath peat
109691	Microlith	Tool with residues	415	Small sandy lens in G/F29/30, tree-bowl
109724	Microlith	Tool with residues	466	Possible fill of feature [467] in F25, fill of bioturbation
110657	Bladelet	Tool with residues	301	Oxidised desiccated peat below overburden
111490	Bladelet	Tool with residues	310	Wood peat
113623	Microlith	Tool with residues	310	Wood peat
93593	Blade	Negative control	308	Dryland clay grey and orange mottled till
98858	Bladelet	Negative control	317	Detrital muds underneath peat
99276	Bladelet	Negative control	312	Reed peat with roundwood
99851	Blade fragment	Negative control	312	Reed peat with roundwood
108206	Scraper	Negative control	310	Wood peat
108205_S	–	Sediment sample	312	Reed peat with roundwood
108373_S	–	Sediment sample	337	Fill of [336]
108397_S	–	Sediment sample	325	Darker siltier feature/not structure, Upper Fill of [330]
109649_S	–	Sediment sample	317	Detrital muds underneath peat
109691_S	–	Sediment sample	415	Small sandy lens in G/F29/30, tree-bowl
109724_S	–	Sediment sample	466	Possible fill of feature [467] in F25, fill of bioturbation
110657_S	–	Sediment sample	301	Oxidised desiccated peat below overburden
111490_S	–	Sediment sample	310	Wood peat
113623_S	–	Sediment sample	310	Wood peat

13.2.1 Extraction

Previous GC-MS studies on lithics and other artefacts have removed large, visible deposits of the proposed resinous material to be characterised. However, during recent excavations led by Nicky Milner and examination of every piece of flint, no signs of residues were visible at the macroscopic level and no further 'resin cakes' like Clark unearthed (1954) were found. Thus, only microscopic quantities of dark-coloured amorphous residues were available for chemical analysis. Theoretically, it was thought possible to extract and characterise lipids from microscopic amounts of residue on stone tools. Since GC-MS works on a molecular level and is a sensitive technique, it should be able to detect minute quantities of only a few hundred ng of lipids in an archaeological sample, if preserved. However, it was not known if these residues were indeed organic, or if GC-MS would be to locate characteristic compounds within such minute samples. Successful and conclusive results of GC-MS analysis to date have only been obtained on stone tools which contain macroscopically visible deposits.

Application of GC-MS analysis to microscopic lithic residues presented a challenge in terms of sample recovery. Specific locations on each lithic containing potential resinous residues could not be sampled by scalpel, drilling, or swabbing, because they were not practical to extract at a microscopic resolution. To ensure the target residues were removed, the lithics were completely immersed in solvent and sonicated. Additionally, unlike pottery, the non-porous nature of flint precludes the recovery of an internal sample that is protected from the surrounding burial environment. Considering this, the sediment surrounding each lithic was tested and compared to determine if chemical markers on the lithic were also present in the sample of the associated sediment.

13.2.2 Sediment samples

The sediment samples were collected directly underneath all tools containing pine compounds were also tested. In addition, a negative archaeological control group of five stone tools that contained no potentially resinous microscopic residues were tested. Blank controls to test for contamination were included as standard protocol during preparation of samples and GC-MS.

13.2.3 Reference resins

Modern reference resins were prepared for comparison with the chemical profiles of the archaeological samples. Reference extracts were prepared separately to avoid any potential cross contamination with artefacts. Potential sources of resin present in Britain during the Mesolithic were chosen as comparative references (listed in Table 13.2) based on 1) the previous finding of birch bark tar (*Betula* sp.) at Star Carr (Aveling and Heron, 1998) and other Mesolithic sites (Chapter 3), and 2) palaeoecological information that indicates that the lake-edge and lake centre pollen sequences from Star Carr that indicate that birch, Scots pine (*Pinus sylvestris*), and Common juniper (*Juniperus communis*) (rare pollen type) were present in the area during occupation (Dark, 1998a, pp. 128, 135, 144, 1998b, pp. 166, 171). This agrees with the wider European fossil pollen record that shows the Mesolithic presence of birch and two Coniferae: Scots pine and Common juniper (Huntley and Birks, 1983).

Table 13.2. Reference resins.

Sample	Description	Oxygen condition	Age	Dilution
Birch bark (*Betula* sp.)	charred, micocharcoal and resinous deposits	aerobic	1.5 years	no dilution
Birch bark (*Betula* sp.)	tar made with an aceramic method, contains no additives	anaerobic	1.5 years	no dilution
Birch bark (*Betula* sp.)	tar made with a vessel to catch the distilled resin, contains animal fat additive	anaerobic	1.5 years	no dilution
Scots pine (*Pinus sylvestris*)	fresh resin	aerobic	1 years	dilution factor 20x
Scots pine (*Pinus sylvestris*)	fresh resin	aerobic	3 days	no dilution
Scots pine (*Pinus sylvestris*)	fresh resin heated 3h at 70°C in sterile glass hatch tube	aerobic	3 days	no dilution

Common juniper (*Juniperus communis*)	fresh resin		aerobic	3 days	no dilution

Three types of birch bark tar (aceramic method, no additives; vessel for collection, with animal fat additive; charred birch bark) were prepared. The aceramic method produced very little tar, barely visible on one end of the birch bark roll placed in an anaerobic environment. The method involving a vessel to collect resin was also carried out in anaerobic conditions (Figure 13.1), and animal fat was added to improve consistency. Much greater quantities were able to be collected with the vessel method. The third way birch bark tar was obtained was simply by charring a piece of birch bark in a fire and then rubbing the burned end on flint. Any tar produced was not macroscopically on the surface of the flint, but what appeared to be tar containing plant fragments and ash were visible microscopically (Figure 13.2). All three birch preparations were applied to freshly knapped flint prior to extraction. Birch sap, but not the viscous tar used as an adhesive, will exude from the tree when the bark is scarred or wounded.

Figure 13.1. Making birch bark tar with airtight vessels experimentally at Star Carr.
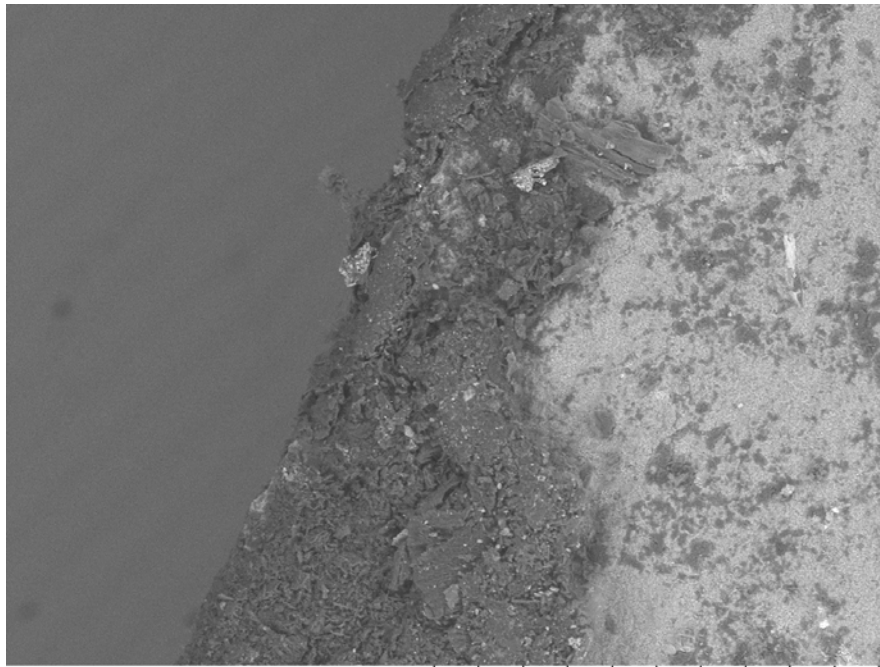
BirchCharr0008   2015/04/29   L   x180   500 um

LacCore, UMN, funded by NSF

Figure 13.2. Experimental potential birch bark tar containing plant fragments and ash on flint substrate, SEM. Birch bark set on fire then rubbed on flint.

Three preparations of reference Scots pine resin were made. During resin collection and GC-MS extraction, Scots pine was particularly resinous. Light yellow resin was observed copiously exuding from wounds on the tree bark and also exuding from branches removed from the tree, and it was easy to collect (Figure 13.3). Scots pine it is known to be highly resinous, second only to the European Larch (*Larix decidua*) in resin production across Europe (Godet and Mitchell, 1988, p. 60).

Figure 13.3. Fresh resin exuding from a Scots pine tree in York, UK.

Pinus spp. trees exude resin from the bark when injured as a defence mechanism against attack from pathogens such as insects, fungi, and bacteria. The pitching out process not only kills the attacking agent, it also flushes and seals the wound (Trapp and Croteau, 2001, p. 690). Monoterpene, sesquiterpene, and diterpene compounds found in the resin provide antibacterial and antifungal activity (Savluchinske-Feio et al., 2006, p. 433; Vilanova et al., 2014, p. 1). Resin exudation can also be promoted by mechanical scarification of the sapwood by incising or boring into the bark of the living tree (tapping) (Gale and Cutler, 2000, p. 391), possibly with a stone tool.

The common juniper tree sampled did not appear resinous or juicy, in contrast to the Scots pine. No resin was seen exuding from the ends of juniper branches, but a tiny shiny red resin deposit was noted that had infilled a wound on the branch (Figure 13.4); this was sampled.

Figure 13.4. Common juniper branch with only miniscule amounts of red resin exuding.

13.3 Results

13.3.1 Introduction

Nine of the twelve tools (mostly blades) with black amorphous residues were found to contain compounds consistent with Pinaceae (pine family) tree resin (Figure 13.). The five tools in the negative control group that contained no microscopic potentially resinous residues were negative for pine compounds. The black amorphous residues found on tools did not exhibit a regular pattern of occurrence on tool surfaces. Rather, these deposits were found in several

locations on tools, including places not expected to be associated with hafting such as the distal ends and middle areas of tools (Figure 13.5, Table 13.4).
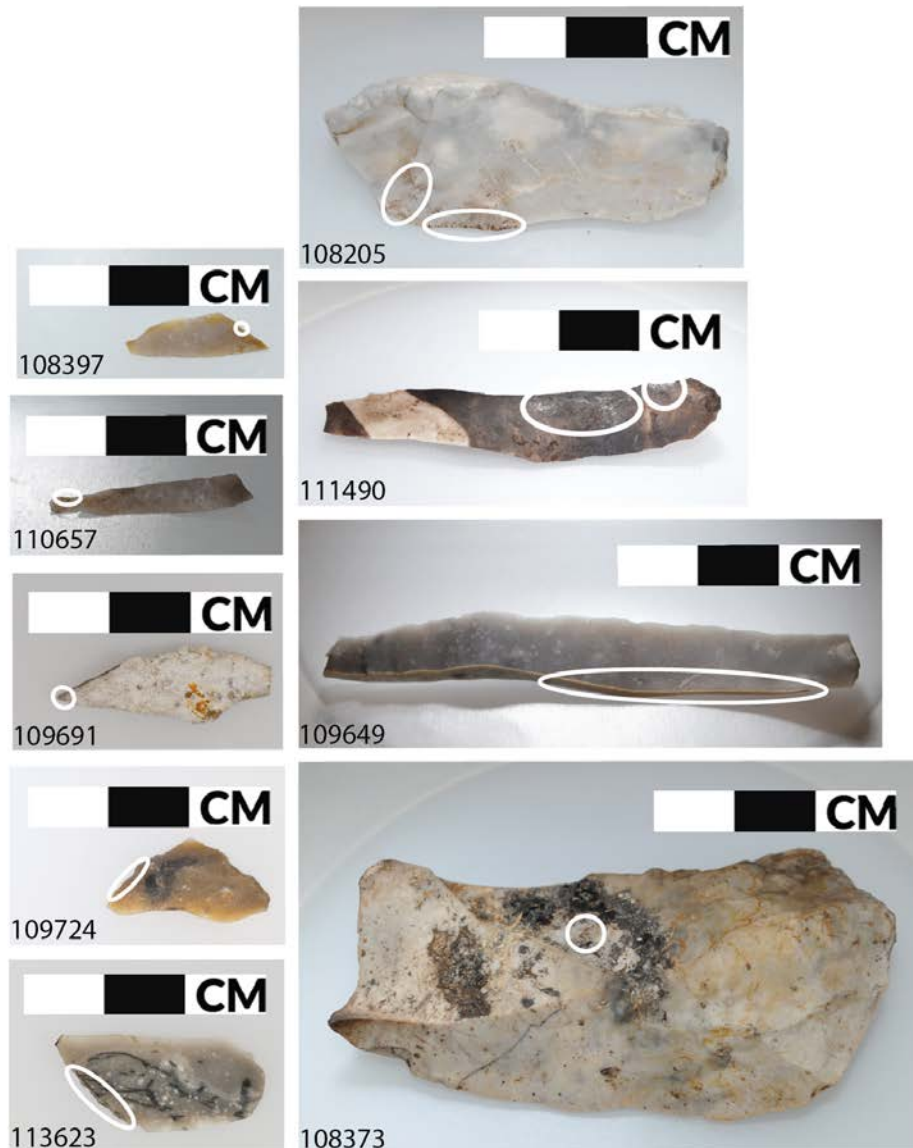
Figure 13.5. Macroscopic images showing the location of black residues found on nine flint tools. The residue extracts from these tools contained compounds consistent with pine resin.

The nine tools containing compounds consistent with pine resin were recovered from both waterlogged and dry areas of Star Carr (Figure 13.6). The tools come from a number of different contexts and features potentially spanning the occupation of the site. There is no apparent clustering spatially of the tools on the site, but three tools were associated with structures on the dry land.
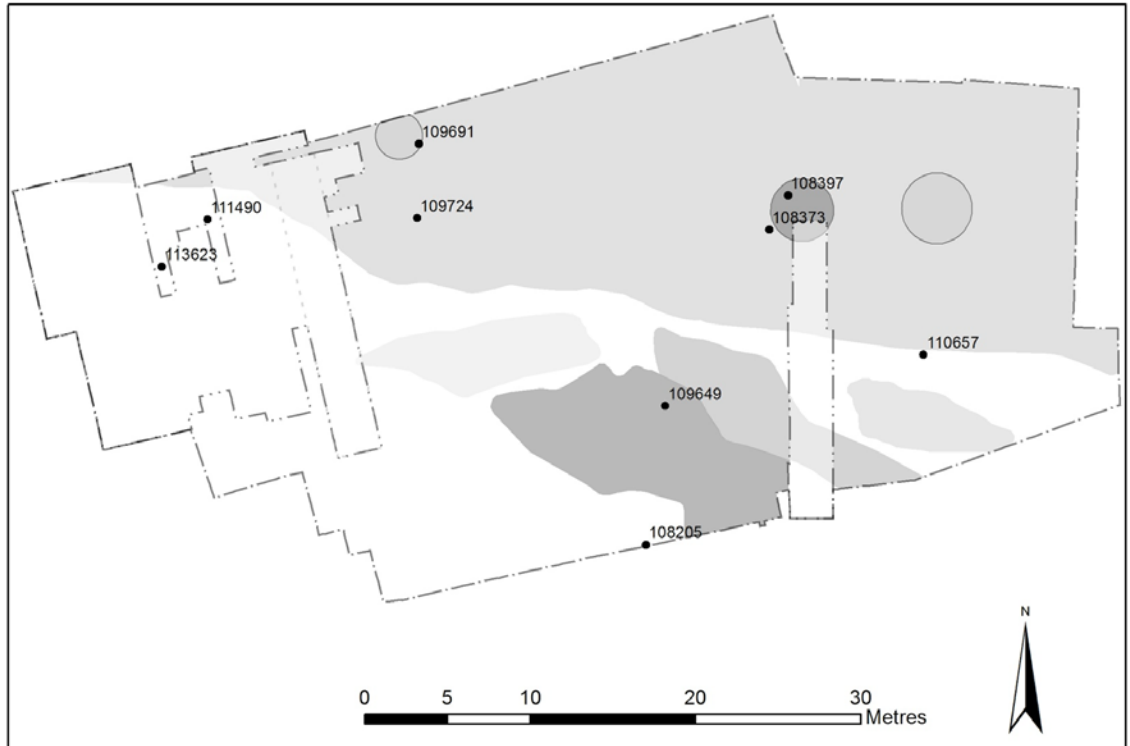
Figure 13.6. Location of nine lithics which contained pine compounds in their residue extracts. Circles represent housing structures. Image by Becky Knight.

13.3.2 Overview of compounds found

A range of organic compounds were found, including saturated fatty acids and dicarboxylic acids (adipic acid, azelaic acid). Some of the saturated fatty acids (e.g. C14:0 myristic acid, also called tetradecanoic acid, C16:0 palmitic acid, also called hexadecanoic acid, C18:0 stearic acid, also called octadecanoic acid) were found in both the tool samples and the sediments. This suggests some compounds from the sediment transfer to the stone surfaces during burial and are not removed by washing with water.

Nine of the tool samples contained products related to common natural fatty acids found in plants and animals, with palmitic acid (C16:0, hexadecanoic acid) at about 18.16 min and stearic acid (C18:0, octadecanoic acid) at about 19.94 min,

found in tool extract samples from 108205, 108373, 108397, 109649, 109691, 109724, 110657, 111490, and 113623. These two lipids were present in six of nine sediment samples, suggesting that plant lipids are contamination from the sediment and are not part of the archaeological residues.

13.3.3 Diterpenoid compounds associated with pine resin

Three altered diterpenoid products of abietic acid were able to be located, all eluting between 20-23 min: dehydro-7-dehydroabietic acid (Dehydro-7-DHA), dehydroabietic acid (DHA), and 7-oxo-dehydroabietic acid (7-oxo-DHA). Table 13.3 lists the diterpenoid compounds found in the lithic residue samples and their characteristic ions.

Table 13.3. Diterpenoid compounds found in extracts from nine Star Car lithics. TMS stands for trimethylsilyl ester.

Biomolecular constituent	tR (min)	Characteristic ions (*m/z*)
Dehydro-7-dehydroabietic acid, TMS	20.904	237, 252, 195, 238, 197, 370, 167, 181, 253, 209
Dehydroabietic acid, TMS	21.097	239, 73, 240, 43, 171, 75, 173, 357, 41, 255
7-oxo-dehydroabietic acid, TMS	22.733	253, 268, 73, 386, 187, 269, 178, 254, 75, 371

Five tools contained three diterpenoid compounds (Dehydro-7-DHA, DHA, and 7-oxo-DHA), and a further four tools contained two diterpenoids (Dehydro-7-DHA and DHA) (Table 13.4). These altered diterpene resin acids have an abietane skeleton and have been reported in archaeological and historical samples as markers indicative of Pinaceae resin (Andreotti et al., 2006; Colombini et al., 2005; Evershed et al., 1985; Fox et al., 1995; Helwig et al., 2008; Hjulström et al., 2006; Mills and White, 1977, 2012; Pastorova et al., 1997; Pérez-Arantegui et al., 2009; Pollard and Heron, 2008; Proefke and Rinehart, 1992; Regert, 2004; Regert et al., 2005, 2003b; Regert and Rolando, 2002; Richardin, 1996;

Robinson et al., 1987; Scalarone et al., 2002; Scalarone and Chiantore, 2009; van den Berg et al., 2000).

The first pine resin alteration marker identified was DHA. DHA was located at retention times of 21.097 and 21.089 min and was found in the extracts of nine flint tools. The characteristic base fragment ion found in the mass spectrum of trimethylsilylated DHA is *m/z* 239. None of the sediment samples taken directly underneath each of these nine tools contained DHA. In the tool extracts examined, DHA was present as a shoulder of another larger chromatographic peak (adipic acid, also known as hexanedioic acid).

The second pine resin compound found was 7-oxo-DHA, which is an oxidation marker of abietic acid (Regert et al., 2005, p. 131). 7-oxo-DHA was located at retention times of 22.733 and 22.741 min and was found in the extracts of five flint tools. The mass spectrum of trimethylsilylated 7-oxo-DHA has a characteristic base peak of 268, followed in relative abundance by an ion peak of *m/z* 253.

The third oxidation product of abietic acid found was dehydro-7-DHA, located at retention times of 20.896 and 20.904 min. Dehydro-7-DHA was found in the extracts of nine flint tools, identified based on the correspondence with the mass spectrum published by Regert (2004, p. 251). The characteristic base peak found in the mass spectrum of trimethylsilylated dehydro-7-DHA is *m/z* 237.

Table 13.4. Compounds found on each tool.

Number	Tool type	Context	Microscopic description of residues	Residue location	Residue in a possible hafting location	Pine resin compounds
108205	Burin	312 reed peat with roundwood	black shiny deposits with bubbly smooth appearance	dorsal left mid edge and dorsal centre distal, slightly left	✗	DHA, Dehydro-7-DHA, 7-oxo-DHA
108373	Blade	337 fill of 336	shiny black deposit associated with microcharcoal, unburnt wood fragments, and sediment adhering	dorsal surface, centre	✗	DHA, Dehydro-7-DHA, 7-oxo-DHA

108397	Microlith	325 feature	black amorphous deposit	ventral proximal mid edge	✗	DHA, Dehydro-7-DHA, 7-oxo-DHA
109649	Blade	317 detrital muds	black granular deposits	on cortex surface, ventral left proximal edge. Same deposit type also along reverse edge of tool, dorsal right side, mid edge	✓	DHA, Dehydro-7-DHA, 7-oxo-DHA
109691	Microlith	415 sandy lens	only residue located is possible microcharcoal	ventral distal tip	✗	DHA, Dehydro-7-DHA
109724	Microlith	466 possible fill of feature 467	only residue located is microcharcoal	ventral left curved edge.Same deposit type also along reverse edge of tool, dorsal right edge	✓	DHA, Dehydro-7-DHA
110657	Bladelet	301 desiccated peat	Q black resinous deposit associated with white crystalline material (Q bone or Q mineral?)	ventral right distal edge	✓	DHA, Dehydro-7-DHA, 7-oxo-DHA
111490	Bladelet	310 wood peat	black shiny material which appears cracked and platelike	large areas of the ventral surface covered	✗	DHA, Dehydro-7-DHA
113623	Microlith	310 wood peat	adhering black plant material, associated with iron oxide	ventral left edge	✓	DHA, Dehydro-7-DHA
94362	Flake	310 wood peat	bright sparkly black deposits containing potential striations (Q tar, Q plant remains?)	dorsal right mid and proximal edges	✗	–
94554	Blade fragment	308 mottled clay till	black spots, Q tar. Translucent residue along edge, contains black specks, Q charcoal frags?	ventral distal edge	✗	–
95828	Burin	310 wood peat	black spots, Q tar, Q charcoal. With polariser and analyser, bright white parts of the residue turn black	dorsal right proximal edge	✗	–
93593 negative control	Blade	308 mottled clay till	No potentially resinous residues	N/A	N/A	–
98858 negative control	Bladelet	317 detrital muds	No potentially resinous residues	N/A	N/A	–
99276 negative control	Bladelet	312 reed peat with roundwood	No potentially resinous residues	N/A	N/A	–
99851 negative control	Blade fragment	312 reed peat with roundwood	No potentially resinous residues	N/A	N/A	–

108206 negative control	Scraper	310 wood peat	No potentially resinous residues	N/A	N/A	–

Retene, a thermal alteration marker resulting from the strong heating of Pinaceae resin and degradation of diterpenoids (Font et al., 2007, p. 120; Modugno and Ribechini, 2009a, p. 221), was not present in any of the extracts from tool residues. Abietic acid was not identified in any tool samples. The most intensive peak in the mass spectra of TMS abietic acid is the ion 256, but other important ions 241, 185, and 374 were not found (discussed further below).

13.3.4 Unknown 1 and Unknown 2: diterpene fragments?

Additionally, two distinctive but unidentified compounds (Unknown 1 and Unknown 2) were found in all nine tool residue extracts that contained compounds consistent with pine resin. Unknown 1 was also found in the sediment sample associated with microlith 109691, but the other eight tool sediment samples did not contain Unknown 1 and no sediment samples contained Unknown 2. Unknown 1 and 2 were not present in the *Pinus sylvestris* fresh reference pine resins. Table 13.5 lists these unknown compounds, their time of elution, and characteristic ions. It is noteworthy that the ion composition is extremely similar between Unknown 1 and 2, suggesting they are very likely to be related. Example mass spectra of Unknown 1 and Unknown 2 are illustrated in Figures 13.7 and 13.8, respectively.

Table 13.5. Unknown but consistently present peaks in tool residue extract samples.

Biomolecular constituent	tR (min)	Characteristic ions (*m/z*) in order of abundance
Unknown 1	15.385	256, 73, 91, 257, 149, 75, 59, 65, 180, 258
Unknown 2	15.955	256, 73, 257, 91, 149, 258, 59, 65, 75, 86
Comparison with abietic acid (Azemard et al. 2016,		256, 241, 185, 213, 257, 242, 143, 129, 374, 91

Supplementary Material)		
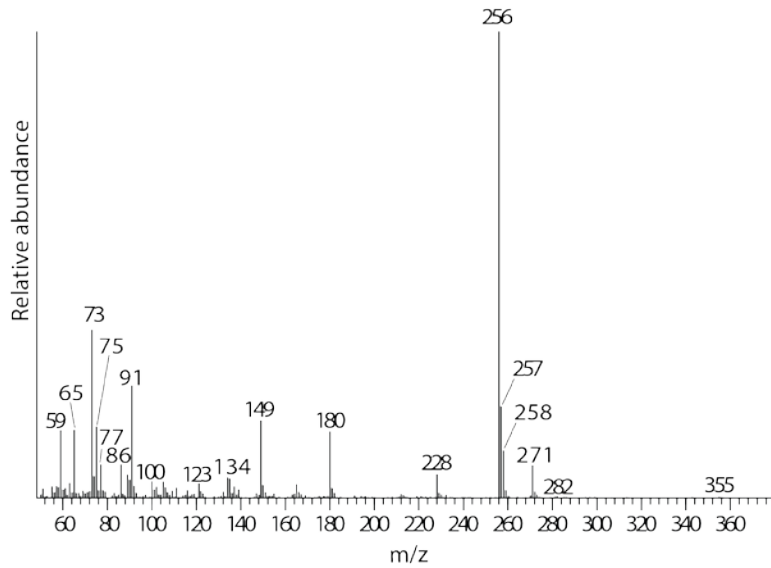
Figure 13.7. Example of a mass spectrum of possible diterpene fragment Unknown 1 from blade 108373.
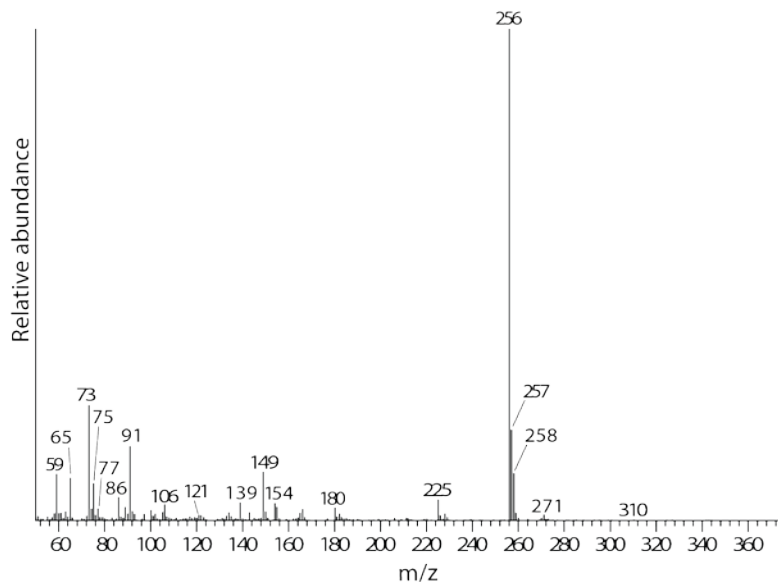
Figure 13.8. Example of a mass spectrum of possible diterpene fragment Unknown 2 from blade 108373.

These interesting peaks may signal the presence of more oxidized diterpenic structures, perhaps diterpenoid fragments. For instance, Čukovska et al. (2012,

p. 1692) identified four peaks that they ascribed to unknown pine resin-related compounds, in addition to the presence of DHA, dehydro-DHA, and 7-oxo-dehydro-DHA, in five samples of wall paintings from Macedonian churches.

The fragmentation mechanisms of diterpenes in abietanes, pimaranes, and labdanes yielding new unknown fragments have been proposed by Azemard et al. (2016) using GC-MS-MS. The closest matches able to found with Unknown 1 and 2, based on the pattern of the most abundant ions seen in mass spectra, was abietic acid (trimethylsilylated with BSTFA) (Azemard et al., 2016, p. 2 supplementary material; cf. Regert et al., 2005, p. 131). Unknown 1 and 2 contain ions 256 and 257 in common with the mass spectrum for abietic acid in Azemard et al. (2016, p. 2 supplementary material). Although Unknown 1 and 2 share similar mass spectral traits with abietic acid as presented in Regert et al. (2005) and Azemard (2016), they are not an exact match. For this reason, it is suggested that Unknown1 and 2 are perhaps fragments of the Pinaceae compound abietic acid.

13.3.5 Results by tool

The tools that contained compounds consistent with pine resin are presented sequentially below, with an analysis of each tool. First, the macroscopic and microscopic observations are presented together, followed by the GC-MS results. Additionally, all tools were revisited microscopically to determine if the target residue had been removed by the solvent extraction procedure.

13.3.5.1 Burin 108205

This tool is an angled burin on a break. On the dorsal side of the burin, macroscopically visible deposits varying in colour from black to golden brown were present over large areas of the dorsal surface but appearing to concentrate at the edges. A black shiny deposit with a bubbly smooth appearance was noted on the dorsal left mid edge (Figures 13.9 and 13.10). Plant material and black

deposits were found together located dorsal centre distal, slightly left. A good deal of the black/brown deposit was removed during microscopic analysis, sticking to the parafilm. This tool was also suspected of containing iron oxide deposits within microchips, along the ventral right distal edge. It appears the tool was used, based on the presence of usewear, with polish noted on the dorsal left proximal corner, and microchipping found on the ventral right distal edge.
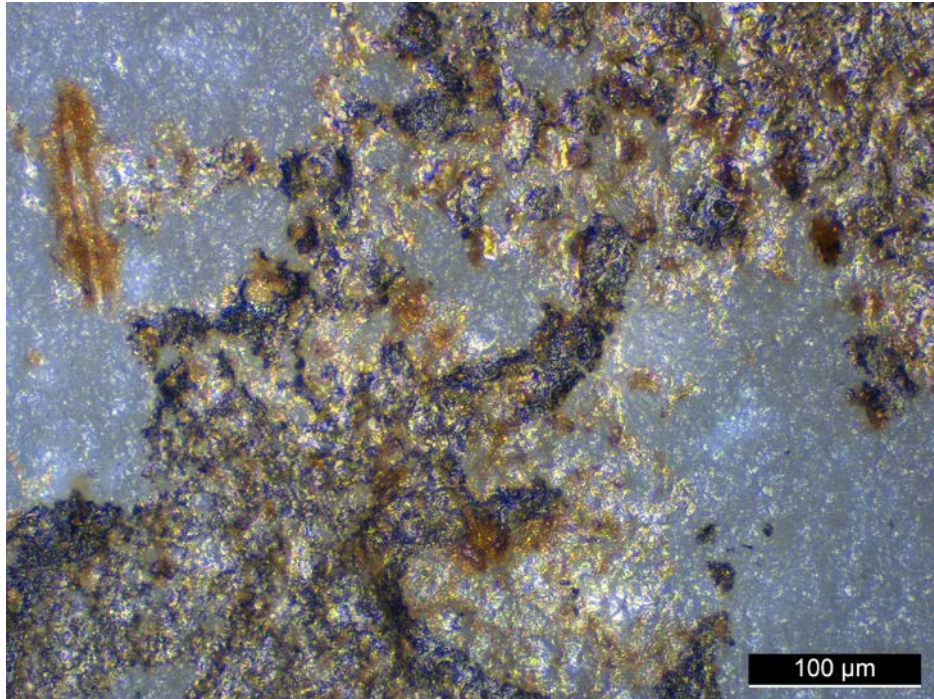
Figure 13.9. Black shiny deposit with bubbly smooth appearance, dorsal left mid edge of burin 108205.
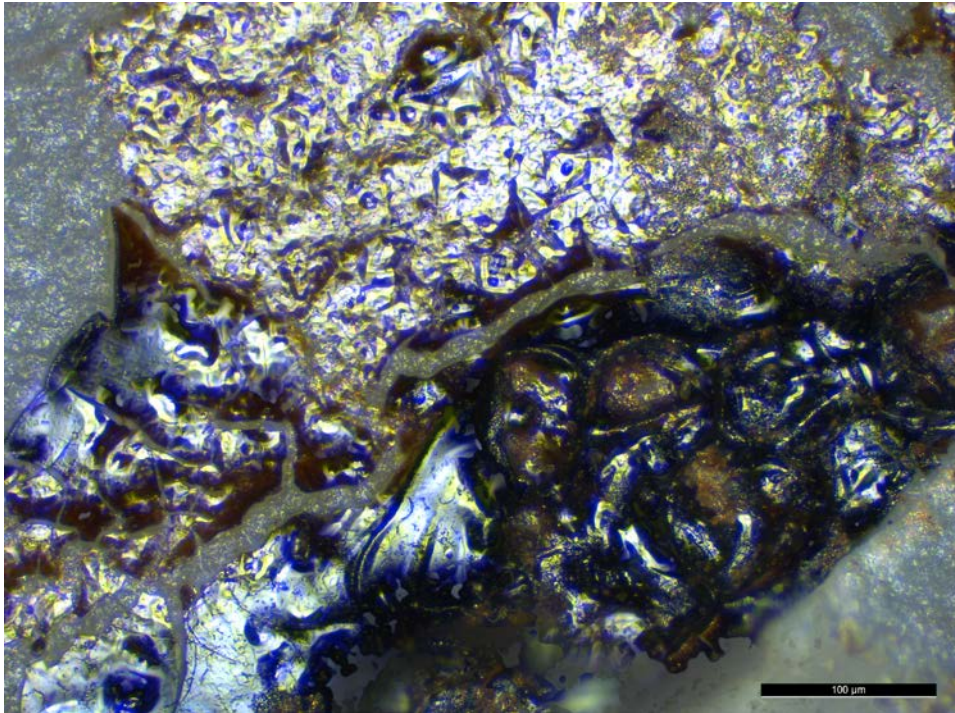
Figure 13.10. Black shiny deposit with bubbly smooth appearance, dorsal left mid edge of burin 108205.

A large portion of the black amorphous deposit was visibly removed by solvent extraction (Figure 13.11). Only a few traces remained after solvent extraction, perhaps less than 5% of the original deposit.

Figure 13.11. Some deposits still remain on burin 108205 after solvent extraction, ventral left mid edge.

The gas chromatogram from burin 108205 contained peaks identified as dehydro-7-DHA, DHA, and 7-oxo-DHA (Figures 13.12 and 13.13).
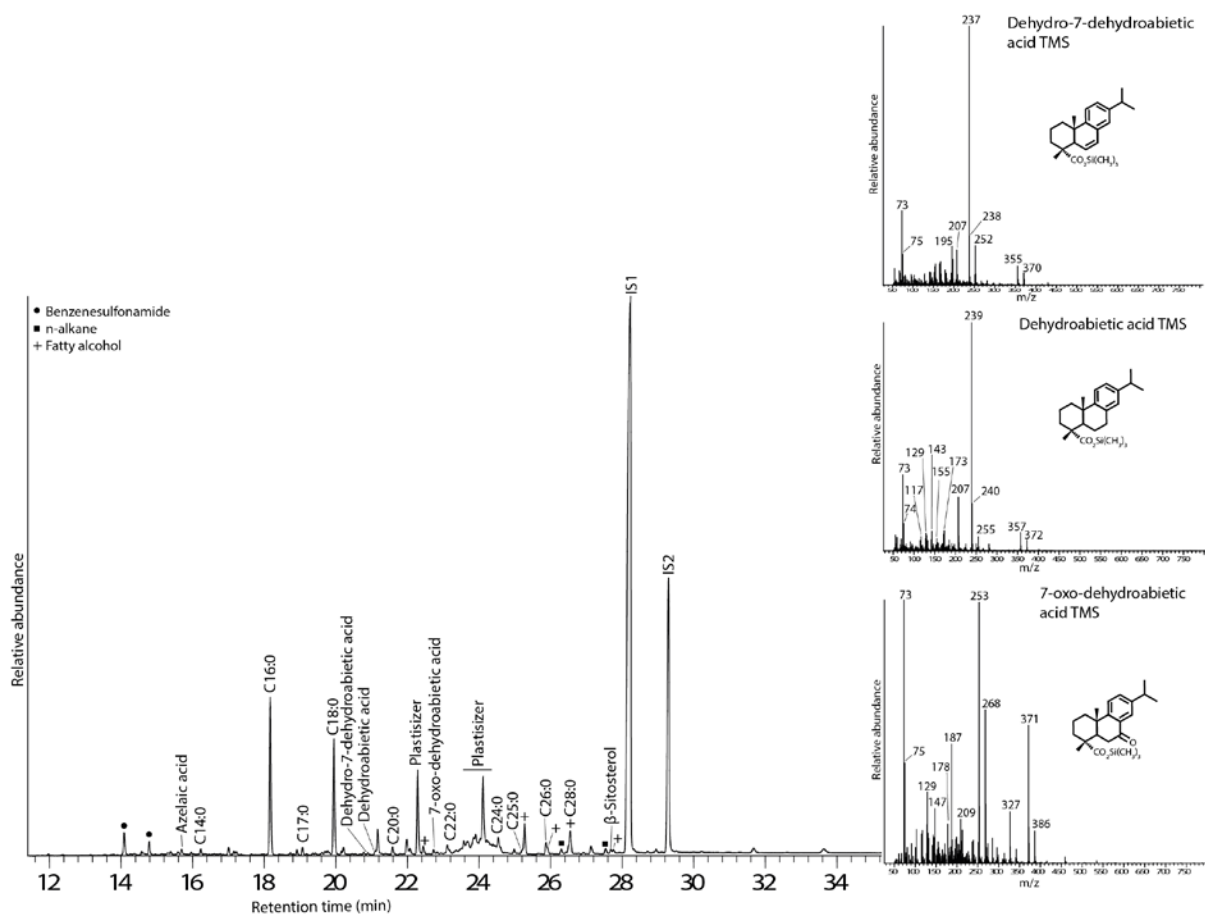
Figure 13.12. Total gas chromatogram of the trimethylsilylated residue extract from burin 108205. Inset shows mass spectra of Dehydro-7-DHA, DHA, and 7-oxo-DHA, present in trace amounts.

Figure 13.13. Partial gas chromatogram of the trimethylsilylated sample extract from burin 108205, zoomed in to show altered markers of pine resin.

13.3.5.2 Blade 108373

Microscopic observations of blade 108373 noted a possible black resinous deposit in the dorsal centre of the blade (Figure 13.14).
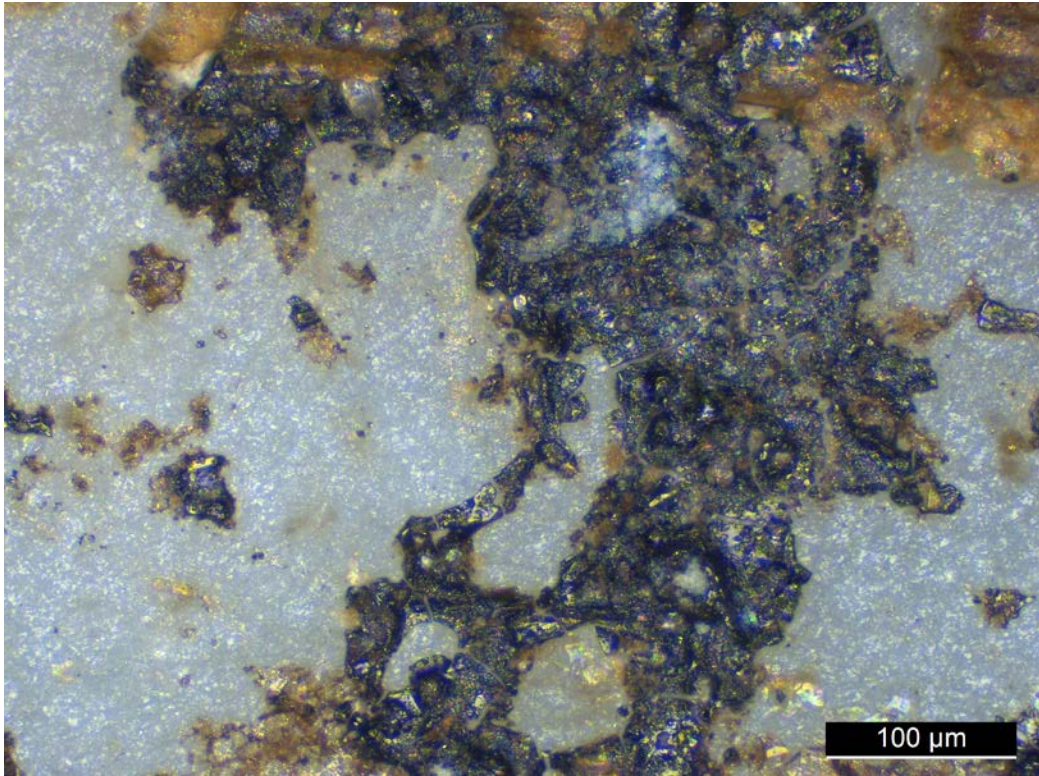
Figure 13.14. Black deposit on blade 108373, dorsal centre.

This blade also contained traces of wood microcharcoal (Figure 13.15), which were too small and fragmentary to allow any taxonomic determination. The context (337) the blade was retrieved from is described as a fill of a pit that contains burnt lithics and bone. Heat exposure on the blade is evident – it is cracked in several places and has two pot lids on the ventral distal area. If the black deposits on this blade are the remnants of tree resin, they may originate from the exudates from the burnt wood in the pit, not necessarily an applied hafting residue. For instance, it has been shown experimentally that green wood fuel in a hearth exudes resin onto any underlying stone in the vicinity (Schmidt et al. 2015).
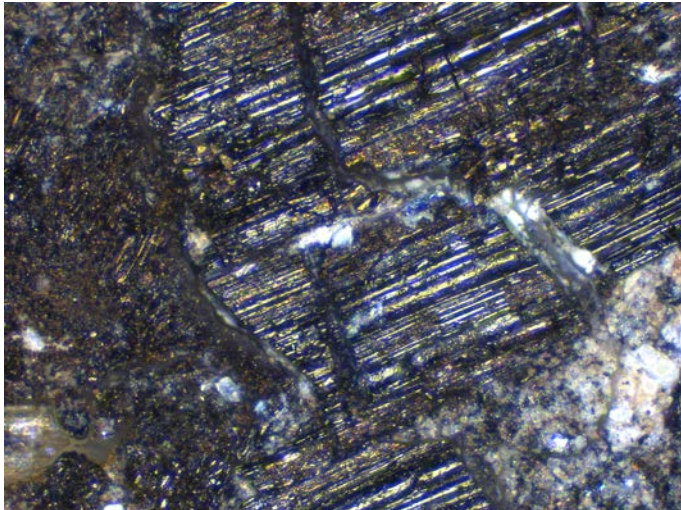
Figure 13.15. Microcharcoal on blade 108373.

The gas chromatogram from blade 108373 contained peaks identified as dehydro-7-DHA, DHA, and 7-oxo-DHA (Figures 13.16 and 13.17).
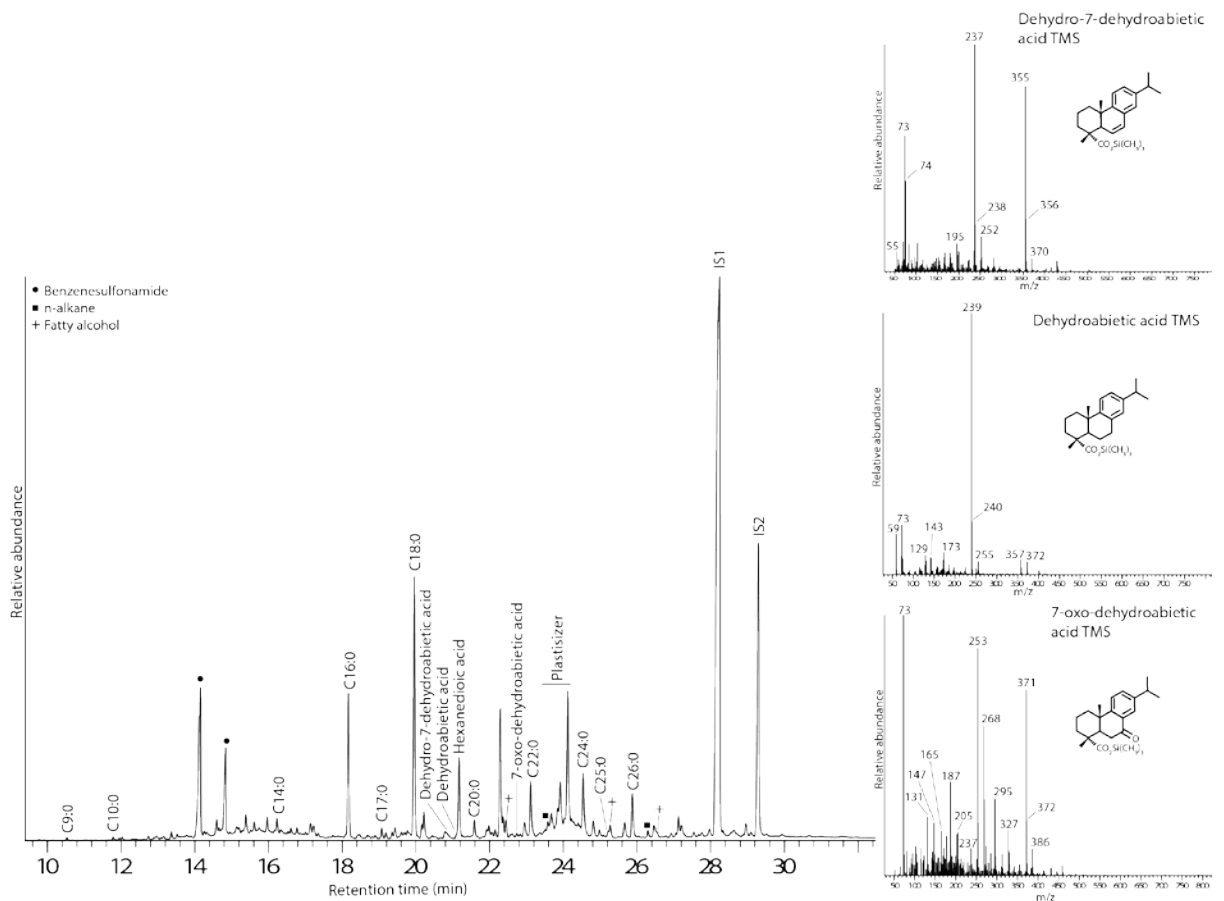
Figure 13.16. Total gas chromatogram of the trimethylsilylated sample extract from blade 108373. Inset shows mass spectra of Dehydro-7-DHA, DHA, and 7-oxo-DHA, present in trace amounts.
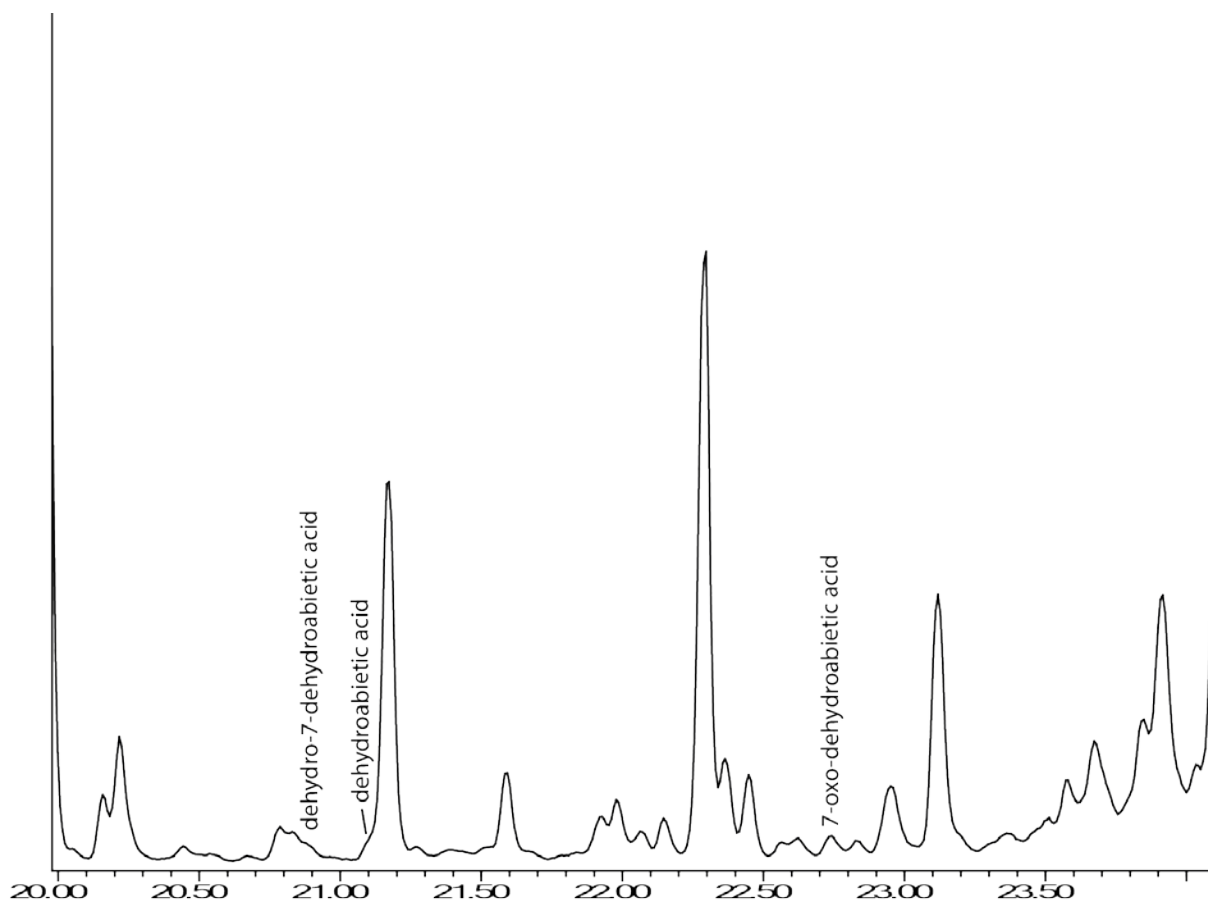
Figure 13.17. Partial gas chromatogram of the trimethylsilylated sample extract from blade 108373, showing derivatives of abietic acid.

13.3.5.3 Microlith 108397

A black amorphous residue originally posited as birch bark tar was located on the ventral proximal mid edge of microlith 108397. Figure 13.18 illustrates this residue residue before and after solvent extraction. As can be seen, not all of the residue was removed by solvent extraction treatment.
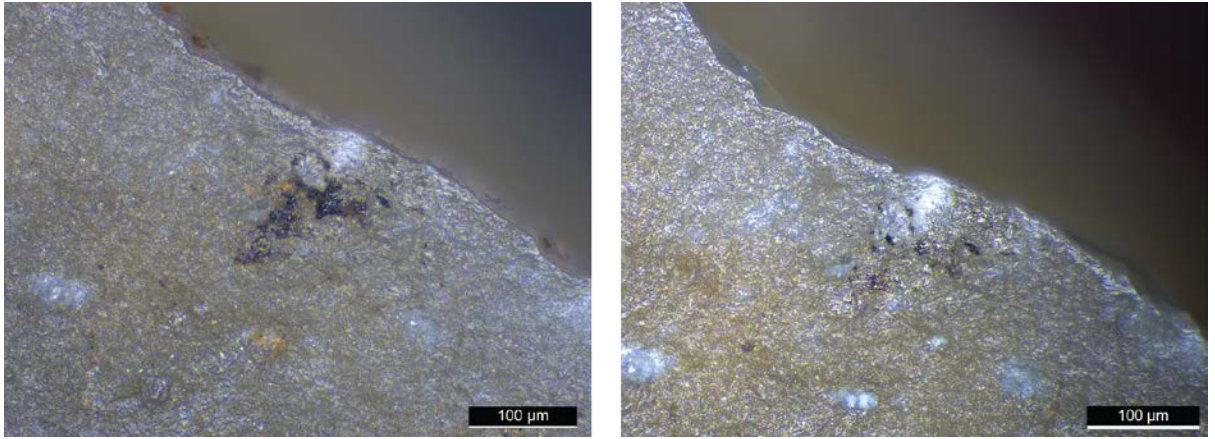
Figure 13.18. Left: black amorphous residue located on the ventral proximal mid edge of microlith 108397, prior to solvent extraction and GC-MS. Right: Black residue deposit after GC-MS. Most of the deposit was removed but some residue still remains.

The gas chromatogram from microlith 108397 did not contain any evidence for the presence of birch bark tar, but rather contained peaks identified as dehydro-7-DHA, DHA, and 7-oxo-DHA (Figures 13.19 and 13.20).
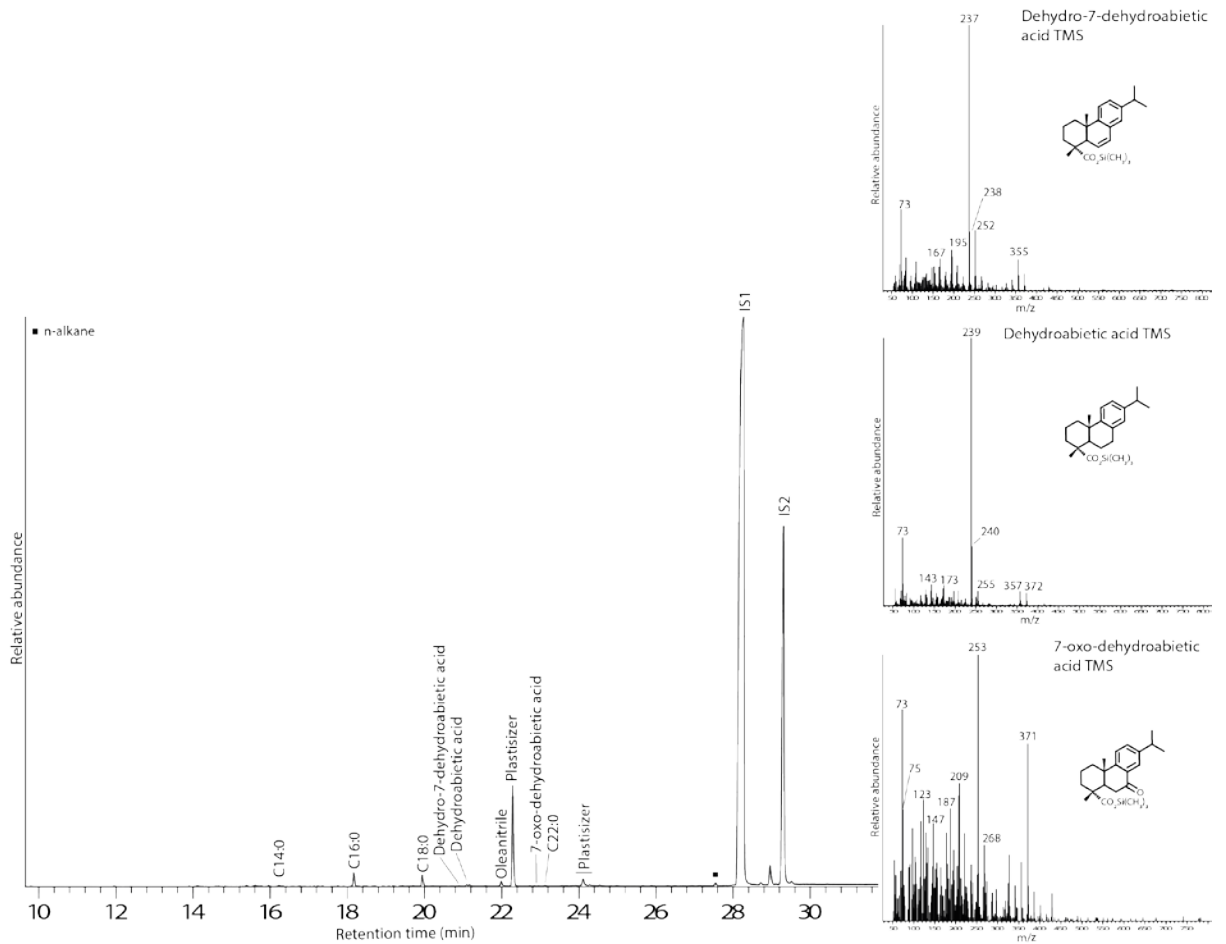
Figure 13.19. Total gas chromatogram of the trimethylsilylated sample extract from microlith 108397. Inset shows mass spectra of Dehydro-7-DHA, DHA, and 7-oxo-DHA, present in trace amounts.
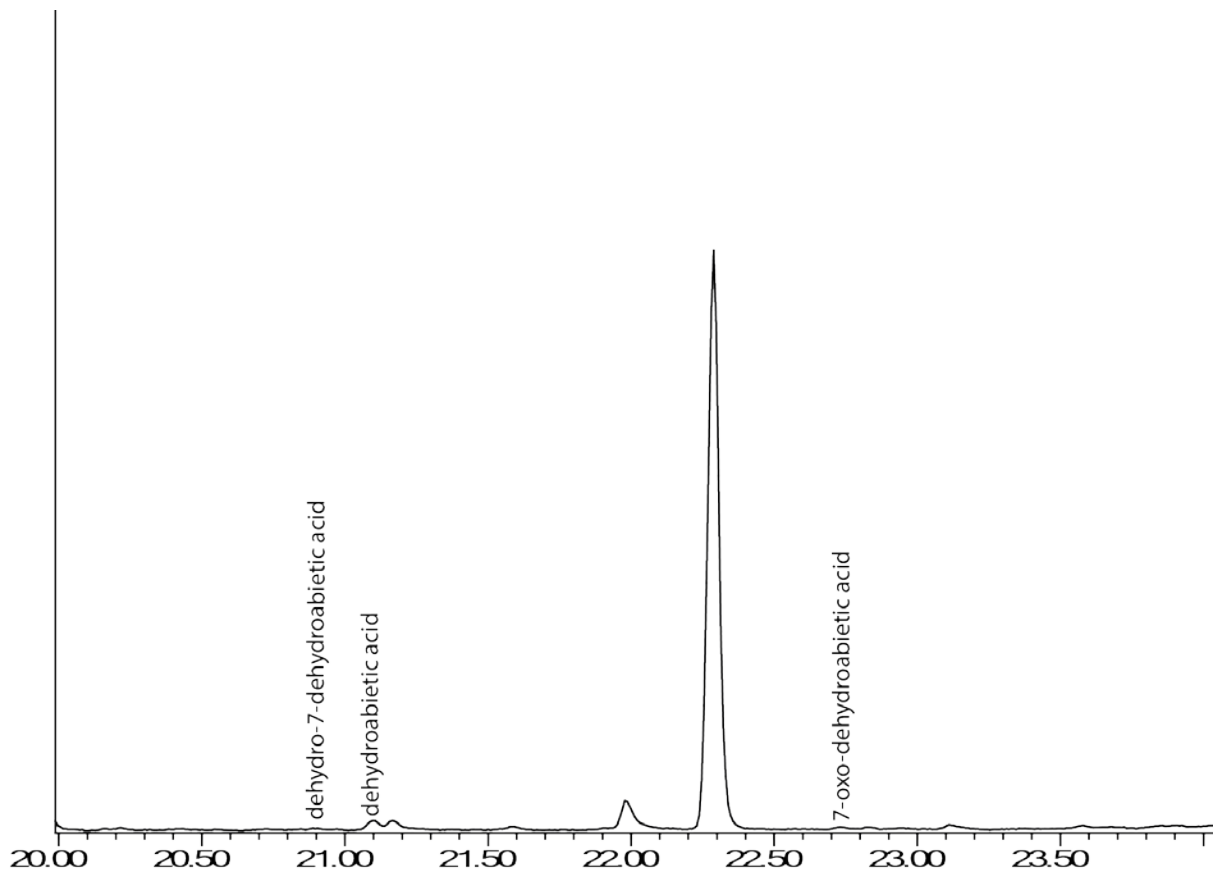
Figure 13.20. Partial gas chromatogram of the trimethylsilylated sample extract from microlith 108397.

13.3.5.4 Blade 109649

Black granular deposits (Figure 13.21) were found overtop of cortex along the dorsal right mid edge and right distal edge on blade SC 14 109649 (317) P7. These black granular deposits also continued on the ventral side of the blade.
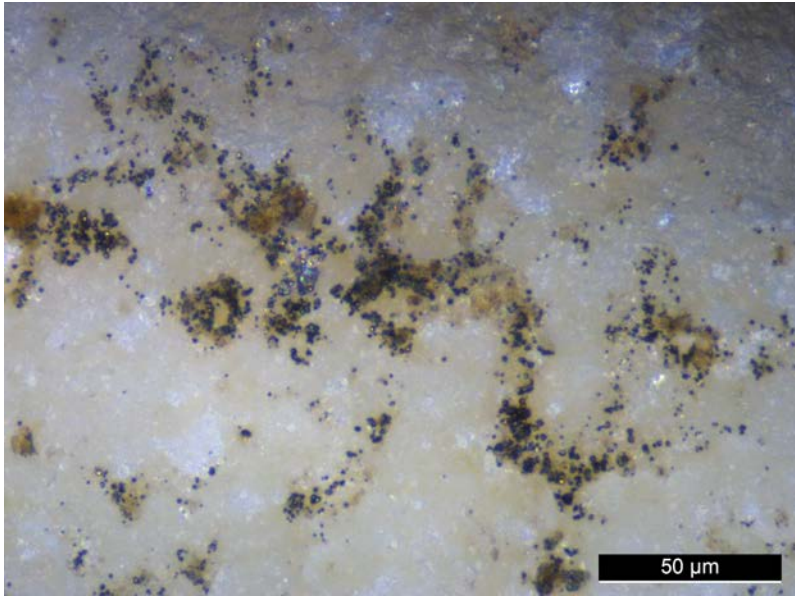
Figure 13.21. Black granular deposits on the right mid edge on blade 109649.

The gas chromatogram from blade 109649 contained dehydro-7-DHA, DHA, and 7-oxo-DHA (Figures 13.22 and 13.23).
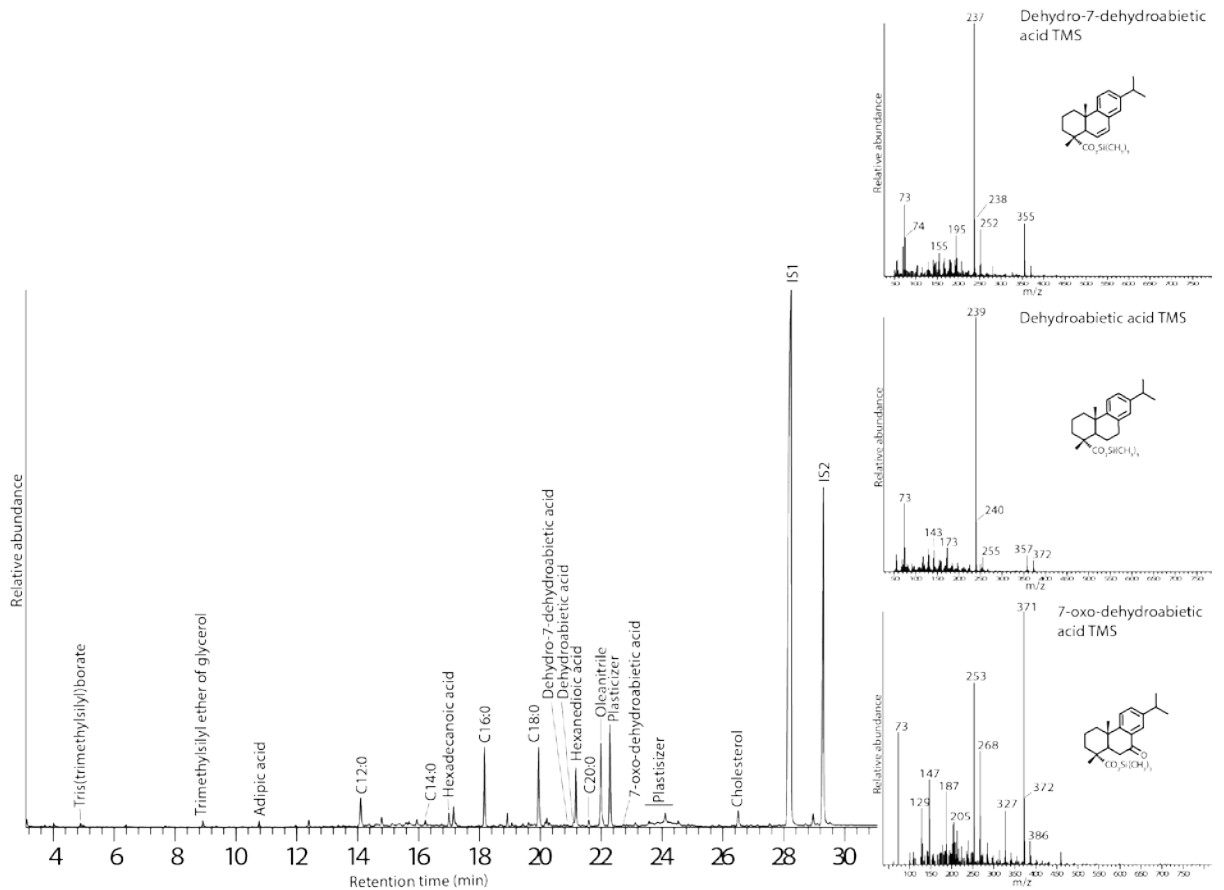
Figure 13.22. Total gas chromatogram of the trimethylsilylated sample extract from blade 109649. Inset shows mass spectra of Dehydro-7-DHA, DHA, and 7-oxo-DHA, present in trace amounts.

394
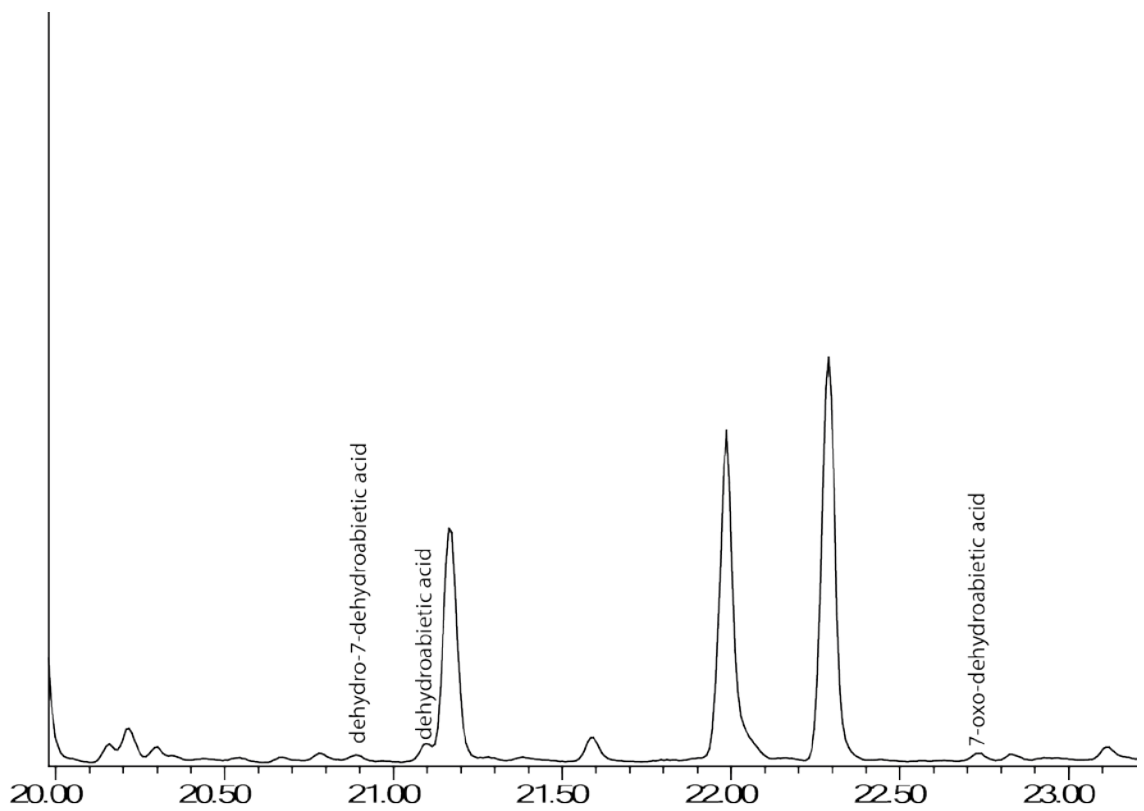
Figure 13.23. Partial gas chromatogram of the trimethylsilylated sample extract from blade 109649.

13.3.5.5 Microlith 109691

Tool 109691 was a microlith that had the proximal end broken. It contained black deposits and microcharcoal on the ventral distal tip (Figure 13.24).

Figure 13.24. Black deposits and microcharcoal on the right mid edge on bladelet 109691.

The gas chromatogram from blade 109649 contained dehydro-7-DHA and DHA (Figures 13.25 and 13.26).
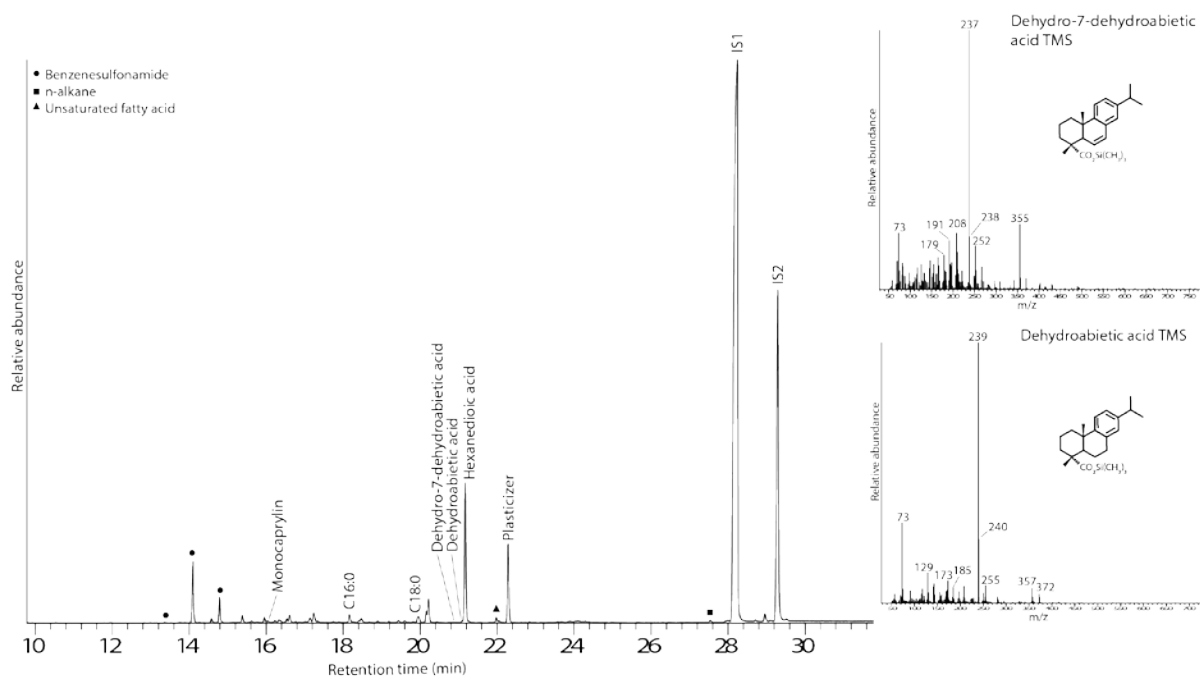
Figure 13.25. Total gas chromatogram of the trimethylsilylated sample extract from microlith 109691. Inset shows mass spectra of Dehydro-7-DHA, and DHA, present in trace amounts.
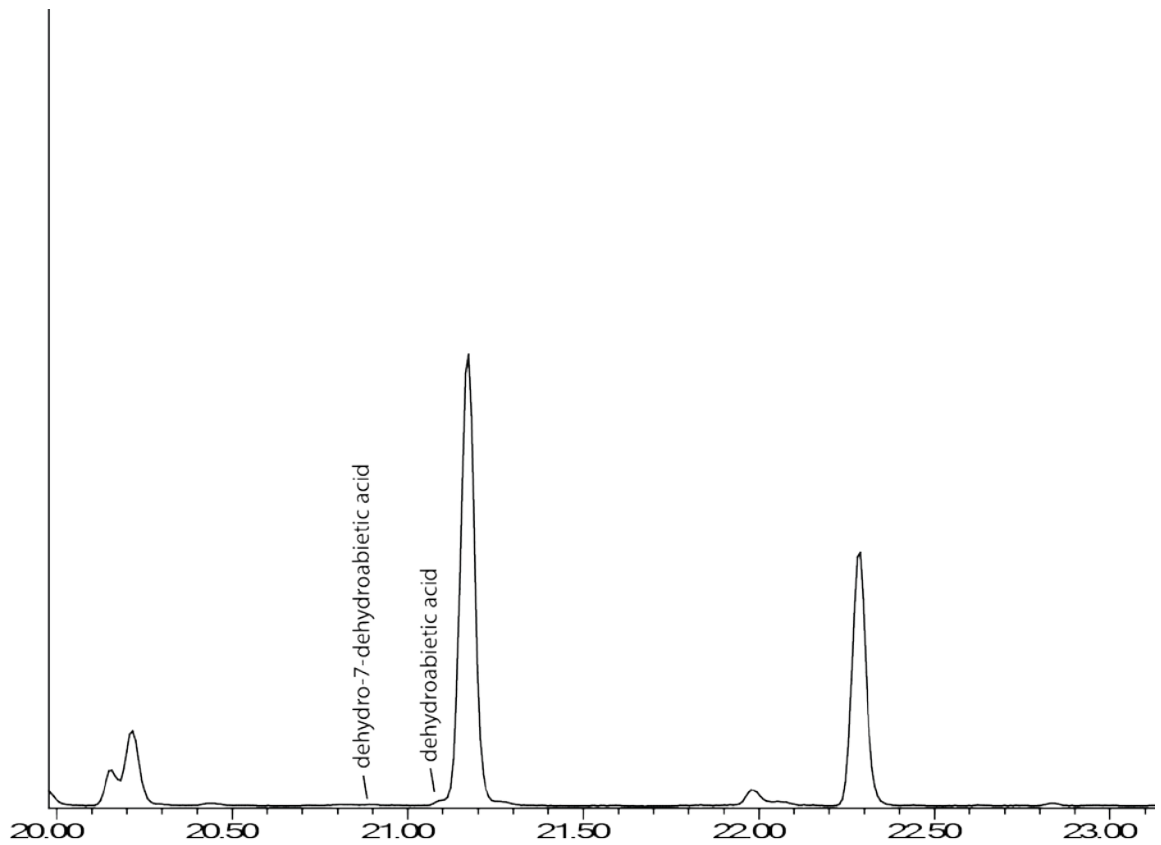
Figure 13.26. Partial gas chromatogram of the trimethylsilylated sample extract from microlith 109691.

13.3.5.6 Microlith 109724

Microlith 109724 contained black traces of microcharcoal on the right distal edge (Figure 13.27). Only the 'curved' long edge of the tool contained microcharcoal, other edges did not.
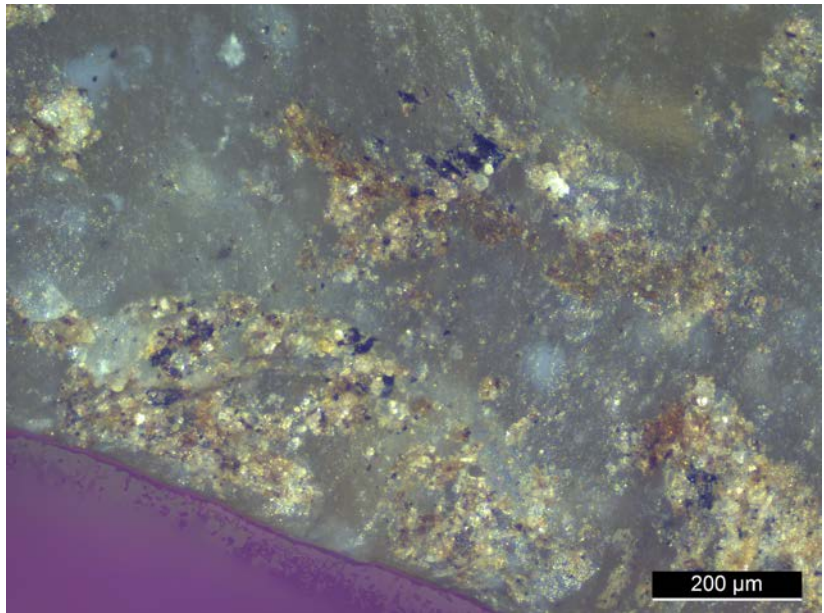
Figure 13.27. Black microcharcoal on microlith 109724, right distal edge.

The gas chromatogram from microlith 109724 contained dehydro-7-DHA and DHA (Figures 13.28 and 13.29).
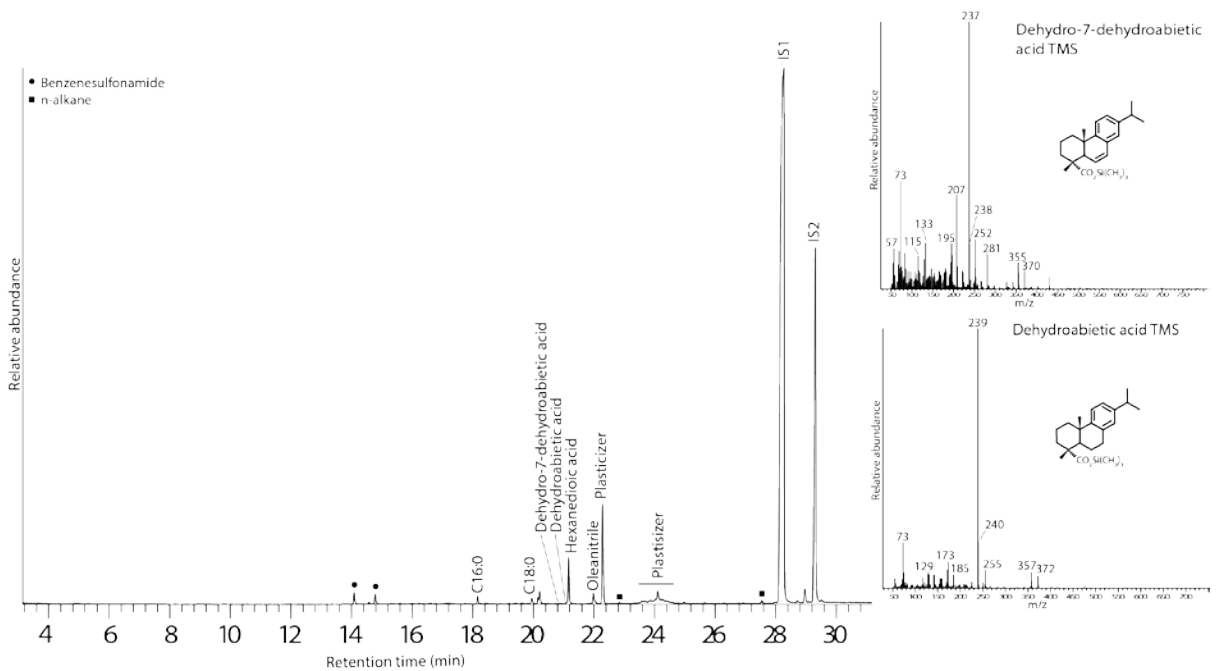
Figure 13.28. Total gas chromatogram of the trimethylsilylated sample extract from microlith 109724. Inset shows mass spectra of Dehydro-7-DHA, and DHA, present in trace amounts.
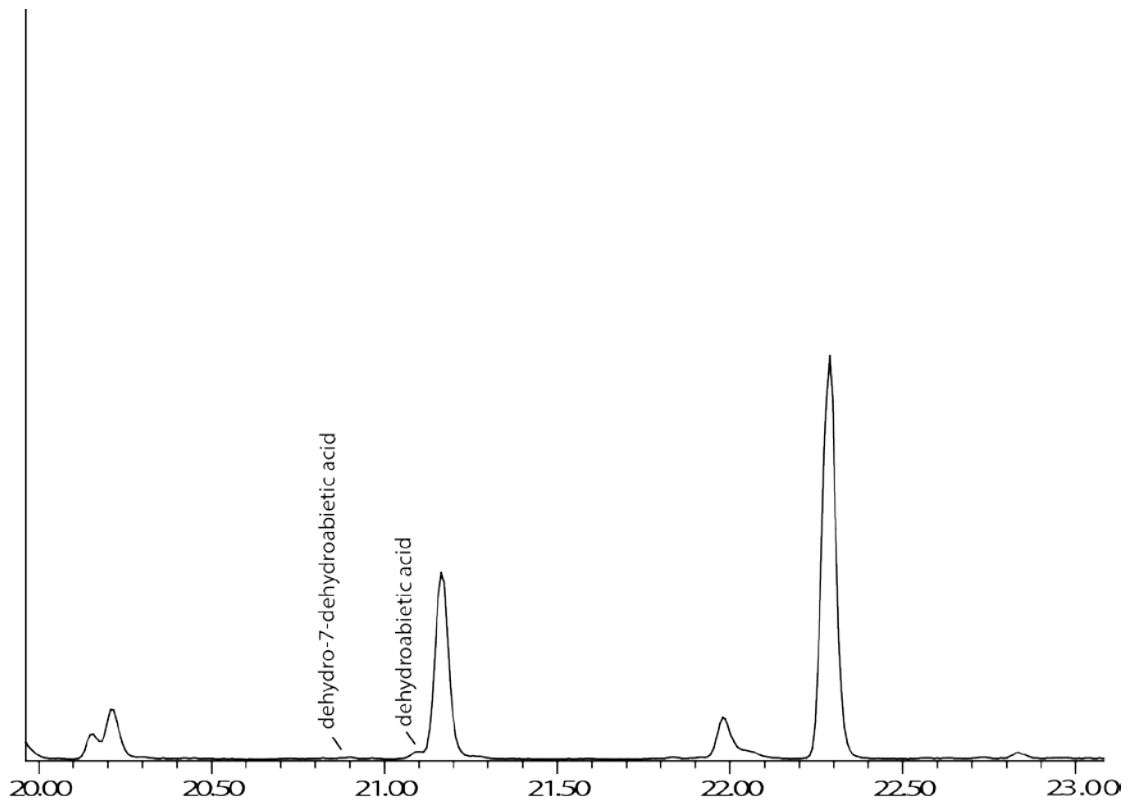
Figure 13.29. Partial gas chromatogram of the trimethylsilylated sample extract from microlith 109724.

13.3.5.7 Bladelet 110657

Bladelet 110657 was part of a sequence of bladelets (microblades) recovered together (110656-110659). A black deposit was found associated with white crystalline material on the ventral right distal edge (Figure 13.30).
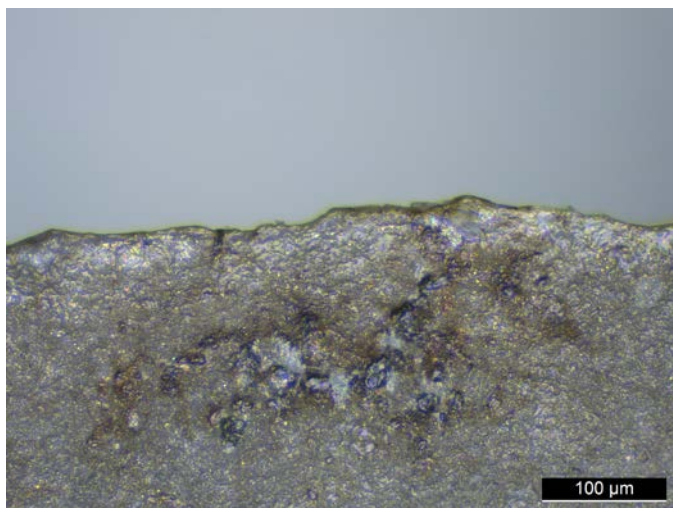
Figure 13.30. Black deposit and white crystalline material, bladelet 110657, ventral right distal edge.

The gas chromatogram from microlith 110657 contained dehydro-7-DHA, DHA, and 7-oxo-DHA (Figures 13.31 and 13.32).
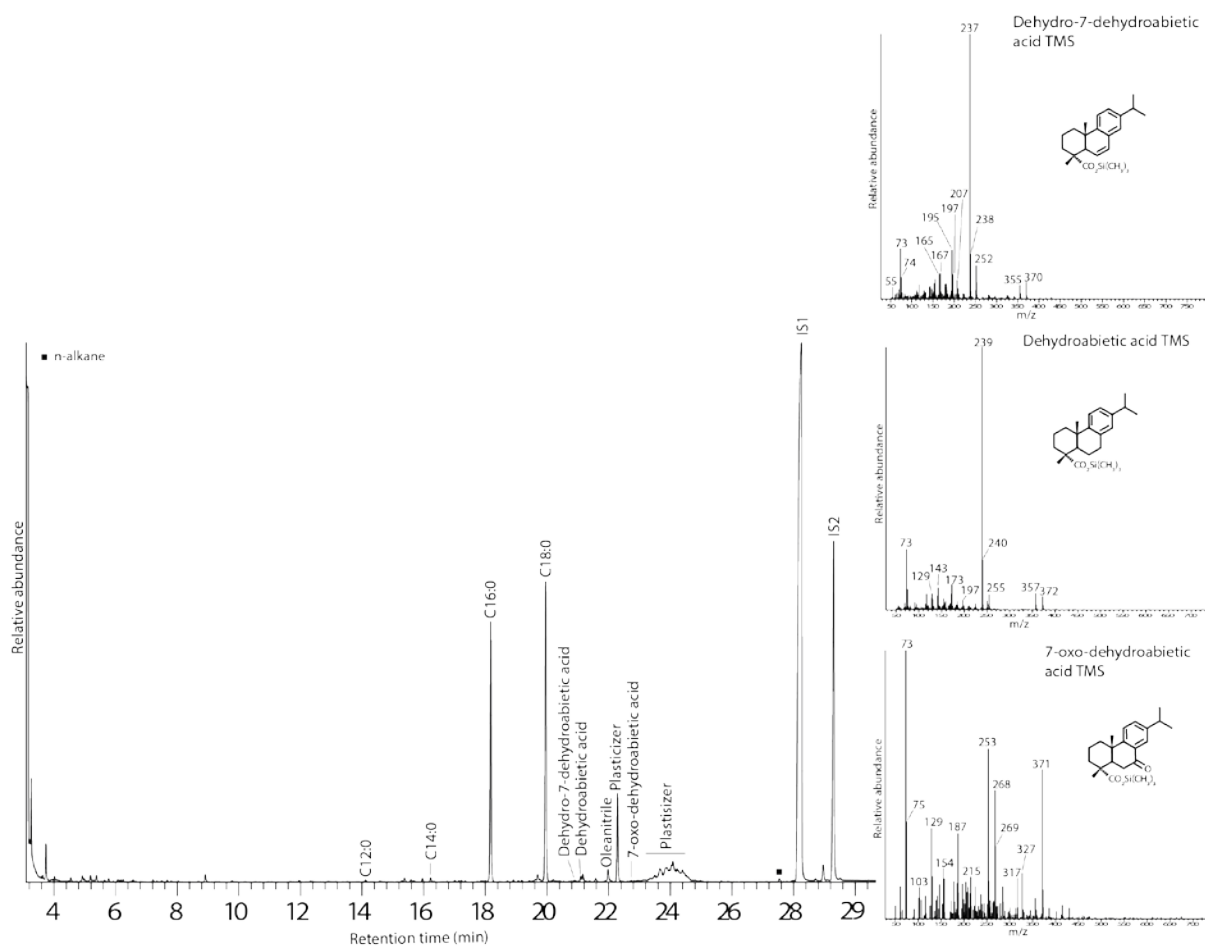
Figure 13.31. Total gas chromatogram of the trimethylsilylated extract from bladelet 110657. Inset shows mass spectra of Dehydro-7-DHA, DHA, and 7-oxo-DHA, present in trace amounts.
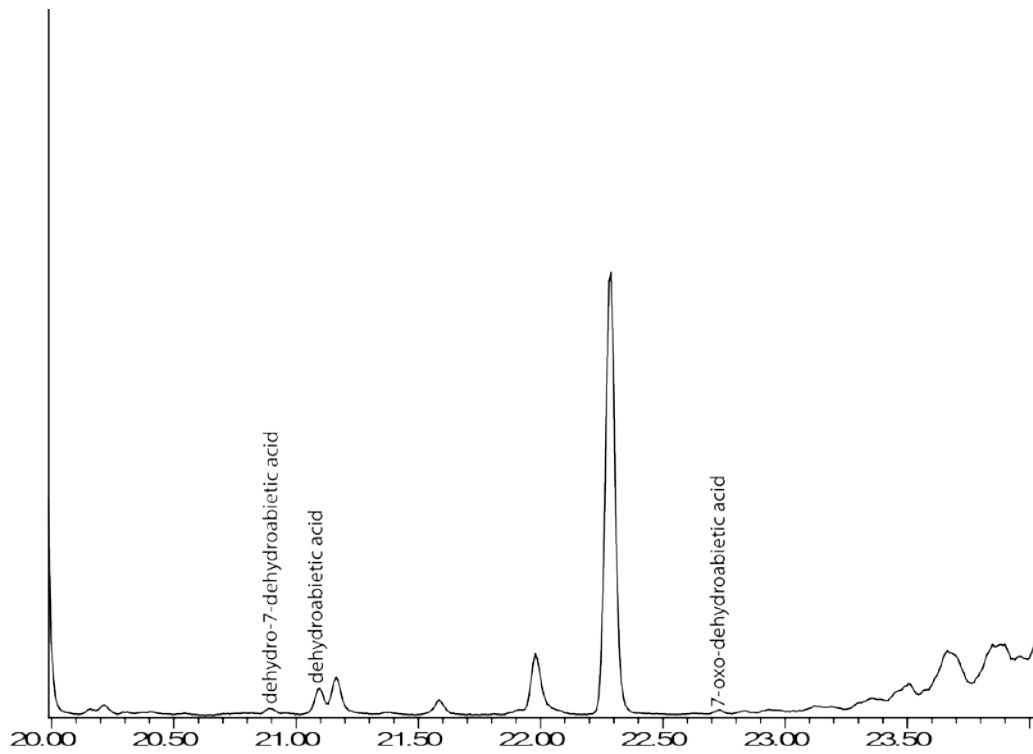
Figure 13.32. Partial gas chromatogram of the trimethylsilylated sample extract from bladelet 110657.

13.3.5.8 Bladelet 111490

Large areas of the ventral surface were covered with a black shiny material on bladelet 111490 (Figure 13.33).
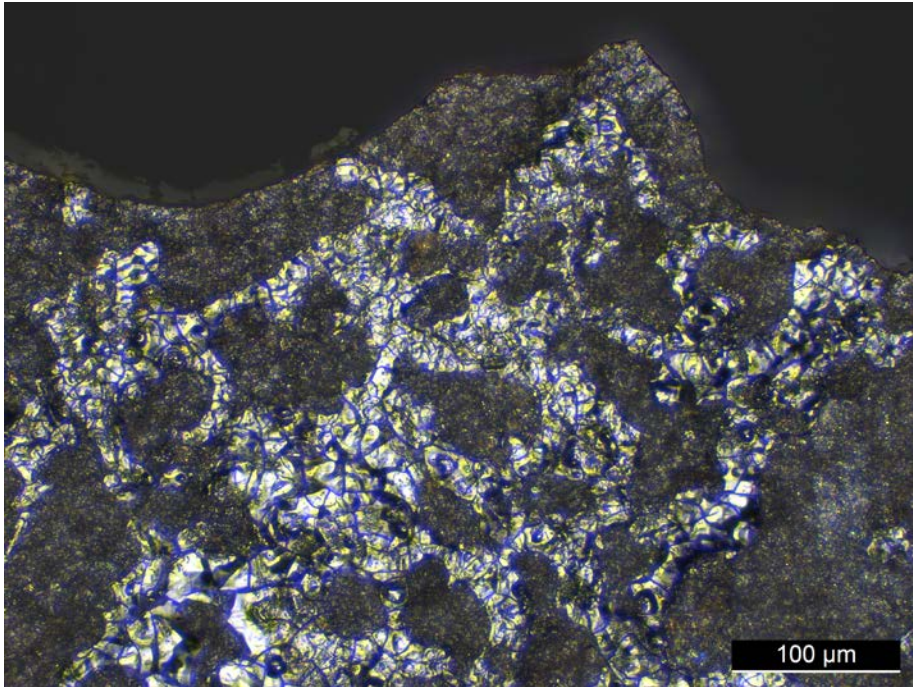
Figure 13.33. Large black shiny deposit on bladelet 111490, ventral proximal right edge.

The gas chromatogram from bladelet 111490 contained dehydro-7-DHA and DHA (Figures 13.34 and 13.35).
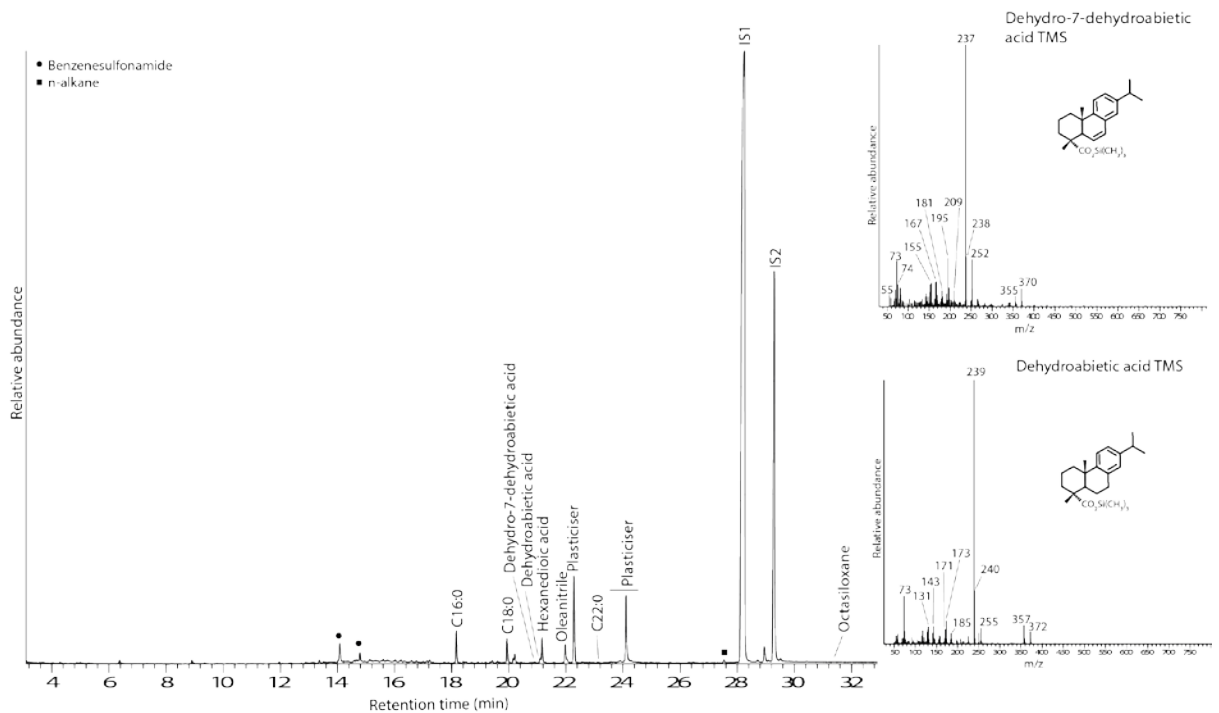
Figure 13.34. Total gas chromatogram of the trimethylsilylated sample extract from bladelet 111490. Inset shows mass spectra of Dehydro-7-DHA, and DHA, present in trace amounts.
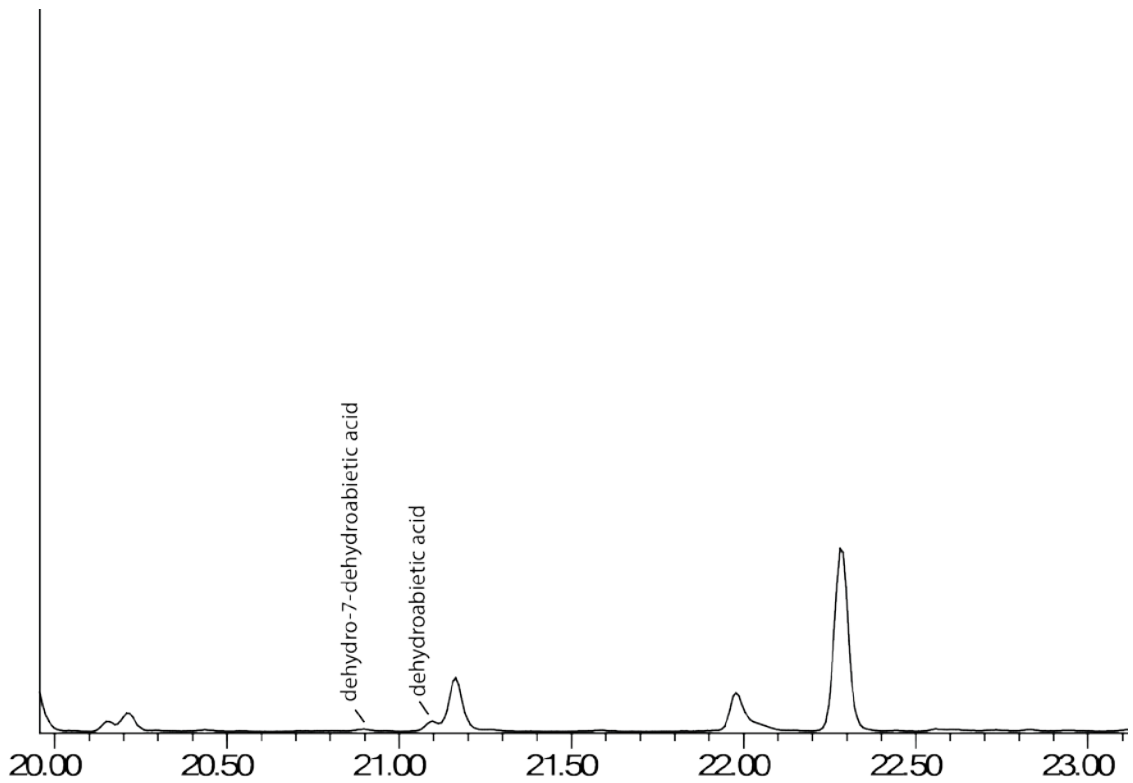
Figure 13.35. Partial gas chromatogram of the trimethylsilylated sample extract from bladelet 111490.

13.3.5.9 Microlith 113623

The ventral left edge of microlith 113623 contained a black plant material (Figure 13.36). This tool also contained orange iron oxide deposits in a tideline morphology.
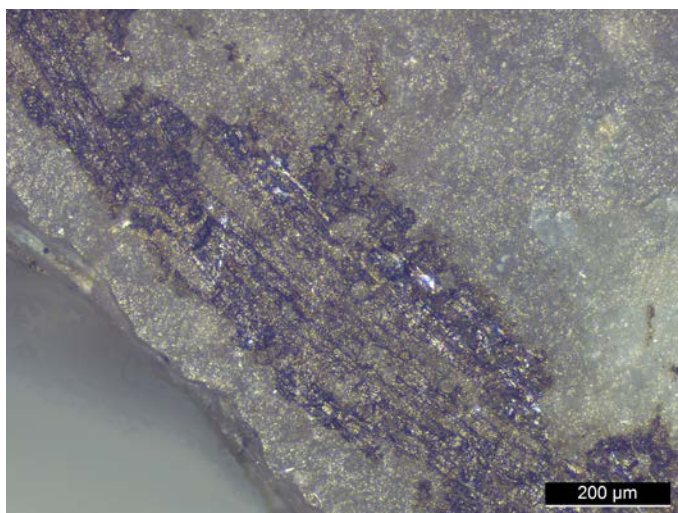
Figure 13.36. Black deposit showing outlines of plant cells on microlith 113623, ventral left edge.

The gas chromatogram from microlith 113623 contained dehydro-7-DHA and DHA (Figures 13.37 and 13.38).
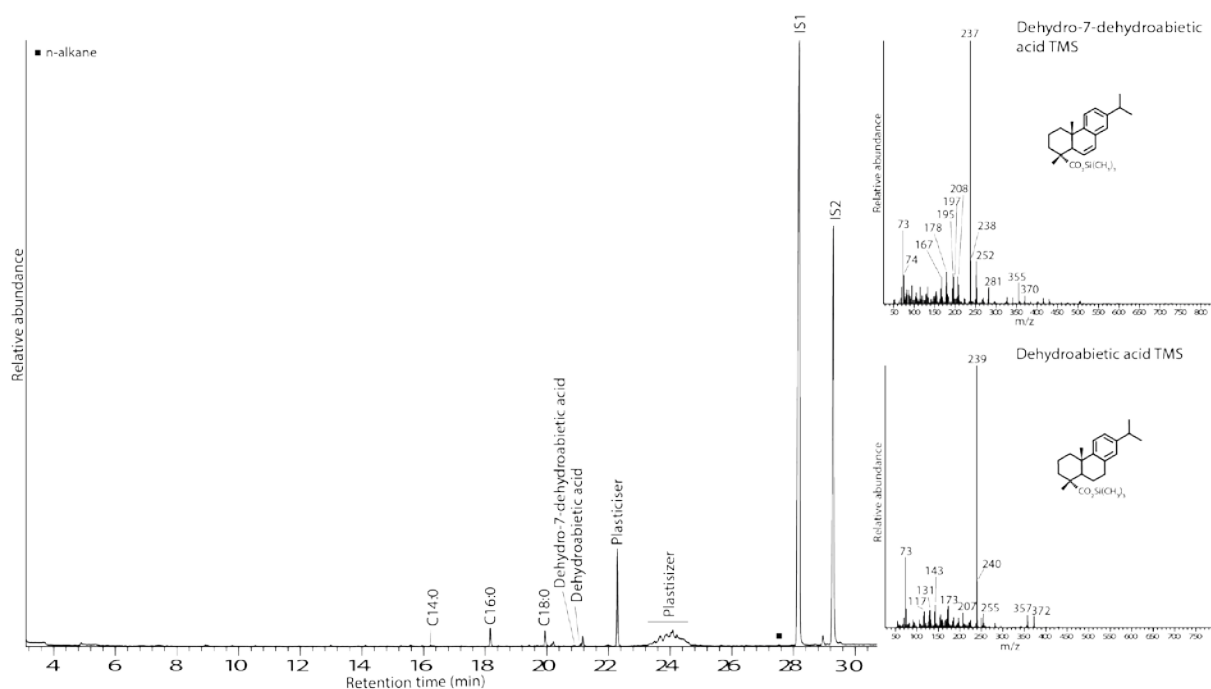
Figure 13.37. Total gas chromatogram of the trimethylsilylated sample extract from microlith 1113623. Inset shows mass spectra of Dehydro-7-DHA, and DHA, present in trace amounts.
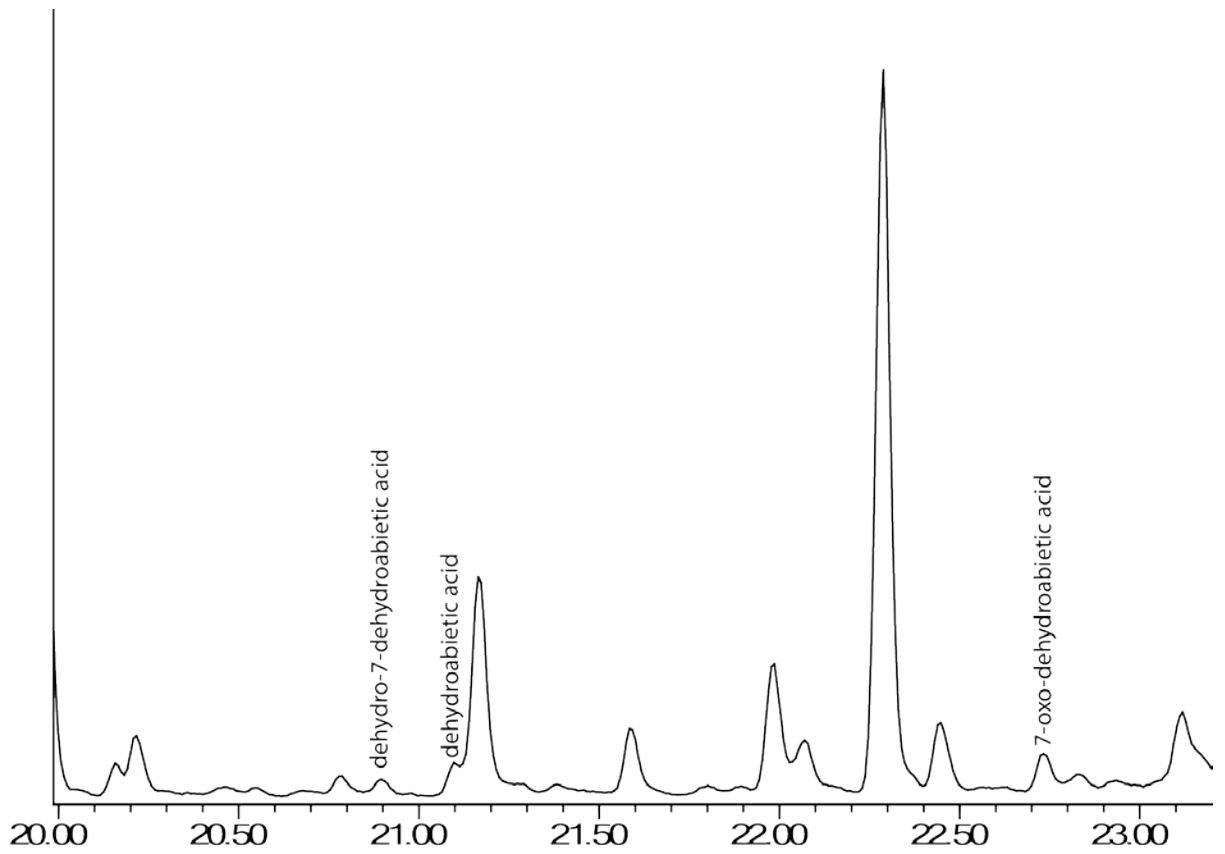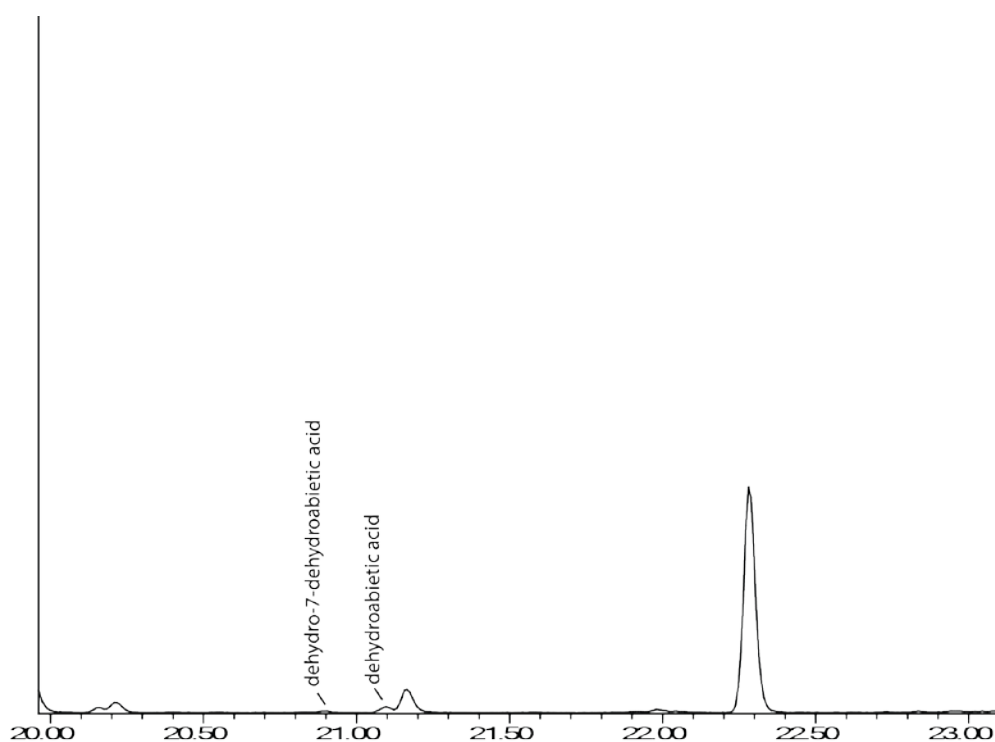

Figure 13.38. Partial gas chromatogram of the trimethylsilylated sample extract from microlith 1113623.

13.3.6 Comparison with reference resins

13.3.6.1 Birch

The reference birch bark tars were characterised by high amounts of betulin. Birch bark tar specifically contains the following triterpenoid markers: betulin, betulinic aldehyde, betulone, allobetulinol, lupenone, and lupeol (Aveling and Heron, 1998; Grünberg, 2002; Hayek et al., 1990, p. 2040; Mills and White, 2012, p. 65; Urem-Kotsou et al., 2002, p. 964), but none of these were identified in the lithic residue samples.

13.3.6.2 Scots pine

The three preparations of reference Scots pine resin contained the following compounds: abietic acid, DHA, pimaric acid, and isopimaric acid. Almost all pine resin acids have abietane, pimarane, isopimarane, or labdane skeletons (Zinkel et al., 1971). As can be seen in Figures 13.39 and 13.40, natural Scots pine resin contains abietic acid, DHA, as well as pimaric and isopimaric acid. It was originally thought that abietic acid would be an important compound to identify in the archaeological samples to find evidence of pine resin, given that abietic acid represents the largest peak in the reference Scots pine resin. It was not found in any archaeological samples, but this is actually to be expected, since abietic acid usually completely disappears in aged samples, degrading to form derivative compounds (van den Berg et al., 2000, p. 521).

DHA is only found as a minor component in fresh conifer resins, but during aging of the resin, the abundance of DHA increases (Rontani et al., 2015, p. 1606). In fact, DHA is the most abundant molecule in aged *Pinus* samples (Pollard and Heron, 2008, p. 242). In the reference Scots pine resin, we see that the altered marker compounds dehydro-7-DHA and 7-oxo-DHA, which were found in the archaeological samples, were not present. It makes sense that dehydro-7-DHA and 7-oxo-DHA are not present in the fresh pine resins, since they are derivative compounds arising from the degradative oxidation of the original biomarker abietic acid.
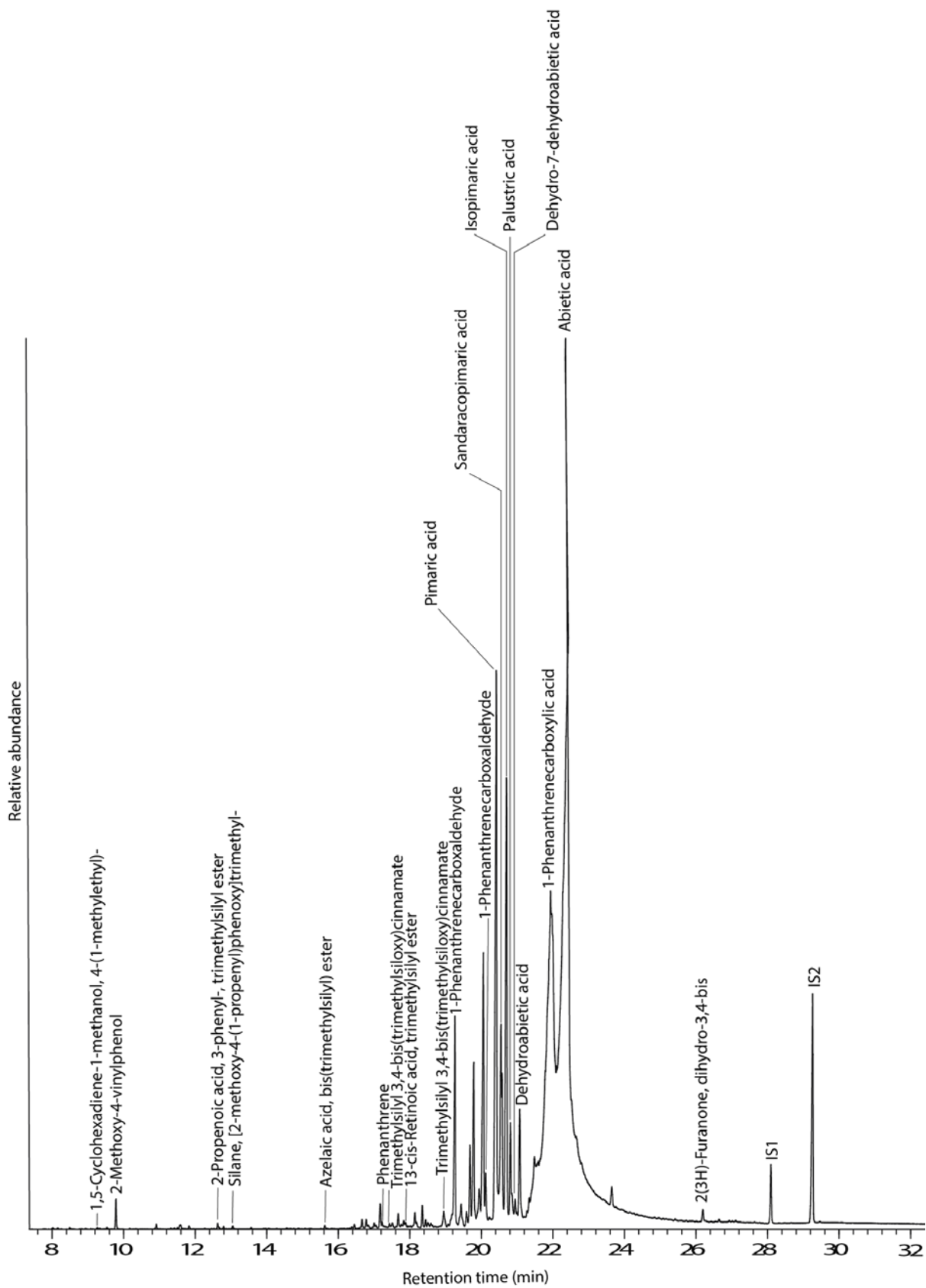
Figure 13.39. Trimethylsilylated total gas chromatogram of reference *Pinus sylvestris* resin, one year old. The sample was diluted by a factor of 20x.
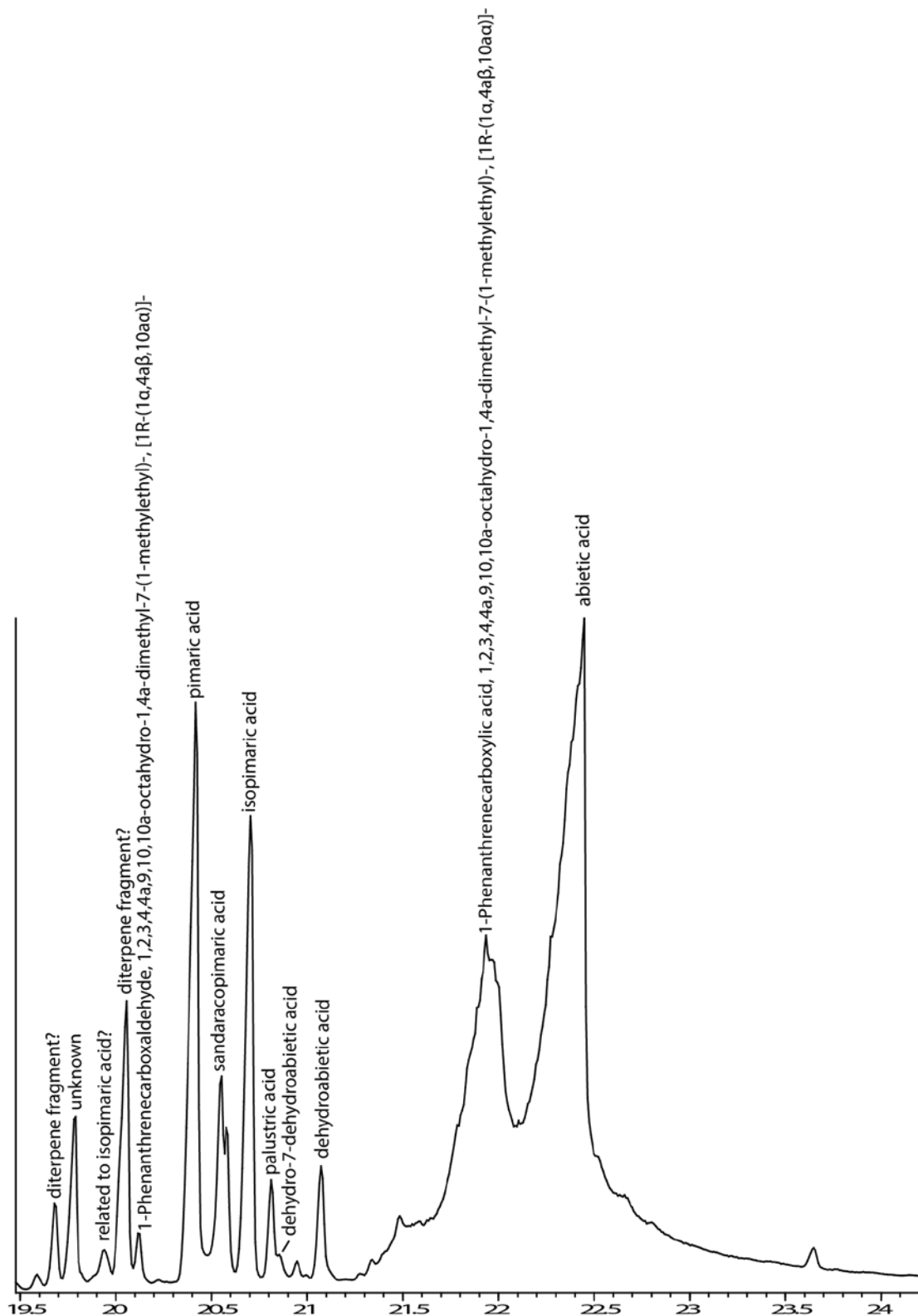
Figure 13.40. Partial gas chromatogram of reference *Pinus sylvestris* resin, one year old. The sample was diluted by a factor of 20x. Two peaks are labelled in Figure 13. as possible diterpene fragments. The peak occurring at 19.688 min has ions of 257, 73, 75, 91, similar to unknown 2 (but occurring at a different retention time), and the peak at 20.057 min has ions of 257, 91, 93, 79. The closest match to the peak marked as 'related to isopimaric acid?' is isopimaric acid TMS, with ions of 73, 255, and 241.

407

13.3.5.3 Common juniper

Common juniper had a different chemical profile to Scots pine as well as the lithic residue samples and did not contain abietic acid, DHA, 7-oxo-DHA, Dehydro-7-DHA, or isopimaric acid.

13.3.7 Sediment samples

It was important to exclude the sediment as a possible contamination source on the stone tools. All sediment sample gas chromatograms were searched for DHA, 7-oxo-DHA, and dehydro-7-DHA – none were found to contain these compounds. The fact that DHA, 7-oxo-DHA, and dehydro-7-DHA were found on stone tools but not their associated sediment samples indicates they are not contaminants from the burial environment. As a group, the sediment samples were typically characterised by the presence of saturated fatty acids (C14:0, C15:0, C16:0, C18:0, C22:0, C24:0, C25:0, C26:0), as well as benzeneacetic acid and benzoic acid (Figures 13.41 and 13.42).
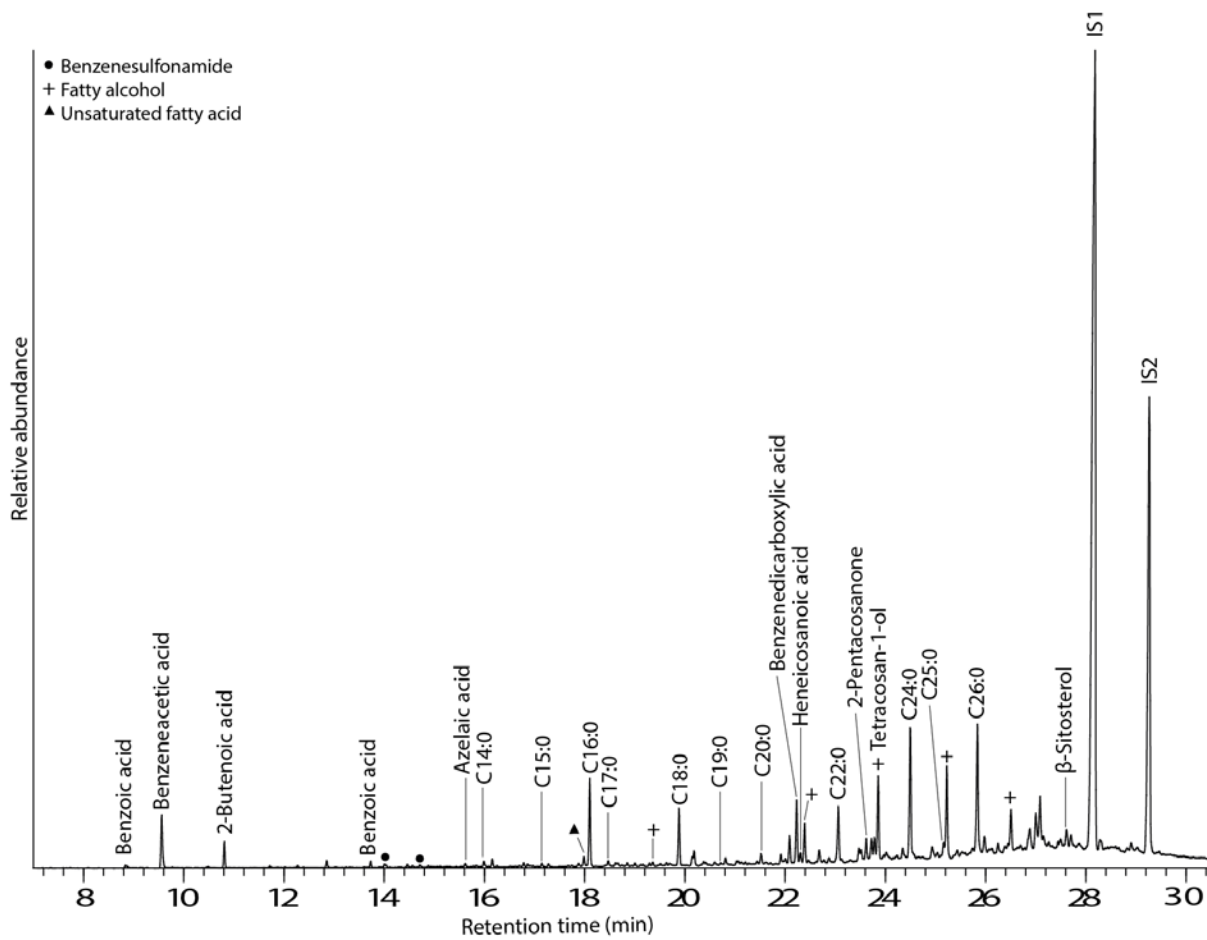
Figure 13.41. Example of a sediment sample total gas chromatogram collected underneath tool 108373 (context 337). Note Dehydro-7-DHA, DHA, and 7-oxo-DHA are not present.
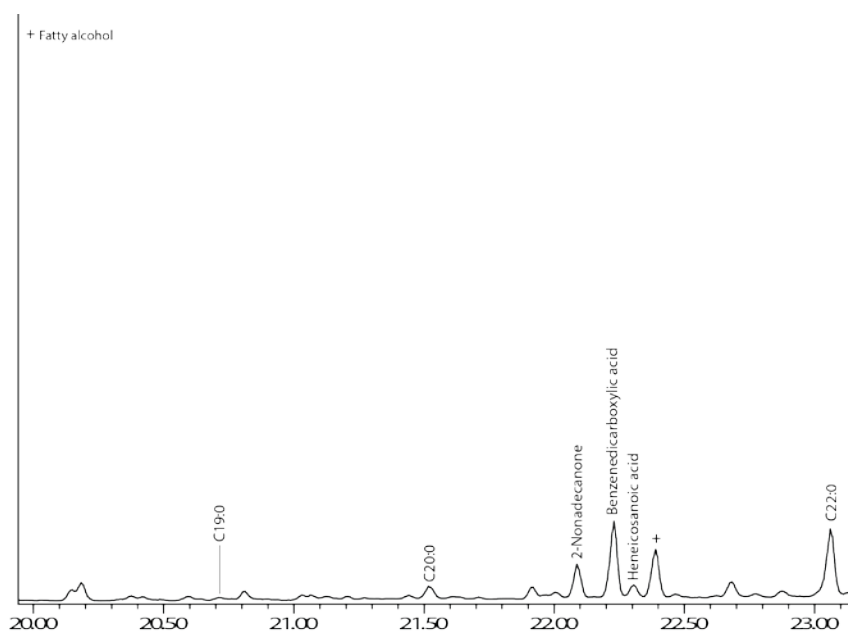
Figure 13.42. Partial gas chromatogram of the trimethylsilylated sample extract from sediment sample 10873, zoomed in from the previous image to show Dehydro-7-DHA, DHA, and 7-oxo-DHA are not present.

Spectra of tool extracts were compared to their underlying sediment samples. An example is presented in Table 13.6.

Table 13.6. Example of comparison of compounds found in a tool extract and its associated sediment sample collected directly underneath it, in this case from blade 108737. TMS stands for trimethylsilyl ester.

Compound	108737	108737_S
Pimaric acid, TMS	✗	✗
Isopimaric, TMS	✗	✗
Abietic acid, TMS	✗	✗
Dehydroabietic acid, TMS	✓	✗
7-oxo-dehydroabietic acid, TMS	✓	✗
Dehydro-7-dehydroabietic acid, TMS	✓	✗
Noanoic acid, TMS	✓	✗
Decanoic acid, TMS	✓	✓
Cycloheptasiloxane, tetradecamethyl-	✓	✗
Heneicosanoic acid, TMS	✓	✓
Tetradecanoic acid, TMS	✓	✓
n-Pentadecanoic acid, TMS	✓	✓
Hexadecanoic acid, TMS	✓	✓
Heptadecanoic acid, TMS	✓	✓
Octadecanoic acid, TMS	✓	✓
Nonadecanoic acid, TMS	✓	✗
Eicosanoic acid, TMS	✓	✓
Docosanoic acid, TMS	✓	✓
13-Docosenamide, (Z)-	✓	✗
Tetracosanoic acid, TMS	✓	✓
Pentacosanoic acid, TMS	✓	✓

Hexacosanoic acid, TMS	✓	✓

13.3.8 Controls

The method blanks and lithics with no microscopic traces of potentially resinous residues (negative controls) did not contain DHA, 7-oxo-DHA, or dehydro-7-DHA. An example of a method blank from a GC-MS run on June 15, 2016 is shown in Figure 13.43.
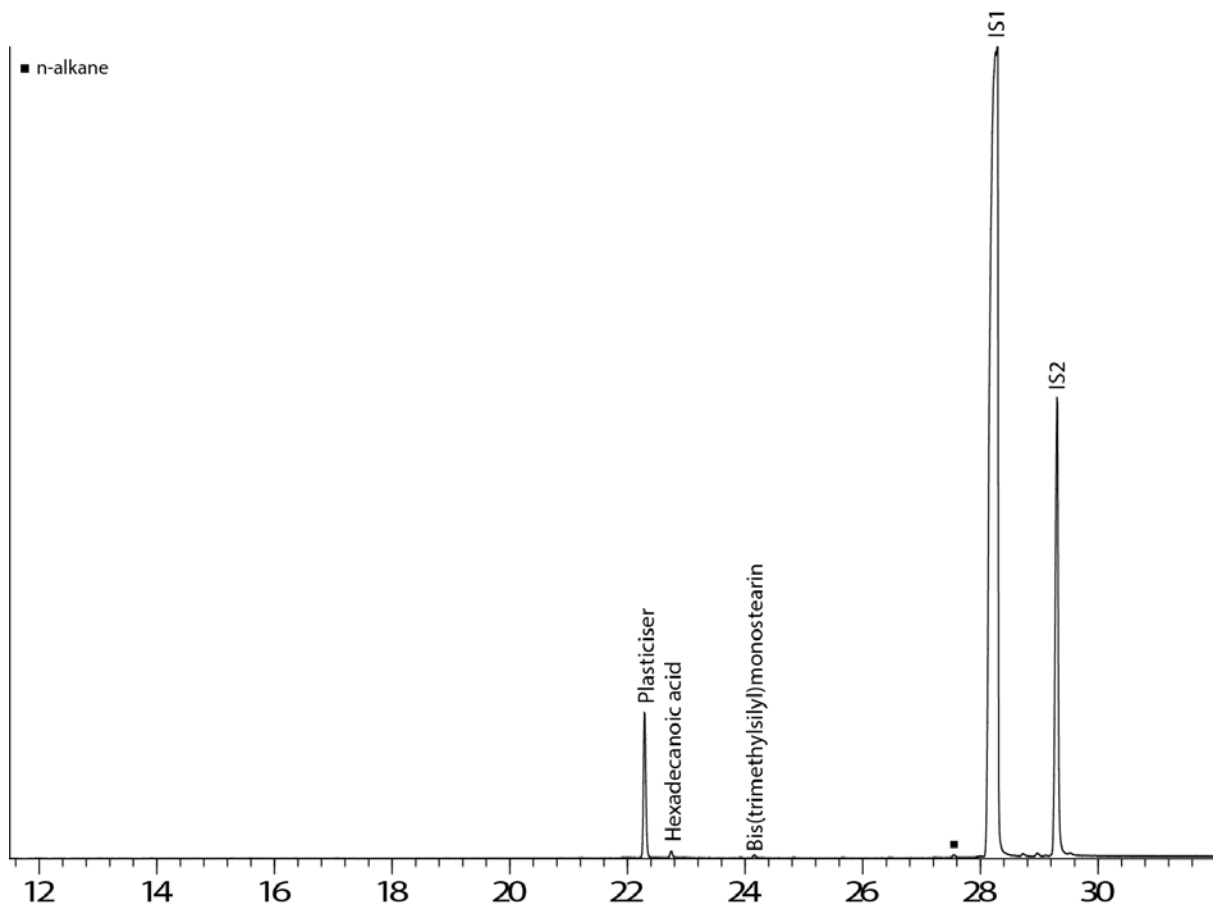
Figure 13.43. Partial gas chromatogram of the trimethylsilylated method blank.

13.3.9 Tools without resin compounds

Three of the twelve tools that were hypothesised to contain resinous residues based on microscopic observations did not contain them. The fact that some of the lithics suspected of containing resinous residues were negative highlights that microscopic visual observations should be tested by chemical characterisation techniques. The importance of objective hypothesis-testing to confirm or refute visual observations of amorphous residues is paramount to the methodological development of lithic residue analysis.

13.3.10 Contaminants

Some peaks in the mass spectra from both tools and sediments were identified as common modern contaminants. The mass spectral peak seen in nearly all samples at 24.0 min in chromatograms containing *m/z* ion 149 is $C_6H_4((CO)OC_nH_{2n+1})_2$ alkyl ester of phthalic acid, a compound found in plastic (Ji et al., 2013; Li et al., 2013). This most likely originates from the plastic zip lock bags used to store artefacts and sediment samples. Compounds further associated with plastic were found in tool TICs at retention times around 24 min (see tool extract chromatograms in Figures illustrated above). It is possible that the signal from these contaminant compounds has overlapped or masked compounds in archaeological residues. For instance, erucamide (13-Docosenamide, (Z)-) was a large peak commonly found in tool extracts at 24.1 min, a compound used as a slip agent in polyethylene products such as plastic bags (Lv et al., 2009). Hexanedioic acid, bis(2-ethylhexyl) ester was also found in four tool samples at ~ 21.16 min, which is also a plasticizer (Middleditch, 1989, p. 77).

Also commonly seen in all samples was a mass spectral peak *m/z* ion value of 73, which is $(CH_3)_3Si$ ions, representing the residue from trimethylsilyl derivatising reagents, in this case BSTFA. Some samples showed the combination of the following peaks: 73, 147, 207, 281, 295, 355, 429, identified as $((-CH_2)_2SiO)_n$

dimethyl polysiloxane, representing bleed from methyl silicone GC columns and septa (Sparkman et al., 2011, p. 514).

13.4 Discussion

13.4.1 Introduction

The context of pine resin residues found on nine stone tools from Star Carr is discussed below. Alteration compounds of pine resin, followed by the pathways of abietic acid degradation are examined. Concerns about the data obtained are appraised, and then a case is made for the intentional presence of archaeological pine resin on the stone tools based on the molecular, pollen, and ethnographic lines of evidence.

13.4.2 Compounds in fresh and altered Pinaceae resin

Pine tree resins contain several compounds specific to the family Pinaceae (Accompanying Material 5). Components of pine resin found in chromatograms may be classified into two categories: biomarkers, which are formed naturally in the tree resin, and alteration markers, which are formed by human processing such as heating and distillation of the resin, or formed by natural degradation factors of ageing. The presence and combination of specific compounds can be indicative of pine resin in a fresh or aged state, strong heating, and the level of degradation that has occurred. Identification of such a suite of diterpenoid molecular constituents in a total ion current (TIC) chromatogram is the most secure way to the diagnostic assignation of pine resin.

13.4.3 Alteration of pine resin compounds

The procedure for the identification of terpene resins in a gas chromatogram is not the straightforward matching between the chemical signature of fresh reference resins and the archaeological samples. Rather, resin compounds are altered by degradation and ageing, and the type of processing that took place (i.e. heating, distillation) – factors which can change the functional groups (van der Doelen and Boon, 1995). The physical properties of a resin residue such as volume or quantity of the residue present, its shape and thickness, and surface area exposed to light and oxygen will contribute to the chemical signals resulting from degradation processes. An additional factor to consider is the natural biological variation present in resins across different plant species and environmental conditions.

There are three main degradative factors which fragment or chemically alter the compounds in a fresh conifer resin: heat, light (photooxidation), and oxidation from air (autoxidation) or bacterial metabolic activity (Doménech-Carbó et al., 2006, p. 1267; Enoki, 1976; Milanova et al., 1995). It is known that molecular changes to pine resin occur just a few weeks after the exudation of the fresh resin from the tree, but the precise transformation pathways the original compounds take due to ageing and degradation processes in *Pinus* species resins are not yet fully described by gas chromatography-mass spectrometry (GC-MS), Fourier transform infrared spectroscopy (FTIR), or nuclear magnetic resonance (NMR) (Beltran et al., 2016, p. 4073; Enoki, 1976, p. 52; Langenheim, 2003, p. 26). However, research has elucidated some of the changes in resin compounds due to degradation and heating.

13.4.3.1 Alteration products of abietic acid

The chemical profile of raw unprocessed resin from Pinaceae trees contains levopimaric acid, neoabietic acid, abietic acid, dehydroabietic acid (in trace amounts), paulstric acid, and pimaric acid (Enoki, 1976, p. 57). Abietic acid in particular is found in abundance in the fresh (bleed) resin, but is transformed in

atmospheric conditions into more oxidised compounds (Beltran et al., 2016, p. 4073). Diagenetic processes lead to the chemical alteration of pine resin (Regert, 2004, p. 250). Aging and chemical alteration begins with oxidation of conjugated double bonds of abietane diterpenoids (levopimaric, abietic, and neoabietic acids), to form DHA, and oxygen is further incorporated to yield several derivative products of DHA (Scalarone et al., 2003, p. 615). Oxidation and isomerisation of the primary compound abietic acid produces several characteristic altered compounds: DHA, 7-hydroxy-DHA, 15-hydroxy-DHA, 3-hydroxy-DHA, 7-oxo-DHA, and 7-oxo-15-hydroxy-DHA (Pastorova et al., 1997, p. 43).

In addition to being markers for diagenetic ageing and natural oxidation, many pine compounds can also be interpreted as signals for heating of pine resin. High temperatures applied to pine resin compounds cause acceleration of oxidation reactions and the formation of altered derivative compounds, and there are examples of archaeological pine resin compounds being interpreted as a result of resin processed by heating (Egenberg et al., 2002; Font et al., 2007; Robinson et al., 1987). However, as Regert (2004, p. 250) points out, it is difficult to determine whether anthropogenic heating of the resin or simple natural decay is the origin of some of the derivative pine compounds, in particular DHA, 7-oxo-DHA, and dehydro-7-DHA.

Models of the alteration of abietic acid to produce derived compounds have been proposed by GC-MS studies (Proefke and Rinehart, 1992, p. 585; Scalarone and Chiantore, 2009, p. 333; 2000, p. 514, 1998, p. 565), FTIR (Beltran et al., 2016, p. 4081), and NMR (Enoki, 1976, p. 52), but are not yet completely resolved. Figure 13 illustrates a simplified version of the proposed oxidation and isomerisation reaction pathways of abietic acid, based on Proefke and Rinehart (1992, p. 585), Pastorova et al. (1997/8, p. 43), van den Berg et al. (2000, p. 514, 1998, p. 565) (1998; 2000), Modugno and Ribechini (2009b, p. 221 Fig. 8.5), and Lattuati-Derieux et al. (2014, p. 4). The pathways to produce the abietic acid alteration products 3,15-dihydroxy-DHA; 7,15-dihydroxy-DHA; and 7-oxo-15-hydroxy-DHA are not agreed upon in the literature. Additionally, dehydro-7-DHA (found in this study) is not present in any published oxidation model of abietic

acid, but it is clearly a derivative of DHA, so its position is suggested in Figure 13.44.
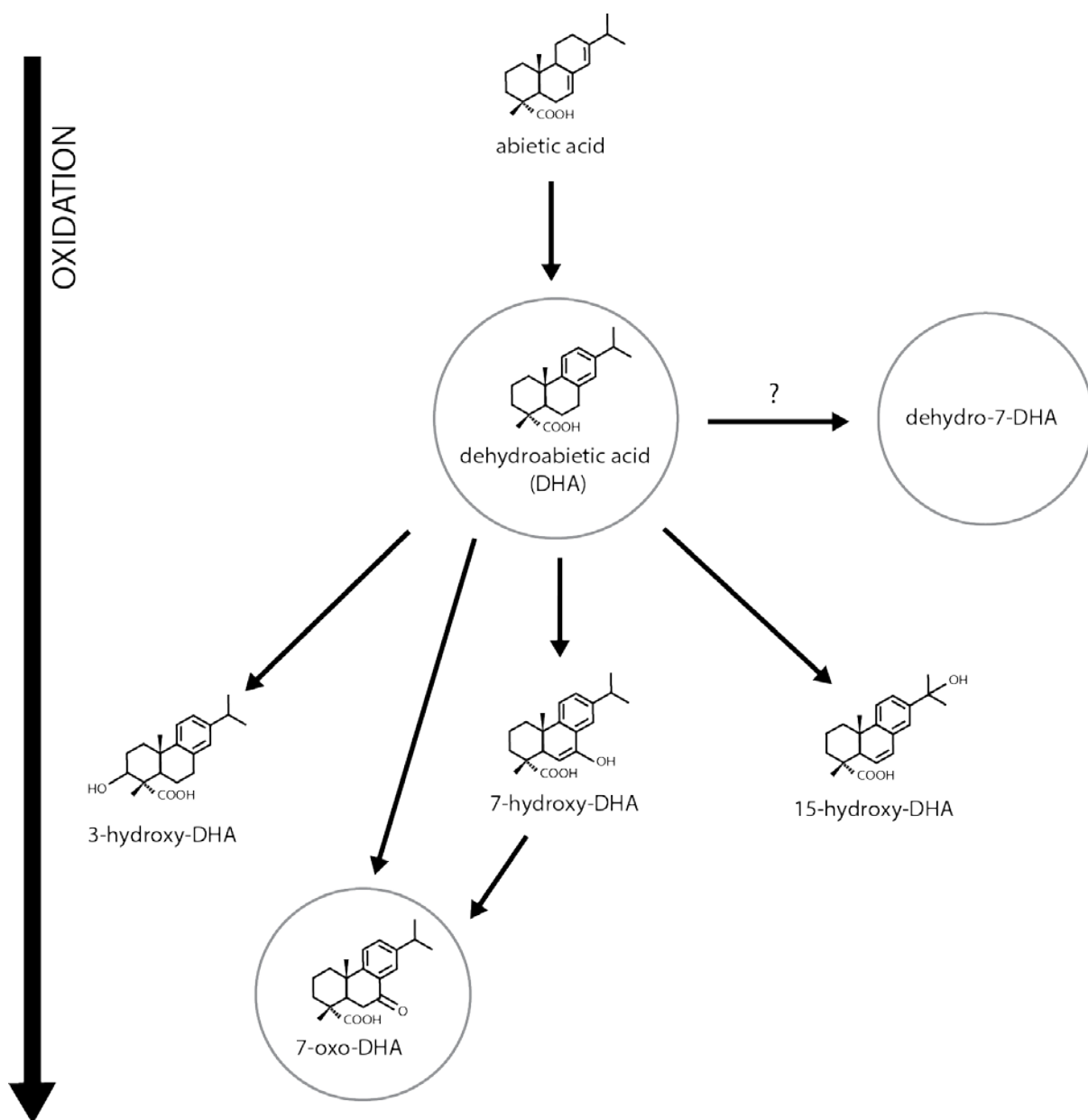
Figure 13.44. Proposed degradation of abietic acid into derivative compounds by oxidation and isomerisation. Compounds identified in this study are circled. Degree of oxidation increases moving down the flow chart. Based on Proefke and Rinehart (1992), Pastorova et al. (1997), van den Berg et al. (1998; 2000), van den Berg (2003), Modugno and Ribechini (2009), and Lattuati-Derieux et al. (2014).

13.4.4 Incidental or anthropogenic pine diterpenoid markers?

It is important to discuss the limitations of the data presented here. Interpretation of the results is particularly challenging given that we do not know what results to expect – no one else has attempted to use mass spectrometry techniques on lithics where the residues were only available in microscopic quantities. However, a liquid chromatography-mass spectrometry (LC-MS) analysis by Evans (David, 1998), reported successful chemical characterisation even when the lithics were completely devoid of microscopically-visible residues (discussed further below). There are four issues with the data presented here which prevent the definitive ascription of the pine compounds dehydro-7-DHA, DHA, 7-oxo-DHA to an archaeological pine resin source.

13.4.4.1 Lack of macrobotanical pine remains at Star Carr

The literature indicates that at the earliest Mesolithic sites in Britain, such as Star Carr and Thatcham, pine existed in relatively open landscapes (Milner and Mithen, 2009, p. 53). However, the evidence of pine macrobotanical remains at Star Carr is not strong enough to corroborate the chemical findings. In an archaeological mud layer at Star Carr, Walker and Godwin (1954, p. 59) identified *Pinus sylvestris* as present, although they state "... only one small piece of pine bark was discovered" (1954, p. 60). The presence of pine might also be suggested at Star Carr by two pieces of wood excavated in 2008 that were identified by Alan Hall to the level of division Coniferae. However, over the last excavation seasons (2013-2015), the POSTGLACIAL Project did not find any macrobotanical remains of pine wood, needles, or cones during excavations or within flotation samples (Radini et al., in press). The analysed wood assemblage shows willow (*Salix* sp.), birch (*Betula* sp.), and aspen (*Populus* sp.) were common (Bamforth et al., in press a, b). However, the fact that no macrobotanical remains have recently been located at Star Carr does not negate the idea that pine resin could have been collected when people traveled outside of the

immediate landscape. It is also possible that tools already containing pine resin were brought to site from elsewhere.

It might be posited that the tools found to contain pine resin compounds at Star Carr were heat treated in a fire containing embers of pine wood, and hence diterpenoid compounds would have transferred to the surfaces of the flint. Schmidt et al. (2016, 2015) proposed that heat treatment of silcrete was carried out at the Middle Stone Age site of Diepkloof Rock Shelter, South Africa, as evidenced by the similar presence and locations of black heat tempering-residues on both experimental and archaeological tools. Perhaps it is possible that Mesolithic people at Star Carr were heat treating the flint prior to knapping, but again there are no pine macrobotanical remains on site, so no evidence of fires with pine wood are present.

Terpenoid pine resin compounds can also be found within smoke particulates from burning pine wood (Simoneit, 2002). Wood burning experiments by Simoneit et al. (2000) and Fine et al. (2002, p. 1448) showed that dehydroabietic acid and 7-oxo-dehydroabietic acid, among others, were found in smoke residues from two pine species (*Pinus taeda* and *Pinus elliottii*). The tool samples from Star Carr did contain dehydroabietic acid and 7-oxo-dehydroabietic acid, which were also found in particulates in smoke from modern pine wood campfires. Other major markers reported in pine smoke by Simoneit et al. (2000) (pimaric acid, isopimaric acid, sandaracopimaric acid, abietic acids, retene, pimanthrene, methylcyclopentenophenanthrene, levoglucosan, and lignin phenolics such as vanillic acid) were not found in any of the tool samples or sediment samples. Also, dehydro-7-dehydroabietic acid (found in some tool samples), has not been reported in pine wood smoke, but has been reported in archaeological resin samples (see references in Accompanying Material 5). Additionally, the appropriateness of modern woodsmoke for comparison to ancient woodsmoke, that may contain compounds which have degraded or transformed over time, has not been examined.

Refitting sequences evidence tool manufacture both on and off site (Conneller et al., in press), so pine compounds originating from both locations must be

considered. Because no macrobotanical pine remains have been securely identified from Star Carr, there are a number of scenarios which are less likely or difficult to support: 1) the tools found to contain pine resin compounds were heat treated on site at Star Carr in a fire with pine wood embers, and further excavations may recover the pine wood, 2) tools were exposed to pine woodsmoke following discard at Star Carr, and further excavations may recover the pine wood, 3) people made tools off site using a fire treatment with pine wood, although no heat tempering-residues like those Schmidt et al. (2016, 2015) reported were found, or 4) people made tools off site that were exposed to pine woodsmoke that were brought to Star Carr.

Heat treatment does not make sense as a practical manufacturing choice for the flint artefacts found at Star Carr. Heat treatment is a sensible technique to use prior to knapping when the raw material is grainy and poor quality, such as silcrete. However, the majority of flint tools from the Star Carr are made of a high quality cryptocrystalline glacial till flint, so the fracturing properties would not be improved significantly by heating.

13.4.4.2 Variable morphology of posited resinous residues

Secondly, a clear and consistent connection between the microscopic appearance of black deposits and the positive identification of the pine resin compounds in tool extracts could not be established. Rather, a variety of black residue morphologies were seen on the tools from Star Carr, including granular, cracked, shiny and bubbly. Perhaps pine resin residues can exhibit multiple morphologies under the microscope; this seems to be supported by observations made during the experimental phase of research (Chapters 5 and 6). Experimentally buried pine resin residues were found in variable conditions, appearing granular, smooth, textured, amorphous, diffuse, shiny, opaque, and with colours ranging from white to red to brown/black. Aged Pinaceae residues from a wig dated to 895–1123 cal AD from Britain containing DHA (methyl ester), Dehydro-DHA (TMS derivative), DHA (TMS derivative), and 7-oxo-DHA (TMS derivative), identified with GC-MS were also a black colour (Cameron et al., 2017, p. 270).

13.4.4.3 Very small concentrations of pine compounds

Thirdly, the pine resin-related peaks (alteration markers dehydro-7-DHA, DHA, and 7-oxo-DHA) in samples were small, in every case yielding signals lower in abundance than other fatty acids and plasticizers present in the chromatograms. The quantity of dehydro-7-DHA in tool samples was between 0.013–0.636 µg, DHA between 0.120–0.328 µg, and 7-oxo-DHA between 0.028–0.440 µg.

The low abundance of pine resin compounds present might suggest contamination of the samples, but lab contamination can be ruled out as the source of the diterpenoid markers since none of the pine compounds were found in the method blanks. Also, a sediment source of the pine compounds from environmental contamination of the flint can also be excluded, since no sediments samples contained Dehydro-7-DHA, DHA, or 7-oxo-DHA. Recently, Costa et al. (2016) found abietic acid and/or DHA are produced by eight of 15 types of cyanobacteria from marine, estuarine and inland habitats. Thus, the status of abietic acid and DHA as biomarkers specific to conifer plants has been called into question, since abietic acid and DHA can be found in a diverse range of prokaryotic cyanobacteria. If the abietic acid and DHA found here on stone tools originated from cyanobacterial contamination, we would expect it to be present in the surrounding burial environment as well, but this was not the case. It is important to consider the minimal traces that were available for sampling in this study – microscopic residues – which may have contributed to the finding of only low concentrations of pine compounds detected in chromatograms.

It might be argued that the quantities of pine compounds present on the artefacts are too low to base archaeological interpretations upon. However, relatively low concentrations have been reported on other archaeological samples. For instance, Giachi et al. (2013, p. 1195) interpreted low concentrations of DHA and 7-oxo-DHA relative to the internal standard as indicating the presence of pine resin in a 2,000-year-old medicine tablet from an Etruscan shipwreck. Similarly, Bianchin et al. (2009, p. 444) found dehydro-DHA, DHA, and 7-oxo-DHA from an Italian Renaissance altarpiece painting, all in concentrations a tiny fraction of the concentration of the internal standards. Bianchin et al. (2009) argue that even

when pine resin compounds are found in low amounts, like their sample, they attest to the presence of Pinaceae resin.

13.4.4.4 Suites of related pine compounds

Fourthly, just three altered abietic acid marker compounds were able to be found in the tool samples. The identification of a full suite (five or more) of pine resin-related compounds from historical and archaeological samples have been described (Bailly et al., 2016; Burger et al., 2013; Egenberg et al., 2002; Fox et al., 1995; Helwig et al., 2008; Hjulström et al., 2006; Modugno and Ribechini, 2009a; Rageot et al., 2016; Regert, 2004; Regert et al., 2005; Ribechini et al., 2009, 2008), and such reports provide stronger evidence for the interpretation of ancient pine resin. On the other hand, there are also reports which identify pine resin on the basis of two (Giachi et al., 2013), three (Bianchin et al., 2009; Pérez-Arantegui et al., 2009; Proefke and Rinehart, 1992), or four (Čukovska et al., 2012) altered abietic acid marker compounds.

13.4.5 The case for an anthropogenic origin of pine resin

13.4.5.1 Pollen evidence

Perhaps the strongest argument for an anthropogenic origin to explain the presence of the pine compounds on stone tools from Star Carr is found in pollen records. At Star Carr, Scots pine (*Pinus sylvestris*) pollen is present throughout all the sequences taken from both the lake-edge (four monoliths) and from the lake centre (one monolith) of Palaeolake Flixton (Dark, 1998a, 1998b) (see examples). It likely that there was at least some pine among the predominantly birch woodland at Star Carr (Petra Dark 2017, pers. comm.). Dates published from 'Star Carr Monolith 1' (lake-edge), range from 9272–8756 cal BC (95.4% probability) to 8295–7789 cal BC (95.4% probability), and 'Star Carr Clark site' monolith (lake-edge), range from 9151–8629 cal BC (95.4% probability) to 8846–8423 cal BC (89.3% probability) (14C ages calibrated with OxCal v4.3.2, IntCal

13, Bronk Ramsey, 2017). These dates overlap with occupation dates obtained from a recent high-resolution dating programme at Star Carr (Bayliss et al., in press). The first Mesolithic human activity at Star Carr is modelled with radiocarbon dates to start at *9385–9260 cal BC* (*95% probability*), and end at *8555–8380 cal BC* (*95% probability*) (Bayliss et al., in press Fig. 17.2). Overall, the continuous pollen curves for Scots pine, in conjunction with pollen percentages of c. 10–20% and concentration curves that also suggest its pervasiveness indicate that Scots pine was highly likely to have been present in the wider landscape during occupation of Star Carr (Suzi Richer 2017, pers. comm.).

Example of a pollen percentage diagram of 'Star Carr Clark site' monolith (lake-edge), showing *Pinus sylvestris* pollen throughout the sequence. From Dark 2017 Fig. 2. Image for examination purposes only, to be removed prior to publication.

Example of pollen and spore concentrations from 'M1' monolith (lake-edge), showing *Pinus sylvestris* pollen throughout the sequence. From Dark 1998a Fig. 11.3. Image for examination purposes only, to be removed prior to publication.

Similarly, analysis of a pollen sequence sampled in 1949 by Donald Walker (Dark, 2017, p. 242; Walker and Godwin, 1954, p. 42) noted that *Pinus* pollen densities increased to replace *Betula* in dominance over the course of occupation of Star Carr, but no specific dates are given. Pollen data depicting the local and regional Mesolithic environments around Star Carr by Innes et al. (2011, p. 90) reports: "The forests of the Early Mesolithic were less variable, predating the major spread of oak and with alder and lime hardly present at all, but with pine present as a common constituent in specialist ecological niches on favourable soils."

Macrofossil and pollen evidence suggest that Scots pine entered England just after 10,000 BP, or c. 9655–9391 cal BC, (95.4% probability) (Bennett 1984) (14C age calibrated with OxCal v4.3.2, Bronk Ramsey 2017). Furthermore, palynological studies support the notion that pine, specifically Scots pine, was present across Europe the times of site occupation. Although all genera within the Pinaceae family are resin-producing, such as *Abies* (fir), *Picea* (spruce), and *Larix* (larch), the only genus documented in Early Mesolithic pollen records from south-east England, deposits spanning c. 9655–9391 cal BC, (95.4% probability) to 7580–7541 cal BC (95.4% probability), is *Pinus* (pine) (Reynier, 2005, p. 73) (14C ages calibrated with OxCal v4.3.2, Bronk Ramsey, 2017). At the beginning

of the Holocene (9655–9391 cal BC (95.4% probability), or ~10,000 BP), densities of *Pinus* pollen indicate that pine forests were extensive in the European mountains and the northern European lowlands. Also, refugia of pine existed in early Holocene Ireland and Scotland, and may have also been present in or near western Britain (Huntley and Birks, 1983, p. 308).

Two factors must be considered about pine pollen: 1) it is produced in great quantities, and 2) it can disperse great distances by wind.

Concerning the first factor, plant species differ in the amounts of pollen they contribute to sediments, and interpretation of pollen diagrams must take this into account (Davis, 1963, p. 897). Pine species are known to be high pollen producers – a pine tree can produce up to six million grains of pollen in a season (Buhner, 2011) (Figure 13.45). Thus, even though at times Scots pine pollen accounts for up to 20% of the total pollen during occupation at Star Carr (Dark, 1998a, p. 126, 1998b, p. 142), in reality this may mean pine trees were not in the immediate vicinity of Star Carr, but present in a few stands the wider landscape but still contributing heavily to the pollen assemblage.

Figure 13.45. Scots pine tree (*Pinus sylvestris*) in May releasing large quantities of pollen from the male flowers in York, UK.

In terms of the second factor, pine pollen is bisaccate (two air-filled sacs are attached to each pollen grain) and able to travel considerable distances from the tree, up to 100+ kilometers (Schuster and Mitton, 2000, p. 348). However, in a study of Scots pine pollen dispersal, Robledo-Arnuncio and Gil (2005, p. 13) found the tree has an average pollen dispersal distance of 135 m, with only 7% of effective pollen moving beyond 200 m of the source tree. Even when the pollen evidence is considered in light of the fact that a fraction of pine pollen can disperse great distances by wind currents, palynologists have still ascribed *Pinus* as present, although likely restricted to specific habitats, in Early Mesolithic environments near Star Carr.

13.4.5.2 Molecular evidence from a nearby Mesolithic site

Potentially supporting evidence for an anthropogenic origin of pine resin compounds exists from the nearby Mesolithic site of Seamer Carr (about 1.5 km northeast of Star Carr). There, *Pinus* resin, beeswax and traces of proteins (glutamic acid and glycine) were identified on one scalene triangle microlith, found in Boreal peat deposits (David, 1998). This tool was found within a group of microliths thought to be related in a multi-component tool, but no haft survived to confirm this idea. Although microscopic analysis of the tool did not detect any adhering materials, the organic residues were reportedly identified by differential infrared spectroscopy, GC, and high performance liquid chromatography (HPLC) by John Evans (David, 1998, p. 200). This scalene triangle was the only microlith which yielded organic residues out of 33 microliths analysed from the site. The organic residue analysis was described as inconclusive, likely because the methods were not very sensitive and no mass spectrometry was carried out. Sadly, any specific pine resin compounds that might have been identified were not described, the chromatograms were not included, which undermines the reported findings. Additionally, the original data from Evans study was not possible to obtain for comparison to the results presented here.

13.4.5.3 Long-term preservation

Conifer resins are known to preserve long-term, so even miniscule archaeological amounts like those found here are possible to trace. The burial conditions at Star Carr (in the waterlogged peat and the dry land, along with an additional alkaline control burial condition located off site), were experimentally shown to allow preservation of pine resin on flint, albeit within a short timeframe of 11 months (Croft et al. 2016; Chapters 5 and 6). Indeed, pine tree resin survived extremely well microscopically from all burial conditions tested.

Long-term preservation of conifer resin lipid compounds is very good, for instance lithified as amber. In fact, pine diterpenoid compounds, including abietic acid, dehydroabietic acid, and 15-hydroxy-dehydroabietic acid in conifer remains are known to preserve for millions of years. The discovery of diterpenoids by GC-MS in Eocene and Miocene deposits and macrobotanical pine fossils attests to their longevity (Otto et al., 2002, p. 1544; Otto and Simoneit, 2001, p. 3519; Stefanova et al., 2005, p. 96; Životić et al., 2013, p. 20).

13.4.5.4 Ethnographic evidence

The case for an anthropogenic origin of pine resin on stone tools from Star Carr is further supported in an analogical way by multiple ethnographic sources. Among hunter-gatherers, pine resin is universally viewed as a useful resource. Its exploitation for utilitarian items, medicines, and even food, is well-documented and remains widespread. Simple small incisions made in pine bark cause resin to ooze out of the wounds that is then easily collected (Hurcombe, 2014, p. 58).

In British Columbia, Canada, the Saanich and other indigenous nations used pine pitch (from *Pinus contorta*) as a glue to put arrowheads in shafts, and the Sechelt used the pitch (*Pinus contorta* and *Pinus monticola*) to waterproof canoes and baskets (Turner, 1998, p. 91). The Lower Stl'atl'imx used pine pitch to to seal fish hooks and mixed it with bear grease as a protective coating on fishing line and to glue the joints of harpoons and other tools (Turner, 1998, p. 91). The Nlaka'pamux gave stone pipes a glossy finish by using pine pitch with grease as a coating (Turner, 1998, p. 91).

Native Americans in California collected great quantities of pinyon pine (*Pinus edulis*) resin for use in a range of medicines. It was applied to the skin for treating splinters and boils, cuts, sores, insect bites, plastered hot on cloth for pneumonia, sciatica, and muscle soreness, chewed for sore throats, and also ingested in a tea as a remedy for colds, rheumatism, tuberculosis, influenza, and chronic indigestion. Native Californians also used sugar pine (*Pinus lambertiana*) resin as chewing gum, and applied it to burns and sores to aid healing, ingested as mild laxative and used dried and powdered to cure ulcers (Balls, 1962, p. 29). Also in California, people used pine resin to fasten flint points to arrow shafts (Laylander, 2000, p. 133) (originally in Eastwood, 1924), and one tribe (the Wintu) used pine resin as a sealant for whistles (Du Bois, 1935, p. 124). Additionally, most species of pines were used by some tribes of California for cement or glue (Balls, 1962, p. 29).

The Tarahumara people in Northern Mexico burned pitch pine sticks as torches for use in ceremonies (Bennett and Zingg, 1935, p. 284). The Maya in Mesoamerica collected *Pinus* resin at higher elevations and used it for incense, likely in ceremonial contexts (Langenheim, 2003, p. 296). In Malaysia, the Semelai people use pine resin (*Pinus merkusii*) for batik-making (wax-resist prepared cloth), paints, and soaps (Gianno, 1990, p. 94). The resinous inner bark of Scots pine was used as a food source by the Sami, and the practice of bark removal is evidenced by the presence of scarring still visible on culturally modified trees in Sweden, Norway, and Finland (Bergman et al., 2004).

The above ethnographic examples show that hunter-gatherers the word over view pine resin as a valued resource used it in myriad ways. Thus, it is suggested that any pine resin available to Mesolithic people in Britain could have been put to many applications.

13.5 Conclusion

To the authors knowledge, this was the first attempt to chemically test and identify microscopic amounts of lithic residues using GC-MS. Nine tool samples contained traces of DHA, 7-oxo-DHA, and Dehydro-7-DHA. These three compounds are derivatives of abietic acid – a biomarker found in the resin of trees of the Pinaceae family. Although the results should be considered preliminary, they are supported by the fact that the pine compounds could not be traced to sediments of the burial environment or a modern contaminant source from the lab. Additionally, the negative control group that contained no potentially resinous residues were negative for pine compounds, as expected, suggesting there may be a real link between the black amorphous residues observed and the positive identification of pine resin.

As Aveling and Heron (1998) showed, at least one plant-based adhesive, birch bark tar, was clearly used by the people visiting Star Carr. Contrary to expectation, and particularly considering the shiny black appearance of many residue deposits on artefacts, no chemical evidence of birch bark tar was found on tools, based on comparison with three different reference birch bark tars and the literature. Further research may be able to confirm the results here for pine resin at Star Carr. Positive replication for other lithics containing pine compounds in tandem with negative findings from their associated sediment samples is necessary. However, the finding of compounds consistent with pine resin may have significant implications for our understanding of the hunter-gatherers that visited Star Carr.

For instance, confirmation of pine resin at Star Carr would demonstrate that early Mesolithic people actively curated useful plant resources in the landscape. The fact that the only macrobotanical remains to suggest pine was present at Star Carr are one unconfirmed piece of Scots pine bark, and two pieces of wood identified to conifer (section 13.4.4.1), might suggest that people used pine at off-site locations, perhaps at higher elevations. Since pine resin naturally exudes from the tree, it could have been collected by people casually on an encounter

basis, when it was seen during travelling to or from Star Carr. Alternatively, perhaps resin production was made more predictable than the naturally occurring resin exudation by purposeful scarification of pine trees, as a type of plant management practice. The results presented here might also hint that a tradition of resin use existed. The radiocarbon dated deposits from which the nine tools were recovered range from about 9300-8500 cal BC (Radini et al., in press), suggesting the product was being used from the early phases of the site and continuing for perhaps about 800 years. It would not be surprising that Mesolithic people exploited any pine resin available. Ethnographic accounts of native peoples everywhere document the the use of pine resin, and also an intimate understanding of botanical resources within a wider network of traditional ecological knowledge (Turner, 2014).

On a methodological level, this study has supported the findings of previous investigations of residues in this thesis – microscopic observations of amorphous or ambiguous residues must be examined chemically. Again, chemical characterisation as a test for microscopic observations of lithic residues has shown that microscopic observations are not sufficient to identify amorphous residues or residues which lack diagnostic structures due to degradation, supporting the results of Monnier et al. (2012), Croft et al. (2016), and Pedergnana and Blasco (2016).

Improved results for the analysis of potentially resinous microscopic residues on stone tools may be possible with the use of highly sensitive chemical fingerprinting methodologies. Headspace solid-phase microextraction (HS-SPME) and GC-MS, with comprehensive two-dimensional gas chromatography-time-of-flight mass spectrometry (HS-SPME-GC×GC-TOFMS) was recently tested on modern reference residues including ivory, bone, antler, animal tissue, human tissue, sediment, and resin (Cnuts et al., 2016; Perrault et al., 2016). HS-SPME-GC×GC-TOFMS has the advantages of being a technique that 1) provides better resolution than traditional GC-MS, 2) is non-destructive to the residue, preserving ancient samples for replication or further chemical characterisation, 3) can be conducted on residues in their original state, and 4) extraction does not require solvents or derivatisation. Currently, it is not known if removal with a simple water

extraction like that used by Perrault et al. (2016) and HS-SPME-GC×GC-TOFMS would be successful on archaeological tools with resinous residues, especially tools that only have degraded microscopic quantities of resin available for testing. Perrault et al. (2016, p. 5) found that when tested with HS-SPME-GC×GC-TOFMS, the modern Norway spruce (*Picea abies*) resin, and two mixtures of the spruce resin and beeswax (one mixture heated only until melting point, the other mixture heated for an hour), had the most complex volatile profiles of all reference residues tested. Fascinatingly, unique volatile signatures were produced for the all spruce resin samples, even between the mixture heated to melting point and the mixture heated for an hour. These are exciting results since we may be able to gain even more nuanced information than is currently possible with GC-MS about ancient adhesive manufacturing methods using HS-SPME-GC×GC-TOFMS, perhaps differentiating quite sensitively between the time length of heating and temperatures used.

CHAPTER 14 DISCUSSION AND CONCLUSION

14.1 Introduction

When this project began, it was thought possible to locate and identify anthropogenic residues in situ on flint surfaces with relative ease, using only reflected visible light microscopy (VLM). This assumption was incorrect; the identification of microscopic lithic residues is in fact not usually a straightforward task. Archaeological lithic residues are complex, usually heterogeneous materials which have undergone degradation and interaction with the burial environment. It was proposed in Chapter 1 that a fourth major issue exists in the field of residue analysis: residues may be identified incorrectly. This is a substantial problem because a number of archaeological interpretations of ancient human and neanderthal behaviour, as well as inferences about cognitive abilities, have hinged on microscopic results. The findings of the experimental phase of research showed that many residue types are actually unidentifiable with reflected VLM because no specifically diagnostic structures were present (Croft et al., 2016). Thus, previously published claims of the discovery of particular lithic residues may need to be re-examined.

The results of this thesis stand as a crucial contribution to the methodological development of lithic residue analysis. The results showed that microscopic interpretations of residues should not be taken at face-value unless the residue being identified contains diagnostic structural characteristics. Ideas about the identity of amorphous residues are conjecture and should be formulated as hypotheses – serving as a jumping-off point to start further inquiry. Thus, for now, lithic residue analysis remains a time-intensive approach, requiring conservative microscopic analysis, and usually additional chemical interrogation techniques.

Many residues encountered on lithics from Star Carr might have been incorrectly interpreted as anthropogenic on the basis of the visual microscopic analysis alone. However, the testing of the visual observations of residues by application of further techniques (SEM-EDS, Micro-Raman, GC-MS) showed that:

- Red-orange deposits that appeared like resin were actually the alpha phase of iron (III) oxide (α-Fe_2O_3).
- Tiny clear crystal formations that appeared as silica plant phytoliths were actually gypsum crystals.
- Fibrous sheet formations which appeared like elongated articulated wood residues were actually gypsum.
- The white angular crystalline deposits that appeared like bone residues and were most likely related to quartz.
- Shiny gold deposits on the pendant that resembled the remnants of pigments were actually framboidal pyrite microcrystals.
- Brown stains within the lines of the pendant that resembled the remnants of pigments were actually organic detritus.
- Black amorphous residues that appeared like birch bark tar residues were not birch bark tar. Some samples contained compounds consistent with pine (Pinaceae) tree resin, but the results are considered preliminary.

The identification and minimisation of contaminants on artefacts is an ever-present issue in residue analysis. In fact, the results from the microscopic examination of 138 lithics from Star Carr combined with selected chemical characterisation of residues reinforced the importance of the first major issue in residue analysis: non-use related residues might contaminate artefacts. Most residues seen on stone tools in this study were natural: minerals including iron (III) oxide, gypsum, and pyrite were common, likely originating from complex and changing chemical interactions within the sediments at Star Carr (Boreham et al., 2011a, 2011b; Milner et al., 2011). The investigations of residues found on stone tools from Star Carr have yielded results which are surprising and of limited use in terms of contributing to our understanding of the archaeology. However, preliminary microscopic and GC-MS evidence suggested pine (*Pinus* sp.)

compounds were present in trace amounts on nine stone tools, and could be related to activities of Early Mesolithic people.

These findings have implications for the practice of lithic residue analysis, importantly demonstrating that microscopic identification of residues based on visual observations can be misleading. Thus, the use of chemical characterisation methods for testing residues is strongly recommended. This is especially true of those residues whose structure is non-distinct and nonspecific (e.g. resin, fat, bone, muscle, red ochre) and residues that are easily mistakable for other items (e.g. red blood cells for fungal spores, starch for bordered pits found on plant tracheids and vessel elements).

14.2 Research questions revisited

It is important to critically revisit the research questions posed in Chapter 1 of this thesis. Below, the extent to which the research questions were answered is addressed.

1. Is there potential for residues to survive on lithics at Star Carr?

This question was addressed during the experimental phase of research (Chapter 5 and 6). The preservation of a variety of plant, animal, and mineral residues on flint flakes were tested in two archaeological burial contexts at Star Carr (wetland, dryland), and one off-site control context (alkaline). Some experimental residues did survive across all burial conditions and over the short time intervals tested (one month and eleven months). These surviving residues included bird feathers, squirrel hair, softwood tissue, tree resin, and red ochre, although it was noted that keratinised remains were unlikely to survive over longer time scales at Star Carr. It was surprising that the microscopic remains of bone and antler working – expected to exhibit long-term durability – did not survive after 11 months burial in the wetland or dryland contexts at Star Carr.

2. Which residues can be identified on stone tools from Star Carr and what do they tell us about the lives of Early Mesolithic hunter-gatherers?

Given the exploratory nature of the application of lithic residue analysis at Star Carr and the techniques used in this project, it was necessary to pose an open-ended question without prejudgement of potential results. The investigation of the modern reference residues showed that not all residue types contained structural features which would allow them to be diagnostically identified. Thus, an identification guide was devised that grouped residues commonly found in the literature into diagnostic, distinct, and non-distinct categories, along with the specific structural features which are present/absent in each residue.

In terms what was gained from the residues that informs us about the lives of Early Mesolithic people, the results are disappointing, but challenge the discipline of residue analysis to build a firmer methodological foundation. The results of this study have mainly yielded identification of environmental contaminant residues from that originated from the archaeological burial environment. Nevertheless, preliminary evidence was presented that suggests pine (*Pinus* sp.) compounds may be present in trace amounts on nine stone tools from Star Carr.

3. What techniques are most useful for the discipline of lithic residue analysis?

The techniques that were found to be the most useful for the analysis of lithic residues in this study were VP-SEM-EDS, GC-MS, and Micro-Raman. Other techniques outside of those used here, such as FTIRM, DESI-MS or MALDI-TOF, might also be successfully applied to archaeological residues. VP-SEM-EDS makes an excellent screening technique for lithics since organic (carbon-rich) vs inorganic residues can be quickly identified. This is especially useful in cases where information regarding the soil chemistry and specific burial conditions are not available. GC-MS and Micro-Raman were found to provide the most specific, and therefore most conclusive, data, yielding identifications made at the molecular level. Both GC-MS and Micro-Raman are considered techniques that

can provide adequate resolution to be molecularly specific. Structural information and identity of the molecule is determined in GC-MS by calculation of the mass fragmentation pattern containing the ions from broken up molecules and Micro-Raman by measurement of the vibrational modes of the molecules detected by the movement of atoms and bonds.

Reproducibility is a problem when using GC-MS to investigate microscopic lithic organic residues, since the immersive sonication method used here for residue extraction usually removes visual traces of the original residues in their entirety. On the other hand, replication is not an issue for the application of Micro-Raman to investigate in situ lithic residues because it does not require total destruction or removal of the residue (the laser burns an area of the residue of only a few microns or less). The Micro-Raman technique and its surrounding literature appears to be ideally positioned for the identification of items which have a crystalline structure, such as mineral components, and not as easily able to achieve high specificity when organic residues are tested, but this partly due to the usually fluorescent nature of organic residues.

14.3 Implications

14.3.1 Amorphous residues cannot be identified visually

As was established during the experimental phase of research (in Chapter 5 and Croft et al. 2016), there are many residues which defy identification because they lack diagnostic structural features. These amorphous residues are ambiguous even in the unaltered 'fresh' state, and require chemical characterisation for successful identification. Thus, hypothesis-testing of visual observations with specific and sensitive techniques is imperative for amorphous residues. Residue analysts need to recognise which residue types are diagnostic, distinct, and non-distinct (amorphous) (Croft et al., 2016). By acknowledging cases when

microscopic residues are actually ambiguous, as recommended by Monnier et al. (2012), lithic residue analysis can avoid interpretations built on shaky evidence.

14.3.2 Consideration of the burial environment

The cases presented in this thesis have provided evidence that indicates residue and usewear analysts need to understand as much as possible about the chemical and physical processes occurring within the burial environment from the beginning of the project. The contribution of the burial environment has probably led to false positive identifications of archaeological residues. A good understanding of the soils and/or sediments from which archaeological material was recovered is important so that suspected contaminants can be discounted quickly. For instance, it was not expected that mineral deposits would be present on top of flint surfaces as both amorphous concretions and crystalline structures. These items could have perhaps been identified faster if geochemistry sources were consulted first. In the case of the iron oxides, gypsum, and shiny deposits, the burial environment can be responsible for non-anthropogenic, false traces on flint stone tools. The way to ameliorate this problem is to increase our knowledge of sediment chemistry, geochemistry, taphonomy, biological agents, and the reactions that can lead to the observed phenomena on stone tools.

The collection of small (~ 5 g) sediment samples with each artefact recovered in the field for residue analysis is recommended to assist in the identification of contaminants. Sediment sampling has been suggested by other residue analysis workers, although no one has applied this measure on the systematic scale as was protocol at Star Carr. These sediment samples can be compared both microscopically and chemically to results obtained from residues on the stone tool surfaces. Here, this evidence was used to rule out the origin of residues as contaminants from the burial environment in the case of the Pinaceae resin compounds. Additionally, the sediment samples provided the basis to identify contaminants. The pyrite framboids and gypsum microcrystals observed on several artefacts were also found within their corresponding sediment samples.

14.3.3 Consideration of post-excavation handling and processing

Some traces on flint can appear post-excavation that may be mistaken for anthropogenic residues or usewear. It was discovered that the formation of several shiny deposits on stone tools (Chapter 10) were linked to simply washing tools in ultrapure water. This was evidenced by the presence of macroscopically visible shiny deposits mirroring the very locations on the tools where water had pooled in contact with the drying tray. Sometimes these deposits were found to contain exact impressions of the folds of the clingfilm with which the tool was in contact. This confounds the identification of any usewear polish on tools from Star Carr, since it is clear that some shiny deposits formed as a result of, or were altered significantly altered by, basic washing with water. The following question is raised: can the polish and shiny deposits observed on tools from Star Carr arising from post-excavation handling, natural, or cultural processes be differentiated by microscopic techniques?

14.3.4 Multiple independent lines of evidence

Multiple independent lines of evidence provide more rigorous interpretations that can support or refute subjective visual observations of lithic residues. When the residue observed is amorphous and cannot be securely identified, these additional lines of evidence should include characterisation by chemical means, such as energy dispersive x-ray spectroscopy (EDS or EDX), gas chromatography–mass spectrometry (GC-MS), confocal Raman microspectroscopy, and Fourier transform infrared spectroscopy (FTIR). And indeed, several researchers have already chemically characterised amorphous residues suspected to be hafting residues (Bleicher et al., 2015; Boëda et al., 2008, 1996; Cârciumaru et al., 2012; Charrié-Duhaut et al., 2013; Dinnis et al.,

2009; Grünberg, 2002; Hauck et al., 2013; Helwig et al., 2014; Koller et al., 2001; Matheson and McCollum, 2014; Mazza et al., 2006; Monnier et al., 2013; Ollé et al., 2014; Pawlik and Thissen, 2011; Villa and Roebroeks, 2014).

Current thought has advocated establishing a connection between usewear and residues together to make a case for anthropogenic stone tool use, but this may be unjustified, as the locations of usewear and residues may not always be closely related spatially. Xhauflair et al. (2017) found random residue distributions without apparent links to usewear locations on experimental tools. That residue locations can be random agrees with the findings from the experimental phase of research presented in Chapter 5. Rather, during the use of experimental flint tools on a variety of plant and animal materials, residues were not confined to working edges, but occurred all over the tool. It is possible for residues to be concentrated on edges, but requiring this pattern to interpret the residue as anthropogenic may be unfounded.

14.4 Is lithic residue analysis 'scientific'?

The trend of recent publications in lithic residue analysis suggests more researchers in the discipline are striving to become increasingly scientific. With more examples of archaeology in general employing new techniques borrowed from chemistry, physics, and biology, increasing availability and decreasing costs of sample processing, this development is perhaps not surprising. 'Scientific' here means employing the scientific method to systematically observe a phenomenon, test a hypothesis, collect empirical data using the senses that is measurable, and then evaluate the original hypothesis.

That the phenomenon under investigation (in this case residues on stone tools) is measurable or quantifiable in some way is an important attribute because it removes analyst bias, and allows clear and objective results to be obtained that

can be assessed by other researchers. Measurability of the phenomenon in question brings transparency to the process and production of novel findings, and demystifies residue identifications. For lithic residue identification, Monnier et al. (2017a, p. 159) are proponents of the development of analytical techniques that are: "1) preferably less dependent upon analyst expertise, 2) more objective in data interpretation, and 3) can help us to understand the processes of alteration and degradation." These considerations are important to address and are integral to the development of residue analysis. While no method is completely objective, if we aim to strategically use subjective modes of inquiry (such as microscopic observations of nondiagnostic residues) as the basis to generate hypotheses for testing with objective methods, this will be a solid foundation upon which to move forward in the discipline. The adoption of more objective methods will also permit independent confirmation of results and better levels of reproducibility to be achieved between researchers. This adoption should include a validation process for each method used in residue analysis to assess its adequacy to suit its intended purpose, its reliability, whether it has suitable operational conditions for obtaining results, and its limitations (Hlinka et al., 2009, p. 151).

The results of the investigation of lithic residues at Star Carr have fortified an argument that science is well-positioned to provide reliable answers. As Wylie (2000, p. 228) and others have pointed out, science of course does not operate in a vacuum or transcend the contexts of its production. Rather, it is operated by variable human actors, and is subject to the social and political climate in which it takes place. The separation between theory and method is considered as a central methodological problem in lithic residue studies and has been addressed via multiple studies presented in this thesis. If there are a number of competing hypotheses to explain the presence and identity of a particular residue, the method used must be independent and neutral, rather than predicated on one theory being true (Johnson, 2010). Overall, the author supports the recent move towards lithic residues being tested by scientifically verifiable means, and believes this should become standard practice.

14.5 Future residue work recommendations

Research is beginning to focus on bringing new techniques into residue analysis in addition to microscopy. Residue analysts are working to form closer ties with researchers in chemistry, physics, biology, materials science, geology, and other areas, and this is certainly a productive direction for the discipline. The formation of more interdisciplinary collaborations between archaeologists and scientists is not, however, without challenges. For instance, as Nigra (2015, p. 12) point out, one stumbling block is the differing backgrounds and research interests between anthropological archaeologists and analytical chemists. Another barrier to collaboration is communication. Use of language, concepts, and theories which are not mutually understood between the parties involved can be an obstacle to progress.

In future, the analysis of residues from stone artefacts would be most profitably applied to: 1) lithics with visible surface deposits from which micro-samples can be retrieved, 2) ground stone objects such as querns, grinding vessels, lamps, stone containers, that have pores which absorb and protect residues, as recommended by Evershed (2008, p. 915). Targeting artefact types which have a porous mineral surface or obviously contain deposits on their surfaces will mean residue analysts have a higher chance of recovering residues significant to the reconstruction of human behaviours and archaeological interpretations.

This research has built upon current methodological strides that have been made in the field of residue analysis. Of most pressing concern, this research has found the sole use of visual microscopy as an accepted practice in residue analysis is certainly questionable. A healthy level of scientific skepticism is warranted in residue analysis and provides a sound base for further technical and methodological development.

APPENDIX 1 DETAILED RESULTS FROM RESIDUE BURIAL EXPERIMENT

Introduction

This appendix accompanies Chapter 6. It presents the detailed results from the microscopic observation of each experimental tool from each of three experimental conditions (n= 78) from the residue burial experiment. Chapter 6 contains the synthesis of these observations.

Results: detailed

The reference collection containing residues in a 'fresh' state was first analysed to form the basis to interpret experimentally degraded residues. These observations of unaltered residues were compared to residue appearance after burial. Then, microscopic analysis was carried out on each buried flake from each unit and time interval. VLM and SEM micrographs were collected for the twelve residue types in the reference collection, as well as the blank stone material. Figure A1.1 is a visual presentation of the results from each individual flake included in the experiment. The two left columns of the table show residues from the reference collection in the fresh state. The columns to the right show the extent of preservation for each residue type in each experimental condition. Comments and observations specific to burial unit and time are detailed below.

Residue type	Fresh state	Fresh state	Dryland 1 month	Dryland 11 months	Wetland 1 month	Wetland 11 months	Alkaline 1 month	Alkaline 11 months
Bone				no bone residues identified	no bone residues identified	no bone residues identified		
Antler				no antler residues identified	no antler residues identified	no antler residues identified		
Muscle				no muscle residues identified			no muscle residues identified	no muscle residues identified
Fish				no fish residue identified	no fish residue identified			no fish residue identified
Bird								
Squirrel								
Potato				no starch residues identified		no starch residues identified	no starch residues identified	no starch residues identified
Reeds								
Softwood								
Hardwood				no hardwood residues identified				
Resin								
Red ochre								
Control								

Figure A1.1. Residue preservation by type, burial condition, and burial time.

Bone

Reference collection bone

The bone residues in the reference collection had no diagnostic traits but appeared as white to cream crystalline flakes with jagged angular edges. The

442

max diameter of reference bone residue flakes measured in micrographs was 500 µm.

Bone 1 Month dry land

Preservation index rating (0-5): 1

Very little bone was preserved, and of the natural crystalline pieces were difficult to distinguish as bone. A greasy film and associated fat was present on ventral side.

Bone 11 Months dryland

Preservation index rating (0-5): 1

A translucent light brown residue with no diagnostic features was found restricted to working edge on both dorsal and ventral sides of the tool (see Figure A1.2). The residue is sometimes associated with white crystal flakes, located at the inner boundary of the residue. This translucent brown edge residue possibly originated from tissues still attached to bone while it was worked. It can be suggested that the white crystal flakes represent flint attrition and damage accrued during use, since they are not comparable to the morphology of bone flakes seen in the reference collection.
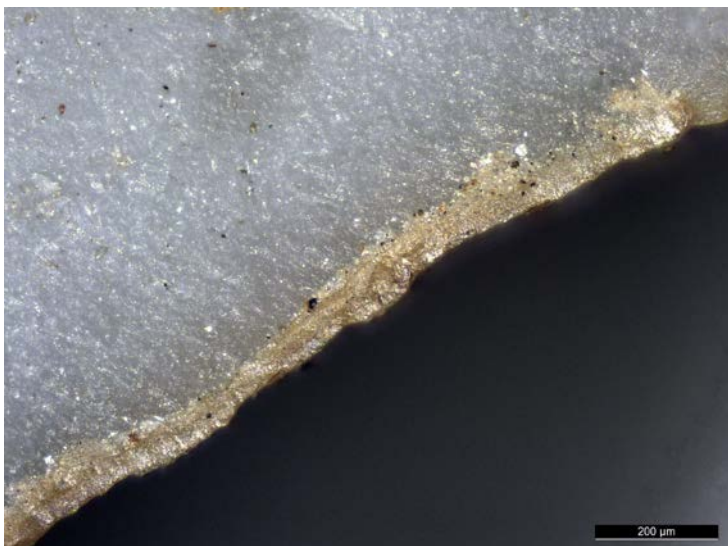
Figure A1.2 Residue line present on a flake that was used to work fresh bone with tissues, after burial for 11 months in the dry land unit at Star Carr. Note the absence of bone flakes.

Bone 1 Month wetland

Preservation index rating (0-5): 1

Bone residues were difficult to identify from the wetland. White material, probably bone microremains, appeared as lumpy white granular bumps with relatively smooth edges and with brown/translucent tissues associated (Figures A1.3 and A1.4). In contrast, the bone in the reference collection was greasy, and bone crystalline pieces were jagged irregularly shaped with ragged edges.
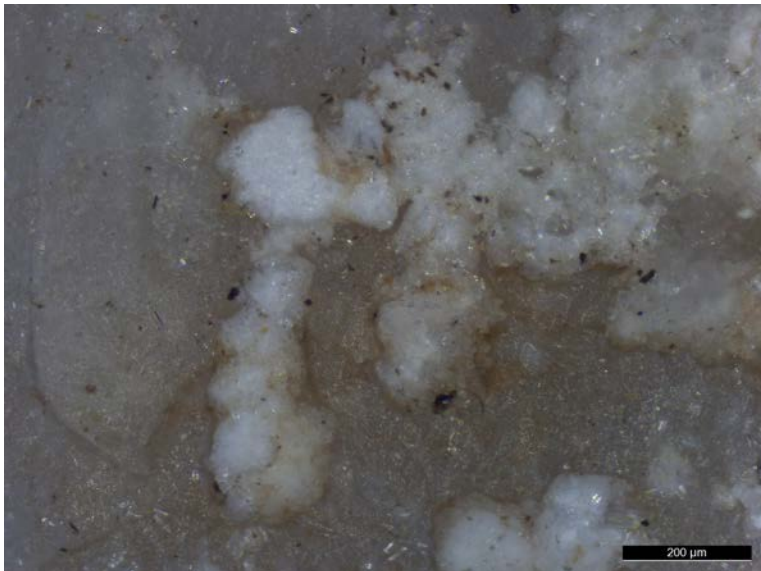
Figure A1.3. Possible bone residue on flint buried in the wetland for 1 month.
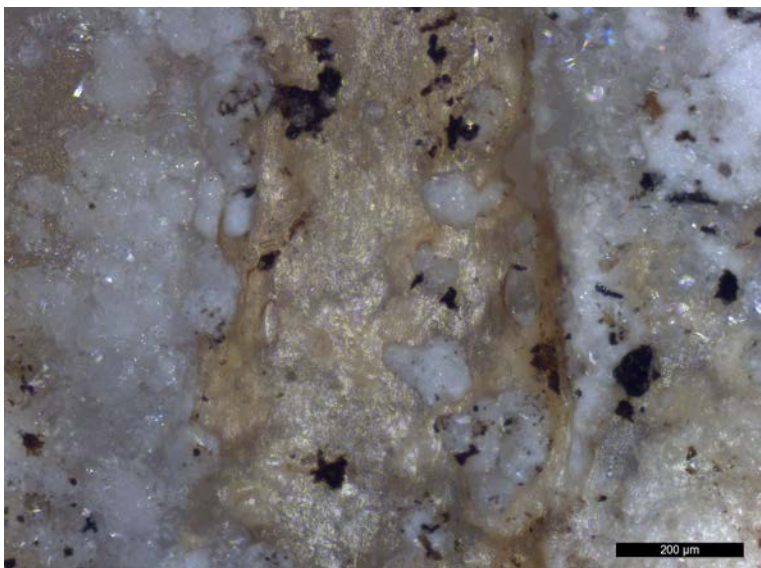
Figure A1.4. Possible bone residue on flint buried in the wetland for 1 month.

In terms of post-depositional alterations, brown/green staining and crystal formations were found all over this flake, and crystals were found growing on the potential bone residues, complicating identification. In addition, the remains of saprophytic fungi with septa were found on top of the potential bone. Jans (2005), provides images of histological sections of archaeological bone showing tunnelling by microbes and fungi that remove collagen and mineral components of bone. According to Jans, bone can be greatly altered due to the nature of the burial environment, for instance by crystal formation such as framboidal pyrites and microbial action. Extensive microbial alteration and corrosive environments with low pH can cause bone microscopic structure to become unrecognisable. Calcium-deficient apatite crystals have a granular surface texture (see Legeros and Legeros, 2008, p. 385), which is consistent with the visual appearance of the putative bone residues. This may suggest that the calcium in the bone has been dissolved in the acidic peat sediment by demineralization.

The presence of bone residues on the flint flake could not be confirmed due to morphological dissimilarity with the bone from the reference collection. However, it is likely that bone residues were present, but unrecognisable due to being degraded and smoothed on a microscopic level from the acidic burial condition and digestion by fungi and/or bacteria (Figures A1.5, A1.6).
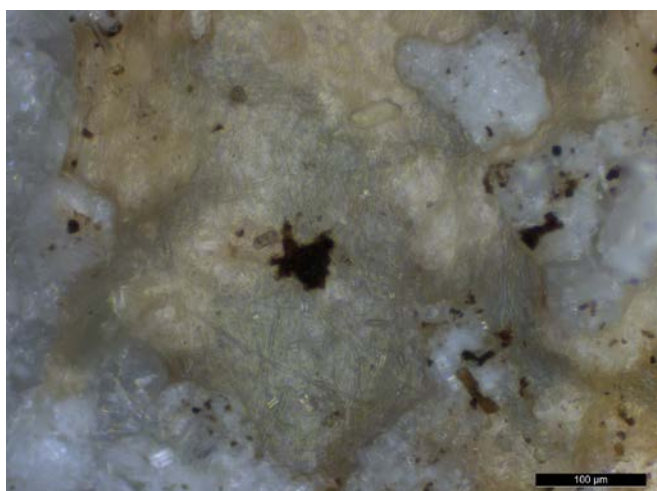
Figure A1.5. Possible bone residue and fungal hyphae on flint buried in the wetland unit for 1 month.
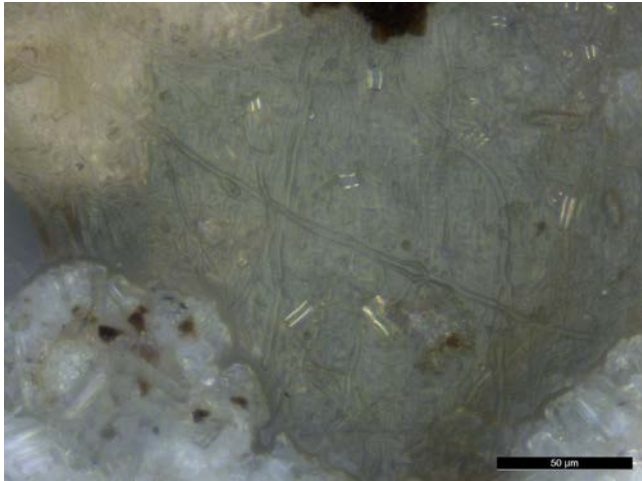
Figure A1.6. Possible bone residue and fungal hyphae.

Bone 11 Months wetland

Preservation index rating (0-5): 0

There were no identifiable bone fragments identified. Macroscopically, white crystalline material was present on the edge of the flake. The crystal formations are clear lath, rhomboid, and fine rosettes, most likely gypsum.

Bone 1 Month alkaline

Preservation index rating (0-5): 2

No residues were visible to the naked eye on the flint. When viewed with the microscope, crystalline translucent to yellow fatty bone pieces with irregular edges were seen on both dorsal and ventral surfaces (Figure A1.7). Non-bone crystal pieces were present as natural parts of the stone (Figure A1.8). These flint crystals were always found as rectangular crystals within a rectangular depression with brown to amber staining. These non-bone stone crystals are larger and more regularly shaped than bone pieces.
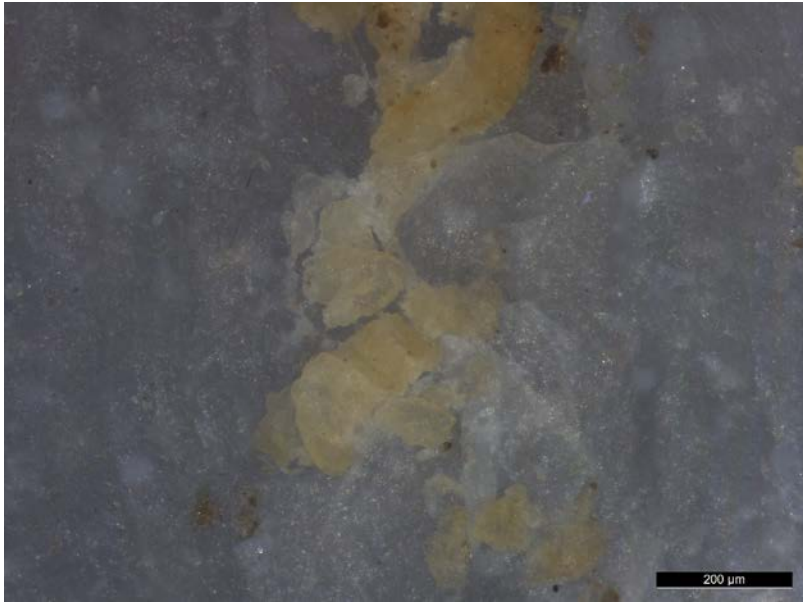
Figure A1.7. Bone residue on lithic after 1 month burial in the alkaline control condition.

Figure A1.8. Natural crystal structure in the flint.

Bone 11 Months alkaline

Preservation index rating (0-5): 1

Probable fatty bone residue was located on the ventral side of the flake accompanied by yellow fat, but no diagnostic features were present to make a secure identification. White patches were visible macroscopically, but these were found to be non-bone white mineral inclusions on surface of the flint. The white patches were composed of small granular crystals of roughly uniform size, visible

with the 50x objective lens. These white granular mineral deposits did not appear as individual jagged bone fragments as seen in the reference collection. Photographs of tool before and during tool use show the white patches are part of the natural stone, not bone residues.

Antler

Reference collection antler

Similar to the bone residue, antler showed no diagnostic morphological traits. This residue had a crystalline flake-like appearance but occasionally an elongate crystalline structure, with no discernible substructure, was also seen. Antler residues were white to taupe in colour. The largest antler flakes seen in the reference residue had a max diameter of about 575 μm.

Antler 1 Month dry land

Preservation index rating (0-5): 1

This flake most likely does contain antler, however, no distinctive traits of potential antler flakes were found. The morphology of antler residues in the reference collection appear as crystalline flakes with ragged edges and variable colour. On the dorsal side of the flake, a light brown residue line was present representing the extent of penetration of the flake into the antler was discerned. Large deposits of cortex were found on this flake, which appear as granular, chalky, bright white inclusions that contain sub ovate pieces.

Antler 11 Months dryland

Preservation index rating (0-5): 1

Translucent brown residue present on both dorsal and ventral sides of the working edge, roughly similar in appearance to the translucent brown residue seen on the bone working tool. Again, white crystals were present in association with the translucent brown residue, which could arise from flint damage.

Antler 1 Month wetland

Preservation index rating (0-5): 1

Antler preservation at a microscopic level within the wetland burial context appears to be poor, similar to bone. On the ventral side of the flake, one white deposit with shiny translucent material associated was found. This might be degraded antler, but it is not morphologically similar to the reference collection examples. Orange and clear colourless crystal formations were present on this flake.

Antler 11 Months wetland

Preservation index rating (0-5): 0

No identifiable antler fragments were located. Rosette and lath crystals were found on the edges and center of the tool (Figure A1.9).
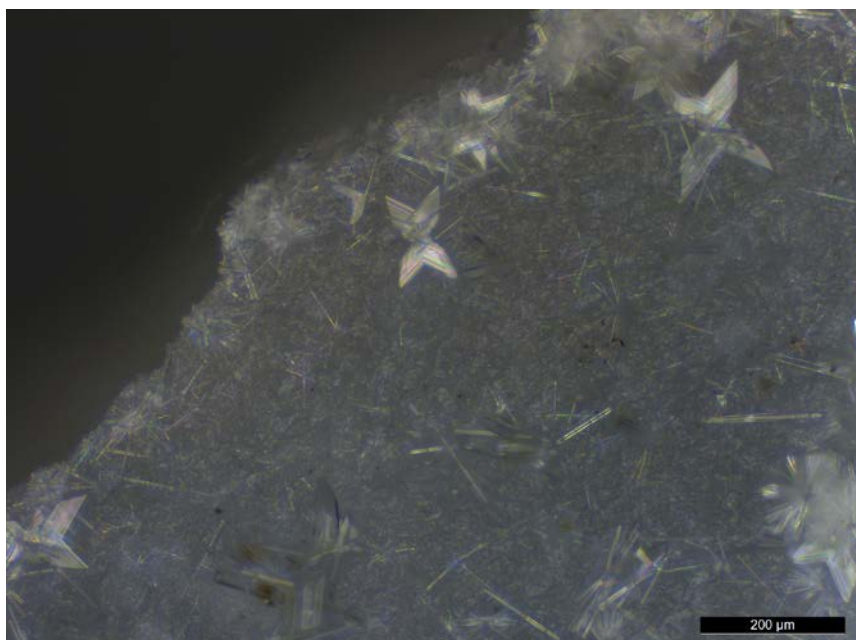
Figure A1.9. Rosette types 1 and 2, and lath crystals on experimental flint piece used on antler, buried in the wetland unit for 11 months.

Antler 1 Month alkaline

Preservation index rating (0-5): 4

A visible thick white crumbly deposit was present macroscopically on the flint. Under the microscope, the antler residues appear as crystalline pieces or

irregularly shaped flakes with jagged edges, ranging from white to cream to light brown. The morphology of the microscopic residues provide a comparable morphological match to antler in the reference collection, although there are no specific diagnostic characteristics. Adhesion was not very strong, as a large piece of the antler residues detached from the dorsal side of the flake.

Antler 11 Months alkaline

Preservation index rating (0-5): 1

Probable yellow crystalline antler residues were found in crevices on both the dorsal and ventral sides of the flake, some with hyphal invasion. No diagnostic features of this residue but there was general agreement between reference collection antler residue and the residues seen on this flake, both have crystals of various sizes with jagged edges.

Muscle

Reference collection muscle

The reference residue for muscle was from beef and during cutting with the flint probably contained some fat as well. The muscle residue was dried and myofibres with cross striations (also known as 'banding') characteristic of striated muscle (Kenyon 2012, page 1273), were sometimes visible with reflected VLM (see images in Croft et al. 2016). Surprisingly, the distinctive banding seen within the myofibre structure with VLM, was not found in the SEM images taken even at 500x. Identification of muscle tissue residues are not expected in archaeological materials, since no beef muscle myofibres with banding were found on any flint flakes buried in the experiment.

Muscle 1 Month dry land

Preservation index rating (0-5): 1

Possible striated muscle tissue was found remaining on the dorsal edge of the flint, appearing as light brown thin translucent residue or stain. The residue was not able to be confidently identified visually due to lack of diagnostic structures.

Muscle 11 Months dryland

Preservation index rating (0-5): 1

Probable muscle tissue and fat deposits were found on both dorsal and ventral sides of the flake. This residue was light brown and translucent, somewhat reflective, with small white crystalline pieces sometimes incorporated within it, but no diagnostic structural features of muscle (myofibres with banding) could be identified. However, the locational restriction of this residue to used edges is highly suggestive that this is the remnants of the original muscle tissue. While this residue was most likely muscle residue, no distinctive features were present to be able to identify the residue as muscle without question.

Muscle 1 Month wetland

Preservation index rating (0-5): 3

This piece had a large sheet of white fibrous tissue visible with the naked eye. At the edges, jumbled overlapping fibers could be seen, and clear translucent muscle fibers stretched out across crevices were also visible. The muscle fibers have a morphology which is ragged, irregularly shaped, with pointed and frayed at ends. It was determined that these items were not fungal hyphae since they lacked septa (cross walls) and smooth outer walls, as would be expected in hyphae.

Muscle 11 Months wetland

Preservation index rating (0-5): 2

A piece of possible muscle tissue was found with crystal formations overlying it, visible macroscopically. The piece of possible muscle appears brown, greasy, stringy, however there are no diagnostic characteristics to form a secure identification. The fine stringy appearance of the observed residue could have been muscle fibers. The possible muscle was found wrapped around the working

edge on both the dorsal and ventral sides of the tool. Poor adhesion of possible muscle residue to the stone substrate was noted, as most of the piece was dislodged during analysis.

Muscle 1 Month alkaline

Preservation index rating (0-5): 0

Concentrations of black fungal spores were found on both dorsal and ventral surfaces. The spores and hyphae could be evidence of the locations where fungi digested the original plant or meat residues (as has been suggested by Haslam, 2006, p. 120), and perhaps a thin fatty residue remains. A residue that looked like possible muscle was found, but it lacked bands of cross striations within myofibres, as would be expected in muscle tissue.

Muscle 11 Months alkaline

Preservation index rating (0-5): 0

No remnants of muscle residues were found remaining. Fungal hyphae were present on the tool.

Fish

Reference collection fish

The reference collection flakes were used to cut into the integument and muscle of a Cyprinid fish. Thus, the fish residues seen in the reference collection contained a suite of residues. These were: scales, chromatophores (at least two types), and muscle tissue. Scales were the most obvious type of residue, with clear concentric ridges (circuli) emanating from around the focus (centre of the scale). Fish, crustaceans, cephalopods, amphibians, and reptiles contain chromatophores, which are pigment containing or light-reflecting cells. There are different types of chromatophores, depending on the hue they display in white light. Melanophores (black/brown) and iridophores (reflective/iridescent) were

observed in the fish residues in the fresh state (see Frohnhöfer et al. 2013). The melanophores were observed as tiny dots and gave the fish residue a speckled appearance. Melanophores were only visible with the 50x objective, and were significantly smaller in size when compared to the iridophores. Iridophores are crystals which are birefringent under the microscope (Parker 2012, page 118).

Fish 1 Month dry land

Preservation index rating (0-5): 1

No scales were found preserved and no distinctive residues were present after one month burial in the dry land at Star Carr. There were light brown, semi-transparent residue lines on the edges of the flint which lack diagnostic structure and were amorphous.

Fish 11 Months dry land

Preservation index rating (0-5): 1

No diagnostic residues such as fish scales were identified on the tool. Both dorsal and ventral sides of the tool showed an abundance of possible circular brown fatty deposits in locations where fish was in contact with the tool (Figure A1.10). The dorsal side also had a possible fatty fish tissue residue. The residue remains on this piece were so different from the fish residues in the reference collection, it was difficult to find congruences apart from the greasy appearance of deposits.
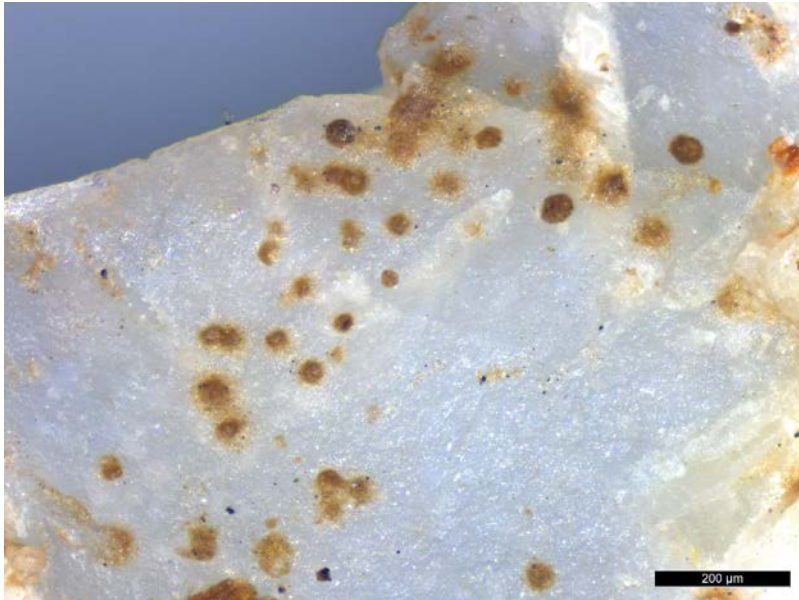
Figure A1.10. Possible circular fatty fish deposits left after 11 months burial in the dry land at Star Carr. Note the absence of diagnostic structural features of this residue.

Fish 1 Month wetland

Preservation index rating (0-5): 1

No scales or morphologically distinct residues were present. Perhaps some fat and muscle residue remained in a small amount on the flake.

Fish 11 Months wetland

Preservation index rating (0-5): 3

A possible greasy fish residue was encountered on the dorsal side of the tool, but it lacked distinctive morphological features. On the ventral surface, two large scales were found preserved. The scales showed some degradation of the annuli, and the lines were not as sharp as when the scales were fresh. Heavy crystal formations were present underneath the scales, which were found lifting from the stone. In fact, both scales fell off during analysis due to poor adhesion.

Fish 1 Month alkaline

Preservation index rating (0-5): 3

Scales and other probable fish residues were visible with bare eyes. The scales, which displayed clear circuli, were found on the ventral surface and appeared

cracked. The cuticle of a worm was also present overlying one of the fish scales, evidence of the high biological activity present in the alkaline burial unit at Star Carr.

Fish 11 Months alkaline

Preservation index rating (0-5): 0
No fish residues were able to be identified on the surfaces of the tool. Fungal hyphae were present. Plumose manganese oxide dendrites were relocated on the flint surface, which were present prior to tool use.

Bird

Reference collection bird

The reference for bird (greylag goose) was a suite of residues including muscle tissue, fat, and feather fragments, however, only the downy feather barbules were able to be identified as diagnostic with VLM. Downy feather barbules were identifiable by the presence of nodes and prongs. Node to node distance, also known as the internode length, was 80 μm. Node max width ranged from 9-13 μm. Downy feather barbules were diagnostically identifiable with VLM, but the prongs were also noted with SEM.

Bird 1 Month dry land

Preservation index rating (0-5): 3
Feather barbules were found on both dorsal and ventral edges.

Bird 11 Months dryland

Preservation index rating (0-5): 3
Feather fragments were visible macroscopically on both dorsal and ventral sides of the tool. Prongs on feather barbules were visible with the 20x and 50x objective lenses.

Bird 1 Month wetland

Preservation index rating (0-5): 4

Feathers were visible with the naked eye during recovery after one month burial (Figure A1.11). Microscopically, nodes and prongs were visible. White crystal formations could be seen all over tool, probably originating from the peat burial environment. The crystals could be gypsum.

Figure A1.11. Recovery of experimental flakes from the acidic wetland unit after one month. Note the preservation of hair and feathers still visible.

Bird 11 Months wetland

Preservation index rating (0-5): 4

Feather fragments were still visible on both dorsal and ventral surfaces of the flint flake, and a whole intact feather was present on the dorsal side. Possible muscle tissue was also located on the ventral side of the tool. Similar to the observations of possible cow muscle residue (see above), crystal formations were found on top of possible bird muscle tissue. Poor adhesion was noted for the large feather, as it appeared that it would easily dislodge from stone surface.

Bird 1 Month alkaline

Preservation index rating (0-5): 3

A large feather was seen macroscopically on the dorsal surface, and feather barbules were visible microscopically on both sides of the flake. On one of the ventral edges, a bright black residue was found. This residue was very reflective in normal light, and turned black when viewed with the polariser/analyser. It is unknown whether the black residue originates from burial in the alkaline unit, although this seems unlikely for two reasons. Firstly, the residue is restricted to the ventral edge, an edge which was used to butcher the goose. If the black residue arose from the sediments of the burial environment, we could expect the residue to be seen in randomly distributed locations over the tool surface. Secondly, all flakes were washed with a gentle stream of ultrapure water prior to analysis, so loose sediments were mainly removed. An interesting bright blue residue was present on the flake edge which appears to be a well adhering contaminant, perhaps incorporated onto the tool when it was used in the laboratory.

Bird 11 Months alkaline

Preservation index rating (0-5): 2

Feather fragments of various sizes were seen macroscopically on both sides of the tool. Feather barbule prongs were visible with the 20x objective lense, and nodes were visible at 50x. Brown shiny globules were associated with feathers, which are probably fat. Hyphae were also present on the flint.

Squirrel

Reference collection squirrel

The squirrel residue suite included dried tissues of muscle, as well as blood and hair, but only the hair was found to be diagnostic. The squirrel hairs in the reference collection were quite variable in size, with the following hair widths

recorded: 13 µm, 19 µm, 20 µm, 48 µm. The presence and pattern of the medulla and cuticular scales were captured in VLM. Hair was diagnostically identifiable with VLM. SEM imaging shows the scale patterns more clearly than the reflected VLM micrographs, but since SEM captures surfaces only, the medullary pattern inside the hair is not visible.

Squirrel 1 Month dry land

Preservation index rating (0-5): 3

This flake contains hair and associated amorphous residues that appear as thin greasy light brown smears. The hairs can be confirmed as originating from a rodent or bat due to the presence of coronal scales. Fungal material was also present. On the ventral side, there is a band of weak polish and light brown colour staining along left edge.

Squirrel 11 Months dryland

Preservation index rating (0-5): 2

Squirrel hairs were present macroscopically on dorsal and ventral surfaces. Hairs were in association with what appear to be brown fat globules and light brown translucent residue, likely from squirrel soft tissue. This piece may represent a case in differences in degradation that can occur on the scale of the individual artefact. Hairs that were observed on ventral surface were very degraded, and the scale pattern was not visible and cuticle not intact, although the medullae were still visible. On the reverse side of the tool, the dorsal surface, hairs showed a clear and well-defined scale pattern. No hyphae were found on this tool.

Squirrel 1 Month wetland

Preservation index rating (0-5): 4

Lots of hair was visible with the naked eye all over the flake, both at the time of recovery (Figure A1.11) and after cleaning. The squirrel hairs displayed much variation in colour, thickness, and the scale pattern appeared slightly different between hair types, and depending on the region of the hair (i.e. basal vs end).

Squirrel 11 Months wetland

Preservation index rating (0-5): 4

On the dorsal and ventral surfaces, an abundance of hair was visible macroscopically. On microscopic inspection, the hairs showed scales and pigmentation was intact. Hair was determined to be in excellent condition, with no discernable degradation detected. However, adhesion of hairs was poor and some hairs were incidentally removed during analysis.

Squirrel 1 Month alkaline

Preservation index rating (0-5): 3

Upon inspection with the naked eye, fine hairs were visible. The red blood crusts that were present before burial were no longer visible during microscopic analysis. Adhesion of the hair was poor and some hairs fell off the flake.

Squirrel 11 Months alkaline

Preservation index rating (0-5): 1

On the dorsal side of the piece, there were four hairs with damaged cuticles but the scale pattern and medullae were still visible. On the ventral side, one blond coloured hair was found with the scale pattern very eroded. All hairs were attacked by clear fine fungal hyphae. Possible red ochre was found on the ventral right corner edge, indicating potential cross-contamination.

Potato

Reference collection potato

Large colourless starch granules of *Solanum tuberosum* were found as expected in the potato residue. During reflected VLM observation of the reference potato residue on flint, round and ovate granules that displayed partial extinction crosses in cross polarised light were found. Eccentric hila within the granules seemed to be present, but the granules would require extraction and viewing with transmitted VLM to confirm. No lamellae, hila, vacuoles, or other features were

visible with SEM. However, the three-dimensional shape of the granules was better imaged with SEM. SEM may be helpful in cases where the 3D shape of the granules are difficult to capture with reflected and transmitted VLM, for instance lenticular shapes that settle on slides in the flat orientation (polar view). The 3D shape of starch granules is routinely examined by applying a small amount of pressure on the coverslip of the slide with a probe, for example with an acupuncture needle or wood skewer. This procedure is only applicable to certain types of slide mounting media (e.g. water and glycerol) and thus ineffective with in situ starch on stone.

Potato 1 Month dry land

Preservation index rating (0-5): 2

Degraded ovate starch granules appeared to be present in an aggregate of about 15-29 granules on the ventral side of the flake, on a projection. The granules are about 25-60 μm in maximum diameter, within the expected size range for potato starch. There was clear fungal attack damage of the potential starch, with hyphae and black fungal spores that resembled caviar. Optical features of starch such as the three dimensional shape, extinction cross, lamellae, hilum, etc. were not visible with reflected light microscopy (metallurgical microscope). These features can be observed by mounting on glass slides and use of transmitted light microscopy. Extraction, mounting on slides and transmitted light microscopy would greatly assist in the identification of starch characteristics, particularly as this is a case where granules appear modified.

Potato 11 Months dryland

Preservation index rating (0-5): 0

No potato starch granules were able to be identified on this tool. It did contain possible potato residue on the dorsal side, which appeared brown to orange and rough surfaced, without distinctive borders or edges, similar in appearance to possible fat globules. On the ventral side, residues of light brown patches with no diagnostic features, probably potato residue, were also found. Some of the light brown patches are heavily overlain with fungal spores, perhaps evidence of

fungal digestion of the original residue and subsequent fruiting, a hypothesis put forth by Haslam (2006, page 120 b).

Potato 1 Month wetland

Preservation index rating (0-5): 4

Starch preserved in great abundance on the flake after one month in the peat, and also in the sediment directly underneath the flake. Starch granules were in excellent condition, as if native starch granules were unmodified by taphonomic processes. Faint extinction crosses appeared small and centric within granules under polarised light. This was unexpected since the hilum is known to be eccentrically located in potato starch. The centric appearance of granule hila may be due to the in situ nature of viewing, which appears to distort conventional optical properties of starch granules.

Potato 11 Months wetland

Preservation index rating (0-5): 1

Nondiagnostic plant residues were located on the dorsal surface. During microscopic scanning of the ventral surface, possible degraded starch was encountered, however only orange outlines remained. Rosette crystal formations were found on the dorsal distal right edge, likely gypsum. A contaminant starch granule was present, lying on top of sediment on the tool. This starch granule could have originated from air/dust in circulation system.

Potato 1 Month alkaline

Preservation index rating (0-5): 1

Some questionable starch was found on the dorsal surface of the flake. Black outlines of circular structures could be defining where starch granules were located. No residues were identified on the ventral surface.

Potato 11 Months alkaline

Preservation index rating (0-5): 0

No starch or other residues were found on the tool.

Reeds

Reference collection reeds

The reference residues from reeds contained cells with an elongate sub-rectangular structure and well-defined cell walls. Green chlorophyll pigments within the reed residue were also still intact at the time of viewing, although these would not be expected to survive in archaeological residues. Examination of the reed residues with SEM illustrated cell wall structure and also showed the reed leaf tissues contained long crystals.

Reeds 1 Month dry land

Preservation index rating (0-5): 3

This flake has green staining penetrating deep into the center of the flake from the edges, which is visible with the naked eye. There are green stained deposits visible on edges, and in cracks and furrows on surface. Chlorophyll must still be relatively intact on the flint surface after one month burial in the dry land. Reed leaf fibres and leaf epidermal tissue fragments with preserved cellular structure present. A well developed polish is also present, probably due to the high-silica content of the worked reeds.

Reeds 11 Months dryland

Preservation index rating (0-5): 3

Large macroscopic pieces of reed leaves were still present on the dorsal side of the tool. Cell walls and stomata in the leaves were visible at 160x magnification. Some chlorophyll was preserved within the reed residues on both dorsal and ventral surfaces, as the original green colour of reed leaves was apparent. Fine black hyphae were seen on the ventral surface.

Reeds 1 Month wetland

Preservation index rating (0-5): 2

This flake contained a large brown stained area with siliceous reed fragments on nearly the whole surface. No green was colour remaining in the reed residues, indicating destruction of the chlorophyll pigments. Reed epidermal tissue was present with visible double walled cells, comparable with the reed reference residue. Clear colourless crystal formations in spiky druse shapes were noted on the piece.

Reeds 11 Months wetland

Preservation index rating (0-5): 2

Large pieces of reflective loosely adhering yellow brown plant material was visible macroscopically on both dorsal and ventral surfaces. Microscopically, double wall cell structure diagnostic of plant remains was visible. It appears that no green chlorophyll from the original reed leaves preserved on this flake. The plant remains were more than likely reed leaves, however, since only one nondiagnostic feature (plant cell structure) was visible and no green colour indication was present, an absolutely certain identification could not be made.

Reeds 1 Month alkaline

Preservation index rating (0-5): 3

On the dorsal and ventral surfaces, silicified tissue with cellular structure in sheets and fibres were seen. Some chlorophyll in the reed leaf tissue was preserved after a month buried in the alkaline unit. Macroscopically, green patches were associated with silicified residues, concentrated on flake edges and in central area of flake.

Reeds 11 Months alkaline

Preservation index rating (0-5): 2

On the dorsal edges of the tool, what appeared to be macerated silicified reed tissue with cell walls was found, well adhering to the stone. This tissue had undergone a colour change after 11 months burial in the alkaline unit from bright

green to shiny brown/green. On the ventral side of the tool, no individual cells from reed leaves were identified, however, likely reed fibrous silicified material was found. These pieces are white and reflective, and exhibit a rainbow effect. Brown and green staining was also present over distal edge region on the ventral side. It was determined that the original reed residue probably had been found, based on the combined presence of cell walls and the location of brown/green staining. The brown and green staining was visible on edges used to work reed leaves, contrasting with clean surface in the interior of the tool. At least three types of hyphae were recognised on the flint.

Softwood

Reference collection softwood

The wood residues from the softwood that were examined in situ on experimental flakes with reflected VLM lacked diagnostic anatomical features. However, many wood residues were distinctive in appearance to allow tentative, but not secure, identification. In particular the presence of bordered pits (structures that assist in the movement of water, nutrients and solutes through plants) are likely indicative of tool contact with woody plant matter. In the softwood, bordered pits were only found with SEM.

Softwood 1 Month dry land

Preservation index rating (0-5): 3

This piece has brown staining concentrated at working edges, visible with the naked eye. On the right ventral edge, tracheids were present with spiral thickening of the secondary walls and bordered pits observed. Wood cells associated with resin deposits were also seen. Curiously, circular structures that resemble starch granules were found embedded in resinous residue. These items are about 10-20 μm in max diameter.

Softwood 11 Months dryland

Preservation index rating (0-5): 1

Very few woody residues were visible macroscopically on this tool. A tracheid with bordered pits was identified on the dorsal left distal edge with the 50x objective. On the ventral side of the tool, translucent brown silicified plant tissue was present on the edge but no diagnostic features could be identified. The translucent brown residues from working wood appears similar to the residue seen from working animal muscle, like a thin brown stain restricted along the edge with some small angular crystalline pieces incorporated. This occurrence of overlapping residue appearance shows that materials which are totally different – plant wood and animal muscle – can present extreme difficulty in their distinction when examined in situ with reflected light microscopy only. Also observed on the tool were plumose manganese oxide dendrites which were present on the flint surface before experimental use and burial. No hyphae were located on the tool surfaces.

Softwood 1 Month wetland

Preservation index rating (0-5): 3

A large piece of wood tissue and wood fibers were easily visible on the flint. Tracheids with discernable bordered pits were identified.

Softwood 11 Months wetland

Preservation index rating (0-5): 3

On the dorsal surface of the flake, woody tissue was visible macroscopically, which was a light tawny colour. Microscopically, this woody tissue revealed bordered pits visible with the 50x objective. Similarly, on the ventral surface, tracheids with bordered pits were found, which are diagnostic to coniferous trees, also identified with the 50x objective. Extensive rosette and lath shaped crystal formations were present. These appeared as salty deposits on the stone with the naked eye.

Softwood 1 Month alkaline

Preservation index rating (0-5): 2

Silicified fibrous softwood residues were found to be present but infrequently occurring. Bordered pits and spiral secondary wall thickening on xylary elements were observed with the 20x microscope objective. Additionally, some likely amorphous softwood residues were also present, ranging from flat and patchy to granular, although these lacked diagnostic features.

Softwood 11 Months alkaline

Preservation index rating (0-5): 1

Vegetative tissues were well adhering to the stone surface, likely softwood residues, found on both dorsal and ventral surfaces. Tracheids with well-defined bordered pits were identified, which were well-adhering to the stone surface. A faint edge staining was visible from working wood on the ventral distal edge. Fungal hyphal networks were present on the tool.

Hardwood

Reference collection hardwood

Reference residues from the hardwood that were examined in situ on experimental flakes with reflected VLM lacked anatomical features that would allow secure identification, similar to the softwood residues. However, closely packed alternate intervessel pits were identified on several vessel elements. Each pit was about 10-12 μm in max diameter. That these pits were visible is surprising since no light passes through the residue when viewed in situ. SEM imaging of the hardwood tissue revealed the presence of crystals, probably calcium oxalates, and permitted better visualisation of intervessel pits.

Hardwood 1 Month dry land

Preservation index rating (0-5): 3

Wood fibres and woody tissue fragments are visible. The wood tissues fragments appear in a range of colours: clear, amber, and dark brown. The dorsal left distal edge contained woody tissue fragments, wood fibres, and vessel elements with large intervessel pits.

Hardwood 11 Months dryland

Preservation index rating (0-5): 1

Few woody residues were visible macroscopically on this tool. Possible hardwood tissue fragments were located on the dorsal and ventral sides, however no diagnostic features were identified. Possible hardwood residues appear to have undergone a colour change from light brown and amber colour to dark brown. Dark brown plant tissue fragments were often found in the soil samples from all three burial units in the experiment.

Hardwood 1 Month wetland

Preservation index rating (0-5): 3

Hardwood fibers were visible with the microscope on the flint, and perhaps also vessel elements, but the presence of pits was unclear. Ambiguous residues were associated with the woody tissues which appeared as thin shiny smear of light brown, highly reflective material.

Hardwood 11 Months wetland

Preservation index rating (0-5): 2

Woody residues were visible macroscopically. Microscopically, intervessel pitting was identified with at 320x magnification. Extensive rosette and lath shaped crystal formations were present on the tool.

Hardwood 1 Month alkaline

Preservation index rating (0-5): 4

On the dorsal left edge, vessel elements with pits were present in broken up fibrous clumps. Brown deposit were visible macroscopically on the ventral

surface. Also on the ventral side of the tool, silicified vascular tissues including vessel elements with pits were associated flat translucent plant exudates.

Hardwood 11 Months alkaline

Preservation index rating (0-5): 2

Vegetative tissue, probably hardwood residue was found on the dorsal and ventral edges, but no diagnostic morphological features were identified, such as individual vessel elements with pitting. There is no way to confidently exclude that the vegetative tissue did not originate from the burial environment. It is assumed here that hardwood residues were present, due to their location and associated staining restricted to edge areas. A clear stain line was present on the ventral left edge visible macroscopically, extending about 5 mm inwards.

Resin

Reference collection resin

The pine tree resin reference residue was amorphous, with no anatomical structural units. It appeared granular at low magnifications (160x or less) and shiny and orange at higher magnifications (320x or more). It is worth noting that while raw pine resin was used in the experiment, other resins will probably exhibit different characteristics in terms of colour and texture. With SEM, the resin still appeared relatively rough in texture and amorphous. Resin residues that were experimentally buried underwent a change in colour from semi-translucent reddish-orange to largely opaque grey/white with only small spots of shiny orange remaining visible.

Resin 1 Month dry land

Preservation index rating (0-5): 4

Large blobs of resin covered in dirt is visible macroscopically on this flake. Much of the resin surface occluded by sediment, but some portions still appear amber-coloured and shiny.

Resin 11 Months dryland

Preservation index rating (0-5): 4

Large white resin lumps visible macroscopically on both sides of the flint, and orange amber shiny areas were visible microscopically. The white surfaces of the resin residue were invaded by black hyphae.

Resin 1 Month wetland

Preservation index rating (0-5): 4

Outstanding preservation was apparent, as a very large resin deposit was visible with the naked eye. The resin now looks mostly greyish white probably due to burial debris adhering to the surface, but some of the original amber colour was still visible in small patches.

Resin 11 Months wetland

Preservation index rating (0-5): 4

The pine resin was abundant, well-preserved, and visible macroscopically, covering half or more of the dorsal and ventral surfaces. The resin exhibited an orange amber to light honey colour. The texture of the resin was granular to relatively smooth and shiny.

Resin 1 Month alkaline

Preservation index rating (0-5): 4

An abundance of macroscopically visible and well preserved resin was present on both sides of the flake. Interestingly, the resin underwent a change in colour from amber orange to mostly a white. Heavy black fungal attack was apparent around the resin residues as hyphae.

Resin 11 Months alkaline

Preservation index rating (0-5): 4

A large area of resin was found intact and visible macroscopically on both dorsal and ventral surfaces. After 11 months buried in the alkaline unit, the resin residue underwent a distinct colour change from orange amber to white with small amber patches.

Red ochre

Reference collection red ochre

The red ochre reference residue can be described as a distinctive red powdery material that is granular in texture and has a small grain size, in this case about 2-3 μm. However, there were no diagnostic characteristics detected using reflected VLM and there are a number of iron-based soil contaminants that are also red and granular. During SEM imaging, the ochre residue appeared as dark accumulations within depressed areas of the flint microtopography.

Red ochre 1 Month dry land

Preservation index rating (0-5): 4

Lots of ochre is visible with the naked eye, covering all surfaces of the flake. The red ochre changed colour from bright red to a duller red after one month burial, indicative of some taphonomic process. The red ochre also appeared less granular after one month burial.

Red ochre 11 Months dryland

Preservation index rating (0-5): 4

With the naked eye, diffuse ochre deposits were visible covering entire dorsal, and especially the ventral, surfaces. The deep red colour and granular appearance of the red ochre was maintained at a microscopic level after 11 months burial in the dry land unit. Authigenic crystal growth not observed on the tool, in contrast to crystal abundance on the red ochre, 11 Months piece from the wetland unit.

Red ochre 1 Month wetland

Preservation index rating (0-5): 4

An abundance of red ochre was distributed throughout the flint surface, and particularly on the ventral side, apparent with the naked eye. There appears to be slight colour change of the ochre to a duller, less bright red, but otherwise appears very intact. The flint contained red crystal formations with ochre incorporated into their structure.

Red ochre 11 Months wetland

Preservation index rating (0-5): 4

Red ochre was visible macroscopically on edges and covering the dorsal surface. The red colour was maintained after 11 months burial in acidic wetland conditions. Extensive crystal growth on top of the red ochre occluded the original granular appearance of the ochre. An abundance of rosette and lath crystals were present on this tool.

Red ochre 1 Month alkaline

Preservation index rating (0-5): 4

Large amount of macroscopically visible red ochre was found covering entire piece, which was dark red and granular. The ochre maintained its original deep red colour.

Red ochre 11 Months alkaline

Preservation index rating (0-5): 4

A large amount of red ochre was visible with the naked eye on both flake surfaces. The ochre maintained its dark red colour and granular appearance after burial. The washing treatment with jet bath stream of water removed a portion of the ochre.

Control flakes

Untreated flint

Blank flakes of the flint raw material type used in the experiment were examined microscopically. The Yorkshire Wolds flint was a light grey colour with white powdery chalk cortex and sometimes natural inclusions, such as chalk vesicles, mineral crystals, brown to orange discolourations, and foraminifera. Wolds flint is one of two flint types found on site at Star Carr, the other is the glacial till flint. The Wolds flint is relatively fine-grained, however, the glacial till flint is more fine-grained. This difference in surface texture is visible with reflected VLM, with the Wolds flint appearing rough.

Control 1 Month dry land

Only natural flint crystals were visible.

Control 11 Months dryland

On the ventral side of the flake, a light brown translucent material that appears similar to animal tissue residue. This material is likely sediment.

Control 1 Month wetland

Crystals were present on the ventral edge of the control flake in the wetland. Some polish was noted on ridges due to possible abrasion with other stone flakes prior to use.

Control 11 Months wetland

No residues were found on the control flake. However, rosette crystal formations were located on several dorsal surfaces, likely gypsum.

Control 1 Month alkaline

No residues were found on the control flake. However, green material, possibly algae or lichen, was present (Figure A1.12).
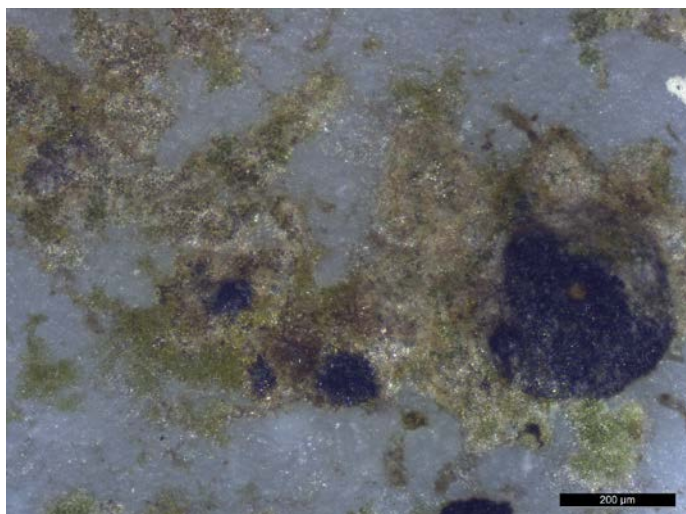
Figure A1.12. Green growth, possibly algae or lichen on blank flake buried for 1 month in the alkaline unit.

Control 11 Months alkaline

No residues were found on the control flake.

Sediment samples

Sediment samples were taken directly underneath each experimental piece and were examined microscopically with reflected VLM.

Sediment samples 1 Month dry land

The sediment samples from the dry land after 1 month burial contained no residues.

Sediment samples controls 11 Months dryland

No residues were found in the sediment samples associated with the set of flakes buried in the dry land for 11 months.

Sediment samples 1 Month wetland

Residues from the flake were found in the following instances: hardwood, potato starch, and likely muscle. Sediment samples from the wetland have shown that some movement occurred, which transferred some of the residue from the tool to the underlying sediment.

Sediment samples 11 Months wetland

The sediment sample taken underneath the flake used to butcher a squirrel (Flake 142) contained squirrel hair. Apart from this soil sample, no other soil samples yielded residues.

Sediment samples 1 Month alkaline

All sediment samples examined with each flake in the alkaline burial unit did not contain residues. The control sediment sample contained a pink thread, a modern contaminant, likely from clothing.

Sediment samples 11 Months alkaline

The sediment sample taken underneath the red ochre experimental piece was found to contain a small amount of what appears to be granular ochre, although ochre lacks diagnostic structure (see Figure A1.13). Because the visual identification is not sufficient in this case to confirm the suspected ochre in the sediment sample originated from the ochre that was placed on the flint surface, it would be necessary to chemically characterise both materials and find agreement in the chemical signature. If one accepts the visual identification of ochre in the sediment sample, it suggests that ochre moved from the flint surface to the sediment, perhaps by water movement. This sediment sample also contained

contaminant pink and blue threads. All other sediment samples examined contained no residues.
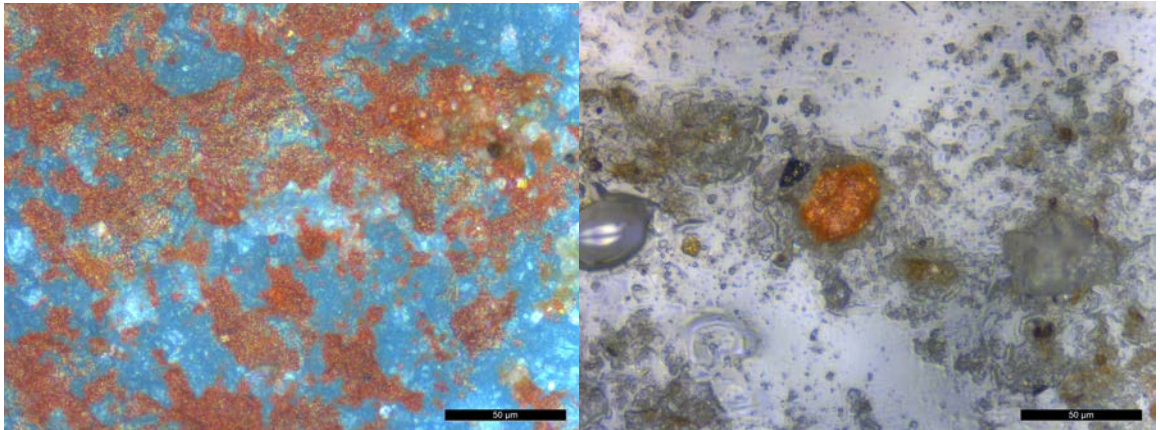
Figure A1.13. Left: Red ochre on experimental flint flake after 11 months burial in the alkaline unit. Right: Likely red ochre recovered in the soil sample taken underneath the flint.

Other comments

Nearly all animal related products have left a light brown, shiny, semi-transparent residue line on the edges of the flint which lacks diagnostic structure, and were thus amorphous. This residue pattern was persistent after one month burial in the dry land and found on the tools used to process squirrel, beef muscle, fish, fresh bone, and dry antler. However, a similar deposit along the edge of the control was also seen (Figure A1.14).
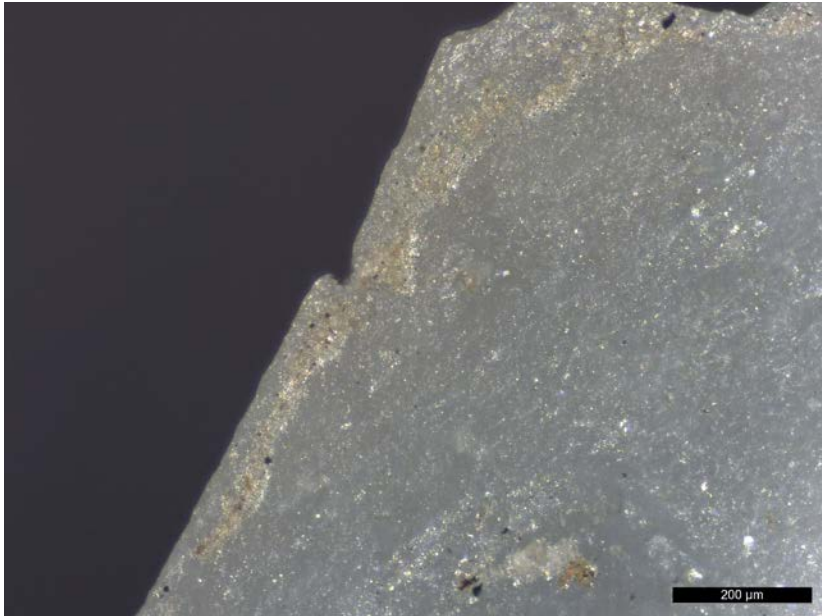
Figure A1.14. Non-residue edge deposit on control buried 1 month in the dry land.

Comments on unit 1: Star Carr dry land, 11 months burial

Interestingly, the probable muscle residue from this unit context (dry land, 11 months burial) looks more or less identical to the bone and antler residues observed from the same burial conditions. When the residues of bone, antler, and muscle were compared from the other two unit contexts (alkaline, 11 months and wetland, 11 months), the similar shared appearance of the residue seen in the dyland, 11 months unit was not observed.

Comments on unit 2: Star Carr wetland

The experimental flakes that were buried in the acidic peat wetland area of Star Carr had crystal formations on the stone surfaces after both one month and 11 months time intervals of the experiment. Crystal formation was so heavy in the wetland unit after 11 months, fine white deposits were visible macroscopically over the top of the unit (Figure A1.15) and also on some tools (Figure A1.16). These crystals are angular elongate lath and acicular micro-rosette shapes, clear and colourless, birefringent, and occur in clumps with pieces jutting out in random positions (Figures A1.17, A1.18). Based on investigations with confocal Raman microspectroscopy, these crystals are interpreted as authigenic gypsum crystals.

476

Figure A1.15. Heavy crystal formation on the top of the soil of the wetland unit after 11 months.

Figure A1.16. Heavy white crystal deposits were visible macroscopically on several experimental tools buried in the wetland at Star Carr. Pictured: crystals on the tool used to work fish after 11 months.
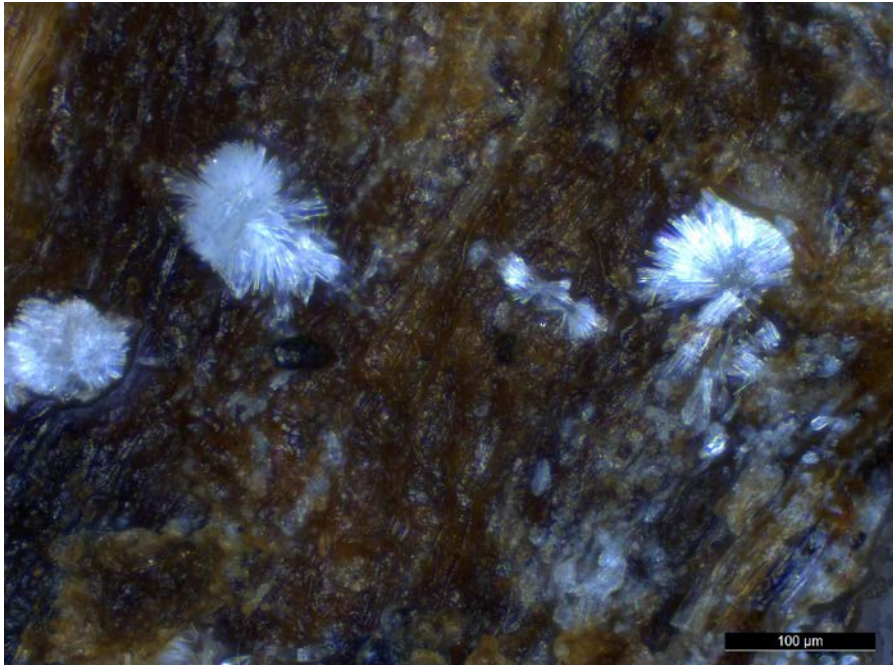
Figure A1.17. Colourless rosette shaped crystals that formed after 11 months burial in the wetland Unit 2. This tool was used to work reeds leaves.
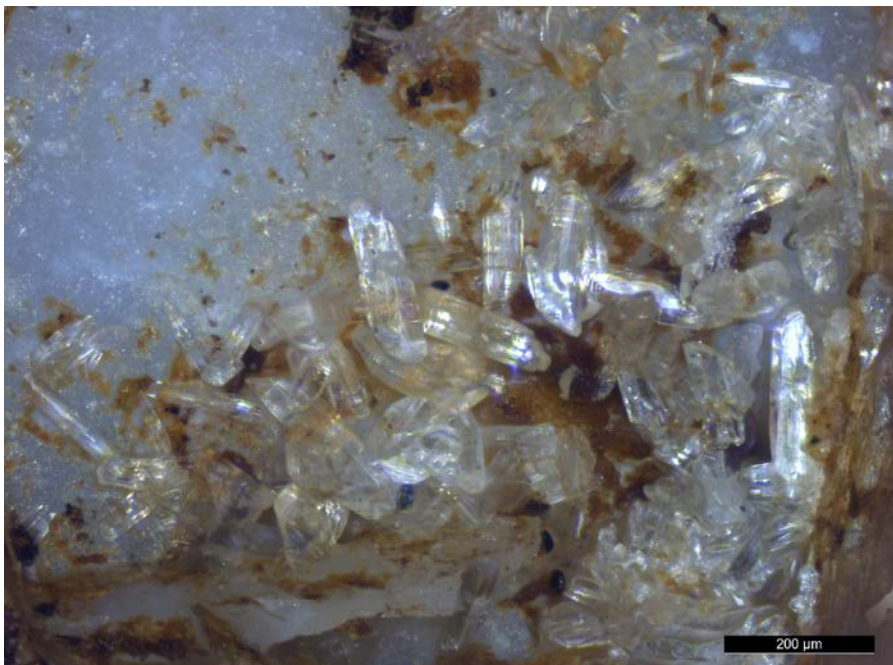
Figure A1.18. Clear lath shaped crystals on the tool used to work reeds, likely gypsum from the peat burial environment. Buried 11 Months, wetland.

APPENDIX 2 RESIDUE IDENTIFIABILITY RESULTS

Introduction

This appendix accompanies Chapter 6. Specifically, it presents results from the analysis of the modern reference residues to assess the visual identifiability of residues in situ on flint. These results are published in Croft et al. (2016). Reference residues were sorted into three categories based on their microscopic structural features: diagnostic, distinct, and non-distinct.

Diagnostic residue types

The residue types that were found to have diagnostic microscopic characteristics were fish scales, bird downy feather barbules, and mammal hair. Each residue in this group contains enough specific visual traits to diagnostically identify it in situ on stone with reflected light microscopy. These residues are not easily mistaken for other materials.

Fish Scales

Fish scales are diagnostic and able to be identified with visible light microscopy (Figure A2.1), but no distinctive structures could be located in the fish tissue residues. There are four main types of extant fish scales: placoid, cosmoid, ganoid, and cycloid and ctenoid, which are considered together (Helfman et al., 2009, p. 36). Placoid scales found in the cartilaginous fishes (class Chondrichthyes) have a rectangular base and spines. Cosmoid scales are found in lungfishes and consist of two basal layers of bone (lamellar and cancellous), overlain with cosamine. Lamellar bone layers are added to the basal layers during growth. Ganoid scales are typically rhomboid and have articulating peg

and socket joints between them. Fishes with ganoid scales include the bichirs, Bowfin, paddlefishes, gars, and sturgeons. The majority of bony fishes (superclass Osteichthyes) have cycloid and ctenoid scales (Elliott, 2000, p. 100). Cycloid and ctenoid scales contain enough distinct morphological features to be used for identification purposes in archaeology (Casteel, 1974, p. 560) and comparative reference collections of fish scales are available. The diagnostic features of cycloid and ctenoid scales are: focus, calcified concentric ridges called circuli, radii grooves radiating from centre focus (Lagler, 1947). Cycloid scales are circular, thin and flat. Ctenoid scales are similar to cycloid but additionally have posterior projections, such as a stiff-comb, cilia, or tubercles, modifications which are collectively called granulation (Elliott, 2000, p. 102).

In an archaeological residue publication, Hardy et al. (2013, p. 30) state that a feature of fish scales is that they are birefringent in normal light and non-birefringent under cross-polarised light. Presumably, this observation is based on the reference residues on experimental artefacts used in the study. In terms of SEM improving identifiability, fish scales were already diagnostically identifiable with VLM, thus did not require SEM. VLM and SEM images of fish tissue were amorphous.
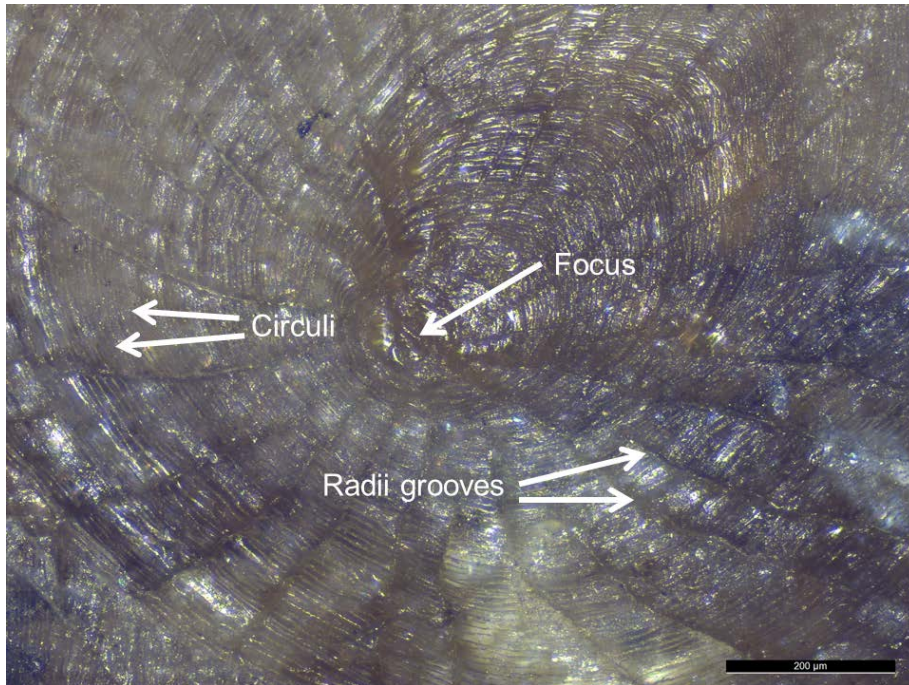
Figure A2.1. Cycloid scale from a tench (*Tinca tinca*) present on flint used to descale the fish, reference collection. Note radii grooves radiating out from central focus, and concentric circuli. Fish scale on flint, reference collection.

Downy feather barbules

The downy barbule is a long subunit of the feather structure with tiny branches. Downy barbules are found in the plumulaceous region at the base of wing, tail, contour, and semiplume feather types, and throughout the length of down feathers. The characteristics of downy feather barbules can identify bird order, family, and sometimes even species (Dove and Koch, 2010; Dove and Peurach, 2002). The features that can be observed in feather barbule fragments are: shape of nodes, distance between nodes, presence and shape of prongs, and pigmentation (Figure A2.2). However, experiments by Pedergnana and Blasco (2016, page 266) have found that small feather fragments overlap with other residue categories, noting this is likely particularly problematic in cases where taphonomic damage has occurred, causing obscuring or loss of diagnostic feather features. As a cautionary note, modified setae or bristle hairs on the larvae of some species of the Carpet Beetle (Family Dermestidae) can also appear similar to feather barbule nodes and prongs when viewed with light microscopy. There are two main types of Dermestid larval setae: spicisetae

481

(occur in most Dermestids) and hastisetae (occur in megatomine Dermestids). Both types of setae are segmented, often long, easily detachable, and spinulate or barbed to entangle predators (Kingsolver, 2002, p. 228; Lawrence and Ślipiński 2013, pp. 67, 91). Hastisetae are found on the posterior tergites of some species of Dermestid larvae (Kingsolver, 1991, p. 131) and can be identified as insect, not avian, in origin since their distal ends or apex terminations are spear or arrow shaped (this is an elaboration of barbed spicisetae) (Kadej, 2012, p. 8), termination structures which are not present in avian feathers. Spicisetae can also be differentiated based on a fine structure showing numerous spikes (Ma et al., 1978, p. 719), which are overlapping and more densely-packed than individual nodes of feather downy barbules. Another caution to be aware of in terms of potential misidentification of feather downy barbules is rodent and bat hair. The coronal scales commonly seen in rodent and bat hair (a feature uncommon in humans) might also appear similar on first inspection to the nodes and prongs of feathers. However, coronal scales encircle the diameter of the hair and appear more closely stacked than the nodes of feather downy barbules (Deedrick and Koch, 2004a).

As residues on archaeological lithic artefacts, Hardy et al. (2001), Hardy et al. (2008), Hardy et al. (2013) note that the nodes and prongs were used as identifying features of feather barbules. Downy feather barbules were diagnostically identifiable with VLM, and SEM did not reveal any further structural features helpful for identification.
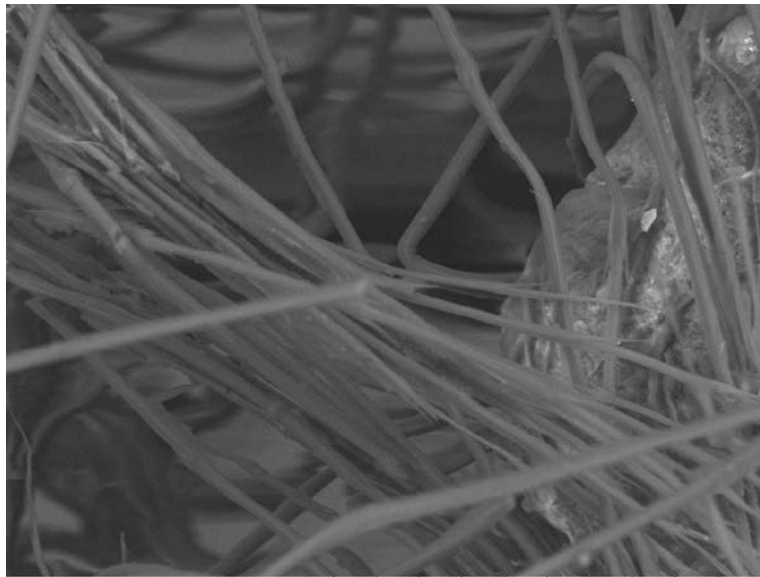
Bird0011   2015/04/30   L   x1.0k 100 um

LacCore, UMN, funded by NSF

Figure A2.2. Feather barbules with visible nodes and prongs. Bird residues on flint, reference collection.

Hair

Mammal overhairs. The two main components of an animal's coat are the fine underhair (fur hairs) and the overhairs (guard hairs), which are longer and coarser. The overhairs are preferred for identification, having better taxonomic differentiation value than underhairs (Ludwig and Bryce, 1996, p. 166; Teerink, 1991, p. 6). A hair has three layers: the outer cuticle or cuticula, the cortex, and the medulla or central channel. The cuticle contains overlapping keratin scales (Figure A2.3), of which different shapes are possible depending on the species. The cortex appears as a homogeneous mass with light microscopy, composed of longitudinal, cornified, shrunken cells. The cortex also contains pigment structures in the form of granules, amorphous masses, or diffuse staining. The medulla is the innermost part of the hair and is composed of an arrangement of cells surrounded by air spaces (Feldhamer et al., 2015, p. 113), in either a unicellular layer or multicellular layers, which form distinctive patterns. The air spaces in the medulla appear dark under light microscopy (Brown, 1942, p. 252). Each hair also has two main regions along its length: the shaft region (proximal) and the thickened shield region (distal). The shield region scale pattern is generally not as good as the shaft region scale pattern for differentiating between

taxonomic groups (Teerink, 1991, p. 6). Major hair features that can be used for identification include: morphology and pattern of cuticular scales, morphology and pattern of cells in the medulla, medullary index, distribution of pigment structures in the cortex (colours and patterns of banding), shaft shape, cross-sectional shape, and root morphology (Hausman, 1920; Petraco and Kubic, 2003; Titus, 1980; Tobin, 2005). Taxa identification of guard hairs down to the species level is possible (Deedrick and Koch, 2004a, 2004b; Teerink, 1991), if features have preserved archaeologically.

Hair has been identified in situ on stone tools by Hardy et al. (2001), Hardy (2004, p. 555), Hardy et al. (2008), Hardy and Moncel (2011), Hardy et al. (2013). There are several features of hair that must be intact and visible to make an identification: cuticle showing scale pattern or medulla showing pattern of cells. Hardy et al. (2001, p. 10973) identified hairs on the basis of the presence of *either* a medulla or cuticle with scale patterns. Combination of a number of hair features is more secure (Petraco and Kubic, 2003). Hair is diagnostically identifiable with reflected VLM. However, SEM did more clearly show the scale patterns than the reflected VLM micrographs.

Squirrel0005   2015/04/30   L   x400   200 um
LacCore, UMN, funded by NSF
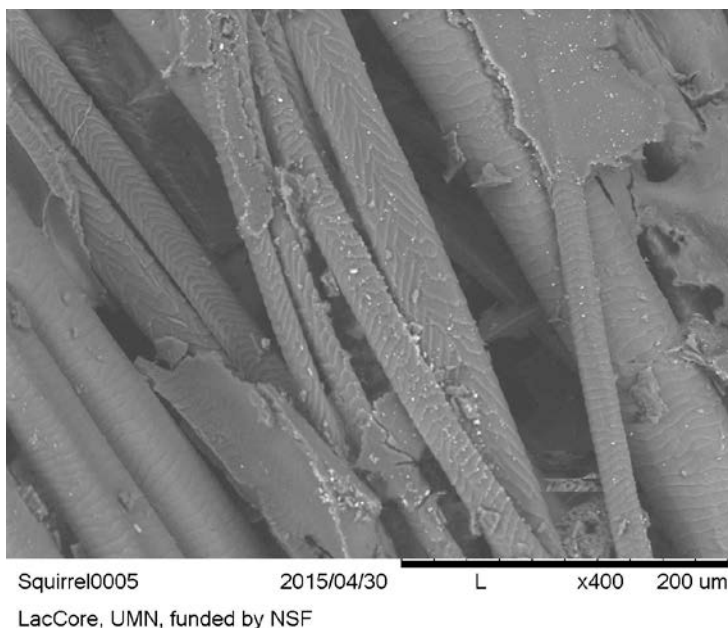
Figure A2.3. Hairs with scale patterns visible. Squirrel residues on flint, reference collection.

Distinct residue types

When viewed with reflected light microscopy, this group of residues appear distinctive, but not diagnostic. Thus, it is possible for these residue types to be identified incorrectly or mistaken for other materials originating from the soil or substrate. Reeds, potato, softwood, and hardwood all contained residues belonging to this distinct category. These residue types are potentially recognisable, however, identification with reflected light microscopy should be considered tentative and preliminary.

Plant cells

The cell wall in land plants is composed of a primary (growing) cell wall, a middle lamella, and a secondary (dead tissue) cell wall, the molecular composition and structural arrangement of which differs among species (Carpita et al. 2015, page 45). From an archaeological standpoint, the durable material examined at a cellular level are the secondary cell walls. The structural rigidity and durability of the secondary cell wall is due to 1) the fact that it is primarily made of cellulose, hemicellulose, and lignin (Noguchi, 2014, p. 137), and 2) the arrangement of cellulose microfibrils in three dense layers of different orientations that provide strength (Raven et al. 1999, page 65; Evert 2006, page 66, 74). The layered substructure of the cell wall and microfibrils are not visible when viewing in situ residues with reflected light microscopy, but have been characterised by atomic force microscopy (Kirby et al., 1996; Morris et al., 1997; Radotić et al., 2008). Evidence suggests cell walls are very strong structures that can survive hostile burial environments. For instance, cell walls are sometimes found after a palynological processing technique called acetolysis (Moore and Webb, 1978, p. 24), which is meant to digest and remove cellulose and other organics from pollen preparations.

Although there is great diversity in both morphology and size, plant cells appear distinct under the microscope: their walls always have a clear bounded structure

(Figure A2.4). The reed, softwood, and hardwood tissues all exhibited distinctive cell walls. SEM did not improve identification of plant cell walls.

Reeds0004   2015/04/28   L   x150   500 um
LacCore, UMN, funded by NSF
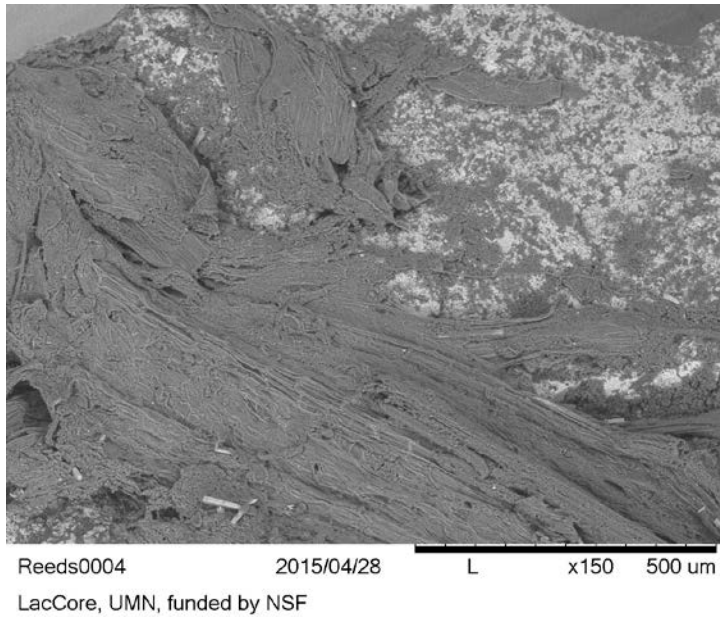
Figure A2.4. Rectangular plant cell walls, likely epidermal tissue due to elongate brick-like cell arrangement. Reed residues on flint, reference collection.

Starch

Starch granules are composed of alternating layers of two polysaccharides: amylose (unbranched helical chains), and amylopectin (highly branched), emanating from an origin point called the hilum (Evert 2006, page 52). The layers, or lamellae, of a starch granule are usually visible under a light microscope. Amylose is considered crystalline and amylopectin contains crystalline and amorphous areas. It is the semi-crystalline nature of starch granules that yields the quality of birefringence under cross polarised light. The proportion of amylose to amylopectin in the starch granule is under genetic control.

Starch granules in situ on stone surfaces can sometimes be suggested when examined with reflected VLM. Extinction crosses of undamaged starch granules are sometimes visible with in situ viewing and cross polarised light, but the presence of extinction crosses is not diagnostic to starch. Starch granules show

up most clearly on smooth surfaces, such as fine-grained flint or obsidian (Michael Haslam, 2016, pers. comm.). However, starch granules in situ on stone surfaces cannot be identified diagnostically with reflected light microscopy. Rather, starch is identifiable with transmitted light microscopy combined with polarised light, which requires extraction of the putative starch from the artefact and mounting on slides to properly see granule features (Kooyman, 2015). Starch granule features valuable to taxonomic identification include: size, three dimensional shape of the granule, surface texture, position and features of hilum, fissures or grooves originating from hilum, lamellae visibility, facets, presentation of and rotation of extinction cross under cross polarised light, morphology of extinction cross (sharp or diffuse, wavy or straight arms), and presence of facets on the margins of granules (Croft, 2012; García-Granero et al., 2016; Torrence and Barton, 2006; Zarrillo and Kooyman, 2006).

The degree of specificity that can be attained in terms of taxon identification is variable with starch, depending on the quality of the reference collection consulted, and how much morphological and size overlap is present between species. When distinctive starch granule features are no longer visible, a destructive test involving digestion of the starch by a starch specific enzyme, such as α-amylase (Hardy et al., 2009) determines that starch is present without question. However, a bath in a weak solution of HCl can clarify if the putative starch granules are calcium carbonate formations, such as calcareous spherulites.

Starch granules must be present in patterned aggregations or in some quantity on a stone tool to be considered of anthropogenic origin. This is to take account of the fact that the presence of only a few starch granules on an artefact might represent ancient incidental contact or modern contamination, particularly since starch can be a contaminant in modern environments, including laboratories (Crowther et al., 2014). Items that can potentially be mistaken for starch are: mineral or faecal spherulites (Canti, 1999, 1998), and conidia fungal spores (Haslam, 2006b). Spherulites are small (5-25 μm) rounded aggregates of radiating crystals, which can originate in the soil (mineral spherulites) or within faeces from animal dung (coprolitic or faecal spherulites). Like starch granules,

spherulites also display birefringence, possess lamellae and extinction crosses when viewed with a polarising lens under transmitted light. However, the extinction cross in spherulites is fixed and does not rotate when the polarising lens is rotated, thus confusion with starch can be avoided. Conidia fungal spores are common to soils, less than 5 μm in diameter, and have extinction crosses which rotate under cross polarised light, they also appear more "transparent" than starch granules.

Starch has been a major lithic residue of archaeological interest for dietary reconstruction and has been found in variable preservation conditions and dated contexts (see Chapter 2, section 2.3.2.3). When reference potato starch was viewed in situ with reflected VLM, it appeared distinct, but was not diagnostic. No lamellae, hila, vacuoles, or other features were visible with SEM. However, the three dimensional shape of the granules was better observed with SEM (Figure A2.5). SEM may be helpful in cases where the 3D shape of the granules are difficult to capture with reflected and transmitted VLM, for instance lenticular shapes which settle on slides in the flat orientation (polar view).

Potato0007 2015/04/29 x1.0k 100 um
LacCore, UMN, funded by NSF
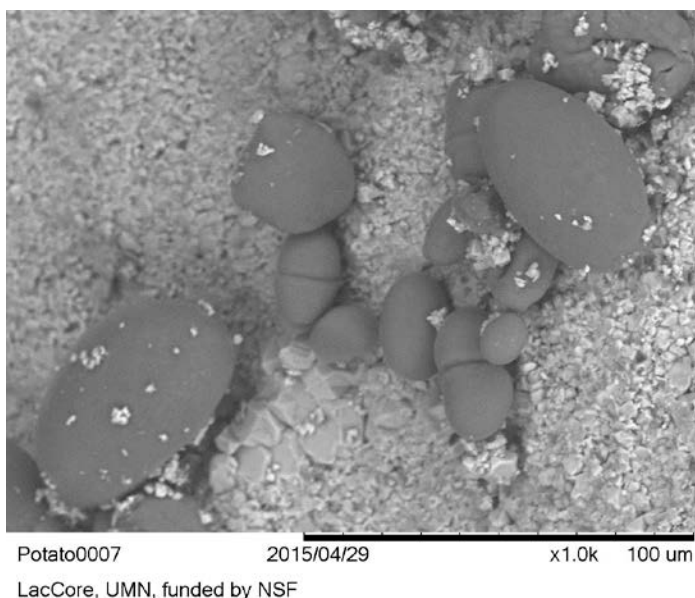
Figure A2.5. Starch granules. Potato residues on flint, reference collection.

Wood

Wood is the xylem of a tree or woody plant (Larson 1969, page 2), and is porous and fibrous. Different levels of identification can be attained with microscopic wood remains, from generic 'wood' down to species, depending on the number of features that are visible and the microscopic techniques used. An in depth description of wood anatomy is beyond the scope of this thesis, but in general conifer wood (softwood) has a lower differentiation among cells and simpler structure than in dicotyledon wood (hardwoods). That being said, wood residues that were examined in situ on experimental flakes with reflected VLM lacked diagnostic anatomical features. However, many wood residues were distinctive in appearance to allow suggested, but not secure, identification. This is in agreement with Hardy and Garufi (1998, p. 180), who found that most experimental wood residues on stone tools do not have microscopically visible diagnostic features. In particular the presence of bordered pits (structures that assist in the movement of water, nutrients and solutes through plants) are likely indicative of tool contact with woody plant matter.

In conifers, pits are circular or slightly elliptical in face view, large (usually 10-20 μm), and have wide borders which are raised above the level of the inner secondary wall, with a torus in the center of the pit opening (Evert, 2006b, p. 260). Across the bordered pit aperture, there is a membrane which has a round torus thickening in the center, a feature characteristic of softwoods (Wilson and White, 1986, p. 56). Unfortunately, the torus is not visible with reflected light microscopy when tracheids are viewed in situ on the artefact, which necessitates viewing with SEM. When viewed under transmitted cross polarised light, bordered pits display maltese crosses, which will rotate when the polarizing filter is rotated. This positive birefringence is due to the arrangement of the cellulose microfibrils in the bordered pit (Wayne, 2009, p. 376).

SEM improved the identifiability of wood residues. For instance, in the softwood (*Picea abies*), bordered pits were found with SEM (Figure A2.6). In the hardwood (*Salix alba*), the presence of crystals (likely calcium oxalate crystals, calciphytoliths, CaOx) were detected with SEM and better visualisation of the pits

was possible (Figure A2.7). Prismatic CaOx crystals are very abundant in bast wood fibres of *Salix*, *Quercus*, and *Populus* and occur in rows of rectangular, thin-walled cells (Schneider 1901, page 143).
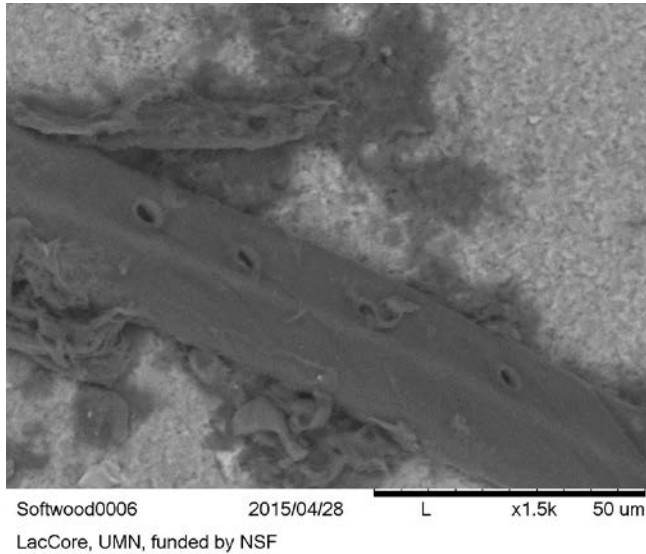
Figure A2.6. Pits with borders on a wood cell, perhaps a tracheid. Softwood residues on flint, reference collection. Note linear arrangement of pits.
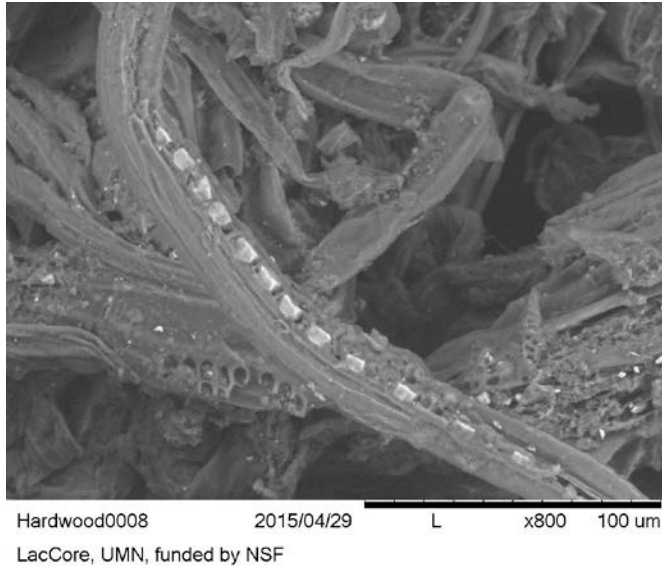
Figure A2.7. Crystals (light coloured) and intervessel pits (bottom left). The crystals in the wood fibre are likely to be calcium oxalate. Hardwood residues on flint, reference collection.

Non-distinct residue types

The residue types that were found to have no diagnostic microscopic characteristics were: bone, antler, muscle, resin, and red ochre, or five out of twelve residue types examined (42%). Blood and fat, which were observed but not specifically tested in the experimental design, are also discussed in this group. This group of residues could easily be mistaken for other residue types or materials originating from the soil or substrate, since they do not contain any specific distinctive traits that can be seen with reflected light microscopy. Identification of these residue types with reflected light microscopy should be considered tentative and preliminary.

Bone

Bone is a complex composite material. Mature compact bone is composed of approximately 70% carbonate hydroxylapatite (bone mineral) and 30% Type 1 collagen (protein) (Monnier et al., 2012, p. 3291). Patterning reflective of structure is present in different types of bone, and these patterns are potentially observable. Patterning which reflects structure is present in different types of bone, which are possible to observe. However, these patterns are only visible when the sample is prepared and viewed at the correct plane or axis, and viewed with transmitted light microscopy or SEM. Currey (2008, pp. 6–8) defines four types of bone that display distinctive characteristics visible with SEM: 1) lamellar bone, 2) woven bone, 3) fibrolamellar bone, 4) secondary osteons (Haversian systems).

On histological transverse thin sections viewed with transmitted light microscope, it is possible to differentiate between bone, antler, and ivory (Anderson, 1980, p. 190). In practice, residue researchers do not tend to make the distinction between bone and antler residues if both might be expected within the geographic area of the archaeology. In compact bone, distinctive features of osteon units are visible only in prepared cross thin sections with a transmitted light microscope or SEM, not with the reflected light microscope used in this study. These features of the

osteon include concentric bone lamellae surrounding Haversian canals, and several osteocytes with branched canaliculi (Jans, 2005, p. 7; Rhinelander, 1972, p. 7; White and Folkens, 2005, p. 43). Spongy or cancellous bone does not contain osteons, however osteocytes composing the bony trabeculae are arranged in a lacunar-canalicular system similar to compact bone (Eurell, 2004, p. 17). Canaliculi openings on the surface of spongy bone are visible in histological preparations.

According to Lombard, bone fragments have sharp jagged edges that may show perforations at magnifications over 200x. Langejans and (Langejans, 2009, p. 64) Langejans and Lombard (2015, p. 207) describe bone and fatty bone deposits on experimental tools as amorphous, opaque, non-birefringent, and having no characterising structure, but state that angular bone flakes are identifiable.

Cortical bone is semi-crystalline in structure due to apatite crystals around collagen fibrils, and is formed in ordered layers. Well-preserved cortical bone will show extinction crosses in transmitted cross polarised light. This has been observed in micromorphological thin sections. Bone, and sometimes degraded bone, will show distinct extinction crosses when prepared as a histological sample on a glass slide, with the osteons cut in cross section and viewed under polarised light with a transmitted light microscope (Jans, 2005). However, bone fragment residues are never encountered in this particular orientation on lithic tools. Even if by chance a cross-sectional cut through osteons and orientation was encountered during reflected light examination of in situ residues, maltese crosses it would probably fail to be recognised since birefringent qualities of anisotropic residues are only weakly visible while they are being viewed in situ.

Fresh scraped bone exhibited a white colour, angular shapes, and had opaque to translucent portions, but no features with a distinctive morphology that can be used to make a secure identification with reflected VLM. Secure identification of tiny bone residue fragments located in situ on a stone tool is not possible, as the distinctive morphological features present in cortical bone are invisible with reflected light microscopy. Also, extraction and viewing on slides is unlikely to orient archaeological cortical bone residues by random chance in such a way as

to allow location of features. A cross-sectional orientation of thin cortical bone fragments remaining from tool use is unlikely to occur by chance.

No osteons were observed in the SEM micrographs. Bone fragments appeared somewhat angular and jagged (Figure A2.8). SEM viewing of in situ bone residues did not improve identifiability; this agrees with SEM observations of experimental bone residues on stone by Jahren et al. (1997, p. 248).

Bone0004   2015/05/01   L   x100   1 mm
LacCore, UMN, funded by NSF
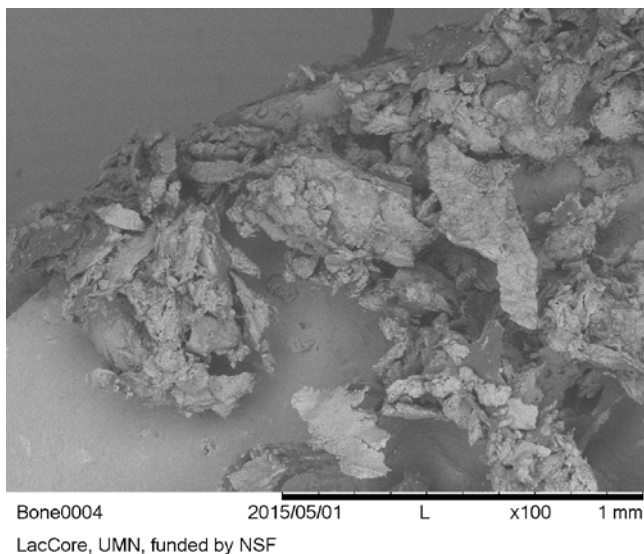
Figure A2.8. Fresh angular bone fragments. No osteons were able to be located, even at high magnifications. Bone residues on flint, reference collection.

Antler

Antlers are paired cephalic appendages found in the Cervidae family (deer, moose, elk, caribou and reindeer) that are periodically shed and regrown (Kierdorf et al. 2003, page 741; Hall 2005, page 103). In contrast to horn, which is living permanent tissue mostly composed of keratin, antler is dead ossified tissue covered with epithelial velvet for part of each year. Prepared histological cross sections of antler, like bone, reveal osteons and trabecular bone tissue (Landete-Castillejos et al., 2012, p. 248). Additionally, a comparative study of antler and limb bones showed that they are similar in chemical composition and microstructure (Chen et al. 2009). Specifically, "both are primarily composed of type I collagen and a mineral phase (carbonated apatite), arranged in osteons in compact (cortical bone) sections and a lamellar structure in the cancellous

(spongy or trabecular bone) sections" (Chen et al. 2009, page 693). Thus, it is not surprising that the reference antler residues were indistinguishable to bone residues. The reference antler residues appeared as jagged crystalline pieces of a light brown to translucent colour, and their edges sometimes appear 'frayed'. Occasionally irregular elongate antler pieces were seen that appeared somewhat fibrous. As with bone residues, the structure of the osteons could not be located in the reference antler residues on stone tools. Thus, antler residues were considered amorphous with no distinct structure. Also like bone, antler residues could be mistaken for minerals originating in the sediment.

SEM did not improve the identifiability of antler residues. However, SEM images showed that antler residues appeared more fibrous and net like than the bone residues, but still contained angular fragments (Figure A2.9).
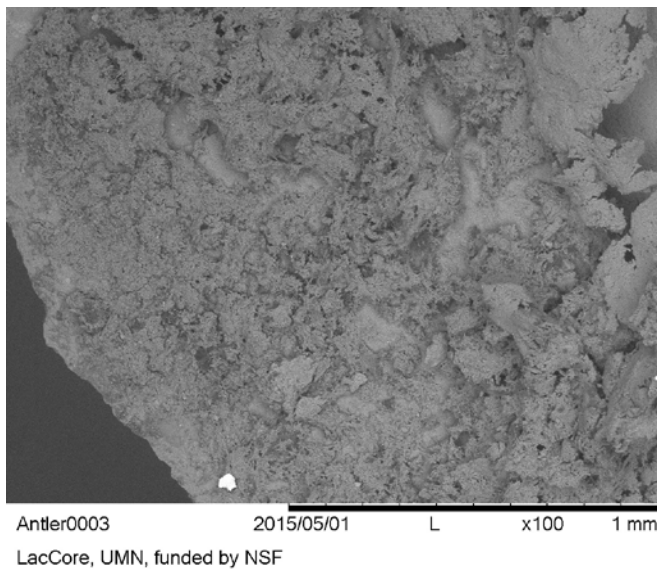
Figure A2.9. Dry antler residues on flint, reference collection.

Muscle tissue

There are three main types of muscle tissue in animals: smooth, cardiac, and skeletal (Martini, 2005, p. 236). Smooth muscle cells are spindle-shaped, nonstriated, and uninuclear. Cardiac muscle cells are striated, branched, and uninucleated. Skeletal muscle cells are striated, tubular, and multinucleated. Skeletal muscle makes up the majority of muscle mass in an animal and is under

voluntary control. The muscle fibre, or myofibre, is the basic unit of skeletal muscle (Stocum, 2012, p. 127). Myofibres are long and range in size from less than 100 μm wide and a few millimeters long to several hundred microns wide and a few centimeters long (Lieber, 2009), depending on where the muscle is located in the body. A myofibre contains many long smaller structures called myofibrils that run the length of the myofibre (Clark, 2005, p. 143). Myofibrils are in turn composed of thick, thin, and elastic myofilaments, arranged into repeating subunits called sarcomeres. The arrangement of the sarcomeres results in the appearance of cross striations on the myofibre, seen as a dark and light banding pattern with VLM (Lieber and Fridén, 1991, p. 691).

The individual cells of striated muscle tissue were not visible on any flint pieces that were buried. Muscle tissue seen in the reference collection was shiny, fibrous and stringy, and ranged in colour from dark brown to translucent. Myofibres with cross striations or banding patterns characteristic of striated muscle (Kenyon, 2012, p. 1273), were sometimes visible with reflected VLM in the reference beef muscle residue (Croft et al. 2016 Fig. 40). After burial in the wetland for one month, suspected muscle tissue was devoid of colour and appeared as a translucent fibrous sheet with holes. However, these traits are not distinctive to muscle, since other residues can appear essentially identical. Langejans (2009, 171, 285, 292, 400) found that gelatinous hyphae can look very similar to muscle tissue, both appearing as networks of translucent fibres containing holes, which can sometimes display birefringence. When the micrographs of gelatinous hyphae and muscle tissue are compared, they are indistinguishable (Langejans 2009, 285, 292).

No additional structural characteristics were visible with SEM. The muscle residue appeared somewhat fibrous (Figure A2.10). Surprisingly, the distinctive banding seen within the myofibre structure with VLM, was not found in the SEM images taken even at 500 x.
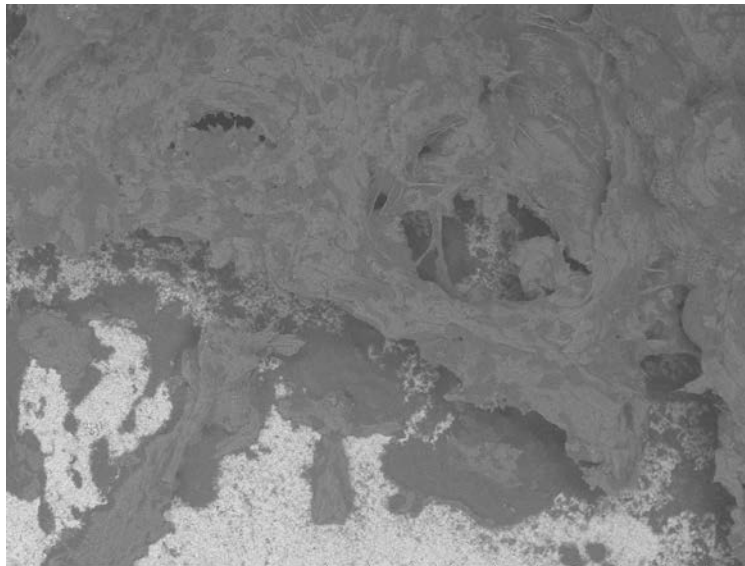
Muscle0003   2015/05/01   L   x100   1 mm

LacCore, UMN, funded by NSF

Figure A2.10. Muscle residues on flint, reference collection.

Blood cells

Although isolated blood was not a specific category of residue tested in the experiment, it was present on all flakes used on the beef muscle, fish, bird, and especially on flakes used to cut the squirrel.

Blood contains 4 major components: red blood cells (erythrocytes), white blood cells (leukocytes), platelets (thrombocytes), and plasma (the liquid portion), but it is the red blood cells that have been reported as being identifiable microscopically on ancient stone tools by a number of archaeologists (see discussion in section 2.3.2.2, Chapter 2). The membranes of red blood cells (RBCs) contain hemoglobin proteins that transport oxygen and carbon dioxide in the body (Larson, 2016, p. 240). Each hemoglobin molecule contains four subunits, and each subunit contains a heme group with an iron atom – the binding site for O_2 molecules (Honig and Adams, 1986, p. 19). RBCs in fresh blood samples from fish, amphibians, reptiles and birds are nucleated (Claver and Quaglia, 2009), but mammal RBCs do not have nuclei or any other cytoplasmic organelles at maturity (Telen, 2009, p. 126). RBCs vary in shape, depending on the animal. Nonmammalian RBCs are oval, whereas the morphology of RBCs seen in fresh mammalian blood are flattened biconcave

discs (discocytes). Adult human RBCs have an average diameter of about 7.2-7.4 µm (Price-Jones, 1933) and a max thickness of 2.2 µm (Smith and Wilson, 2001). Most animal RBCs fall within 5-10 µm in diameter (Seaman, 1975, p. 1183).

While the 'mud-cracked' appearance of blood films is often used as an identifiable feature (Langejans and Lombard, 2015, p. 208), other processes can also create a similar effect on stone. Sediment and iron oxide deposits displaying a mud-cracked appearance can also be found on archaeological stone tools, even after washing.

No individual red or white blood cells could be identified among any animal residues in the reference collection, which were examined with reflected light microscopy and SEM. Additionally, no blood cells were found on any experimentally buried flints. On the reference collection flints used to work squirrel, large mud-cracked blood stains (without identifiable blood cells) were present; these blood stains could not be found on flints from any burial condition. No blood cells were possible to securely identify with VLM or SEM on the basis of visual characteristics (Figures A2.11-A2.13).
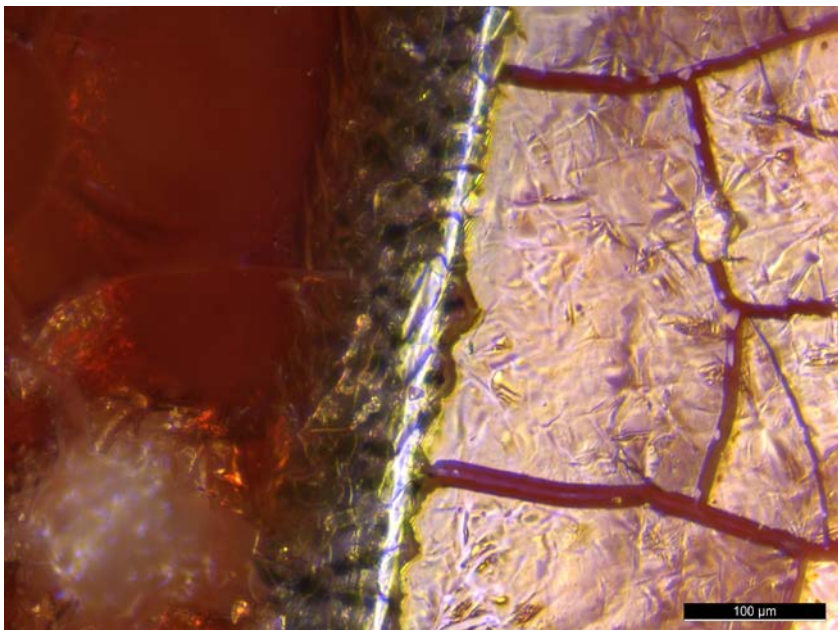
Figure A2.11. Dry squirrel blood film encrustation and hair viewed in situ on flint from the reference collection. Note lack of recognisable RBCs.
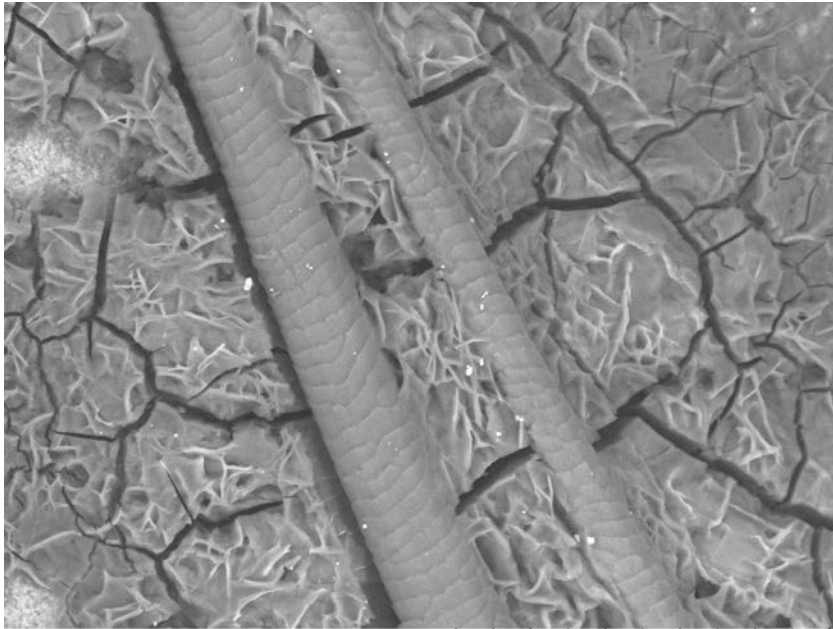
Squirrel0010   2015/04/30   L   x800   100 um
LacCore, UMN, funded by NSF

Figure A2.12. Squirrel blood encrustation and two hairs on flint from the reference collection, stored in fridge for 11.5 months prior to imaging. Note lack of recognisable RBCs. Hairs show coronal scales which encircle the shaft diameter, a feature common to rodents and bats. Distal ends of the hairs towards the top of the image.
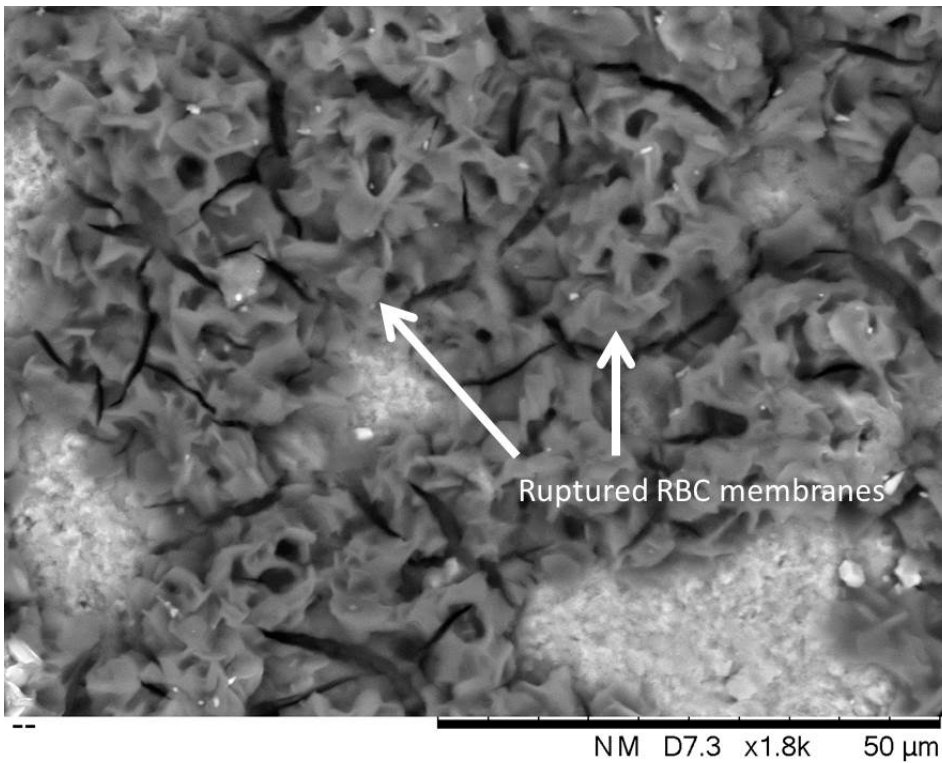
Figure A2.13. Squirrel blood film on flint from the reference collection. Note amorphous ruptured RBC membranes (SEM-BSE).

498

Fat

In all animals (the Metazoa), long-term lipid storage occurs in specialised cell types, but adipose tissue formation is only found in the vertebrates (Birsoy et al., 2013, p. 1541), including fish, amphibians, reptiles, birds, and mammals. The vertebrates store lipids in a semi-liquid state as triacylglycerol and cholesterol esters (Birsoy et al., 2013, p. 1543) in fat cells or adipocytes. White adipose tissue is found in the abdominal and subcutaneous regions of birds, mammals (Azeez et al., 2014, p. 4), and some fish (Pond, 2011a, p. 230). Amphibians, reptiles, and most fish, store fat intra-abdominally, and have essentially no subcutaneous fat storage (Azeez et al., 2014, p. 4; Birsoy et al., 2013, p. 1544). In addition to white adipose tissue, mammals also have brown adipose tissue (Pond 2011, page 227). Brown adipose tissue has a thermoregulatory function and is found only in mammals (Klingenspor and Fromme, 2011, p. 40). The adipocytes that make up the white adipose tissue are unilocular, or composed of a single compartment, and brown adipose tissue occurs in a multilocular, or multi-compartmentalised arrangement (Cinti et al., 2001). In prepared slides, individual adipocytes are visible at low magnifications (2.5 x) (Cinti et al., 2001, p. 21).

Even in the fresh, non-degraded reference collection residues, no diagnostic features were present to allow identification. No individual adipocytes could be isolated from the suites of residues examined (such as the fish, goose, squirrel, or beef steak muscle) and identified as white or brown fat cells. Fat residues lack diagnostic structure, rather appearing as amorphous globules and shiny smears, that are white to yellow to translucent. Examination of potential fat residues with SEM did not reveal any micromorphological structures that could be linked with the residue. Thus, it is suggested that archaeological fat residues are impossible to securely identify visually, but GC-MS might be possible to use to detect lipids.

Resin

Natural plant resin is a type of plant exudate that is viscous or solid, flammable, and non-water soluble, but lipid or spirit soluble (Langenheim, 2003, p. 45).

Secreted tree resin seals injuries from wind, fire, lightning, and herbivory, and prevents invasion of fungi and insects.

Reference pine tree resin appeared granular at low magnifications (160x or less) and shiny and orange at higher magnifications (320x or more). Resin residues which were experimentally buried underwent a changed colour from semi-translucent reddish orange to largely opaque grey/white with only small spots of shiny orange visible within the deposits. It is worth noting that raw pine resin was used in the experiment, and it is expected that other resins display different characteristics in terms of colour and texture.

When viewed with SEM, the resin exhibited similar appearance as the VLM observations – amorphous with a relatively rough in texture (Figure A2.14).
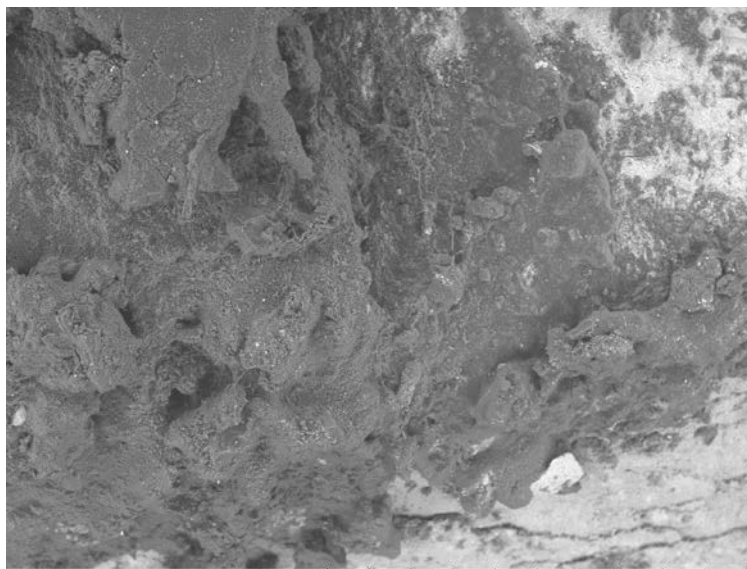
Resin0007   2015/04/29   L   x100   1 mm
LacCore, UMN, funded by NSF

Figure A2.14. Amorphous natural pine resin with a rough texture. Resin on flint, reference collection.

Red ochre

Ochre is a natural earth pigment which is comprised of clay, quartz, and iron oxides or oxyhydroxides (Dayet et al., 2013, p. 3492). In archaeology, ochre is used in a broader sense to mean any mineral material containing iron oxide

(Mortimore et al., 2004, p. 1179) that can be used for colouring by leaving a red or yellow mark when rubbed against a surface. Red ochre takes its reddish colour from the mineral hematite (α-Fe_2O_3), which is dehydrated iron oxide. The hematite mineral itself is hexagonal (Rafferty, 2012, p. 267), but red ochre occurs as nodules in nature.

Ochre is described by Langejans and Lombard (2015, p. 210) as granular and appearing dull in cross-polarised light. Gibson et al. (2004, p. 3), describes ochre residues on stone tools as iron oxides which have grain sizes smaller than sand and can be dark red to mustard yellow.

Microscopically, the red ochre reference residue can be described as a distinctive red powdery material that is granular in texture and has a small grain size, in this case about 2-3 μm. However, there were no diagnostic characteristics detected using reflected VLM and there are a number of iron-based soil contaminants that are also red and granular. During SEM imaging, the ochre residue appeared as dark accumulations within depressed areas of the flint microtopography (Figure A2.15).
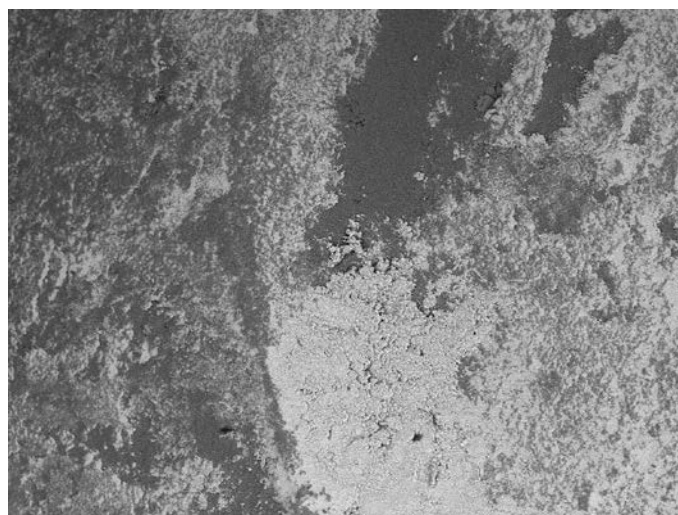
RedOchre0003   2015/04/29   L   x100   1 mm
LacCore, UMN, funded by NSF

Figure A2.15. Red ochre on flint, reference collection.

APPENDIX 3 LIST OF STAR CARR ARTEFACTS MICROSCOPICALLY ANALYSED

Artefact number	Site and year	Trench	Context	Grid Square	Type
93199	SC13	34	312	A17	Flake fragment
93312	SC13	34	308	C23	Blade
93318	SC13	34	308	C26	Flake
93327	SC13	34	308	C22	Blade
93338	SC13	34	??	??	Bladelet
93351	SC13	34	308	C26	Blade
93360	SC13	34	310	C22	Blade fragment
93368	SC13	34	308	B26	Blade
93380	SC13	34	308	C26	Flake
93463	SC13	34	308	F31	Blade
93593	SC13	34	308	G31	Blade
93770	SC13	34	308	U30	Blade
93807	SC13	34	312	A18	Blade
93823	SC13	34	312	A18	Blade
93871	SC13	34	308	D25	Blade fragment
94066	SC13	34	310	A25	Blade
94067	SC13	34	310	A26	Blade fragment
94083	SC13	34	310	A25	Blade
94146	SC13	34	310	B25	Bladelet
94255	SC13	34	310	A26	Flake
94362	SC13	34	310	S12	Flake
94377	SC13	34	310	H12	Bladelet fragment
94405	SC13	34	308	F31	Bladelet fragment
94409	SC13	34	308	F31	Shatter fragment
94445	SC13	34	308	G31	Blade
94554	SC13	34	308	G29	Blade fragment
94859	SC13	34	308	A25	Flake
94878	SC13	34	310	A23	Burin
94882	SC13	34	308	B25	Flake

95076	SC13	34	302	AA21	Blade
95243	SC13	34	310	V12	Blade
95301	SC13	34	310	V8	Bladelet fragment
95308	SC13	34	310	V8	Bladelet
95310	SC13	34	310	V8	Bladelet
95431	SC13	34	308	H23	Meche de foret
95828	SC13	34	310	X13	Burin
97308	SC13	34	310	T13	Blade fragment
97331	SC13	34	310	X9	Fragment
97859	SC13	34	312	V8	Bladelet
98086	SC13	34	310	T12	Blade
98305	SC13	34	310	V10	Flake
98306	SC13	34	312	V9	Blade
98333	SC13	34	310	K13	Blade
98375	SC13	34	312	U9	Flake
98376	SC13	34	312	V12	Wedge
98433	SC13	34	310	T12	Crested blade
98638	SC13	34	308	J26	Blade fragment
98817	SC13	34	310	P14	Blade
98855	SC13	34	317	B17	Blade
98857	SC13	34	317	B17	Fragment
98858	SC13	34	317	C18	Bladelet
98859	SC13	34	317	A17	Bladelet
98901	SC13	34	312	W7	Flake
98902	SC13	34	312	W7	Flake
98938	SC13	34	312	V12	Bladelet
98942	SC13	34	312	V12	Blade
98945	SC13	34	312	U12	Blade
98950	SC13	34	312	V12	Fragment
98957	SC13	34	312	X6	Wedge
99276	SC13	34	312	R8/R9	Bladelet
99454	SC13	34	312	S10	Axe
99496	SC13	34	312	R8	Blade
99516	SC13	34	312	S10	Blade
99568	SC13	34	312	T9	Microlith

99569	SC13	34	312	T9	Blade
99756	SC13	34	312	O13	Flake
99765	SC13	34	312	P11	Blade
99800	SC13	34	312	V9	Blade
99851	SC13	34	312	Q13	Blade fragment
107871	SC14	34	310	B6	Burin
108205	SC14	34	312	N2	Burin
108206	SC14	34	310	B9	Scraper
108219	SC14	34	308	I28	Burin
108220	SC14	34	310	B15	Axe
108225	SC14	34	308	I26	Burin
108228	SC14	34	308	I27	Blade
108229	SC14	34	310	M17	Blade fragment
108237	SC14	34	317	Q8	Flake
108244	SC14	34	310	D15	Flake
108351	SC14	34	326	U18	Microlith
108360	SC14	34	325	AB19	Fragment
108363	SC14	34	325	AA19	Scraper
108371	SC14	34	310	D2	Scraper
108373	SC14	34	337	Z18	Blade
108397	SC14	34	325	AB20	Microlith
109603	SC14	34	326	X21	Burin
109616	SC14	34	308	T21	Blade fragment
109641	SC14	34	308	H28	Blade
109649	SC14	34	317	P7	Blade
109691	SC14	34	415	G29	Microlith
109696	SC14	34	312	L15	Scraper and break burin
109698	SC14	34	312	F13	Blade fragment
109699	SC14	34	308	R21	Blade
109720	SC14	34	317	E9	Blade
109724	SC14	34	466	F25	Microlith
109731	SC14	34	308	N25	Awl
109735	SC14	34	320	P8	Chamfered fragment
109752	SC15	34	312	L5	Microlith, possibly awl
109757	SC15	34	312	AI6	Scraper

109762	SC15	34	317	L11	Blade
109767	SC15	34	317	L11	Core tablet
109783	SC15	34	310	AE9	Blade
109784	SC15	34	310	AD10	Flake
109798	SC15	34	310	ZS29	Axe
109808	SC14	34	312	J12	Blade
109821	SC14	34	308	L28	Hammer stone
109839	SC14	34	308	S24	Scraper
109840	SC14	34	312	J14	Bladelet
110517	SC14	34	320	P6	Flake
110656	SC15	34	301	AG9	Microlith
110657	SC15	34	301	AG9	Microlith
110660	SC15	34	301	AG9	Bladelet
110662	SC15	34	317	L7	Bladelet
110664	SC15	34	310	AJ7	Core tablet
110671	SC15	34	310	ZQ28	Shale bead
110672	SC15	34	310	AJ8	Flake
110679	SC15	34	310	ZQ27	Microlith or awl
110683	SC15	34	310	ZP27	Blade
110685	SC15	34	310	ZP26	Meche de foret
110692	SC15	34	310	ZP26	Crested blade
111456	SC15	34	310	AJ8	Flake
111458	SC15	34	310	A17	Scaper
111460	SC15	34	312	AF7	Bladelet
111467	SC15	34	312	AJ6	Bladelet
111474	SC15	34	312	AC3	Microlith
111479	SC15	34	310	ZP26	Meche de foret
111480	SC15	34	310	ZP26	Meche de foret
111490	SC15	34	310	ZT28	Bladelet
111496	SC15	34	310	ZP27	Meche de foret
113604	SC15	34	312	ZW16	Scraper
113618	SC15	34	312	ZW20	Flake
113623	SC15	34	310	ZP26	Microlith
113624	SC15	34	310	ZP26	Axe, possible
113641	SC15	34	312	ZW19	Burin

113830	SC15	34	310	ZP25	Shale bead
115527	SC15	34	317	ZV12	Pendant
117522	SC15	34	312	ZW20	Blade
Clark's backfill	SC15				Shale bead
					Total= 138

ABBREVIATIONS

2ndGS second-generation sequencing

aDNA ancient dehydroabietic acid

ADS Archaeological Data Service

ATR-FTIR attenuated total reflectance Fourier transform infrared spectroscopy

BSE backscattered electrons

CaOx calcium oxalate

CIEP cross-over immunoelectrophoresis

cm centimeter

DAPI 4,6-diamidion-2-phenylindole

DESI-MS desorption electrospray ionisation mass spectrometry

DHA dehydroabietic acid

DNA deoxyribonucleic acid

DTMS direct temperature resolved mass spectrometry

EDS energy dispersive x-ray spectrometry

EDTA ethylenediaminetetraacetic acid

ELISA enzyme linked immunosorbent assay

FTIR fourier transform infrared spectroscopy

FTIRM fourier transform infrared microspectroscopy

g grams

GC gas chromatography

GC-MS gas chromatography-mass spectrometry

GC×GC-TOFMS comprehensive two-dimensional gas chromatography-time-of-flight mass spectrometry

Hb haemoglobin

HPLC high performance liquid chromatography

HS-SPME headspace solid-phase microextraction

HTS High-throughput sequencing

ICP-AES inductively coupled plasma atomic emission spectroscopy

IBA ion beam analysis

IR infrared

LC-MS-MS liquid chromatography tandem-mass spectrometry

LSCM laser scanning confocal microscopy

MALDI-TOF-MS matrix assisted laser desorption/ionisation-time of flight mass spectrometry

mm millimeter

mtDNA mitochondrial DNA

NGS next-generation sequencing

PDSM post-depositional surface modification

PIXE particle-induced x-ray emission

PMF peptide mass fingerprinting

PCR polymerase chain reaction

RBC red blood cell

RIA radioimmunoassay

SEM scanning electron microscopy

SEM-EDS scanning electron microscopy-energy dispersive x-ray spectrometry

SERS surface enhanced resonance Raman scattering

TIC total ion current

TMS trimethylsilyl ester

µ-XRD – µ-XRF µ-XRF spectroscopy and synchrotron-based 2D µ-XRD coupled with µ-XRF

VP-SEM variable pressure SEM

VLM visible light microscopy

MALDI-MS matrix assisted laser desorption ionisation mass spectrometry

Micro-Raman Confocal Raman microspectroscopy

XRF X-ray fluorescence

BIBLIOGRAPHY

Adam, E., 1989. A technological and typological analysis of upper palaeolithic stone industries of Epirus, northwestern Greece, British Archaeological Reports. BAR, Oxford.

Adamiak, J., Otlewska, A., Tafer, H., Lopandic, K., Gutarowska, B., Sterflinger, K., Piñar, G., 2017. First evaluation of the microbiome of built cultural heritage by using the Ion Torrent next generation sequencing platform. Int. Biodeterior. Biodegradation. doi:10.1016/j.ibiod.2017.01.040

Agashe, S.N., Caulton, E., 2009. Pollen and Spores: Applications with Special Emphasis on Aerobiology and Allergy. Taylor & Francis.

Akoshima, K., Kanomata, Y., 2015. Technological organization and lithic microwear analysis: An alternative methodology. Journal of Anthropological Archaeology 38, 17–24.

Akyuz, S., Akyuz, T., Basaran, S., Bolcal, C., Gulec, A., 2008. Analysis of ancient potteries using FT-IR, micro-Raman and EDXRF spectrometry. Vib. Spectrosc. 48, 276–280.

Albert, B., Innes, J., 2014. Multi-profile fine-resolution palynological and micro-charcoal analyses at Esklets, North York Moors, UK, with special reference to the Mesolithic-Neolithic transition. Veg. Hist. Archaeobot.

Albert, B., Innes, J., Blackford, J., Taylor, B., Conneller, C., Milner, N., 2016. Degradation of the wetland sediment archive at Star Carr: An assessment of current palynological preservation. Journal of Archaeological Science: Reports 6, 488–495.

Aleksandrova, O.I., Kireeva, V.N., Leonova, E.V., 2014. Study of Organic and Inorganic Residues on the Stone Tools from the Early Mesolithic Layer in the Dvoinaya Cave (Northwestern Caucasus)1. Archaeology, Ethnology and Anthropology of Eurasia 42, 2–12.

Alessi, A., Agnello, S., Buscarino, G., Gelardi, F.M., 2013. Structural properties of core and surface of silica nanoparticles investigated by Raman spectroscopy. J. Raman Spectrosc. 44, 810–816.

Alexander, M.P., 1969. Differential staining of aborted and nonaborted pollen. Stain Technol. 44, 117–122.

Allen, J., Newman, M.E., Riford, M., Archer, G.H., 1995. Blood and Plant Residues on Hawaiian Stone Tools from Two Archaeological Sites in Upland Kāne'ohe, Ko'olau Poko District, O'ahu Island. Asian Perspectives 34, 283–302.

Andersen, H.H., Whitlow, H.J., 1983. Wear traces and patination on Danish flint artefacts. Nuclear Instruments and Methods in Physics Research 218, 468–474.

Anderson, P.C., 1980. A Testimony of Prehistoric Tasks: Diagnostic Residues on Stone Tool Working Edges. World Archaeol. 12, 181–194.

Andrefsky, W., 2008. Lithic Technology: Measures of Production, Use and Curation. Cambridge University Press, Cambridge.

Andreotti, A., Bonaduce, I., Colombini, M.P., Gautier, G., Modugno, F., Ribechini, E., 2006. Combined GC/MS analytical procedure for the characterization of glycerolipid, waxy, resinous, and proteinaceous materials in a unique paint microsample. Anal. Chem. 78, 4490–4500.

Antonakos, A., Liarokapis, E., Leventouri, T., 2007. Micro-Raman and FTIR studies of synthetic and natural apatites. Biomaterials 28, 3043–3054.

Asell, J.F., Nicol, M., 1968. Raman spectrum of α quartz at high pressures. J. Chem. Phys. 49, 5395–5399.

Aveling, E.M., 1998. Characterization of natural products from Mesolithic sites in Northern Europe. University of Bradford.

Aveling, E.M., Heron, C., 2000. Gluing and chewing: identification and use of amorphous organic substances of Mesolithic date in Northern Europe, in: Young, R. (Ed.), Mesolithic Lifeways: Current Research from Britain and Ireland, Leicester Archaeology

Monographs. School of Archaeological Studies, University of Leicester, Leicester, pp. 47–52.

Aveling, E.M., Heron, C., 1999. Chewing tar in the early Holocene: an archaeological and ethnographic evaluation. Antiquity 73, 579–584.

Aveling, E.M., Heron, C., 1998. Identification of birch bark tar at the Mesolithic site of Star Carr. Anc. Biomol. 2, 69–80.

Awonusi, A., Morris, M.D., Tecklenburg, M.M.J., 2007. Carbonate assignment and calibration in the Raman spectrum of apatite. Calcif. Tissue Int. 81, 46–52.

Azeez, O.I., Meintjes, R., Chamunorwa, J.P., 2014. Fat body, fat pad and adipose tissues in invertebrates and vertebrates: the nexus. Lipids in Health and Disease 13, 1–13.

Azemard, C., Menager, M., Vieillescazes, C., 2016. Analysis of diterpenic compounds by GC-MS/MS: contribution to the identification of main conifer resins. Anal. Bioanal. Chem. 408, 6599–6612.

Babot, M. del P., 2003. Starch grain damage as an indicator of food processing. Terra Australis, Phytolith and Starch Research in the Australian-Pacific-Asian Regions 19, 69–81.

Babot, M. del P., Apella, M.C., 2003. Maize and Bone: Residues of Grinding in Northwestern Argentina. Archaeometry 45, 121–132.

Badillo-Sanchez, D., Baumann, W., 2016. Comparative palette characterization of oil-on-canvas paintings of two well-known 19th-century Colombian artists by confocal Raman spectroscopy. J. Raman Spectrosc. doi:10.1002/jrs.5065

Bahn, P.G., 1987. Getting blood from stone tools. Nature 330, 14–14.

Bailey, G.N., 1983. Concepts of time in quaternary prehistory. Annu. Rev. Anthropol. 12, 165–192.

Bailey, J.M., Whelan, W.J., 1961. Physical properties of starch. I. Relationship between iodine stain and chain length. J. Biol. Chem. 236, 969–973.

Bailly, L., Adam, P., Charrié, A., Connan, J., 2016. Identification of alkyl guaiacyl dehydroabietates as novel markers of wood tar from Pinaceae in archaeological samples. Org. Geochem. 100, 80–88.

Bain, B.J., 2006. Blood cell morphology in health and disease, in: Lewis, S.M., Bain, B.J., Bates, I. (Eds.), Dacie and Lewis Practical Haematology, MD Consult. Churchill Livingstone/Elsevier, Philadelphia, pp. 79–114.

Balls, E.K., 1962. Early Uses of California Plants, California natural history guides. University of California Press, Berkeley.

Balme, J., Garbin, G., Gould, R., 2001. Residue analysis and palaeodiet in arid Australia. Australian Archaeology 53, 1–6.

Bamforth, M., Taylor, M., Pomstra, D., Little, A., Radini, A., b, in press. Woodworking technology, in: Milner, N., Conneller, C., Taylor, B. (Eds.), Star Carr Monograph. White Rose Press, York.

Bamforth, M., Taylor, M., Taylor, B., Robson, H.K., Radini, A., Milner, N., a, in press. Wooden structures, in: Milner, N., Conneller, C., Taylor, B. (Eds.), Star Carr Monograph. White Rose Press, York.

Bang-Andersen, S., 1989. Mesolithic adaptations in the southern Norwegian Highlands, in: Bonsall, C. (Ed.), The Mesolithic in Europe: Papers Presented at the Third International Mesolithic Symposium, Edinburgh, 1985. John Donald Publishers, Edinburgh, pp. 338–350.

Barber, D.L., Lott, J.N.A., Harris, D.A., 1991. Practical methods for identification of rice endosperm protein bodies and fecal protein particles in light microscopy. Food Structure 10, 4.

Barker, A., Dombrosky, J., Chaput, D., Venbles, B., Wolverton, S., Stevens, S.M., 2015. Validation of a non-targeted LC-MS approach for identifying ancient proteins: method development on bone to improve artifact residue analysis. Ethnobiology Letters 6, 162–174.

Barnard, T., 1962. Polymorphinidae from the Upper Cretaceous of England. Palaeontology 5, 712–736.

Barton, H., 2009. Starch granule taphonomy: the results of a two year field experiment, in: Haslam, M., Robertson, G., Crowther, A., Nugent, S., Kirkwood, L. (Eds.), Archaeological Science Under a Microscope: Studies in Residue and Ancient DNA Analysis in Honour of Thomas H. Loy, Terra Australis. Australian National University Press, Canberra, pp. 129–140.

Barton, H., 2007. Starch residues on museum artefacts: implications for determining tool use. J. Archaeol. Sci. 34, 1752–1762.

Barton, H., n.d. Organic residue analysis, in: Warren, G. (Ed.), Recent Fieldwork at the Sands of Forvie, Aberdeenshire., 2. Scottish Archaeological Internet Reports (www.sair.org.uk).

Barton, H., Matthews, P.J., 2006. Taphonomy, in: Torrence, R., Barton, H. (Eds.), Ancient Starch Research. Left Coast Press, Walnut Creek, California, pp. 75–94.

Barton, H., Torrence, R., Fullagar, R., 1998. Clues to stone tool function re-examined: comparing starch grain frequencies on used and unused obsidian artefacts. J. Archaeol. Sci. 25, 1231–1238.

Barton, H., White, J.P., 1993. Use of Stone and Shell Artifact at Balof 2, New Ireland, Papua New Guinea. Asian Perspectives 32, 169–181.

Bart, Z.R., Hammond, M.A., Wallace, J.M., 2014. Multi-scale analysis of bone chemistry, morphology and mechanics in the oim model of osteogenesis imperfecta. Connect. Tissue Res. 55 Suppl 1, 4–8.

Bates, J.B., Hendricks, R.W., Shaffer, L.B., 1974. Neutron irradiation effects and structure of noncrystalline SiO2. J. Chem. Phys. 61, 4163–4176.

Bayliss, A., Taylor, B., Ramsey, C.B., Dunbar, E., M., K.B.B., Conneller, C., Elliot, B., Knight, B., Milner, N., in press. Dating the archaeology and environment of the Star Carr embayment, in: Milner, N., Conneller, C., Taylor, B. (Eds.), Star Carr Monograph. White Rose Press, York.

Beattie, I.R., Gilson, T.R., 1970. The single-crystal Raman spectra of nearly opaque materials. Iron (III) oxide and chromium (III) oxide. J. Chem. Soc. A 980–986.

Bebber, M.R., Logan Miller, G., Boulanger, M.T., Andrews, B.N., Redmond, B.G., Jackson, D., Eren, M.I., 2017/4. Description and microwear analysis of Clovis artifacts on a glacially-deposited secondary chert source near the Hartley Mastodon discovery, Columbiana County, Northeastern Ohio, U.S.A. Journal of Archaeological Science: Reports 12, 543–552.

Bell, M., 2015. Experimental archaeology at the crossroads: a contribution to interpretation or evidence of "xeroxing"?, in: Chapman, R., Wylie, A. (Eds.), Material Evidence: Learning from Archaeological Practice. Routledge, London, pp. 42–58.

Bell, M., 2009. Experimental archaeology: changing science agendas and perceptual perspectives, in: Allen, M.J., Sharples, N., O'Connor, T. (Eds.), Land and People: Papers in Memory of John G. Evans. Oxbow, Oxford, pp. 31–45.

Bellot-Gurlet, L., Pagès-Camagna, S., Coupry, C., 2006. Raman spectroscopy in art and archaeology. J. Raman Spectrosc. 37, 962–965.

Beltran, V., Salvadó, N., Butí, S., Pradell, T., 2016. Ageing of resin from *Pinus* species assessed by infrared spectroscopy. Anal. Bioanal. Chem. 408, 4073–4082.

Benjamin, D.C., Berzofsky, J.A., East, I.J., Gurd, F.R., Hannum, C., Leach, S.J., Margoliash, E., Michael, J.G., Miller, A., Prager, E.M., 1984. The antigenic structure of proteins: a reappraisal. Annu. Rev. Immunol. 2, 67–101.

Bennett, P.C., 1991. Quartz dissolution in organic-rich aqueous systems. Geochimica et Cosmochimica Acta 55, 1781–1797.

Bennett, P.C., Melcer, M.E., Siegel, D.I., Hassett, J.P., 1988. The dissolution of quartz in dilute aqueous solutions of organic acids at 25°C. Geochim. Cosmochim. Acta 52, 1521–1530.

Bennett, W.C., Zingg, R.M., 1935. The Tarahumara: An Indian Tribe of Northern Mexico, Ethnological series. University of Chicago Press, Chicago.

Bergman, I., Östlund, L., Zackrisson, O., 2004. The use of plants as regular food in ancient subarctic economies: a case study based on Sami use of Scots pine innerbark. Arctic Anthropol. 41, 1–13.

Bianchin, S., Casellato, U., Favaro, M., Vigato, P.A., Munerato, E., Andreotti, A., Colombini, P., 2009. Romanino's altarpiece at civic museum of Padua: from the diagnosis to the scientifically guided intervention, in: Ferrari, A. (Ed.), Proceedings of the 4th International Congress on "Science and Technology for the Safeguard of Cultural Heritage in the Mediterranean Basin", Cairo, Egypt. CNR, Inst. of Chemical Methodologies, Italy, pp. 440–446.

Bicho, N., Marreiros, J.M., Gibaja, J.F., 2015. Use-Wear and Residue Analysis in Archaeology, in: Marreiros, J.M., Gibaja Bao, J.F., Bicho, N. (Eds.), Use-Wear and Residue Analysis in Archaeology, Manuals in Archaeological Method, Theory and Technique. Springer, London, pp. 1–4.

Binford, L.R., 1980. Willow Smoke and Dogs' Tails: Hunter-Gatherer Settlement Systems and Archaeological Site Formation. Am. Antiq. 45, 4–20.

Birsoy, K., Festuccia, W.T., Laplante, M., 2013. A comparative perspective on lipid storage in animals. Journal of Cell Science 126, 1541–1552.

Bleicher, N., Kelstrup, C., Olsen, J.V., Cappellini, E., 2015. Molecular evidence of use of hide glue in 4th millennium BC Europe. J. Archaeol. Sci. 63, 65–71.

Blinkhorn, E., Milner, N., 2013. Mesolithic research and conservation framework 2013. University of York, York.

Boëda, E., Bonilauri, S., Connan, J., Jarvie, D., Mercier, N., Tobey, M., Valladas, H., Sakhel, H. al, Muhesen, S., 2008. Middle Palaeolithic bitumen use at Umm el Tlel around 70,000 BP. Antiquity 82, 853–861.

Boëda, E., Connan, J., Dessort, D., Muhesen, S., Mercier, N., Valladas, H., Tisnérat, N., 1996. Bitumen as a hafting material on Middle Palaeolithic artefacts 380, 336–338.

Boëda, E., Connan, J., Muhesen, S., 2002. Bitumen as Hafting Material on Middle Paleolithic Artifacts from the El Kowm Basin, Syria, in: Neandertals and Modern Humans in Western Asia. Springer US, pp. 181–204.

Boisvert, J.-P., Domenech, M., Foissy, A., Persello, J., Mutin, J.-C., 2000. Hydration of calcium sulfate hemihydrate ($CaSO_4·12H_2O$) into gypsum ($CaSO_4·2H_2O$). The influence of the sodium poly(acrylate)/surface interaction and molecular weight. Journal of Crystal Growth 220, 579–591.

Bokelmann, K., Averdieck, F.-R., Willkomm, H., 1981. Duvensee, Wohnplatz 8, Neue Aspekte zur Sammelwirtschaft im frühen Mesolithikum. Offa. Berichte und Mitteilungen zur Urgeschichte, Frühgeschichte und Mittelalterarchäologie Neumünster 38, 21–40.

Bokelmann, V.K., 1994. Frühboreale Mikrolithen mit Schäftungspech aus dem Heidmoor im Kreis Segeberg. Offa 51, 37–47.

Bonaduce, I., Andreotti, A., 2009. Py-GC/MS of organic paint binders, in: Colombini, M.P., Modugno, F. (Eds.), Organic Mass Spectrometry in Art and Archaeology. Wiley, Chichester, UK, pp. 303–326.

Bonaduce, I., Ribechini, E., Modugno, F., Colombini, M.P., 2017. Analytical Approaches Based on Gas Chromatography Mass Spectrometry (GC/MS) to Study Organic Materials in Artworks and Archaeological Objects, in: Mazzeo, R. (Ed.), Analytical Chemistry for Cultural Heritage, Topics in Current Chemistry Collections. Springer, Gewerbestrasse, pp. 291–327.

Bonneau, A., Moyle, J., Dufourmentelle, K., Arsenault, D., Dagneau, C., Lamothe, M., 2017. A Pigment Characterization Approach to Selection of Dating Methods and Interpretation of Rock Art: The Case of the Mikinak Site, Lake Wapizagonke, Quebec, Canada. Archaeometry. doi:10.1111/arcm.12289

Boon, M.E., Suurmeijer, A.J.H., 1996. The Pap Smear, 3rd ed. Hardwood Academic Publishers, Amsterdam.

Boot, P., 1999. Preservation of use related residues on stone artefacts from Graman, in: Mountain, M.-J., Bowdery, D. (Eds.), Taphonomy: The Analysis of Processes from Phytoliths to Megafauna, Research Papers in Archaeology and Natural History, No. 30. ANH Publications, Department of Archaeology and Natural History, RSPAS, The Australian National University, Canberra, Australia, pp. 35–40.

Bordes, L., Prinsloo, L.C., Fullagar, R., Sutikna, T., Hayes, E., Jatmiko, Wahyu Saptomo, E., Tocheri, M.W., Roberts, R.G., in press. Viability of Raman microscopy to identify micro-residues related to tool-use and modern contaminants on prehistoric stone artefacts. J. Raman Spectrosc. doi:10.1002/jrs.5202

Boreham, S., Boreham, J., Rolfe, C.J., 2011b. Physical and Chemical Analyses of Sediments from around Star Carr as Indicators of Preservation. Journal of Wetland Archaeology 11, 20–35.

Boreham, S., Conneller, C., Milner, N., Taylor, B., Needham, A., Boreham, J., Rolfe, C.J., 2011a. Geochemical indicators of preservation status and site deterioration at Star Carr. J. Archaeol. Sci. 38, 2833–2857.

Borel, A., Ollé, A., Vergès, J.M., Sala, R., 2014. Scanning Electron and Optical Light Microscopy: two complementary approaches for the understanding and interpretation of usewear and residues on stone tools. J. Archaeol. Sci. 48, 46–59.

Bouma, J., Fox, C.A., Miedema, R., 1990. Micromorphology of Hydromorphic Soils: Applications for Soil Genesis and Land Evaluation, in: Douglas, L.A. (Ed.), Soil Micromorphology: A Basic and Applied Science, Developments in Soil Science. Elsevier, New York, pp. 257–278.

Bozzola, J.J., 2007. Conventional specimen preparation techniques for scanning electron microscopy of biological specimens, in: Kuo, J. (Ed.), Electron Microscopy: Methods and Protocols, Methods in Molecular Biology. Humana Press, Totowa, New Jersey, pp. 449–466.

Bradshaw, R., Bleay, S., Clench, M.R., Francese, S., 2014. Direct detection of blood in fingermarks by MALDI MS profiling and imaging. Sci. Justice 54, 110–117.

Bradtmöller, M., Sarmiento, A., Perales, U., Zuluaga, M.C., 2016. Investigation of Upper Palaeolithic adhesive residues from Cueva Morín, Northern Spain. Journal of Archaeological Science: Reports 7, 1–13.

Brehm, U., Gorbushina, A., Mottershead, D., 2005. The role of microorganisms and biofilms in the breakdown and dissolution of quartz and glass. Palaeogeogr. Palaeoclimatol. Palaeoecol. 219, 117–129.

Brettell, R., 2017. Resins from Roman mortuary contexts, in: Dunne, J. (Ed.), Organic Residue Analysis and Archaeology: Guidance for Good Practice. Historic England, pp. 35–38.

Brinker, C.J., Kirkpatrick, R.J., Tallant, D.R., Bunker, B.C., Montez, B., 1988. NMR confirmation of strained "defects" in amorphous silica. J. Non-Cryst. Solids 99, 418–428.

Briuer, F.L., 1976. New Clues to Stone Tool Function: Plant and Animal Residues. American Antiquity 41, 478–484.

Broderick, M., 1982. Appendix 2: Residue analysis of artifacts and flakes recovered from the Telep site DhRp 35, in: Peacock, W.R.B. (Ed.), The Telep Site: A Late Autumn Fish Camp of the Locarno Beach Culture Type. Unpublished consultant's report on file, Heritage Conservation Branch, Victoria, British Columbia.

Bronk Ramsey, C., 2017. OxCal.

Brown, A.G., Ellis, C., Roseff, R., 2010. Holocene sulphur-rich palaeochannel sediments: diagenetic conditions, magnetic properties and archaeological implications. J. Archaeol. Sci. 37, 21–29.

Brown, F.M., 1942. The microscopy of mammalian hair for anthropologists. Proceedings of the American Philosophical Society 85, 250–274.

Brown, T.A., Brown, K., 2011. Biomolecular archaeology: An introduction. John Wiley & Sons.

Brown, T., Bradley, C., Grapes, T., Boomer, I., 2011. Hydrological Assessment of Star Carr and the Hertford Catchment, Yorkshire, UK. Journal of Wetland Archaeology 11, 36–55.

Buck, B.J., Van Hoesen, J.G., 2002. Snowball morphology and SEM analysis of pedogenic gypsum, southern New Mexico, U.S.A. Journal of Arid Environments 51, 469–487.

Buck, B.J., Wolff, K., Merkler, D.J., McMillan, N.J., 2006. Salt Mineralogy of Las Vegas Wash, Nevada. Soil Sci. Soc. Am. J. 70, 1639–1651.

Buckley, M., Collins, M., Thomas-Oates, J., Wilson, J.C., 2009. Species identification by analysis of bone collagen using matrix-assisted laser desorption/ionisation time-of-flight mass spectrometry. Rapid Commun. Mass Spectrom. 23, 3843–3854.

Buckley, M., Kansa, S.W., 2011. Collagen fingerprinting of archaeological bone and teeth remains from Domuztepe, South Eastern Turkey. Archaeol. Anthropol. Sci. 3, 271–280.

Buhner, S.H., 2011. Pine Pollen: Ancient Medicine for a New Millennium. SurThrival.

Bunaciu, A.A., Fleschin, Ş., Aboul-Enein, H.Y., 2014. Biomedical investigations using Fourier transform-infrared microspectroscopy. Crit. Rev. Anal. Chem. 44, 270–276.

Burger, P., Gros-Balthazar, M., Stacey, R.J., 2013. The Newport Medieval Ship Project, Specialist Report: TAR. Newport City Council.

Burgio, L., Clark, R.J., 2001. Library of FT-Raman spectra of pigments, minerals, pigment media and varnishes, and supplement to existing library of Raman spectra of pigments with visible excitation. Spectrochim. Acta A Mol. Biomol. Spectrosc. 57, 1491–1521.

Burroni, D., Donahue, R.E., Pollard, A.M., Mussi, M., 2002. The Surface Alteration Features of Flint Artefacts as a Record of Environmental Processes. J. Archaeol. Sci. 29, 1277–1287.

Butler, I.B., Rickard, D., 2000. Framboidal pyrite formation via the oxidation of iron (II) monosulfide by hydrogen sulphide. Geochimica et Cosmochimica Acta 64, 2665–2672.

Butt, R.W., 1983. Identification of human blood stains by radioimmunoassay. J. Forensic Sci. Soc. 23, 291–296.

Buzgar, N., Buzatu, A., Sanislav, I.V., 2009. The Raman study on certain sulfates. Analele Ştiintifice ale Universităţii Al Cuza din Iaşi. Sect. 2, Geologie 55, 5–23.

Cahn, R.W., 1954. Twinned crystals. Advances in Physics 3, 363–445.

Cameron, D.W., 1993. Uniformitarianism And Prehistoric Archaeology. Australian Archaeology 36, 42–49.

Cameron, J., Devièse, T., Green, F., 2017. Scientific analysis of a preserved head of hair at Romsey Abbey, UK. Journal of Archaeological Science: Reports 13, 265–271.

Canti, M.G., 1999. The Production and Preservation of Faecal Spherulites: Animals, Environment and Taphonomy. J. Archaeol. Sci. 26, 251–258.

Canti, M.G., 1998. The Micromorphological Identification of Faecal Spherulites from Archaeological and Modern Materials. J. Archaeol. Sci. 25, 435–444.

Cappella, A., Bertoglio, B., Castoldi, E., Maderna, E., Di Giancamillo, A., Domeneghini, C., Andreola, S., Cattaneo, C., 2015. The taphonomy of blood components in decomposing bone and its relevance to physical anthropology. American Journal of Physical Anthropology 154, 636–645.

Cappellini, E., Collins, M.J., Gilbert, M.T.P., 2014a. Unlocking ancient protein palimpsests. Science 343, 1320–1322.

Cappellini, E., Gentry, A., Palkopoulou, E., Ishida, Y., Cram, D., Roos, A.-M., Watson, M., Johansson, U.S., Fernholm, B., Agnelli, P., Barbagli, F., Littlewood, D.T.J., Kelstrup, C.D., Olsen, J.V., Lister, A.M., Roca, A.L., Dalén, L., Gilbert, M.T.P., 2014b. Resolution of the type material of the Asian elephant, Elephas maximus Linnaeus, 1758 (Proboscidea, Elephantidae). Zool. J. Linn. Soc. 170, 222–232.

Cappellini, E., Jensen, L.J., Szklarczyk, D., Ginolhac, A., da Fonseca, R.A.R., Stafford, T.W., Holen, S.R., Collins, M.J., Orlando, L., Willerslev, E., Gilbert, M.T.P., Olsen, J.V., 2012. Proteomic analysis of a pleistocene mammoth femur reveals more than one hundred ancient bone proteins. J. Proteome Res. 11, 917–926.

Cârciumaru, M., Ion, R.-M., Niţu, E.-C., Ştefănescu, R., 2012. New evidence of adhesive as hafting material on Middle and Upper Palaeolithic artefacts from Gura Cheii-Râşnov Cave (Romania). J. Archaeol. Sci. 39, 1942–1950.

Carlson, L., Schwertmann, U., 1981. Natural ferrihydrites in surface deposits from Finland and their association with silica. Geochim. Cosmochim. Acta 45, 421–429.

Carpita, N.C., Ralph, J., McCann, M.C., 2015. The cell wall, in: Buchanan, B.B., Gruissem, W., Jones, R.L. (Eds.), Biochemistry and Molecular Biology of Plants. Wiley, Chichester, pp. 45–110.

Cartechini, L., Palmieri, M., Vagnini, M., Pitzurra, L., 2017. Immunochemical Methods Applied to Art-Historical Materials: Identification and Localization of Proteins by ELISA and IFM, in: Mazzeo, R. (Ed.), Analytical Chemistry for Cultural Heritage, Topics in Current Chemistry Collections. Springer International Publishing, Gewerbestrasse, pp. 241–261.

Carvalho, M.A., Calil Júnior, C., Savastano Junior, H., Tubino, R., Carvalho, M.T., 2008. Microstructure and mechanical properties of gypsum composites reinforced with recycled cellulose pulp. Materials Research 11, 391–397.

Casadio, F., Daher, C., Bellot-Gurlet, L., 2016. Raman Spectroscopy of cultural heritage Materials: Overview of Applications and New Frontiers in Instrumentation, Sampling Modalities, and Data Processing. Top. Curr. Chem. 374, 62.

Casteel, R.W., 1974. On the remains of fish scales from archaeological sites. American Antiquity 39, 557–581.

Cattaneo, C., Gelsthorpe, K., Phillips, P., Sokol, R.J., 1992. Reliable identification of human albumin in ancient bone using ELISA and monoclonal antibodies. American Journal of Physical Anthropology 87, 365–372.

Cattaneo, C., Gelsthorpe, K., Sokol, R.J., Phillips, P., 1994. Immunological Detection of Albumin in Ancient Human Cremations using ELISA and Monoclonal Antibodies. J. Archaeol. Sci. 21, 565–571.

Caudullo, G., Caruso, V., Cappella, A., Sguazza, E., Mazzarelli, D., Amadasi, A., Cattaneo, C., 2017. Luminol testing in detecting modern human skeletal remains: a test on different types of bone tissue and a caveat for PMI interpretation. Int. J. Legal Med. 131, 287–292.

Cavallo, G., Fontana, F., Gonzato, F., Guerreschi, A., Riccardi, M.P., Sardelli, G., Zorzin, R., 2015. Sourcing and processing of ochre during the late upper Palaeolithic at Tagliente rock-shelter (NE Italy) based on conventional X-ray powder diffraction analysis. Archaeol. Anthropol. Sci. 1–13.

Cesare, B., Maineri, C., 1999. Fluid-present anatexis of metapelites at El Joyazo (SE Spain): constraints from Raman spectroscopy of graphite. Contrib. Mineral. Petrol. 135, 41–52.

Cesaro, N.S., Lemorini, C., 2012. The function of prehistoric lithic tools: A combined study of use-wear analysis and FTIR microspectroscopy. Spectrochim. Acta A Mol. Biomol. Spectrosc. 86, 299–304.

Charrié-Duhaut, A., Porraz, G., R. Cartwright, C., Igreja, M., Connan, J., Poggenpoel, C., Texier, P.-J., 2013. First molecular identification of a hafting adhesive in the Late Howiesons Poort at Diepkloof Rock Shelter (Western Cape, South Africa). J. Archaeol. Sci. in press, 1–13.

Chatzipanagis, K., Iafisco, M., Roncal-Herrero, T., Bilton, M., Tampieri, A., Kroger, R., Delgado-López, J.M., 2016. Crystallization of citrate-stabilized amorphous calcium phosphate to nanocrystalline apatite: a surface-mediated transformation. CrystEngComm. doi:10.1039/C6CE00521G

Chen, P.-Y., Stokes, A.G., McKittrick, J., 2009. Comparison of the structure and mechanical properties of bovine femur bone and antler of the North American elk (Cervus elaphus canadensis). Acta Biomater. 5, 693–706.

Child, A.M., Pollard, A.M., 1992. A review of the applications of immunochemistry to archaeological bone. J. Archaeol. Sci. 19, 39–47.

Child, R.E., 1995. Pitch, tar, bitumen and asphalt? A sticky problem, in: Wright, M.M., Townsend, J.H. (Eds.), Resins Ancient and Modern. Presented at the SSCR 2nd Resins Conference, Department of Zoology, University of Aberdeen, Edinburgh, pp. 111–113.

Chriazomenou, E., Papoulia, C., Kopaka, K., 2014. Associating residues and wear traces as indicators of hafting methods: a view from the chipped stone industries from the island of Gavdos, Crete, in: Marreiros, J., Bicho, N., Gibaja, J.F. (Eds.), International Conference on Use-Wear Analysis. Presented at the Use-Wear 2012, Cambridge Scholars, Cambridge, pp. 714–726.

Christensen, M., Calligaro, T., Consigny, S., Dran, J.C., Salomon, J., Walter, P., 1998. Insight into the usewear mechanism of archaeological flints by implantation of a marker ion and PIXE analysis of experimental tools. Nucl. Instrum. Methods Phys. Res. B 136–138, 869–874.

Christensen, M., Grime, G., Menu, M., Walter, P., 1993. Usewear studies of flint tools with microPIXE and microRBS. Nucl. Instrum. Methods Phys. Res. B 77, 530–536.

Christensen, M., Walter, P., Menu, M., 1992. Usewear characterisation of prehistoric flints with IBA. Nucl. Instrum. Methods Phys. Res. B 64, 488–493.

Cinti, S., Zingaretti, M.C., Cancello, R., Ceresi, E., Ferrara, P., 2001. Morphologic techniques for the study of brown adipose tissue and white adipose tissue, in: Ailhaud, G. (Ed.), Adipose Tissue Protocols, Methods in Molecular Biology. Humana Press, Totowa, New Jersey, pp. 21–52.

Ciupiński, Ł., Fortuna-Zaleśna, E., Garbacz, H., Koss, A., Kurzydłowski, K.J., Marczak, J., Mróz, J., Onyszczuk, T., Rycyk, A., Sarzyński, A., Skrzeczanowski, W., Strzelec, M., Zatorska, A., Zukowska, G.Z., 2010. Comparative laser spectroscopy diagnostics for ancient metallic artefacts exposed to environmental pollution. Sensors 10, 4926–4949.

Clarke, A., 2014. Stainton West: ochre and haematite.

Clark, G., 1954. Excavations at Star Carr: an Early Mesolithic site at Seamer near Scarborough, Yorkshire. Cambridge University Press, Cambridge.

Clark, G., 1954. Miscellaneous Finds, in: Excavations at Star Carr: An Early Mesolithic Site at Seamer near Scarborough, Yorkshire. Cambridge University Press, Cambridge, pp. 165–178.

Clark, G., 1972. Star Carr: A Case Study in Bioarchaeology. Addison-Wesley, Reading.

Clark, R.K., 2005. Anatomy and Physiology: Understanding the Human Body. Jones and Bartlett Publishers, Sudbury, MA.

Claver, J.A., Quaglia, A.I.E., 2009. Comparative Morphology, Development, and Function of Blood Cells in Nonmammalian Vertebrates. Journal of Exotic Pet Medicine 18, 87–97.

Cloutman, E.W., 1988. Palaeoenvironments in the Vale of Pickering. Part I: Stratigraphy and Palaeogeography of Seamer Carr, Star Carr and Flixton Carr. Proceedings of the Prehistoric Society.

Cloutman, E.W., Smith, A.G., 1988. Palaeoenvironments in the Vale of Pickering. Part 3: Environmental History at Star Carr, in: Proceedings of the Prehistoric Society. Cambridge Univ Press, pp. 37–58.

Cnuts, D., Perrault, K., Dubois, L., Stefanuto, P.-H., Focant, Jean-François, Rots, V., 2016. A new method for identifying experimental and Palaeolithic hafting adhesives using GC×GC-HRTOFMS.

Cnuts, D., Rots, V., 2017. Extracting residues from stone tools for optical analysis: towards an experiment-based protocol. Archaeol. Anthropol. Sci. 1–20.

Collins, M.J., Copeland, L., 2011. Ancient starch: Cooked or just old? Proc. Natl. Acad. Sci. U. S. A. 108, E145.

Collins, M.J., Nielsen–Marsh, C.M., Hiller, J., Smith, C.I., Roberts, J.P., Prigodich, R.V., Wess, T.J., Csapò, J., Millard, A.R., Turner–Walker, G., 2002. The survival of organic matter in bone: a review. Archaeometry 44, 383–394.

Collins, M.J., Westbroek, P., Muyzer, G., de Leeuw, J.W., 1992. Experimental evidence for condensation reactions between sugars and proteins in carbonate skeletons. Geochim. Cosmochim. Acta 56, 1539–1544.

Colomban, P., 2011a. Pigment identification of a rare 18th century wallpaper from Buffon library. J. Raman Spectrosc. 42, 192–194.

Colomban, P., 2011b. Pigment identification of a rare 18th century wallpaper from Buffon library. J. Raman Spectrosc. 42, 192–194.

Colomban, P., 2005. Raman u-Spectrometry, a Unique Tool for On-Site Analysis and Identification of Ancient Ceramics and Glasses, in: Materials Research Society Symposium Proceedings. Cambridge, pp. 1–15.

Colomban, P., Tournie, A., Bellot-Gurlet, L., 2006. Raman identification of glassy silicates used in ceramics, glass and jewellery: a tentative differentiation guide. J. Raman Spectrosc. 37, 841–852.

Colombini, M.P., Modugno, F., Ribechini, E., 2005. Direct exposure electron ionization mass spectrometry and gas chromatography/mass spectrometry techniques to study organic coatings on archaeological amphorae. J. Mass Spectrom. 40, 675–687.

Conklin, A.R., 2013. Introduction to Soil Chemistry: Analysis and Instrumentation, 2nd ed, Chemical Analysis: A Series of Monographs of Analytical Chemistry and Its Applications. Wiley, Oxford.

Conneller, C., 2014. Star Carr, Archaeology of, in: Smith, C. (Ed.), Encyclopedia of Global Archaeology. Springer New York, pp. 7003–7009.

Conneller, C., 2007. Inhabiting new landscapes: settlement and mobility in Britain after the last glacial maximum. Oxford Journal of Archaeology 26, 215–237.

Conneller, C., 2000. Space, time and technology: the Early Mesolithic of the Vale of Pickering, North Yorkshire (PhD). University of Cambridge.

Conneller, C., Bayliss, A., Milner, N., Taylor, B., 2016. The Resettlement of the British Landscape: Towards a chronology of Early Mesolithic lithic assemblage types. Internet Archaeol. 42. doi:10.11141/ia.42.12

Conneller, C., Ellis, C., Allen, M.J., Macphail, R., Scaife, R., 2007. A Final Upper Palaeolithic Site at La Sagesse Convent, Romsey, Hampshire. Proceedings of the Prehistoric Society 73, 191–227.

Conneller, C., Higham, T., 2015. The early Mesolithic colonisation of Britain: preliminary results, in: Ashton, N., Harris, C.R.E. (Eds.), No Stone Unturned: Papers in Honour of Roger Jacobi. LSS, London.

Conneller, C., Little, A., Birchenall, J., in press. Spatial Analysis of the Flint, in: Milner, N., Conneller, C. and Taylor, B. (Ed.), Star Carr Monograph. White Rose Press, York.

Conneller, C., Milner, N., Taylor, B., Taylor, M., 2012. Substantial settlement in the European Early Mesolithic: new research at Star Carr. Antiquity 86, 1004–1020.

Conneller, C., Schadla-Hall, T., 2003. Beyond Star Carr: the Vale of Pickering in the 10th millennium BP. Proceedings of the Prehistoric Society 69, 85–106.

Cormack, D.H., 2001. Essential Histology, 2nd ed, Medicine Series. Lippincott Williams & Wilkins, Philadelphia.

Cornell, R.M., Schwertmann, U., 2003. The Iron Oxides: Structure, Properties, Reactions, Occurrences and Uses, 2nd ed. Wiley-VCH, Weinheim.

Cosano, D., Mateos, L.D., Jiménez-Sanchidrián, C., Ruiz, J.R., 2017/1. Identification by Raman microspectroscopy of pigments in seated statues found in the Torreparedones Roman archaeological site (Baena, Spain). Microchem. J. 130, 191–197.

Cosgrove, R., 1985. New evidence for early Holocene aboriginal occupation in northeast Tasmania. Australian Archaeology 21, 19–36.

Costa, M.S., Rego, A., Ramos, V., Afonso, T.B., Freitas, S., Preto, M., Lopes, V., Vasconcelos, V., Magalhães, C., Leão, P.N., 2016. The conifer biomarkers dehydroabietic and abietic acids are widespread in Cyanobacteria. Sci. Rep. 6, 23436.

Coughlin, E., Claassen, C., 1982. Siliceous and microfossil residues on stone tools: a new methodology for identification and analysis, in: Gramly, R.M. (Ed.), The Vail Site: A Paleo-Indian Encampment in Maine. Bulletin of the Buffalo Society of Natural Sciences, Buffalo, NY.

Courtin-Nomade, A., Grosbois, C., Marcus, M.A., Fakra, S.C., Beny, J.-M., Foster, A.L., 2009. The weathering of a sulfide orebody: speciation and fate of some potential contaminants. Canadian Mineralogist 47, 493–508.

Craig, O.E., Collins, M.J., 2002. The Removal of Protein from Mineral Surfaces: Implications for Residue Analysis of Archaeological Materials. J. Archaeol. Sci. 29, 1077–1082.

Crane, N.J., Popescu, V., Morris, M.D., Steenhuis, P., Ignelzi, M.A., Jr, 2006. Raman spectroscopic evidence for octacalcium phosphate and other transient mineral species deposited during intramembranous mineralization. Bone 39, 434–442.

Creamer, J.I., Quickenden, T.I., Crichton, L.B., Robertson, P., Ruhayel, R.A., 2005. Attempted cleaning of bloodstains and its effect on the forensic luminol test. Luminescence 20, 411–413.

Cristiani, E., Pedergnana, A., Gialanella, S., 2014. The use of microliths in the Eastern Alpine region between the Late Mesolithic and Early Neolithic. Use-wear and residue analysis of trapezes from Riparo Gaban, in: Lemorini, C., Cesaro, S.N. (Eds.), An Integration of the Use-Wear and Residue Analysis for the Identification of the Function of Archaeological

Stone Tools. Proceedings of the International Workshop, Rome, March 5th-7th, 2012. Archaeopress, Oxford, pp. 91–112.

Cristiani, E., Pedrotti, A., Gialanella, S., 2009. Tradition and innovation between the Mesolithic and early Neolithic in the Adige Valley (northeast Italy). New data from a functional analysis of trapezes from the Gaban rock-shelter. Documenta Praehistorica XXXVI, 191–205.

Cristiani, E., Živaljević, I., Borić, D., 2014. Residue analysis and ornament suspension techniques in prehistory: cyprinid pharyngeal teeth beads from Late Mesolithic burials at Vlasac (Serbia). J. Archaeol. Sci. 46, 292–310.

Croft, S., 2012. Traces of the past: microscopic residue analysis on the Canadian Plateau, British Columbia. University of Calgary, Calgary.

Croft, S., Monnier, G., Radini, A., Little, A., Milner, N., 2016. Lithic residue survival and characterisation at Star Carr: a burial experiment. Internet Archaeology 42. doi:10.11141/ia.42.5

Crook, K.A.W., 1968. Weathering and roundness of quartz sand grains. Sedimentology 11, 171–182.

Crowther, A., Haslam, M., 2007. Blind tests in microscopic residue analysis: comments on Wadley et al. (2004). Journal of Archaeological Science 34, 997–1000.

Crowther, A., Haslam, M., Oakden, N., Walde, D., Mercader, J., 2014. Documenting contamination in ancient starch laboratories. J. Archaeol. Sci. 49, 90–104.

Crowther, J.R., 2001. The ELISA Guidebook, Methods in Molecular Biology. Humana Press, Totowa, New Jersey.

Cuesta, A., Dhamelincourt, P., Laureyns, J., Martínez-Alonso, A., Tascón, J.M.D., 1994. Raman microprobe studies on carbon materials. Carbon N. Y. 32, 1523–1532.

Čukovska, L.R., Minčeva – Šukarova, B., Lluveras-Tenorio, A., Andreotti, A., Colombini, M.P., Nastova, I., 2012. Micro-Raman and GC/MS analysis to characterize the wall painting technique of Dicho Zograph in churches from Republic of Macedonia. J. Raman Spectrosc. 43, 1685–1693.

Cummings, L.S., 2007. Manual for Pollen, Phytolith, Starch, FTIR, AMS Radiocarbon, and Macrofloral Sampling.

Cummins, G.E., 2003. Impacts of hunter-gatherers on the vegetation history of the eastern vale of pickering, Yorkshire. Durham University.

Currey, J., 2008. The structure and mechanical properties of bone, in: Kokubo, T. (Ed.), Bioceramics and Their Clinical Applications. Woodhead Publishing, Cambridge, pp. 3–27.

Custer, J.F., Ilgenfritz, J., Doms, K.R., 1988. A cautionary note on the use of chemstrips for detection of blood residues on prehistoric stone tools. J. Archaeol. Sci. 15, 343–345.

Czamara, K., Majzner, K., Pacia, M.Z., Kochan, K., Kaczor, A., Baranska, M., 2015. Raman spectroscopy of lipids: a review. J. Raman Spectrosc. 46, 4–20.

Dark, P., 2017. Pollen and preservation at Star Carr: A 60-year perspective. Journal of Archaeological Science: Reports 13, 240–248.

Dark, P., 1998a. Lake-edge Sequences: Results, in: Mellars, P., Dark, P. (Eds.), Star Carr in Context, McDonald Institute Monographs. Oxbow Books, Cambridge, pp. 125–146.

Dark, P., 1998b. The Lake-centre Sequences: Results, in: Mellars, P., Dark, P. (Eds.), Star Carr in Context, McDonald Institute Monographs. Oxbow Books, Cambridge, pp. 163–178.

Darwin, C., 1859. On the origin of species by means of natural selection, or, The preservation of favoured races in the struggle for life /. John Murray, London.

Das, S., Hendry, M.J., 2011. Application of Raman spectroscopy to identify iron minerals commonly found in mine wastes. Chem. Geol. 290, 101–108.

David, A., 1998. Two Assemblages of Later Mesolithic Microliths from Seamer Carr, North Yorkshire: Fact and Fancy, in: Ashton, N., Healy, F., Pettitt, P. (Eds.), Stone Age Archaeology: Essays in Honour of John Wymer, Oxbow Monograph 102, Lithic Studies Occasional Paper 6. Oxbow Books, Oxford, pp. 196–204.

Davis, M.B., 1963. On the theory of pollen analysis. Am. J. Sci. 261, 897–912.

Dayet, L., Texier, P.-J., Daniel, F., Porraz, G., 2013. Ochre resources from the Middle Stone Age sequence of Diepkloof Rock Shelter, Western Cape, South Africa. J. Archaeol. Sci. 40, 3492–3505.

Day, P., 1996. Devensian Late-glacial and early Flandrian environmental history of the Vale of Pickering, Yorkshire, England. J. Quat. Sci. 11, 9–24.

Deedrick, D.W., Koch, S.L., 2004a. Microscopy of Hair Part I: A Practical Guide and Manual for Human Hairs. Forensic Science Communications 6.

Deedrick, D.W., Koch, S.L., 2004b. Microscopy of Hair Part II: A Practical Guide and Manual for Animal Hairs. Forensic Science Communications 6.

de Faria, D.L.A., Lopes, F.N., 2007. Heated goethite and natural hematite: Can Raman spectroscopy be used to differentiate them? Vib. Spectrosc. 45, 117–121.

de Faria, D.L.A., Venâncio Silva, S., de Oliveira, M.T., 1997. Raman microspectroscopy of some iron oxides and oxyhydroxides. J. Raman Spectrosc. 28, 873–878.

DeForest, J.L., 2009. The influence of time, storage temperature, and substrate age on potential soil enzyme activity in acidic forest soils using MUB-linked substrates and l-DOPA. Soil Biol. Biochem. 41, 1180–1186.

Degano, I., La Nasa, J., 2016. Trends in High Performance Liquid Chromatography for Cultural Heritage. Topics in Current Chemistry 374, 1–28.

De Gelder, J., De Gussem, K., Vandenabeele, P., Moens, L., 2007. Reference database of Raman spectra of biological molecules. J. Raman Spectrosc. 38, 1133–1147.

Delagnes, A., Wadley, L., Villa, P., Lombard, M., 2006a. Crystal quartz backed tools from the Howiesons Poort at Sibudu Cave. Southern African Humanities 18, 43–56.

Delagnes, A., Wadley, L., Villa, P., Lombard, M., 2006b. Crystal quartz backed tools from the Howiesons Poort at Sibudu Cave. Southern African Humanities 18, 43–56.

Delgado-López, J.M., Iafisco, M., Rodríguez, I., Tampieri, A., Prat, M., Gómez-Morales, J., 2012. Crystallization of bioinspired citrate-functionalized nanoapatite with tailored carbonate content. Acta Biomater. 8, 3491–3499.

Demarchi, B., Hall, S., Roncal-Herrero, T., Freeman, C.L., Woolley, J., Crisp, M.K., Wilson, J., Fotakis, A., Fischer, R., Kessler, B.M., Rakownikow Jersie-Christensen, R., Olsen, J.V., Haile, J., Thomas, J., Marean, C.W., Parkington, J., Presslee, S., Lee-Thorp, J., Ditchfield, P., Hamilton, J.F., Ward, M.W., Wang, C.M., Shaw, M.D., Harrison, T., Domínguez-Rodrigo, M., MacPhee, R.D.E., Kwekason, A., Ecker, M., Kolska Horwitz, L., Chazan, M., Kröger, R., Thomas-Oates, J., Harding, J.H., Cappellini, E., Penkman, K., Collins, M.J., 2016. Protein sequences bound to mineral surfaces persist into deep time. Elife 5. doi:10.7554/eLife.17092

Demoisson, F., Mullet, M., Humbert, B., 2008. Pyrite oxidation in acidic medium: overall reaction pathway. Surf. Interface Anal. 40, 343–348.

Denham, T.P., Haberle, S.G., Lentfer, C., Fullagar, R., Field, J., Therin, M., Porch, N., Winsborough, B., 2003. Origins of agriculture at Kuk Swamp in the highlands of New Guinea. Science 301, 189–193.

Derrick, M.R., Stulik, D., Landry, J.M., 1999. Infrared Spectroscopy in Conservation Science, Scientific tools for conservation. The Getty Conservation Institute, Los Angeles .

Der Sarkissian, C., Allentoft, M.E., Ávila-Arcos, M.C., Barnett, R., Campos, P.F., Cappellini, E., Ermini, L., Fernández, R., da Fonseca, R., Ginolhac, A., Hansen, A.J., Jónsson, H., Korneliussen, T., Margaryan, A., Martin, M.D., Moreno-Mayar, J.V., Raghavan, M., Rasmussen, M., Velasco, M.S., Schroeder, H., Schubert, M., Seguin-Orlando, A., Wales, N., Gilbert, M.T.P., Willerslev, E., Orlando, L., 2015. Ancient genomics. Philos. Trans. R. Soc. Lond. B Biol. Sci. 370, 20130387.

de Tercero, M.D., Röder, C., Fehrenbacher, U., Teipel, U., Türk, M., 2014. Continuous supercritical hydrothermal synthesis of iron oxide nanoparticle dispersions and their characterization. J. Nanopart. Res. 16, 1–27.

Dhakal, B., Armitage, R.A., 2013. GC-MS Characterization of Carbohydrates in an Archaeological Use Residue: A Case Study from the Coahuila Desert, in: Archaeological Chemistry VIII, ACS Symposium Series. American Chemical Society, pp. 157–170.

Dietze, B., Cialla, D., Schmitt, M., Popp, J., 2010. Introduction to the fundamentals of Raman spectroscopy, in: Dieing, T., Hollricher, O., Toporski, J. (Eds.), Confocal Raman Microscopy, Springer Series in Optical Sciences. Springer, Heidelberg, pp. 21–42.

Dinnis, R., Pawlik, A., Gaillard, C., 2009. Bladelet cores as weapon tips? Hafting residue identification and micro-wear analysis of three carinated burins from the late Aurignacian of Les Vachons, France. J. Archaeol. Sci. 36, 1922–1934.

Doménech-Carbó, M.T., Osete-Cortina, L., de la Cruz Cañizares, J., Bolívar-Galiano, F., Romero-Noguera, J., Fernández-Vivas, M.A., Martín-Sánchez, I., 2006. Study of the microbiodegradation of terpenoid resin-based varnishes from easel painting using pyrolysis–gas chromatography–mass spectrometry and gas chromatography–mass spectrometry. Anal. Bioanal. Chem. 385, 1265–1280.

Dominguez- Rodrigo, M., Serrallonga, J., Juan-Tresserras, J., Alcala, L., Luque, L., 2001. Woodworking activities by early humans: a plant residue analysis on Acheulian stone tools from Peninj (Tanzania). J. Hum. Evol. 40, 289–299.

Dove, C.J., Koch, S.L., 2010. Microscopy of Feathers: A Practical Guide. Journal of American Society of Trace Evidence Examiners 1, 15–61.

Dove, C.J., Peurach, S.C., 2002. Microscopic Analysis of Feather and Hair Fragments associated with Human Mummified Remains from Kagamil Island, Alaska. Smithsonian Institution, Washington, DC.

Downs, E.F., Lowenstein, J.M., 1995. Identification of archaeological blood proteins: A cautionary note. J. Archaeol. Sci. 22, 11–16.

Drees, L.R., Wilding, L.P., Smeck, N.E., Senkayi, A.L., 1989. Silica in soils: quartz and disordered silica polymorphs, in: Dixon, J.B., Weed, S.B. (Eds.), Minerals in Soil Environments, SSSA Book Series. Soil Science Society of America, Madison, Madison, Wisconsin, pp. 913–974.

Dresselhaus, M.S., Jorio, A., Hofmann, M., Dresselhaus, G., Saito, R., 2010. Perspectives on carbon nanotubes and graphene Raman spectroscopy. Nano Lett. 10, 751–758.

Du Bois, C.A., 1935. Wintu Ethnography, University of California publications in American archaeology and ethnology. University of California Press, Berkeley.

Dudd, S.N., Evershed, R.P., 1999. Unusual triterpenoid fatty acyl ester components of archaeological birch bark tars. Tetrahedron Lett. 40, 359–362.

Dypvik, H., 1984. Geochemical compositions and depositional conditions of Upper Jurassic and Lower Cretaceous Yorkshire clays, England. Geological Magazine 121, 489–504.

Eales, T., Westcott, C., Lilley, I., Ulm, S., Brian, D., Clarkson, C., 1999. Roof Fall Cave, Cania Gorge: site report. Queensland Archaeological Research 11, 14.

Eastwood, A., 1924. Menzies' California Journal. Calif. Hist. Soc. Q. 2, 265–340.

Edwards, H.G., 2006. Raman Spectroscopic Analysis of Art and Archaeological Materials, in: Encyclopedia of Analytical Chemistry. John Wiley & Sons, Ltd.

Edwards, H.G.M., Chalmers, J.M., 2005. Practical Raman Spectroscopy and Complementary Techniques, in: Edwards, H.G.M., Chalmers, J.M. (Eds.), Raman Spectroscopy in Archaeology and Art History. Royal Society of Chemistry, Cambridge, pp. 41–47.

Edwards, H.G.M., Farwell, D.W., de Faria, D.L.A., Monteiro, A.M.F., Afonso, M.C., De Blasis, P., Eggers, S., 2001. Raman spectroscopic study of 3000-year-old human skeletal remains from a sambaqui, Santa Catarina, Brazil. J. Raman Spectrosc. 32, 17–22.

Edwards, H.G.M., Farwell, D.W., Wynn-Williams, D.D., 1999. FT-Raman spectroscopy of avian mummified tissue of archaeological relevance. Spectrochim. Acta A Mol. Biomol. Spectrosc. 55, 2691–2703.

Egenberg, I.M., Aasen, J.A.B., Holtekjølen, A.K., Lundanes, E., 2002. Characterisation of traditionally kiln produced pine tar by gas chromatography-mass spectrometry. J. Anal. Appl. Pyrolysis 62, 143–155.

Eisele, J.A., Fowler, D.D., Haynes, G., Lewis, R.A., 1995. Survival and detection of blood residues on stone tools. Antiquity 69, 36–46.

Elias, M., Chartier, C., Prévot, G., Garay, H., Vignaud, C., 2006. The colour of ochres explained by their composition. Mater. Sci. Eng. B 127, 70–80.

Elliott, B.J., 2012. Antlerworking practices in Mesolithic Britain. University of York, England, York.

Elliott, B.J., Milner, N., 2010. Making a Point: a Critical Review of the Barbed Point Manufacturing Process Practised at Star Carr. Proceedings of the Prehistoric Society 76, 75–94.

Elliott, B., Knight, B., Little, A., in press. Antler frontlets, in: Milner, N., Conneller, C., Taylor, B. (Eds.), Star Carr Monograph. White Rose Press, York.

Elliott, D.G., 2000. Integumentary System, in: Ostrander, G.K. (Ed.), The Laboratory Fish, Handbook of Experimental Animals. Academic Press, San Diego, pp. 95–108.

Enoki, A., 1976. Isomerization and autoxidation of resin acids. Wood research: bulletin of the Wood Research Institute Kyoto University 49–57.

ENS de Lyon Handbook of Minerals Raman Spectra, 2000.

Eurell, J.A.C., 2004. Veterinary Histology. Teton NewMedia, Jackson, Wyoming.

Evans, A.A., 2014. On the importance of blind testing in archaeological science: the example from lithic functional studies. J. Archaeol. Sci. 48, 5–14.

Evans, A.A., Donahue, R.E., 2008. Laser scanning confocal microscopy: a potential technique for the study of lithic microwear. J. Archaeol. Sci. 35, 2223–2230.

Evans, A.A., Donahue, R.E., 2005. The elemental chemistry of lithic microwear: an experiment. J. Archaeol. Sci. 32, 1733–1740.

Evans, A.A., Macdonald, D.A., Giusca, C.L., Leach, R.K., 2014. New method development in prehistoric stone tool research: evaluating use duration and data analysis protocols. Micron 65, 69–75.

Evans, W.D., 1964. The organic solubilization of minerals in sediments, in: Colombo, U., Hobson, G.D. (Eds.), Advances in Organic Geochemistry: Proceedings of the International Meeting. Pergamon Press, Oxford, pp. 263–270.

Evershed, R.P., 2008. Organic residue analysis in archaeology: the archaeological biomarker revolution. Archaeometry 50, 895–924.

Evershed, R.P., 1993. Biomolecular archaeology and lipids. World Archaeol. 25, 74–93.

Evershed, R.P., Jerman, K., Eglinton, G., 1985. Pine wood origin for pitch from the Mary Rose. Nature 314, 528–530.

Evershed, R.P., Payne, S., Sherratt, A.G., Copley, M.S., Coolidge, J., Urem-Kotsu, D., Kotsakis, K., Özdoğan, M., Özdoğan, A.E., Nieuwenhuyse, O., 2008. Earliest date for milk use in the Near East and southeastern Europe linked to cattle herding. Nature 455, 528–531.

Evert, R.F., 2006a. Esau's plant anatomy: meristems, cells, and tissues of the plant body: their structure, function, and development, 3rd ed. Wiley, Hoboken, New Jersey.

Evert, R.F., 2006b. Xylem: Cell Types and Developmental Aspects, in: Esau's Plant Anatomy, Meristems, Cells, and Tissues of the Plant Body: Their Structure, Function, and Development, 10. Wiley, Hoboken, New Jersey, pp. 255–290.

Faivre, D., 2016. Iron Oxides: From Nature to Applications. Wiley-VCH, Weinheim.

Fanning, D.S., 2006. Acid Sulfate Soils, in: Lal, R. (Ed.), Encyclopedia of Soil Science. Taylor & Francis, New York, pp. 11–14.

Fazeli, S., Abtahi, A., Poch, R.M., Abbaslou, H., 2017. Gypsification processes and porosity changes in soils from southern Iran (Jooyom region-Fars province). Arid Ecosyst 7, 80–91.

Feldhamer, G.A., Drickamer, L.C., Vessey, S.H., Merritt, J.F., Krajewski, C., 2015. Mammalogy: Adaptation, Diversity, Ecology, 4th ed, Mammalogy. Johns Hopkins University Press, Baltimore.

Fellows, C.M., Al-Hamzah, A., 2015. Thermal desalination: current challenges, in: Amjad, Z., Demadis, K.D. (Eds.), Mineral Scales and Deposits: Scientific and Technological Approaches. Elsevier, Amsterdam, pp. 583–602.

Feng, N., Lu, J., He, Y., Du, J., 2005. Post-chemiluminescence behaviour of Ni^{2+}, Mg^{2+}, Cd^{2+} and Zn^{2+} in the potassium ferricyanide-luminol reaction. Luminescence 20, 266–270.

Feuillie, C., Merheb, M.M., Gillet, B., Montagnac, G., Daniel, I., Hänni, C., 2014. Detection of DNA sequences refractory to PCR amplification using a biophysical SERRS assay (Surface Enhanced Resonant Raman Spectroscopy). PLoS One 9, e114148.

Fiedel, S., 1996. Blood from Stones? Some Methodological and Interpretive Problems in Blood Residue Analysis. J. Archaeol. Sci. 23, 139–147.

Fine, P.M., Cass, G.R., Simoneit, B.R.T., 2002. Chemical Characterization of Fine Particle Emissions from the Fireplace Combustion of Woods Grown in the Southern United States. Environ. Sci. Technol. 36, 1442–1451.

FitzPatrick, E.A., 1984. Micromorphology of Soils. Chapman and Hall, London.

Fletcher, L., Milner, N., Taylor, M., Bamforth, M., Croft, S., Little, A., Pomstra, D., Robson, H.K., Knight, B., in press. The use of birch bark, in: Milner, N., Conneller, C. and Taylor, B. (Ed.), Star Carr Monograph. White Rose Press, York.

Flörke, O.W., Jones, J.B., Schmincke, H.-U., 1976. A new microcrystalline silica from Gran Canaria. Zeitschrift für Kristallographie-Crystalline Materials 143, 156–165.

Font, J., Salvadó, N., Butí, S., Enrich, J., 2007. Fourier transform infrared spectroscopy as a suitable technique in the study of the materials used in waterproofing of archaeological amphorae. Anal. Chim. Acta 598, 119–127.

Fox, A., Heron, C., Sutton, M.Q., 1995. Characterization of natural products on Native American archaeological and ethnographic materials from the Great Basin region, U.S.A.: a preliminary study. Archaeometry 37, 363–375.

Fredericksen, C., 1985. The detection of blood on prehistoric flake tools. New Zealand Archaeological Association Newsletter 28, 155–164.

French, D., 1984. Organization of starch granules, in: Whistler, R.L., BeMiller, J.N., Paschall, E.F. (Eds.), Starch: Chemistry and Technology, Food Science and Technology. Academic Press, San Diego, pp. 183–247.

Frohnhöfer, H.G., Krauss, J., Maischein, H.-M., Nüsslein-Volhard, C., 2013. Iridophores and their interactions with other chromatophores are required for stripe formation in zebrafish. Development 140, 2997–3007.

Froment, F., Tournié, A., Colomban, P., 2008. Raman identification of natural red to yellow pigments: ochre and iron-containing ores. J. Raman Spectrosc. 39, 560–568.

Fullagar, R., 2014. Residues and usewear, in: Balme, J., Paterson, A. (Eds.), Archaeology in Practice: A Student Guide to Archaeological Analysis. Wiley-Blackwell, Chichester, England, pp. 232–263.

Fullagar, R., 2006. Residues and Usewear, in: Balme, J., Paterson, A. (Eds.), Archaeology in Practice: A Student Guide to Archaeological Analyses, 8. Wiley Blackwell, Oxford, pp. 232–263.

Fullagar, R., 1993. Flaked stone tools and plant food production: a preliminary report on obsidian tools from Talasea, West New Britain, PNG, in: Anderson, P.C., Beyries, S., Otte, M., Plisson, H. (Eds.), Traces et Fonction: Les Gestes Retrouvés. Erual, Liège, pp. 331–337.

Fullagar, R., 1989. The potential of lithic use-wear and residues studies for determining stone tool functions, in: Gorecki, P.P., Gillieson, D. (Eds.), A Crack in the Spine: Prehistory and Ecology of the Jimi-Yuat Valley, Papua New Guinea. James Cook University, Townsville, Queensland, pp. 209–223.

Fullagar, R., 1988. Recent developments in Australian use-wear and residue studies, in: Beyries, S. (Ed.), Industries Lithiques: Traceologie et Technologie, British Archaeological Reports International Series 411. pp. 133–145.

Fullagar, R., 1986. Use-wear and residues on stone tools: Functional analysis and its application to two southeastern Australian archaeological assemblages. LaTrobe University, Melbourne.

Fullagar, R., David, B., 1997. Investigating Changing Attitudes Towards an Australian Aboriginal Dreaming Mountain Over >37,000 Years of Occupation via Residue and Use Wear Analyses of Stone Artefacts. Cambridge Archaeological Journal 7, 139–144.

Fullagar, R., Field, J., 1997. Pleistocene seed-grinding implements from the Australian arid zone. Antiquity 71, 300–307.

Fullagar, R., Field, J., Denham, T., Lentfer, C., 2006. Early and mid Holocene tool-use and processing of taro (*Colocasia esculenta*), yam (*Dioscorea* sp.) and other plants at Kuk Swamp in the highlands of Papua New Guinea. J. Archaeol. Sci. 33, 595–614.

Fullagar, R., Furby, J., Hardy, B., 1996. Residues on stone artefacts: state of a scientific art. Antiquity 70, 740–745.

Fullagar, R., Hayes, E., Stephenson, B., Field, J., Matheson, C., Stern, N., Fitzsimmons, K., 2015. Evidence for Pleistocene seed grinding at Lake Mungo, south-eastern Australia. Archaeology in Oceania 50, 3–19.

Fullagar, R., 1991. The role of silica in polish formation. J. Archaeol. Sci. 18, 1–24.

Fullagar, R., Matheson, C., 2014. Stone tool usewear and residue analysis, in: Smith, C. (Ed.), Encyclopedia of Global Archaeology. Springer, New York, pp. 7062–7065.

Fürst, S., Müller, K., Gianni, L., Paris, C., Bellot-Gurlet, L., Pare, C., Reiche, I., 2016. Raman Investigations to Identify Corallium rubrum in Iron Age Jewelry and Ornaments. Minerals 6, 56.

Galanidou, N., 2006. Analytical and Ethical Issues concerning Organic Residues on Paleolithic Chipped Stone Tools from NW Greece. J. Field Archaeol. 31, 351–362.

Galeener, F.L., 1982. Planar rings in glasses. Solid State Commun. 44, 1037–1040.

Gale, R., Cutler, D.F., 2000. Plants in Archaeology: Identification Manual of Vegetative Plant Materials Used in Europe and the Southern Mediterranean to c. 1500, Plants in archaeology: identification manual of vegetative plant materials used in Europe and the Southern Mediterranean to c.1500. Westbury and Royal Botanic Gardens, Kew.

Gamsjaeger, S., Masic, A., Roschger, P., Kazanci, M., Dunlop, J.W.C., Klaushofer, K., Paschalis, E.P., Fratzl, P., 2010. Cortical bone composition and orientation as a function of animal and tissue age in mice by Raman spectroscopy. Bone 47, 392–399.

García-Granero, J.J., Lancelotti, C., Madella, M., 2016. A methodological approach to the study of microbotanical remains from grinding stones: a case study in northern Gujarat (India). Veg. Hist. Archaeobot. 1–15.

Garling, S.J., 1998. Megafauna on the menu? Haemoglobin crystallisation of blood residues from stone artefacts at Cuddie Springs. A Closer Look: Recent Australian Studies of Stone Tools 29–48.

Garnier, N., Cren-Olivé, C., Rolando, C., Regert, M., 2002. Characterization of archaeological beeswax by electron ionization and electrospray ionization mass spectrometry. Anal. Chem. 74, 4868–4877.

Garrett, R.H., Grisham, C.M., 2012. Biochemistry, 5th ed. Brooks/Cole, Belmont, CA.

Gerlach, S.C., Newman, M., Knell, E.J., Jr., E.S.H., 1996. Blood Protein Residues on Lithic Artifacts from Two Archaeological Sites in the De Long Mountains, Northwestern Alaska. Arctic 49, 1–10.

Gernaey, A.M., Waite, E.R., Collins, M.J., Craig, O.E., Sokol, R.J., 2001. Survival and interpretation of archaeological proteins, in: Brothwell, D.R., Pollard, A.M. (Eds.), Handbook of Archaeological Sciences. Wiley, Chichester, pp. 323–329.

Giachi, G., Pallecchi, P., Romualdi, A., Ribechini, E., Lucejko, J.J., Colombini, M.P., Mariotti Lippi, M., 2013. Ingredients of a 2,000-y-old medicine revealed by chemical, mineralogical, and botanical investigations. Proc. Natl. Acad. Sci. U. S. A. 110, 1193–1196.

Gianno, R., 1990. Semelai Culture and Resin Technology, Connecticut Academy of Arts and Sciences New Haven, Conn: Memoirs of the. Connecticut Academy of Arts and Sciences, Connecticut.

Gibson, N.E., Wadley, L., Williamson, B.S., 2004. Microscopic residues as evidence of hafting on backed tools from the 60 000 to 68 000 year-old Howiesons Poort layers of Rose Cottage Cave, South Africa. Southern African Humanities 16, 1–11.

Gillet, P., Cléac'h, L., Madon, M., Others, 1990. High-temperature raman spectroscopy of SiO_2 and GeO_2 Polymorphs: Anharmonicity and thermodynamic properties at high-temperatures. J. Geophys. Res. [Solid Earth] 95, 21635–21655.

Gíslason, S.R., Heaney, P.J., Oelkers, E.H., Schott, J., 1997. Kinetic and thermodynamic properties of moganite, a novel silica polymorph. Geochim. Cosmochim. Acta 61, 1193–1204.

Glauberman, P.J., Thorson, R.M., 2012. Flint Patina as an Aspect of "Flaked Stone Taphonomy": A Case Study from the Loess Terrain of the Netherlands and Belgium. Journal of Taphonomy 10, 21–43.

Gleisner, M., Herbert, R.B., Jr., Frogner Kockum, P.C., 2006. Pyrite oxidation by Acidithiobacillus ferrooxidans at various concentrations of dissolved oxygen. Chem. Geol. 225, 16–29.

Godet, J.-D., Mitchell, A., 1988. Collins photographic key to the trees of Britain and northern Europe: a guide to identification by leaves and needles. Collins, London.

Goldstein, J., Newbury, D., Joy, D., Lyman, C., Echllin, P., Lifshin, E., Sawyer, L., Michael, J., 2003. Scanning Electron Microscopy and X-ray Microanalysis, 3rd ed. Springer, New York.

Gomes, H., Rosina, P., Holakooei, P., Solomon, T., Vaccaro, C., 2013. Identification of pigments used in rock art paintings in Gode Roriso-Ethiopia using Micro-Raman spectroscopy. J. Archaeol. Sci. 40, 4073–4082.

González-Urquijo, J., Beyries, S., Ibáñez, J.J., 2015. Ethnoarchaeology and functional analysis, in: Marreiros, J.M., Gibaja Bao, J.F., Bicho, N., Schiffer, M.B. (Eds.), Use-Wear and Residue Analysis in Archaeology, Manuals in Archaeological Method, Theory and Technique. Springer, London, pp. 27–40.

Götze, J., Möckel, R., 2012. Quartz: Deposits, Mineralogy and Analytics. Springer, Berlin.

Götze, J., Nasdala, L., Kleeberg, R., Wenzel, M., 1998. Occurrence and distribution of "moganite" in agate/chalcedony: a combined micro-Raman, Rietveld, and cathodoluminescence study. Contrib. Mineral. Petrol. 133, 96–105.

Gould, S.J., 1965. Is uniformitarianism necessary? American Journal of Science 263, 223–228.

Grace, R., 1996. Use-wear analysis: the state of the art. Archaeometry 38, 209–229.

Grace, R., Graham, I.D., Newcomer, M.H., 1987. Preliminary investigation into the quantification of wear traces on flint tools, in: Sieveking, G., Newcomer, M.H. (Eds.), Papers Presented at the 4th International Flint Symposium. Cambridge University Press, Cambridge, pp. 63–69.

Graham, D., Faulds, K., 2008. Quantitative SERRS for DNA sequence analysis. Chem. Soc. Rev. 37, 1042–1051.

Gramsch, B., Kloss, K., 1989. Excavations near Friesack: an Early Mesolithic Marshland Site in the Northern Plain of Central Europe, in: Bonsall, C. (Ed.), The Mesolithic in Europe: Papers Presented at the Third International Mesolithic Symposium, Edinburgh, 1985. John Donald Publishers, Edinburgh, pp. 313–324.

Grattan-Bellew, P.E., Eden, W.J., 1975. Concrete Deterioration and Floor Heave Due to Biogeochemical Weathering of Underlying Shale. Can. Geotech. J. 12, 372–378.

Green, E.J., Speller, C.F., 2017. Novel Substrates as Sources of Ancient DNA: Prospects and Hurdles. Genes 8. doi:10.3390/genes8070180

Gribble, C.D., Hall, A.J., 1985. A practical introduction to optical mineralogy. Allen & Unwin, London.

Griffiths, P.R., de Haseth, J.A., 2007. Fourier Transform Infrared Spectrometry. John Wiley & Sons.

Grünberg, J.M., 2002. Middle Palaeolithic birch-bark pitch. Antiquity 76, 15–16.

Gurfinkel, D.M., Franklin, U.M., 1988. A study of the feasibility of detecting blood residue on artifacts. J. Archaeol. Sci. 15, 83–97.

Gutarowska, B., Celikkol-Aydin, S., Bonifay, V., Otlewska, A., Aydin, E., Oldham, A.L., Brauer, J.I., Duncan, K.E., Adamiak, J., Sunner, J.A., Beech, I.B., 2015. Metabolomic and high-throughput sequencing analysis-modern approach for the assessment of biodeterioration of materials from historic buildings. Front. Microbiol. 6, 979.

Guthoff, R.F., Baudouin, C., Stave, J., 2006. Atlas of Confocal Laser Scanning In-vivo Microscopy in Ophthalmology: Principles and Applications in Diagnostic and Therapeutic Ophthalmology. Springer, Berlin.

Hahn, F.E., Keck, M., Raymond, K.N., 1995. Catecholate Complexes of Silicon: Synthesis and Molecular and Crystal Structures of $[Si(cat)_2]\cdot 2THF$ and $Li_2[Si(cat)_3]\cdot 3.5dme$ (cat = Catecholate Dianion). Inorg. Chem. 34, 1402–1407.

Hall, B.K., 2005. Bones and Cartilage: Developmental and Evolutionary Skeletal Biology. Elsevier Academic Press, San Diego.

Hall, J., Higgins, S., Fullagar, R., 1989. Plant Residues on Stone Tools, in: Beck, W., Clarke, A., Head, L. (Eds.), Plants in Australian Archaeology, Tempus. University of Queensland, Queensland, pp. 136–160.

Hames, D., Hooper, N., 2000. Instant Notes in Biochemistry, 2nd ed. BIOS Scientific Publishers, Oxford.

Hardesty, D.L., Brodhead, M.J., Grayson, D.K., Lindström, S., Miller, G., 2005. The Archaeology of the Donner Party. University of Nevada Press, Reno, Las Vegas.

Hardy, B., 1999. Preliminary results of residue and use-wear analyses of stone tools from two Mesolithic sites, northern Bohemia, Czech Republic. Archaeologicke Rozhledy 51, 274–279.

Hardy, B.L., 2004. Neanderthal behaviour and stone tool function at the Middle Palaeolithic site of La Quina, France. Antiquity 78, 547–565.

Hardy, B.L., Bolus, M., Conard, N.J., 2008. Hammer or crescent wrench? Stone-tool form and function in the Aurignacian of southwest Germany. J. Hum. Evol. 54, 648–662.

Hardy, B.L., Garufi, G.T., 1998. Identification of Woodworking on Stone Tools through Residue and Use-Wear Analyses: Experimental Results. J. Archaeol. Sci. 25, 177–184.

Hardy, B.L., Kay, M., Marks, A.E., Monigal, K., 2001. Stone tool function at the paleolithic sites of Starosele and Buran Kaya III, Crimea: Behavioral implications. Proceedings of the National Academy of Sciences 98, 10972–10977.

Hardy, B.L., Moncel, M.-H., 2011. Neanderthal use of fish, mammals, birds, starchy plants and wood 125-250,000 years ago. PLoS One 6, e23768.

Hardy, B.L., Moncel, M.-H., Daujeard, C., Fernandes, P., Béarez, P., Desclaux, E., Chacon Navarro, M.G., Puaud, S., Gallotti, R., 2013. Impossible Neanderthals? Making string, throwing projectiles and catching small game during Marine Isotope Stage 4 (Abri du Maras, France). Quat. Sci. Rev. 82, 23–40.

Hardy, B.L., Raff, R.A., Raman, V., 1997. Recovery of Mammalian DNA from Middle Paleolithic Stone Tools. J. Archaeol. Sci. 24, 601–611.

Hardy, B.L., Svoboda, J.A., 2009. Mesolithic stone tool function and site types in Northern Bohemia, Czech Republic, in: Haslam, M., Robertson, G., Crowther, A., Nugent, S., Kirkwood, L. (Eds.), Archaeological Science under a Microscope: Studies in Residue and Ancient DNA Analysis in Honour of Thomas H. Loy, Terra Australis. Australian National University Press, Canberra, pp. 159–174.

Hardy, K., Blakeney, T., Copeland, L., Kirkham, J., Wrangham, R., Collins, M., 2009. Starch granules, dental calculus and new perspectives on ancient diet. J. Archaeol. Sci. 36, 248–255.

Hardy, K., Shiel, R., 2007. Residue and use-wear analyses, in: Waddington, C. (Ed.), Mesolithic Settlement in the North Sea Basin. A Case Study from Howick, Northumberland. Oxbow Books, Oxford.

Haslam, M., 2009. Mountains and molehills: sample size in archaeological microscopic stone-tool residue analysis, in: Haslam, M., Robertson, G., Crowther, A., Nugent, S., Kirkwood, L. (Eds.), Archaeological Science Under a Microscope: Studies in Residue and Ancient DNA Analysis in Honour of Thomas H. Loy, Terra Australis. Australian National University Press, Canberra, pp. 47–79.

Haslam, M., 2008. Initial tests on the three-dimensional movement of starch in sediments, in: Fairbairn, A., O'Connor, S., Marwick, B. (Eds.), New Directions in Archaeological Science, Terra Australis. Australian National University Press, Canberra, pp. 93–103.

Haslam, M., 2006a. Archaeology of the instant? Action and narrative in microscopic archaeological residue analysis. Journal of Social Archaeology 6, 402–424.

Haslam, M., 2006b. Potential misidentification of in situ archaeological tool-residues: starch and conidia. J. Archaeol. Sci. 33, 114–121.

Haslam, M., 2004. The decomposition of starch grains in soils: implications for archaeological residue analyses. J. Archaeol. Sci. 31, 1715–1734.

Hauck, T.C., Connan, J., Charrié-Duhaut, A., Le Tensorer, J.-M., Sakhel, H. al, 2013. Molecular evidence of bitumen in the Mousterian lithic assemblage of Hummal (Central Syria). J. Archaeol. Sci. 40, 3252–3262.

Hausman, L.A., 1920. Structural Characteristics of the Hair of Mammals. The American Naturalist 54, 496–523.

Hayek, E.W.H., Krenmayr, P., Lohninger, H., Jordis, U., Moche, W., Sauter, F., 1990. Identification of archaeological and recent wood tar pitches using gas chromatography/mass spectrometry and pattern recognition. Anal. Chem. 62, 2038–2043.

Hayes, E.H., Cnuts, D., Lepers, C., Rots, V., 2017/2. Learning from blind tests: Determining the function of experimental grinding stones through use-wear and residue analysis. Journal of Archaeological Science: Reports 11, 245–260.

Hazelton, P., Murphy, B., 2016. Interpreting Soil Test Results: What Do All the Numbers Mean?, 3rd ed. Csiro Publishing, Clayton South, Australia.

Heaney, P.J., Post, J.E., 1992. The widespread distribution of a novel silica polymorph in microcrystalline quartz varieties. Science 255, 441–443.

Heaton, K., Solazzo, C., Collins, M.J., Thomas-Oates, J., Bergström, E.T., 2009. Towards the application of desorption electrospray ionisation mass spectrometry (DESI-MS) to the analysis of ancient proteins from artefacts. J. Archaeol. Sci. 36, 2145–2154.

Hedrich, S., Schlömann, M., Johnson, D.B., 2011. The iron-oxidizing proteobacteria. Microbiology 157, 1551–1564.

Hefferan, K., O'Brien, J., 2010. Earth Materials. Wiley-Blackwell.

Helfman, G., Collette, B.B., Facey, D.E., Bowen, B.W. (Eds.), 2009. Skeleton, skin, and scales, in: The Diversity of Fishes: Biology, Evolution, and Ecology. Wiley-Blackwell, Oxford, pp. 23–40.

Helwig, K., Monahan, V., Poulin, J., 2008. The Identification of Hafting Adhesive on a Slotted Antler Point from a Southwest Yukon Ice Patch. American Antiquity 73, 279–288.

Helwig, K., Monahan, V., Poulin, J., Andrews, T.D., 2014. Ancient projectile weapons from ice patches in northwestern Canada: identification of resin and compound resin-ochre hafting adhesives. Journal of Archaeological Science 41, 655–665.

Henry, A.G., Brooks, A.S., Piperno, D.R., 2011. Microfossils in calculus demonstrate consumption of plants and cooked foods in Neanderthal diets (Shanidar III, Iraq; Spy I and II, Belgium). Proceedings of the National Academy of Sciences 108, 486–491.

Henry, A.G., Hudson, H.F., Piperno, D.R., 2009/3. Changes in starch grain morphologies from cooking. J. Archaeol. Sci. 36, 915–922.

Henson, D., 2016. The Meso-what? The public perceptions of the Mesolithic (PhD). University of York.

Hibino, Y., Hanafusa, H., Ema, K., Hyodo, S., 1985. Raman study on silica optical fibers subjected to high tensile stress. Appl. Phys. Lett. 47, 812–814.

High, K., 2014. Fading Star: Understanding Accelerated Decay at Star Carr. University of York.

High, K., Milner, N., Panter, I., Demarchi, B., Penkman, K.E.H., 2016. Lessons from Star Carr on the vulnerability of organic archaeological remains to environmental change. Proc. Natl. Acad. Sci. U. S. A. 113, 12957–12962.

High, K., Milner, N., Panter, I., Penkman, K.E.H., 2015. Apatite for destruction: Investigating bone degradation due to high acidity at Star Carr. Journal of Archaeological Science 59, 159–168.

High, K., Penkman, K., Boreham, S., Boreham, J., Needham, A., Knight, B., Elliott, B., Bamforth, M., Taylor, M., Panter, I., Felter, M., Rowley, C., Milner, N., in press.

Geochemistry of the Central and Western Structures, in: Milner, N., Conneller, C., Taylor, B. (Eds.), Star Carr. White Rose Press, York.

Hill, H.E., Evans, J., 1987. The identification of Plants used in Prehistory from Organic Residues, in: Ambrose, W.R., Mummery, J.M.J. (Eds.), Archaeometry: Further Australasian Studies. Dept. of Prehistory, Research School of Pacific Studies, Australian National University, Canberra, pp. 90–96.

Hjulström, B., Isaksson, S., Hennius, A., 2006. Organic Geochemical Evidence for Pine Tar Production in Middle Eastern Sweden During the Roman Iron Age. J. Archaeol. Sci. 33, 283–294.

Hlinka, V., Muharam, I., Lentile, V.K., 2009. Method validation in forensics and the archaeological sciences, in: Haslam, M., Robertson, G., Crowther, A., Nugent, S., Kirkwood, L. (Eds.), Archaeological Science under a Microscope: Studies in Residue and Ancient DNA Analysis in Honour of Thomas H. Loy, Terra Australis. Australian National University Press, Canberra, pp. 151–158.

Högberg, A., Puseman, K., Yost, C., 2009. Integration of use-wear with protein residue analysis - a study of tool use and function in the south Scandinavian Early Neolithic. J. Archaeol. Sci. 36, 1725–1737.

Holakooei, P., Karimy, A.-H., Hasanpour, A., Oudbashi, O., 2016. Micro-Raman spectroscopy in the identification of wulfenite and vanadinite in a Sasanian painted stucco fragment of the Ghaleh Guri in Ramavand, western Iran. Spectrochim. Acta A Mol. Biomol. Spectrosc. 169, 169–174.

Hollricher, O., 2010. Raman instrumentation for confocal Raman microscopy, in: Dieing T Hollricher O Toporski (Ed.), Confocal Raman Microscopy, Springer Series in Optical Sciences. Springer, Heidelberg, pp. 43–60.

Honig, G.R., Adams, J.G., 1986. Human Hemoglobin Genetics. Springer-Verlag, New York.

Horobin, R.W., 2002. Monoazo dyes, in: Horobin, R.W., Kiernan, J.A. (Eds.), Conn's Biological Stains: A Handbook of Dyes, Stains and Fluorochromes for Use in Biology and Medicine. Taylor & Francis, London, pp. 107–123.

Horrocks, M., Nieuwoudt, M.K., Kinaston, R., Buckley, H., Bedford, S., 2014. Microfossil and Fourier Transform InfraRed analyses of Lapita and post-Lapita human dental calculus from Vanuatu, Southwest Pacific. J. R. Soc. N. Z. 44, 17–33.

Hortolà, P., 2008. Secondary-electron SEM bioimaging of human erythrocytes in bloodstains on high-carbon steel substrate without specimen preparation. Micron 39, 53–55.

Hortolà, P., 2005. SEM examination of human erythrocytes in uncoated bloodstains on stone: use of conventional as environmental-like SEM in a soft biological tissue (and hard inorganic material). Journal of Microscopy 218, 94–103.

Hortolà, P., 2002. Red Blood Cell Haemotaphonomy of Experimental Human Bloodstains on Techno-Prehistoric Lithic Raw Materials. Journal of Archaeological Science 29, 733–739.

Hortolà, P., 2001. Experimental SEM Determination of Game Mammalian Bloodstains on Stone Tools. Environmental Archaeology 6, 97–102.

Hortolà, P., 1992. SEM analysis of red blood cells in aged human bloodstains. Forensic Science International 55, 139–159.

Howard, C.D., 2002. The Gloss Patination of Flint Artifacts. Plains Anthropol. 47, 283–287.

Howard, C.D., 1999. Amorphous Silica, Soil Solutions, and Archaeological Flint Gloss. North American Archaeologist 20, 209–215.

Howard, C.D., 1994. Natural Indicators of Lithic Artifact Authenticity. North American Archaeologist 15, 321–330.

Hübschmann, H.J., 2015. Handbook of GC-MS: Fundamentals and Applications, 3rd ed. Wiley.

Huntley, B., Birks, H.J.B., 1983. An atlas of past and present pollen maps for Europe: 0-13000 years ago. Cambridge University Press, Cambridge.

Hurcombe, L., 2014. Perishable Material Culture in Prehistory: Investigating the Missing Majority. Routledge.

Hutschenreuther, A., Watzke, J., Schmidt, S., Büdel, T., Henry, A.G., 2017. Archaeological implications of the digestion of starches by soil bacteria: Interaction among starches leads to differential preservation. Journal of Archaeological Science: Reports 15, 95–108.

Hutton, J., 1785. Concerning the system of the earth, its duration, and stability. Abstract of dissertation read in the Royal Society of Edinburgh 30.

Hyland, D.C., Tersak, J.M., Adovasio, J.M., Siegel, M.I., 1990. Identification of the Species of Origin of Residual Blood on Lithic Material. Am. Antiq. 55, 104–112.

Hylton, M.D., 2000. Microfaunal investigation of the early Toarcian (Lower Jurassic) extinction event in NW Europe (PhD). University of Plymouth.

Innes, J.B., Blackford, J.J., Simmons, I.G., 2011. Mesolithic Environments at Star Carr, the Eastern Vale of Pickering and Environs: Local and Regional Contexts. Journal of Wetland Archaeology 11, 85–108.

Innes, J., Blackford, J., Simmons, I., 2010. Woodland disturbance and possible land-use regimes during the Late Mesolithic in the English uplands: pollen, charcoal and non-pollen palynomorph evidence from Bluewath Beck, North York Moors, UK. Veg. Hist. Archaeobot. 19, 439–452.

Jacobs, J.A., Testa, S.M., 2014. Acid drainage and sulfide oxidation: introduction, in: Jacobs, J.A., Lehr, J.H., Testa, S.M. (Eds.), Acid Mine Drainage, Rock Drainage, and Acid Sulfate Soils: Causes, Assessment, Prediction, Prevention, and Remediation. Wiley, Hoboken, NJ, pp. 3–8.

Jacobs, J.A., Vance, D.B., 2014a. Biogeochemistry of Acid Drainage, in: Jacobs, J.A., Lehr, J.H., Testa, S.M. (Eds.), Acid Mine Drainage, Rock Drainage, and Acid Sulfate Soils. Wiley, Hoboken, NJ, pp. 15–51.

Jacobs, J.A., Vance, D.B., 2014b. Biogeochemistry of acid drainage, in: Jacobs, J.A., Lehr, J.H., Testa, S.M. (Eds.), Acid Mine Drainage, Rock Drainage, and Acid Sulfate Soils: Causes, Assessment, Prediction, Prevention, and Remediation. Wiley, Hoboken, NJ, pp. 15–52.

Jafarzadeh, A.A., Burnham, C.P., 1992. Gypsum crystals in soils. Journal of Soil Science 43, 409–420.

Jahren, A.H., Toth, N., Schick, K., Clark, J.D., Amundson, R.G., 1997. Determining stone tool use: chemical and morphological analyses of residues on experimentally manufactured stone tools. J. Archaeol. Sci. 24, 245–250.

Janko, M., Stark, R.W., Zink, A., 2012. Preservation of 5300 year old red blood cells in the Iceman. Journal of the Royal Society 9, 2581–2590.

Jans, M.M.E., 2005. Histological Characterisation of Diagenetic Alteration of Archaeological Bone, Geoarchaeological and bioarchaeological studies. Institute for Geo and Bioarchaeology, Vrije Universiteit, Amsterdam.

Jennings, S.R., Neuman, D.R., Blicker, P.S., 2008. Acid mine drainage and effects on fish health and ecology: a review. U.S. Fish and Wildlife Service, Bozeman, MT.

Ji, L., Liao, Q., Wu, L., Lv, W., Yang, M., Wan, L., 2013. Migration of 16 phthalic acid esters from plastic drug packaging to drugs by GC-MS. Anal. Methods 5, 2827–2834.

Johansson, S.A.E., 1995. Introduction to PIXE, in: Johansson, S.A.E., Campbell, J.L., Malmqvist, K.G. (Eds.), Particle-Induced X-Ray Emission Spectrometry (PIXE), Chemical Analysis: A Series of Monographs on Analytical Chemistry and Its Applications . John Wiley & Sons, New York, pp. 1–18.

Johnson, M., 2010. Archaeological Theory: An Introduction, 2nd ed. Wiley Blackwell, Oxford.

Jones, L.H.P., Handreck, K.A., 1967. Silica In Soils, Plants, and Animals. Advances in Agronomy 19, 107–149.

Jones, R., 1990. From Kakadu to Kutikina: the southern continent at 18,000 years ago, in: Gamble, C., Soffer, O. (Eds.), The World at 18000 BP: Low Latitudes. Unwin Hyman, London, pp. 264–295.

Juel Jensen, H., 1988. Functional analysis of prehistoric flint tools by high-power microscopy: A review of West European research. Journal of World Prehistory 2, 53–88.

Kadej, M., 2012. Detailed Description of the Morphology of the Last Instar Larva of Trogoderma megatomoides Reitter, 1881 (Dermestidae: Megatominae: Megatomini) with Comparison to Related Species. J. Kans. Entomol. Soc. 85, 5–13.

Kasten, F.H., 2002. Introduction to dyes and stains, in: Horobin, R.W., Kiernan, J.A. (Eds.), Conn's Biological Stains: A Handbook of Dyes, Stains and Fluorochromes for Use in Biology and Medicine. Taylor & Francis, London, pp. 1–14.

Kealhofer, L., Torrence, R., Fullagar, R., 1999. Integrating Phytoliths within Use-Wear/Residue Studies of Stone Tools. J. Archaeol. Sci. 26, 527–546.

Keeley, L.H., 1980a. Experimental Determination of Stone Tool Uses: a Microwear Analysis, in: Butzer, K.W., Freeman, L.G. (Eds.), Prehistoric Archaeology and Ecology. University of Chicago Press, Chicago.

Keeley, L.H., Newcomer, M.H., 1977. Microwear analysis of experimental flint tools: a test case. J. Archaeol. Sci. 4, 29–62.

Keeley, L.H., Toth, N., 1981. Microwear polishes on early stone tools from Koobi Fora, Kenya. Nature 293, 464–465.

Kemp, A., Nicoll, R.S., 1996. Histology and histochemistry of conodont elements. Mod. Geol. 20, 287–302.

Kendrick, K.J., 2006. Pedogenic silica accumulation, in: Lal, R. (Ed.), Encyclopedia of Soil Science. Taylor & Francis, New York, pp. 1251–1253.

Kenyon, L.C., 2012. Skeletal Muscle, in: Rubin, R., Strayer, D.S., Rubin, E. (Eds.), Rubin's Pathology: Clinicopathologic Foundations of Medicine, Rubin's Pathology. Lippincott Williams & Wilkins, Baltimore, pp. 1273–1294.

Kerns, J.G., Buckley, K., Parker, A.W., Birch, H.L., Matousek, P., Hildred, A., Goodship, A.E., 2015. The use of laser spectroscopy to investigate bone disease in King Henry VIII's sailors. J. Archaeol. Sci. 53, 516–520.

Khan, S., Haq, F., Hasan, F., Saeed, K., Ullah, R., 2012. Growth and biochemical activities of Acidithiobacillus thiooxidans collected from black shale. J. Microbiol. Res. 2, 78–83.

Kierdorf, U., Stoffels, E., Stoffels, D., Kierdorf, H., Szuwart, T., Clemen, G., 2003. Histological studies of bone formation during pedicle restoration and early antler regeneration in roe deer and fallow deer. The Anatomical Record Part A: Discoveries in Molecular, Cellular, and Evolutionary Biology 273, 741–751.

Killick, D., 2015a. Using evidence from natural sciences in archaeology, in: Chapman, R., Wylie, A. (Eds.), Material Evidence: Learning from Archaeological Practice. Routledge, Oxon, pp. 159–172.

Killick, D., 2015b. The awkward adolescence of archaeological science. J. Archaeol. Sci. doi:10.1016/j.jas.2015.01.010

Kimura, B., Brandt, S.A., Hardy, B.L., Hauswirth, W.W., 2001. Analysis of DNA from Ethnoarchaeological Stone Scrapers. J. Archaeol. Sci. 28, 45–53.

Kingma, K.J., Hemley, R.J., 1994. Raman spectroscopic study of microcrystalline silica. American Mineralogist 79, 269–273.

King, R., Miskelly, G.M., 2005. The inhibition by amines and amino acids of bleach-induced luminol chemiluminescence during forensic screening for blood. Talanta 67, 345–353.

Kingsolver, J.M., 2002. Dermestidae, in: Arnett, R.H., Thomas, M.C., Skelley, P.E., Frank, J.H. (Eds.), American Beetles, Volume II: Polyphaga: Scarabaeoidea through Curculionoidea. CRC Press, Boca Raton, pp. 228–232.

Kingsolver, J.M., 1991. Dermestid beetles (Dermestidae, Coleoptera), in: Gorham, J.R. (Ed.), Insect and Mite Pests in Food: An Illustrated Key, Agriculture Handbook No. 655. United States Department of Agriculture and United States Department of Health and Human Services, Washington, DC, pp. 115–135.

Kirby, A.R., Gunning, A.P., Waldron, K.W., Morris, V.J., Ng, A., 1996. Visualization of plant cell walls by atomic force microscopy. Biophysical Journal 70, 1138–1143.

Klein, C., Philpotts, A.R., 2013. Earth Materials: Introduction to Mineralogy and Petrology, Earth Materials: Introduction to Mineralogy and Petrology. Cambridge University Press, Cambridge.

Klepetsanis, P.G., Koutsoukos, P.G., 1989. Precipitation of calcium sulfate dihydrate at constant calcium activity. J. Cryst. Growth 98, 480–486.

Klingenspor, M., Fromme, T., 2011. Brown adipose tissue, in: Symonds, M.E. (Ed.), Adipose Tissue Biology. Springer, New York, pp. 39–70.

Knight, B., Milner, N., Taylor, B., Elliott, B., O'Connor, T., in press. Faunal remains, in: Milner, N., Conneller, C., Taylor, B. (Eds.), Star Carr Monograph. White Rose Press, York.

Koenig, J.L., 2000. Infrared and Raman Spectroscopy of Polymers, Rapra Review Reports: Expert overviews covering the science and technology of rubber and plastics. Smithers Rapra Press, Belfast.

Koller, J., Baumer, U., Mania, D., 2001. High-Tech in the Middle Palaeolithic: Neandertal-Manufactured Pitch Identified. European Journal of Archaeology 4, 385–397.

Kononenko, N., 2011. Experimental and archaeological studies of use-wear and residues on obsidian artefacts from Papua New Guinea. Technical Reports of the Australian Museum.

Kononenko, N., Torrence, R., Sheppard, P., 2016/8. Detecting early tattooing in the Pacific region through experimental usewear and residue analyses of obsidian tools. Journal of Archaeological Science: Reports 8, 147–163.

Kononenko, N., Torrence, R., White, P., 2015. Unexpected uses for obsidian: experimental replication and use-wear/residue analyses of chopping tools. J. Archaeol. Sci. 54, 254–269.

Kooyman, B., 2015. Starch Granules: Preparation and Archaeological Extraction, in: Yeung, E.C.T., Stasolla, C., Sumner, M.J., Huang, B.Q. (Eds.), Plant Microtechniques and Protocols. Springer International Publishing, Heidelberg, pp. 525–540.

Kooyman, B., Newman, M.E., Ceri, H., 1992. Verifying the reliability of blood residue analysis on archaeological tools. J. Archaeol. Sci. 19, 265–269.

Kooyman, B., Newman, M.E., Cluney, C., Lobb, M., Tolman, S., McNeil, P., Hills, L.V., 2001. Identification of Horse Exploitation by Clovis Hunters Based on Protein Analysis. Am. Antiq. 66, 686–691.

Kooyman, B.P., 1985. Moa and moa hunting: an archaeological analysis of big game hunting in New Zealand. University of Otago.

Koukouzas, N., Vasilatos, C., 2008. Mineralogical and chemical properties of FGD gypsum from Florina, Greece. J. Chem. Technol. Biotechnol. 83, 20–26.

Krishnamurthy, N., Soots, V., 1971. Raman Spectrum of Gypsum. Canadian Journal of Physics 49, 885–896.

Krishnan, R.S., 1953. The scattering of light in fused quartz and its Raman spectrum. Proc. Indian Acad. Sci. 37, 377–384.

Kyle, P.B., 2017. Toxicology: GCMS, in: Nair, H., Clarke, W. (Eds.), Mass Spectrometry for the Clinical Laboratory. Elsevier, London, pp. 131–164.

Lagler, K.F., 1947. Lepidological Studies 1. Scale Characters of the Families of Great Lakes Fishes. Trans. Am. Microsc. Soc. 66, 149–171.

Lähdesmäki, P., Piispanen, R., 1988. Degradation products and the hydrolytic enzyme activities in the soil humification processes. Soil Biol. Biochem. 20, 287–292.

Lamb, J., Loy, T., 2005. Seeing red: the use of Congo Red dye to identify cooked and damaged starch grains in archaeological residues. J. Archaeol. Sci. 32, 1433–1440.

Landete-Castillejos, T., Currey, J.D., Ceacero, F., García, A.J., Gallego, L., Gomez, S., 2012. Does nutrition affect bone porosity and mineral tissue distribution in deer antlers? The relationship between histology, mechanical properties and mineral composition. Bone 50, 245–254.

Landsteiner, K., 1936. The Specificity of Serological Reactions. Thomas Books, Springfield, Illinois.

Langejans, G.H.J., 2012a. Middle Stone Age pièces esquillées from Sibudu Cave, South Africa: an initial micro-residue study. J. Archaeol. Sci. 39, 1694–1704.

Langejans, G.H.J., 2012b. Micro-residue analysis on Early Stone Age tools from Sterkfontein, South Africa. South African Archaeological Bulletin 67, 200–213.

Langejans, G.H.J., 2011. Discerning use-related micro-residues on tools: testing the multi-stranded approach for archaeological studies. J. Archaeol. Sci. 38, 985–1000.

Langejans, G.H.J., 2010. Remains of the day-preservation of organic micro-residues on stone tools. J. Archaeol. Sci. 37, 971–985.

Langejans, G.H.J., 2009. Testing Residues: An Experimental Approach. University of Witwatersrand, Johannesburg.

Langejans, G.H.J., 2007. PIXE and residues: examples from Sterkfontein and Sibudu, South Africa. South African Archaeological Bulletin 62, 71–73.

Langejans, G.H.J., Lombard, M., 2015. About small things and bigger pictures: an introduction to the morphological identification of micro-residues on stone tools, in: Marreiros, J.M., Gibaja Bao, J.F., Bicho, N.F., Schiffer, M.B. (Eds.), Use-Wear and Residue Analysis in Archaeology, Manuals in Archaeological Method, Theory and Technique. Springer, London, pp. 199–220.

Langenheim, J.H., 2003. Plant Resins: Chemistry, Evolution, Ecology, and Ethnobotany. Timber Press, Portland.

Larkin, P., 2011. Infrared and Raman Spectroscopy; Principles and Spectral Interpretation. Elsevier.

Larson, D., 2016. Clinical Chemistry: Fundamentals and Laboratory Techniques. Elsevier Health Sciences, Saint Louis, Missouri.

Larson, P.R., 1969. Wood formation and the concept of wood quality. Bulletin of Yale University School of Forestry 74, 1–54.

Lattuati-Derieux, A., Gomes, S., Tirat, S., Thao-Heu, S., Echard, J.-P., 2014. New insights into molecular evolution of oil/colophony varnishes: towards pyrolysis-gas chromatography/mass spectrometry-based quantitation. e-Preservation Science 11, 54–63.

Lawrence, J., Ślipiński, A., 2013. Australian Beetles Volume 1: Morphology, Classification and Keys, Australian Beetles Series. CSIRO Publishing, Collingwood.

Laylander, D., 2000. Early ethnography of the Californias, 1533-1825, Archives of California prehistory. Coyote Press.

Leach, J.D., 1998. A Brief Comment on the Immunological Identification of Plant Residues on Prehistoric Stone Tools and Ceramics: Results of a Blind Test. J. Archaeol. Sci. 25, 171–175.

Leach, J.D., Mauldin, R.P., 1995. Additional comments on blood residue analysis in archaeology. Antiquity 69, 1020–1022.

Legeros, R.Z., Legeros, J.P., 2008. Hydroxyapatite, in: Kokubo, T. (Ed.), Bioceramics and Their Clinical Applications. Woodhead Publishing, Cambridge, England, pp. 367–394.

Legge, A.J., Rowley-Conwy, P.A., 1988. Star Carr revisited: a re-analysis of the large mammals. Centre for Extra-Mural Studies, Birkbeck College, University of London, London.

Legodi, M.A., de Waal, D., 2007. The preparation of magnetite, goethite, hematite and maghemite of pigment quality from mill scale iron waste. Dyes Pigm. 74, 161–168.

Lemorini, C., Cesaro, S.N., 2014. An integration of the use-wear and residue analysis for the identification of the function of archaeological stone tools. Proceedings of the international workshop, Rome, March 5th-7th, 2012, in: BAR International Series 2649. Archaeopress, Oxford.

Lemorini, C., Cesaro, S.N., Celant, A., Nucara, A., Maselli, P., Skakun, N., Abbo, S., Gopher, A., 2014. The function of prehistoric lithic tools: a combined study of use-wear analysis and FTIR microspectroscopy. Results and open problems, in: Lemorini, C., Cesaro, S.N. (Eds.), An Integration of the Use-Wear and Residue Analysis for the Identification of the Function of Archaeological Stone Tools. Proceedings of the International Workshop, Rome, March 5th-7th, 2012. Archaeopress, Oxford, pp. 63–76.

Levi Sala, I., 1996. A study of microscopic polish on flint implements, British Archaeological Reports International Series. British Archaeological Reports, Oxford.

Levi Sala, I., 1986. Use wear and post-depositional surface modification: A word of caution. J. Archaeol. Sci. 13, 229–244.

Lew, K., 2009. Acids and Bases, Essential Chemistry. Infobase Publishing, New York.

Liang, Y., Nikolic, M., Bélanger, R., Gong, H., Song, A., 2015. Silicon in Agriculture: From Theory to Practice. Springer, Dordrecht.

Liao, Z., Chen, G., Mao, Y., Peng, X., Dong, P., Wu, J., 1998. [Morphologic changes of red blood cells in various conditions under scanning electron microscope]. Hua Xi Yi Ke Da Xue Xue Bao [Journal of West China University of Medical Sciences] 29, 192–195.

Lieber, R.L., 2009. Skeletal Muscle Structure, Function, and Plasticity: The Physiological Basis of Rehabilitation, 3rd ed. Lippincott Williams & Wilkins, Philadelphia.

Lieber, R.L., Fridén, J., 1991. Skeletal muscle and tendon microanatomy. Current Opinion in Orthopaedics 2, 691–695.

Lindbo, D.L., Stolt, M.H., Vepraskas, M.J., 2010. Redoximorphic Features, in: Stoops, G, Marcelino, V, Mees, F. (Eds.), Interpretation of Micromorphological Features of Soils and Regoliths. Elsevier, Amsterdam, pp. 129–147.

Little, A., Elliott, B., Conneller, C., Pomstra, D., Evans, A.A., Fitton, L.C., Holland, A., Davis, R., Kershaw, R., O'Connor, S., O'Connor, T., Sparrow, T., Wilson, A.S., Jordan, P., Collins, M.J., Colonese, A.C., Craig, O.E., Knight, R., Lucquin, A.J.A., Taylor, B., Milner, N., 2016. Technological Analysis of the World's Earliest Shamanic Costume: A Multi-Scalar, Experimental Study of a Red Deer Headdress from the Early Holocene Site of Star Carr, North Yorkshire, UK. PLoS One 11, e0152136.

Li, T., Xie, Y.-F., Yang, Y.-M., Wang, C.-S., Fang, X.-Y., Shi, J.-L., He, Q.-J., 2009. Pigment identification and decoration analysis of a 5th century Chinese lacquer painting screen: a micro-Raman and FTIR study. J. Raman Spectrosc. 40, 1911–1918.

Li, X., Xiong, W., Lin, H., Zhuo, L., Lv, S., Tang, X., Chen, M., Zou, Z., Lin, Z., Qiu, B., Chen, G., 2013. Analysis of 16 phthalic acid esters in food simulants from plastic food contact materials by LC-ESI-MS/MS. J. Sep. Sci. 36, 477–484.

Lizama, H.M., Suzuki, I., 1989. Rate Equations and Kinetic Parameters of the Reactions Involved in Pyrite Oxidation by *Thiobacillus ferrooxidans*. Appl. Environ. Microbiol. 55, 2918–2923.

Lloyd, A.J., 1962. Polymorphinid, Miliolid and Rotaliform Foraminifera from the Type Kimmeridgian. Micropaleontology 8, 369–383.

Locquin, M., Langeron, M., 1983. Handbook of Microscopy. Butterworths, London.

Lodish, H., Berk, A., Kaiser, C.A., Krieger, M., Bretscher, A., Ploegh, H., Amon, A., Scott, M.P., 2012. Molecular Cell Biology. W. H. Freeman.

Lombard, M., 2014. In situ presumptive test for blood residues applied to 62 000-year-old stone tools. South African Archaeological Bulletin 199, 80–86.

Lombard, M., 2011. Quartz-tipped arrows older than 60 ka: further use-trace evidence from Sibudu, KwaZulu-Natal, South Africa. J. Archaeol. Sci. 38, 1918–1930.

Lombard, M., 2008. Finding resolution for the Howiesons Poort through the microscope: micro-residue analysis of segments from Sibudu Cave, South Africa. J. Archaeol. Sci. 35, 26–41.

Lombard, M., 2007. The gripping nature of ochre: the association of ochre with Howiesons Poort adhesives and Later Stone Age mastics from South Africa. Journal of Human Evolution 53, 406–419.

Lombard, M., 2006. Direct evidence for the use of ochre in the hafting technology of Middle Stone Age tools from Sibudu Cave. Southern African Humanities 18, 57–67.

Lombard, M., 2005. Evidence of hunting and hafting during the Middle Stone Age at Sibudu Cave, KwaZulu-Natal, South Africa: a multianalytical approach. Journal of Human Evolution 48, 279–300.

Lombard, M., 2004. Distribution Patterns of Organic Residues on Middle Stone Age Points from Sibudu Cave, Kwazulu-Natal, South Africa. The South African Archaeological Bulletin 59, 37–44.

Lombard, M., Phillipson, L., 2010. Indications of bow and stone-tipped arrow use 64 000 years ago in KwaZulu-Natal, South Africa. Antiquity 84.

Lombard, M., Wadley, L., 2009. The impact of micro-residue studies on South African Middle Stone Age research, in: Haslam, M., Robertson, G., Crowther, A., Nugent, S., Kirkwood,

L. (Eds.), Archaeological Science Under a Microscope: Studies in Residue and Ancient DNA Analysis in Honour of Thomas H. Loy, Terra Australis. Australian National University Press, Canberra, pp. 11–28.

Lombard, M., Wadley, L., 2007b. Micro-residues on Stone Tools: The Bigger Picture from a South African Middle Stone Age Perspective, in: Barnard, H., Eerkens, J.W. (Eds.), Theory and Practice of Archaeological Residue Analysis, BAR International Series 1650, 3. Archaeopress, Oxford, England, pp. 18–28.

Lombard, M., Wadley, L., 2007a. The morphological identification of micro-residues on stone tools using light microscopy: progress and difficulties based on blind tests. J. Archaeol. Sci. 34, 155–165.

Lombardo, T., Grolimund, D., Kienholz, A., Hubert, V., Wörle, M., 2016. The use of flint-stone fragments as "fire-strikers" during the Neolithic period: Complementary micro-analytical evidences. Microchem. J. 125, 254–259.

López-Buendía, A.M., Whateley, M.K.G., Bastida, J., Urquiola, M.M., 2007. Origins of mineral matter in peat marsh and peat bog deposits, Spain. International Journal of Coal Geology 71, 246–262.

Lowenstein, J.M., 1980. Species-specific proteins in fossils. Naturwissenschaften 67, 343–346.

Lowenstein, J.M., Reuther, J.D., Hood, D.G., Scheuenstuhl, G., Gerlach, S.C., Ubelaker, D.H., 2006. Identification of animal species by protein radioimmunoassay of bone fragments and bloodstained stone tools. Forensic Sci. Int. 159, 182–188.

Lowenstein, J.M., Sarich, V.M., Richardson, B.J., 1981. Albumin systematics of the extinct mammoth and Tasmanian wolf. Nature 291, 409–411.

Lowenstein, J.M., Scheuenstuhl, G., 1991. Immunological Methods in Molecular Palaeontology. Philos. Trans. R. Soc. Lond. B Biol. Sci. 333, 375–380.

Loy, T., 1985. Preliminary residue analysis: AMHN Specimen 20.4/509, in: Thomas, D.H. (Ed.), The Archaeology of Hidden Cave, Nevada, Anthropological Papers of the AMNH. American Museum of Natural History, New York, pp. 224–225.

Loy, T.H., 1994. Methods in the analysis of starch residues on prehistoric stone tools, in: Hather, J.G. (Ed.), Tropical Archaeobotany: Applications and New Developments, 5. Routledge, London, pp. 86–114.

Loy, T.H., 1993. The Artifact as Site: An Example of the Biomolecular Analysis of Organic Residues on Prehistoric Tools. World Archaeol. 25, 44–63.

Loy, T.H., 1983. Prehistoric Blood Residues: Detection on Tool Surfaces and Identification of Species of Origin. Science 220, 1269–1271.

Loy, T.H., Dixon, E.J., 1998. Blood Residues on Fluted Points from Eastern Beringia. American Antiquity 63, 21–46.

Loy, T.H., Hardy, B.L., 1992. Blood residue analysis of 90,000-year-old stone tools from Tabun Cave, Israel. Antiquity 66, 24–35.

Loy, T.H., Nelson, D.E., 1986. Potential Applications of the Organic Residues on Ancient Tools, in: Olin, J.S., Blackman, M.J. (Eds.), Proceedings of the 24th International Archaeometry Symposium. Smithsonian Institution Press, Washington, pp. 179–186.

Loy, T.H., Spriggs, M., Wickler, S., 1992. Direct evidence for human use of plants 28,000 years ago: starch residues on stone artefacts from the northern Solomon Islands. Antiquity 66, 898–912.

Loy, T.H., Wood, A.R., 1989. Blood Residue Analysis at Çayönü Tepesi, Turkey. J. Field Archaeol. 16, 451–460.

Lu, B., Xu, T., Park, S.K., Yates, J.R., 3rd, 2009. Shotgun protein identification and quantification by mass spectrometry. Methods Mol. Biol. 564, 261–288.

Ludwig, D.H., Bryce, J.R., 1996. Hairs and Feathers, in: Olsen, A.R., Sidebottom, T.H., Knight, S.A. (Eds.), Fundamentals of Microanalytical Entomology: A Practical Guide to Detecting and Identifying Filth in Foods. CRC Press, Boca Raton, pp. 157–215.

Luong, S., Hayes, E., Flannery, E., Sutikna, T., Tocheri, M.W., Wahyu Saptomo, E., Jatmiko, Roberts, R.G., 2017. Development and application of a comprehensive analytical

workflow for the quantification of non-volatile low molecular weight lipids on archaeological stone tools. Anal. Methods. doi:10.1039/C7AY01304C

Lv, G., Wang, L., Liu, J., Li, S., 2009. Method for determination of fatty acid amides in polyethylene packaging materials--gas chromatography/mass spectrometry. J. Chromatogr. A 1216, 8545–8548.

Lyell, C., 1830-1833. Principles of Geology: being an attempt to explain the former changes of the Earth's surface, by reference to causes now in operation. John Murray, London.

Magliulo, M., Simoni, P., Guardigli, M., Michelini, E., Luciani, M., Lelli, R., Roda, A., 2007. A rapid multiplexed chemiluminescent immunoassay for the detection of Escherichia coli O157:H7, *Yersinia enterocolitica*, *Salmonella typhimurium*, and *Listeria monocytogenes* pathogen bacteria. J. Agric. Food Chem. 55, 4933–4939.

Makowski, A.J., Patil, C.A., Mahadevan-Jansen, A., Nyman, J.S., 2013. Polarization control of Raman spectroscopy optimizes the assessment of bone tissue. J. Biomed. Opt. 18, 55005.

Malainey, M.E., 2011c. Ancient DNA and the Polymerase Chain Reaction, in: A Consumer's Guide to Archaeological Science: Analytical Techniques, Manuals in Archaeological Method, Theory and Technique. Springer, New York, pp. 237–253.

Malainey, M.E., 2011b. Blood and protein residue analysis, in: A Consumer's Guide to Archaeological Science: Analytical Techniques, Manuals in Archaeological Method, Theory and Technique. Springer, New York, pp. 219–236.

Ma, M., Burkholder, W.E., Carlson, S.D., 1978. Supra-anal Organ: a Defensive Mechanism of the Furniture Carpet Beetle, *Anthrenus flavipes* (Coleoptera: Dermestidae). Ann. Entomol. Soc. Am. 71, 718–723.

Mandair, G.S., Morris, M.D., 2015. Contributions of Raman spectroscopy to the understanding of bone strength. BoneKEy Reports 4, 620.

Maniatis, Y., Tsirtsoni, Z., 2002. Characterization of a black residue in a decorated Neolithic pot from Dikili Tash, Greece:an unexpected result. Archaeometry 44, 229–239.

Marlar, R.A., Leonard, B.L., Billman, B.R., Lambert, P.M., Marlar, J.E., 2000. Biochemical evidence of cannibalism at a prehistoric Puebloan site in southwestern Colorado. Nature 407, 74–78.

Marreiros, J.M., Gibaja Bao, J.F., Ferreira Bicho, N., 2015. Use-Wear and Residue Analysis in Archaeology. Springer.

Martini, F.H., 2005. Anatomy & Physiology. Pearson, San Francisco.

Matheson, C.D., Hall, J., Viel, R., 2009. Drawing first blood from Maya ceramics at Copán, Honduras. Archaeological science under a microscope: Studies in residue and ancient DNA analysis in honor of Thomas H. Loy 190–197.

Matheson, C.D., McCollum, A.J., 2014. Characterising native plant resins from Australian Aboriginal artefacts using ATR-FTIR and GC/MS. J. Archaeol. Sci. 52, 116–128.

Matheson, C.D., Veall, M.-A., 2014. Presumptive blood test using Hemastix® with EDTA in archaeology. Journal of Archaeological Science 41, 230–241.

Matson, D.W., Sharma, S.K., Philpotts, J.A., 1983. The structure of high-silica alkali-silicate glasses. A Raman spectroscopic investigation. J. Non-Cryst. Solids 58, 323–352.

Mazza, P.P.A., Martini, F., Sala, B., Magi, M., Colombini, M.P., Giachi, G., Landucci, F., Lemorini, C., Modugno, F., Ribechini, E., 2006. A new Palaeolithic discovery: tar-hafted stone tools in a European Mid-Pleistocene bone-bearing bed. J. Archaeol. Sci. 33, 1310–1318.

McKeague, J.A., Cline, M.G., 1963a. Silica in soil solutions I. The form and concentration of dissolved silica in aqueous extracts of some soils. Canadian Journal of Soil Science 43, 70–82.

McKeague, J.A., Cline, M.G., 1963b. Silica in soil solutions II. The adsorption of monosilicic acid by soil and by other substances. Canadian Journal of Soil Science 43, 83–96.

McMurry, J., 2011. Organic Chemistry. Cengage Learning.

Meier, D., Faix, O., 1992. Pyrolysis-Gas Chromatography-Mass Spectrometry, in: Lin, S.Y., Professor Emeritus Dr Carlton (Eds.), Methods in Lignin Chemistry, Springer Series in Wood Science. Springer Berlin Heidelberg, pp. 177–199.

Mellars, P.A., Dark, P., 1998. Star Carr in context: new archaeological and palaeoecological investigations at the Early Mesolithic site of Star Carr, North Yorkshire, in: McDonald Institute Monographs. McDonald Institute for Archaeological Research, Cambridge.

Mellars, P., Schadla-Hall, T., Lane, P., Taylor, M., 1998. The wooden platform, in: Mellars, P.A., Dark, P. (Eds.), Star Carr in Context: New Archaeological and Palaeoecological Investigations at the Early Mesolithic Site of Star Carr, North Yorkshire, 4. McDonald Institute Monographs, Cambridge, pp. 47–64.

Mercader, J., 2009. Mozambican Grass Seed Consumption During the Middle Stone Age. Science 326, 1680–1683.

Mernagh, T.P., Trudu, A.G., 1993. A laser Raman microprobe study of some geologically important sulphide minerals. Chemical Geology 103, 113–127.

Messner, T.C., Schindler, B., 2010. Plant processing strategies and their affect upon starch grain survival when rendering Peltandra virginica (L.) Kunth, Araceae edible. J. Archaeol. Sci. 37, 328–336.

Meteorological Office, 2014. High Mowthorpe. Met Office Library & Archive.

Middleditch, B.S., 1989. Analytical Artifacts: GC, MS, HPLC, TLC and PC. Elsevier, Amsterdam.

Miedema, R., Jongmans, A.G., Slager, S., 1974a. Micromorphological observations on pyrite and its oxidation products in four Holocene alluvial soils in the Netherlands, in: Rutherford, G.K. (Ed.), Soil Microscopy: Proceedings of the Fourth International Working-Meeting on Soil Micromorphology. Department of Geography, Queen's University, Kingston, pp. 772–794.

Miedema, R., Jongmans, A.G., Slager, S., 1974b. Micromorphological observations on pyrite and its oxidation products in four Holocene alluvial soils in the Netherlands, in: Rutherford, G.K. (Ed.), Soil Microscopy: Proceedings of the 4th International Working Meeting on Soil Micromorphology. Queen's University, Kingston, Kingston, Ontario, pp. 772–794.

Miehe, G., Graetsch, H., 1992. Crystal structure of moganite: a new structure type of silica. Eur. J. Mineral.

Mielke, R.E., Pace, D.L., Porter, T., Southam, G., 2003. A critical stage in the formation of acid mine drainage: Colonization of pyrite by Acidithiobacillus ferrooxidans under pH-neutral conditions. Geobiology 1, 81–90.

Milanova, R., Han, K., Moore, M., 1995. Oxidation and glucose conjugation of synthetic abietane diterpenes by Cunninghamella sp. II. Novel routes to the family of diterpenes from Tripterygium wilfordii. J. Nat. Prod. 58, 68–73.

Miller, W., Drautz, D.I., Ratan, A., Pusey, B., Qi, J., Lesk, A.M., Tomsho, L.P., Packard, M.D., Zhao, F., Sher, A., Tikhonov, A., Raney, B., Patterson, N., Lindblad-Toh, K., Lander, E.S., Knight, J.R., Irzyk, G.P., Fredrikson, K.M., Harkins, T.T., Sheridan, S., Pringle, T., Schuster, S.C., 2008. Sequencing the nuclear genome of the extinct woolly mammoth. Nature 456, 387–390.

Mills, J.S., White, R., 1977. Natural Resins of Art and Archaeology Their Sources, Chemistry, and Identification. Stud. Conserv. 22, 12–31.

Mills, J., White, R., 2012. Organic Chemistry of Museum Objects. Taylor & Francis.

Milner, N., 2007. Fading Star. British Archaeology 96, 10–14.

Milner, N., Bamforth, M., Beale, G., Carty, J.C., Chatzipanagis, K., Croft, S., Conneller, C., Elliott, B., Fitton, L.C., Knight, B., Kroger, R., Little, A., Needham, A., Robson, H.K., Rowley, C.C.A., Taylor, B., 2016. A Unique Engraved Shale Pendant from the Site of Star Carr: the oldest Mesolithic art in Britain. Internet Archaeology 40. doi:10.11141/ia.40.8

Milner, N., Blinkhorn, E., Hadley, P., Hellewell, E., 2015. The Meso-What? The Public Perception of the Mesolithic, in: Ashton, N., Harris, C. (Eds.), No Stone Unturned: Papers in Honour of Roger Jacobi. Lithics Studies Society, Oxford, pp. 233–248.

Milner, N., Conneller, C., Elliott, B., Koon, H., Panter, I., Penkman, K., Taylor, B., Taylor, M., 2011a. From riches to rags: organic deterioration at Star Carr. J. Archaeol. Sci. 38, 2818–2832.

Milner, N., Conneller, C., Taylor, B., in press. Introduction, in: Milner, N., Conneller, C., Taylor, B. (Eds.), Star Carr Monograph. White Rose Press, York.

Milner, N., Lane, P., Taylor, B., Conneller, C., Schadla-Hall, T., 2011b. Star Carr in a Postglacial Lakescape: 60 Years of Research. Journal of Wetland Archaeology 11, 1–19.

Milner, N., Mithen, S., 2009. Hunter-gatherers of the Mesolithic, in: Hunter, J., Ralston, I. (Eds.), The Archaeology of Britain: An Introduction from Earliest Times to the Twenty-First Century. Taylor & Francis, Abingdon, pp. 53–77.

Milner, N., Saul, H., Elliott, B., 2013a. Star Carr Archives Project.

Milner, N., Taylor, B., Conneller, C., Boreham, S., Rowley, C., French, C., Craig, O., Williams, H., in press. Sediments and stratigraphy, in: Milner, N., Conneller, C., Taylor, B. (Eds.), Star Carr Monograph. White Rose Press, York.

Milner, N., Taylor, B., Conneller, C., Schadla-Hall, T., 2013b. Star Carr: Life in Britain After the Ice Age. Council for British Archeology, York.

Modugno, F., Ribechini, E., 2009. GC/MS in the Characterisation of Resinous Materials, in: Colombini, M.P., Modugno, F. (Eds.), Organic Mass Spectrometry in Art and Archaeology. Wiley, Chichester, UK, pp. 215–235.

Mohandas, N., Gallagher, P.G., 2008. Red cell membrane: past, present, and future. Blood 112, 3939–3948.

Monnier, G.F., Hauck, T.C., Feinberg, J.M., Luo, B., Le Tensorer, J.-M., Sakhel, H. al, 2013. A multi-analytical methodology of lithic residue analysis applied to Paleolithic tools from Hummal, Syria. Journal of Archaeological Science 40, 3722–3739.

Monnier, G.F., Ladwig, J.L., Porter, S.T., 2012. Swept under the rug: the problem of unacknowledged ambiguity in lithic residue identification. J. Archaeol. Sci. 39, 3284–3300.

Monnier, G., Frahm, E., Luo, B., Missal, K., 2017 b. Developing FTIR Microspectroscopy for the Analysis of Animal-Tissue Residues on Stone Tools. J Archaeol Method Theory 1–44.

Monnier, G., Frahm, E., Luo, B., Missal, K., 2017 a. Developing FTIR microspectroscopy for analysis of plant residues on stone tools. J. Archaeol. Sci. 78, 158–178.

Moore, C.R., Brooks, M.J., Kimball, L.R., Newman, M.E., Kooyman, B.P., 2016. Early Hunter-Gatherer Tool Use and Animal Exploitation: Protein and Microwear Evidence from the Central Savannah River Valley. Am. Antiq. 81, 132–147.

Moore, J., 1954. Excavations at Flixton, Site 2, in: Clark, J.G.D. (Ed.), Excavations at Star Carr: An Early Mesolithic Site at Seamer near Scarborough, Yorkshire. Cambridge University Press, Cambridge, p. 192.

Moore, J.W., 1950. Mesolithic Sites in the Neighbourhood of Flixton, North-east Yorkshire. Proceedings of the Prehistoric Society 16, 101–108.

Moore, P.D., Webb, J.A., 1978. An illustrated guide to pollen analysis. Hodder and Stoughton, London.

Morris, V.J., Gunning, A.P., Kirby, A.R., Round, A., Waldron, K., Ng, A., 1997. Atomic force microscopy of plant cell walls, plant cell wall polysaccharides and gels. International Journal of Biological Macromolecules 21, 61–66.

Mortimore, J.L., Marshall, L.-J.R., Almond, M.J., Hollins, P., Matthews, W., 2004. Analysis of red and yellow ochre samples from Clearwell Caves and Çatalhöyük by vibrational spectroscopy and other techniques. Spectrochimica Acta Part A: Molecular and Biomolecular Spectroscopy 60, 1179–1188.

Motoyama, M., 2012. Structure and Phase Characterization of Triacylglycerols by Raman Spectroscopy. Bulletin of the National Agriculture and Food Research Organization (NARO) Institute of Livestock and Grassland Science 12, 19–68.

Movasaghi, Z., Rehman, S., Rehman, D.I.U., 2007. Raman Spectroscopy of Biological Tissues. Appl. Spectrosc. Rev. 42, 493–541.

Murray, T., Walker, M.J., 1988. Like WHAT? A practical question of analogical inference and archaeological meaningfulness. Journal of Anthropological Archaeology 7, 248–287.

Nastasi, M., Mayer, J.W., Wang, Y., 2015. Ion Beam Analysis: Fundamentals and Applications. CRC Press, Boca Raton.

Nedungadi, T.M.K., 1940. Effect of temperature on the raman spectrum of quartz. Proc. Indian Acad. Sci. 11, 86–95.

Needham, A., 2007. Star Carr Soils Analysis. Unpublished report. University of York.

Needham, A., Little, A., Conneller, C., Pomstra, D., Croft, S., Milner, N., in press. Beads and pendant, in: Milner, N., Conneller, C. and Taylor, B. (Ed.), Star Carr Monograph. White Rose Press, York.

Needham, A.P., Croft, S., Kröger, R., Robson, H.K., Rowley, C.C.A., Taylor, B., Gray Jones, A., Conneller, C., in review. Scratching The Surface of Ochre working in The British Mesolithic: Analysis of Ochre Artefacts from Palaeo-Lake Flixton.

Needham, A., Taylor, B., Jones, A.G., 2014. Preliminary analysis of an engraved pebble from the Mesolithic site of Flixton School House Farm, North Yorkshire, in: Where the Wild Things Are 2.0. Durham, UK.

Nesse, W.D., 1986. Introduction to Optical Mineralogy, 2nd ed. Oxford University Press, Oxford.

Nevin, A., Melia, J.L., Osticioli, I., Gautier, G., Colombini, M.P., 2008/4. The identification of copper oxalates in a 16th century Cypriot exterior wall painting using micro FTIR, micro Raman spectroscopy and Gas Chromatography-Mass Spectrometry. J. Cult. Herit. 9, 154–161.

Newcomer, M., Grace, R., Unger-Hamilton, R., 1986. Investigating microwear polishes with blind tests. J. Archaeol. Sci. 13, 203–217.

Newman, M.E., Ceri, H., Kooyman, B., 1996. The use of immunological techniques in the analysis of archaeological materials — a response to Eisele; with report of studies at Head-Smashed-In Buffalo Jump. Antiquity 70, 677–682.

Newman, M.E., Julig, P., 1989. The identification of protein residues on lithic artifacts from a stratified Boreal Forest site. Canadian Journal of Archaeology 13, 119–130.

Newman, M.E., Yohe, R.M., Ceri, H., Sutton, M.Q., 1993. Immunological Protein Residue Analysis of Non-lithic Archaeological Materials. J. Archaeol. Sci. 20, 93–100.

Nigra, B.T., Faull, K.F., Barnard, H., 2015. Analytical Chemistry in Archaeological Research. Anal. Chem. 87, 3–18.

Nikinmaa, M., 1990. Vertebrate Red Blood Cells: Adaptations of Function to Respiratory Requirements, Zoophysiology. Springer, Berlin.

Nobles, D.R., Brown, R.M., 2007. Many paths up the mountain: tracking the evolution of cellulose biosynthesis, in: Malcolm Jr. Brown, R., Saxena, I.M. (Eds.), Cellulose: Molecular and Structural Biology. Selected Articles on the Synthesis, Structure, and Applications of Cellulose. Springer, Dordrecht, Netherlands, pp. 1–16.

Noguchi, T., 2014. Cell Walls, in: Noguchi, T., Kawano, S., Tsukaya, H., Matsunaga, S., Sakai, A., Karahara, I., Hayashi, Y. (Eds.), Atlas of Plant Cell Structure. Springer, Tokyo, pp. 137–156.

Nolin, L., Kramer, J.K.G., Newman, M.E., 1994. Detection of Animal Residues in Humus Samples from a Prehistoric Site in the Lower Mackenzie River Valley, Northwest Territories. J. Archaeol. Sci. 21, 403–412.

Nowell, A., Walker, C., Cordova, C.E., Ames, C.J.H., Pokines, J.T., Stueber, D., DeWitt, R., al-Souliman, A.S.A., 2016/9. Middle Pleistocene subsistence in the Azraq Oasis, Jordan: Protein residue and other proxies. J. Archaeol. Sci. 73, 36–44.

Odell, G.H., 2001. Stone Tool Research at the End of the Millennium: Classification, Function, and Behaviour. Journal of Archaeological Research 9, 45–100.

Oh, S.J., Cook, D.C., Townsend, H.E., 1998. Characterization of iron oxides commonly formed as corrosion products on steel. Hyperfine Interact.

Ohtsuka, T., Kubo, K., Sato, N., 1986. Raman spectroscopy of thin corrosion films on iron at 100 to 150 C in air. Corrosion 42, 476–481.

Olivares, M., Tarriño, A., Murelaga, X., Baceta, J.I., Castro, K., Etxebarria, N., 2009. Non-destructive spectrometry methods to study the distribution of archaeological and geological chert samples. Spectrochim. Acta A Mol. Biomol. Spectrosc. 73, 492–497.

Ollé, A., Asryan, L., Bazgir, B., Fernández-Marchena, J.L., Hardy, K., Buckley, S., Loza, P., Marro, M., Pedergnana, A., 2014. Creating a reference collection of hafting adhesives to interpret some "black spot" residues on lithic artefacts.

Ollé, A., Vergès, J.M., 2008. SEM functional analysis and the mechanism of microwear formation, in: Longo, L., Skakun, N. (Eds.), "Prehistoric Technology" 40 Years Later: Functional Studies and the Russian Legacy. Proceedings of the International Congress Verona (Italy), 20-23 April 2005, BAR International Series. Archaeopress, Oxford, pp. 39–49.

Ollé, A., Vergès, J.M., Peña, L., Aranda, V., Canals, A., Carbonell, E., 2014. A microwear analysis of handaxes from Santa Ana cave (Cáceres, Extremadura, Spain), in: Marreiros, J., Bicho, N., Gibaja, J.F. (Eds.), International Conference on Use-Wear Analysis. Presented at the Use-Wear 2012, Cambridge Scholars, Cambridge, pp. 270–278.

Önalgil, N., Kadir, S., Külah, T., Eren, M., Gürel, A., 2015/2. Mineralogy, geochemistry and genesis of the modern sediments of Seyfe Lake, Kırşehir, central Anatolia, Turkey. J. Afr. Earth. Sci. 102, 116–130.

Orlando, L., Gilbert, M.T.P., Willerslev, E., 2015. Reconstructing ancient genomes and epigenomes. Nat. Rev. Genet. 16, 395–408.

Orsini, S., Parlanti, F., Bonaduce, I., 2017. Analytical pyrolysis of proteins in samples from artistic and archaeological objects. J. Anal. Appl. Pyrolysis 124, 643–657.

Osticioli, I., Zoppi, A., Castellucci, E.M., 2006. Fluorescence and Raman spectra on painting materials: reconstruction of spectra with mathematical methods. J. Raman Spectrosc. 37, 974–980.

Otto, A., Simoneit, B.R.T., 2001. Chemosystematics and diagenesis of terpenoids in fossil conifer species and sediment from the Eocene Zeitz formation, Saxony, Germany. Geochim. Cosmochim. Acta 65, 3505–3527.

Otto, A., White, J.D., Simoneit, B.R.T., 2002. Natural product terpenoids in Eocene and Miocene conifer fossils. Science 297, 1543–1545.

Overton, N., Elliott, B., in press. Animals in a wider context, in: Milner, N., Conneller, C., Taylor, B. (Eds.), Star Carr Monograph. White Rose Press, York.

Palmer, A.P., Matthews, I.P., Candy, I., Blockley, S.P.E., MacLeod, A., Darvill, C.M., Milner, N., Conneller, C., Taylor, B., 2015. The evolution of Palaeolake Flixton and the environmental context of Star Carr, NE. Yorkshire: stratigraphy and sedimentology of the Last Glacial-Interglacial Transition (LGIT) lacustrine sequences. Proc. Geol. Assoc. 126, 50–59.

Parker, G.H., 1948. Animal Colour Changes and Their Neurohumours: A Survey of Investigations 1910-1943. Cambridge University Press, Cambridge.

Pastorova, I., van der Berg, K.J., Boon, J.J., Verhoeven, J.W., 1997. Analysis of oxidised diterpenoid acids using thermally assisted methylation with TMAH. J. Anal. Appl. Pyrolysis 43, 41–57.

Patel, E., Cicatiello, P., Deininger, L., Clench, M.R., Marino, G., Giardina, P., Langenburg, G., West, A., Marshall, P., Sears, V., Francese, S., 2015. A proteomic approach for the rapid, multi-informative and reliable identification of blood. Analyst 141, 191–198.

Pavia, D., Lampman, G., Kriz, G., Vyvyan, J., 2015. Introduction to Spectroscopy, 5th ed. Cengage Learning, Stamford, CT.

Pawlik, A., 1997. Funktionsanalyse an Artefakten aus Henauhof Nord II. C. -J. Kind, Die letzten Wildbeuter. Henauhof Nord II und das Endmesolithikum in Baden-Württemberg. Materialhefte zur Archäologie in Baden-Württemberg 39, 150178.

Pawlik, A., 1995. Die mikroskopische Analyse von Steingeräten: Experimente, Auswertungsmethoden, Artefaktanalysen. Verlag Archaeologia Venatoria, Tübingen.

Pawlik, A.F., 2004. Identification of hafting traces and residues by scanning electron microscopy and energy-dispersive analysis of X-rays, in: Walker, E.A., Wenban-Smith, F., Healy, F. (Eds.), Lithics in Action: Papers from the Conference Lithic Studies in the Year 2000, Lithic Studies Society Occasional Paper No. 8. Oxbow Books, Oxford, pp. 169–182.

Pawlik, A.F., Thissen, J.P., 2011. Hafted armatures and multi-component tool design at the Micoquian site of Inden-Altdorf, Germany. J. Archaeol. Sci. 38, 1699–1708.

Pearsall, D.M., Chandler-Ezell, K., Zeidler, J.A., 2004. Maize in ancient Ecuador: results of residue analysis of stone tools from the Real Alto site. J. Archaeol. Sci. 31, 423–442.

Pedergnana, A., Asryan, L., Fernández-Marchena, J.L., Ollé, A., 2016. Modern contaminants affecting microscopic residue analysis on stone tools: A word of caution. Micron 86, 1–21.

Pedergnana, A., Blasco, R., 2016. Characterising the exploitation of avian resources: An experimental combination of lithic use-wear, residue and taphonomic analyses. Quat. Int. 421, 255–269.

Pedergnana, A., Ollé, A., 2017. Building an Experimental Comparative Reference Collection for Lithic Micro-Residue Analysis Based on a Multi-Analytical Approach. J Archaeol Method Theory 1–38.

Pedergnana, A., Ollé, A., 2014. Use-wear and residues analyses on quartzite stone tools: setting up a methodology, in: Lemorini, C., Cesaro, S.N. (Eds.), An Integration of the Use-Wear and Residue Analysis for the Identification of the Function of Archaeological Stone Tools. Proceedings of the International Workshop, Rome, March 5th-7th, 2012. Archaeopress, Oxford, pp. 43–62.

Penel, G., Delfosse, C., Descamps, M., Leroy, G., 2005. Composition of bone and apatitic biomaterials as revealed by intravital Raman microspectroscopy. Bone 36, 893–901.

Pérez-Arantegui, J., Ribechini, E., Pardos, C., Colombini, M.P., 2009. Chemical investigation on black pigments in the carved decoration of sixteenth century alabaster tombs from Zaragoza (Spain). Anal. Bioanal. Chem. 395, 2191–2197.

Perlnemolnar, I., Szakacsnepinter, M., Kovago, A., Petroczy, J., Kralovanszky, P.U., Matyas, J., 1985. Investigation of the dye-binding stoichiometry of food and feed-stuff proteins based on reactions with orange-G, acid orange 12 and amino black 10B. Magyar Kemiai Folyoirat 91, 157–166.

Perrault, K., Stefanuto, P.-H., Dubois, L., Cnuts, D., Rots, V., Focant, J.-F., 2016. A New Approach for the Characterization of Organic Residues from Stone Tools Using GC×GC-TOFMS. Sep. Technol. 3, 16.

Perry, L., 2005. Reassessing the traditional interpretation of "manioc" artifacts in the Orinoco Valley of Venezuela. Latin American Antiquity.

Peters, K.E., Walters, C.C., Moldowan, J.M., 2007. The Biomarker Guide: Biomarkers and Isotopes in the Environment and Human History. Cambridge University Press, Cambridge.

Peterson, R., Slovin, J.P., Chen, C., 2010. A simplified method for differential staining of aborted and non-aborted pollen grains. International Journal of Plant Biology.

Petraco, N., Kubic, T., 2003. Color atlas and manual of microscopy for criminalists, chemists, and conservators. CRC press, Boca Raton.

Petraglia, M., Knepper, D., Glumac, P., Newman, M., Sussman, C., 1996. Immunological and Microwear Analysis of Chipped-Stone Artifacts from Piedmont Contexts. Am. Antiq. 61, 127–135.

Phillips, J.L., 1988. The Upper Paleolithic of the Wadi Feiran, Southern Sinai. Paléorient 14, 183–200.

Philp, R.P., Oung, J.N., 1988. Biomarkers - occurrence, utility, and detection. Anal. Chem. 60, 887A–896A.

Piperno, D.R., 2006. Phytoliths: A Comprehensive Guide for Archaeologists and Paleoecologists. Altamira, Lanham.

Piperno, D.R., Holst, I., 1998. The Presence of Starch Grains on Prehistoric Stone Tools from the Humid Neotropics: Indications of Early Tuber Use and Agriculture in Panama. J. Archaeol. Sci. 25, 765–776.

Piperno, D.R., Ranere, A.J., Holst, I., Hansell, P., 2000. Starch grains reveal early root crop horticulture in the Panamanian tropical forest. Nature 407, 894–897.

Piperno, D.R., Weiss, E., Holst, I., Nadel, D., 2004. Processing of wild cereal grains in the Upper Paleolithic revealed by starch grain analysis. Nature 430, 670–673.

Pollard, A.M., Heron, C. (Eds.), 2008. The chemistry and use of resinous substances, in: Archaeological Chemistry. RSC Publishing, Cambridge, pp. 235–269.

Pollard, M., Batt, C., Stern, B., Young, S.M.M., 2007. Analytical Chemistry in Archaeology, Cambridge Manuals in Archaeology. Cambridge University Press, Cambridge.

Polyakova, I.G., 2014. The main silica phases and some of their properties, in: Schmelzer, J.W.P. (Ed.), Glass: Selected Properties and Crystallization. Walter de Gruyter, Berlin, pp. 197–268.

Popa, R., Kinkle, B.K., Badescu, A., 2004. Pyrite Framboids as Biomarkers for Iron-Sulfur Systems. Geomicrobiology Journal 21, 193–206.

Pond, C.M., 2011. The evolution of mammalian adipose tissue, in: Symonds, M.E. (Ed.), Adipose Tissue Biology. Springer, New York, pp. 227–270.

Prager, E.M., Wilson, A.C., Lowenstein, J.M., Sarich, V.M., 1980. Mammoth albumin. Science 209, 287–289.

Prati, S., Bonacini I., S.G., Mazzeo, R., 2017. New frontiers in application of FTIR microscopy for characterization of cultural heritage materials, in: Mazzeo, R. (Ed.), Analytical Chemistry for Cultural Heritage, Topics in Current Chemistry Collections. Springer, Gewerbestrasse, pp. 129–160.

Price-Jones, C., 1933. Red Blood Cell Diameters, Oxford medical publications. Humphrey Milford, Oxford University Press, Oxford.

Prieto-Taboada, N., Gómez-Laserna, O., Martínez-Arkarazo, I., Olazabal, M.Á., Madariaga, J.M., 2014. Raman Spectra of the Different Phases in the $CaSO_4$–H_2O System. Anal. Chem. 86, 10131–10137.

Prinsloo, L.C., Tournié, A., Colomban, P., Paris, C., Bassett, S.T., 2013. In search of the optimum Raman/IR signatures of potential ingredients used in San/Bushman rock art paint. J. Archaeol. Sci. 40, 2981–2990.

Prinsloo, L.C., Wadley, L., Lombard, M., 2014. Infrared reflectance spectroscopy as an analytical technique for the study of residues on stone tools: potential and challenges. J. Archaeol. Sci. 41, 732–739.

Proefke, M.L., Rinehart, K.L., 1992. Analysis of an egyptian mummy resin by mass spectrometry. J. Am. Soc. Mass Spectrom. 3, 582–589.

Prüfer, K., Racimo, F., Patterson, N., Jay, F., Sankararaman, S., Sawyer, S., Heinze, A., Renaud, G., Sudmant, P.H., de Filippo, C., Li, H., Mallick, S., Dannemann, M., Fu, Q., Kircher, M., Kuhlwilm, M., Lachmann, M., Meyer, M., Ongyerth, M., Siebauer, M., Theunert, C., Tandon, A., Moorjani, P., Pickrell, J., Mullikin, J.C., Vohr, S.H., Green, R.E., Hellmann, I., Johnson, P.L.F., Blanche, H., Cann, H., Kitzman, J.O., Shendure, J., Eichler, E.E., Lein, E.S., Bakken, T.E., Golovanova, L.V., Doronichev, V.B., Shunkov, M.V., Derevianko, A.P., Viola, B., Slatkin, M., Reich, D., Kelso, J., Pääbo, S., 2014. The complete genome sequence of a Neanderthal from the Altai Mountains. Nature 505, 43–49.

Quickenden, T.I., Cooper, P.D., 2001. Increasing the specificity of the forensic luminol test for blood. Luminescence 16, 251–253.

Quickenden, T.I., Creamer, J.I., 2001. A study of common interferences with the forensic luminol test for blood. Luminescence 16, 295–298.

Radini, A., McQuilkin, A., Tong, E., Milner, N., in press. The palaeoethnobotanical evidence, in: Milner, N., Conneller, C. and Taylor, B. (Ed.), Star Carr Monograph. White Rose Press, York.

Radley, J., Tallis, J.H., Switsur, V.R., 1974. The Excavation of Three "Narrow Blade" Mesolithic Sites in the Southern Pennines, England. Proceedings of the Prehistoric Society 40, 1–19.

Radotić, K., Djikanović, D., Bogdanović, J., Vasiljević-Radović, D., 2008. Levels of plant cell wall structural organization revealed by atomic force microscopy. Journal of Microscopy 232, 508–510.

Rafferty, J.P., 2012. Minerals, Geology: landforms, minerals, and rocks. Britannica Educational Publishing, New York.

Rageot, M., Pêche-Quilichini, K., Py, V., Filippi, J.-J., Fernandez, X., Regert, M., 2016. Exploitation of Beehive Products, Plant Exudates and Tars in Corsica During the Early Iron Age. Archaeometry 58, 315–332.

Raghavan, M., Sahar, N.D., Kohn, D.H., Morris, M.D., 2012. Age-specific profiles of tissue-level composition and mechanical properties in murine cortical bone. Bone 50, 942–953.

Rankine, W.F., Rankine, W.M., Dimbleby, G.W., 1960. Further Excavations at a Mesolithic Site at Oakhanger, Selborne, Hants. Proceedings of the Prehistoric Society (New Series) 26, 246–262.

Rao, H., Yang, Y., Abuduresule, I., Li, W., Hu, X., Wang, C., 2015. Proteomic identification of adhesive on a bone sculpture-inlaid wooden artifact from the Xiaohe Cemetery, Xinjiang, China. J. Archaeol. Sci. 53, 148–155.

Raven, P.H., Evert, R.F., Eichhorn, S.E. (Eds.), 1999. Introduction to the Plant Cell, in: Biology of Plants. W.H. Freeman and Company, New York, pp. 40–72.

Regert, M., 2004. Investigating the history of prehistoric glues by gas chromatography–mass spectrometry. J. Sep. Sci. 27, 244–254.

Regert, M., Delacotte, J.-M., Menu, M., Pétrequin, P., Rolando, C., 1998. Identification of Neolithic hafting adhesives from two lake dwellings at Chalain (Jura, France). Anc. Biomol. 2, 81–96.

Regert, M., Langlois, J., Colinart, S., 2005. Characterisation of wax works of art by gas chromatographic procedures. J. Chromatogr. A 1091, 124–136.

Regert, M., Rolando, C., 2002. Identification of Archaeological Adhesives Using Direct Inlet Electron Ionization Mass Spectrometry. Anal. Chem. 74, 965–975.

Regert, M., Vacher, S., Moulherat, C., Decavallas, O., 2003a. Adhesive Production and Pottery Function During the Iron Age at the Site of Grand Aunay (Sarthe, France). Archaeometry 45, 101–120.

Regert, M., Garnier, N., Decavallas, O., Cren-Olivé, C., Rolando, C., 2003b. Structural characterization of lipid constituents from natural substances preserved in archaeological environments. Meas. Sci. Technol. 14, 1620–1630.

Reichert, E.T., 1913. The Differentiation and Specificity of Starches in Relation to Genera, Species, etc. Carnegie Institute of Washington, Washington, D.C.

Reinhart, W.H., Chien, S., 1986. Red cell rheology in stomatocyte-echinocyte transformation: roles of cell geometry and cell shape. Blood 67, 1110–1118.

Remington, S.J., 1994. Identifying species of origin from prehistoric blood residues. Science 266, 298–300.

Reuther, J.D., Lowenstein, J.M., Gerlach, S.C., Hood, D., Scheuenstuhl, G., Ubelaker, D.H., 2006. The use of an improved pRIA technique in the identification of protein residues. J. Archaeol. Sci. 33, 531–537.

Revedin, A., Aranguren, B., Becattini, R., Longo, L., Marconi, E., Lippi, M.M., Skakun, N., Sinitsyn, A., Spiridonova, E., Svoboda, J., 2010. Thirty thousand-year-old evidence of plant food processing. Proc. Natl. Acad. Sci. U. S. A. 107, 18815–18819.

Reynier, M.J., 2005. Environment, in: Early Mesolithic Britain: Origins, Development and Directions, British Archaeological Reports British Series. Archaeopress, Oxford, pp. 71–84.

Reynier, M.J., 2005. Typology, in: Early Mesolithic Britain: Origins, Development and Directions, British Archaeological Reports British Series. Archaeopress, Oxford, pp. 11–70.

Rhinelander, F.W., 1972. Circulation of Bone, in: Bourne, G.H. (Ed.), The Biochemistry and Physiology of Bone, 1. Academic Press, New York, pp. 2–78.

Ribechini, E., Modugno, F., Colombini, M.P., Evershed, R.P., 2008. Gas chromatographic and mass spectrometric investigations of organic residues from Roman glass unguentaria. J. Chromatogr. A 1183, 158–169.

Ribechini, E., Orsini, S., Silvano, F., Colombini, M.P., 2009. Py-GC/MS, GC/MS and FTIR investigations on Late Roman-Egyptian adhesives from opus sectile: new insights into ancient recipes and technologies. Anal. Chim. Acta 638, 79–87.

Richardin, P., 1996. Contribution de la spectrométrie de masse à l'étude du patrimoine culturel. Spectra 2000 analyse.

Richards, T., 1989. Initial results of a blood residue analysis of lithic artefacts from Thorpe Common Rockshelter, South Yorkshire, in: Brooks, I., Phillips, P. (Eds.), Breaking the Stony Silence, Sheffield Lithics Conference 1988. BAR British Series, Sheffield.

Rigaud, S., Gutiérrez-Zugasti, I., 2016. Symbolism among the last hunter–fisher–gatherers in northern Iberia: Personal ornaments from El Mazo and El Toral III Mesolithic shell midden sites. Quat. Int. 407, Part B, 131–144.

Ritsema, C.J., Groenenberg, J.E., 1993. Pyrite Oxidation, Carbonate Weathering, and Gypsum Formation in a Drained Potential Acid Sulfate Soil. Soil Science Society of America Journal 57, 968–976.

Roberts, A.J., Barton, R.N.E., Evans, J., 1998. Early Mesolithic mastic: radiocarbon dating and analysis of organic residues from Thatcham III, Star Carr and Lackford Heath, in: Ashton, N., Healy, F., Pettitt, P. (Eds.), Stone Age Archaeology: Essays in Honour of John Wymer, Oxbow Monograph 102, Lithic Studies Occasional Paper 6. Oxbow Books, Oxford, pp. 185–192.

Robertson, G., Attenbrow, V., Hiscock, P., 2009. Multiple uses for Australian backed artefacts. Antiquity 83, 296–308.

Robinson, N., Evershed, R.P., James Higgs, W., Jerman, K., Eglinton, G., 1987. Proof of a pine wood origin for pitch from Tudor (Mary Rose) and Etruscan shipwrecks: application of analytical organic chemistry in archaeology. Analyst 112, 637–644.

Robledo-Arnuncio, J.J., Gil, L., 2005. Patterns of pollen dispersal in a small population of *Pinus sylvestris* L. revealed by total-exclusion paternity analysis. Heredity 94, 13–22.

Robson, H.K., Little, A., Jones, A.K.G., Blockley, S., Candy, I., Matthews, I., Palmer, A., Schreve, D., Tong, E., Pomstra, D., Fletcher, L., Hausmann, N., Taylor, B., Conneller, C., Milner, N., 2016. Scales of analysis: Evidence of fish and fish processing at Star Carr. Journal of Archaeological Science: Reports. doi:10.1016/j.jasrep.2016.02.009

Rodgers, K.A., Hampton, W.A., 2003. Laser Raman identification of silica phases comprising microtextural components of sinters. Mineral. Mag. 67, 1–13.

Roldán, C., Villaverde, V., Ródenas, I., Novelli, F., Murcia, S., 2013. Preliminary analysis of Palaeolithic black pigments in plaquettes from the Parpalló cave (Gandía, Spain) carried out by means of non-destructive techniques. J. Archaeol. Sci. 40, 744–754.

Rontani, J.-F., Aubert, C., Belt, S.T., 2015. EIMS Fragmentation Pathways and MRM Quantification of 7α/β-Hydroxy-Dehydroabietic Acid TMS Derivatives. J. Am. Soc. Mass Spectrom. 26, 1606–1616.

Roomans, G.M., Dragomir, A., 2007. X-ray microanalysis in the scanning electron microscope, in: Kuo, J. (Ed.), Electron Microscopy: Methods and Protocols, Methods in Molecular Biology. Humana Press, Totowa, New Jersey, pp. 507–528.

Ross, M.H., Pawlina, W., 2011. Histology: A Text and Atlas, 6th ed. Wolters Kluwer/Lippincott Williams & Wilkins Health, Philadelphia.

Rothwell, R.G., 1989. Gypsum (and anhydrite), in: Rothwell, R.G. (Ed.), Minerals and Mineraloids in Marine Sediments: An Optical Identification Guide. Elsevier Applied Science, London, pp. 103–108.

Rots, V., Hayes, E., Cnuts, D., Lepers, C., Fullagar, R., 2016. Making Sense of Residues on Flaked Stone Artefacts: Learning from Blind Tests. PLoS One 11, e0150437.

Rots, V., Lentfer, C., Schmid, V.C., Porraz, G., Conard, N.J., 2017. Pressure flaking to serrate bifacial points for the hunt during the MIS5 at Sibudu Cave (South Africa). PLoS One 12, e0175151.

Rots, V., Pirnay, L., Pirson, P., Baudoux, O., 2006. Blind tests shed light on possibilities and limitations for identifying stone tool prehension and hafting. J. Archaeol. Sci. 33, 935–952.

Rots, V., van Peer, P., Vermeersch, P.M., 2011. Aspects of tool production, use, and hafting in Palaeolithic assemblages from Northeast Africa. J. Hum. Evol. 60, 637–664.

Rots, V., Williamson, B.S., 2004. Microwear and residue analyses in perspective: the contribution of ethnoarchaeological evidence. J. Archaeol. Sci. 31, 1287–1299.

Rottländer, R., 1975. The formation of patina on flint. Archaeometry 17, 106–110.

Rottländer, R.C.A., 1991. Untersuchungen an der Kittmasse von geschäfteten Feuersteinklingen, in: Waterbolk, H.T., van Zeist, W. (Eds.), Niederwil, Eine Siedlung Der Pfyner Kultur. IV Holzartefakte Und Textilien. Academica Helvetica, Bern, pp. 249–250.

Rowley, C., French, C., Milner, N., in press. Geochemistry of the Central and Western Structures, in: Milner, N., Conneller, C., Taylor, B. (Eds.), Star Carr. White Rose Press, York.

Rubbo, M., Bruno, M., Aquilano, D., 2011. The (100) Contact Twin of Gypsum. Cryst. Growth Des. 11, 2351–2357.

Rubbo, M., Bruno, M., Massaro, F.R., Aquilano, D., 2011. The five twin laws of gypsum ($CaSO_4 \cdot 2H_2O$): a theoretical comparison of the interfaces of the contact twins. Cryst. Growth Des. 12, 264–270.

Rull, F., 2012. The Raman effect and the vibrational dynamics of molecules and crystalline solids, in: Dubessy, J., Caumon, M.-C., Rull, F. (Eds.), Applications of Raman Spectroscopy to Earth Sciences and Cultural Heritage, European Mineralogical Union Notes in Mineralogy. European Mineralogical Union, London, pp. 1–60.

Sabnis, R.W., 2010. Handbook of Biological Dyes and Stains: Synthesis and Industrial Applications. Wiley, Hoboken, New Jersey.

Salque, M., Bogucki, P.I., Pyzel, J., Sobkowiak-Tabaka, I., Grygiel, R., Szmyt, M., Evershed, R.P., 2013. Earliest evidence for cheese making in the sixth millennium BC in northern Europe. Nature 493, 522–525.

Sánchez, A., Tuñón, J., Montejo, M., Parras, D., 2012. Micro Raman spectroscopy (MRS) and energy dispersive x-ray microfluorescence (µEDXRF) analysis of pigments in the Iberian cemetery of Tutugi (from the fourth to the third century bc, Galera, Granada, Spain). J. Raman Spectrosc. 43, 1788–1795.

Sandermann, W., 1965. Untersuchungen vorgeschichtlicher "Gräberharze" und Kitte. Technische Beiträge zur Archäologie 2, 58–73.

Sarma, L.P., Prasad, P.S.R., Ravikumar, N., 1998. Raman spectroscopic study of phase transitions in natural gypsum. J. Raman Spectrosc. 29, 851–856.

Saverwyns, S., 2010. Russian avant-garde… or not? A micro-Raman spectroscopy study of six paintings attributed to Liubov Popova. J. Raman Spectrosc. 41, 1525–1532.

Savluchinske-Feio, S., Curto, M.J.M., Gigante, B., Roseiro, J.C., 2006. Antimicrobial activity of resin acid derivatives. Appl. Microbiol. Biotechnol. 72, 430–436.

Sawczak, M., Kamińska, A., Rabczuk, G., Ferretti, M., Jendrzejewski, R., Śliwiński, G., 2009. Complementary use of the Raman and XRF techniques for non-destructive analysis of historical paint layers. Appl. Surf. Sci. 255, 5542–5545.

Scalarone, D., Chiantore, O., 2009. Py-GC/MS of natural and synthetic resins, in: Colombini, M.P., Modugno, F. (Eds.), Organic Mass Spectrometry in Art and Archaeology. Wiley, Chichester, UK, pp. 327–362.

Scalarone, D., Duursma, M.C., Boon, J.J., Chiantore, O., 2005. MALDI-TOF mass spectrometry on cellulosic surfaces of fresh and photo-aged di- and triterpenoid varnish resins. J. Mass Spectrom. 40, 1527–1535.

Scalarone, D., Lazzari, M., Chiantore, O., 2002. Ageing behaviour and pyrolytic characterisation of diterpenic resins used as art materials: colophony and Venice turpentine. J. Anal. Appl. Pyrolysis 64, 345–361.

Scalarone, D., van der Horst, J., Boon, J.J., Chiantore, O., 2003. Direct-temperature mass spectrometric detection of volatile terpenoids and natural terpenoid polymers in fresh and artificially aged resins. J. Mass Spectrom. 38, 607–617.

Schäfer, D., Holdermann, C., Pawlik, A., Affolter, J., Ikinger, A., Bertola, S., 2006. Mesolithic subsistence at Ullafelsen/Tyrol. Preliminary studies 1995-2002, in: Kind, C.-J. (Ed.), After the Ice Age: Settlements, Subsistence and Social Development in the Mesolithic of Central Europe. Proceedings of the International Conference, 9th to 12th of September 2003, Rottenburg/Neckar, Baden-Württemberg, Germany. K. Theiss, Stuttgart , pp. 201–210.

Schmidt, P., Bellot-Gurlet, L., Léa, V., Sciau, P., 2013. Moganite detection in silica rocks using Raman and infrared spectroscopy. Eur. J. Mineral. 25, 797–805.

Schmidt, P., Bellot-Gurlet, L., Slodczyk, A., Fröhlich, F., 2012. A hitherto unrecognised band in the Raman spectra of silica rocks: influence of hydroxylated Si–O bonds (silanole) on the Raman moganite band in chalcedony and flint (SiO2). Phys. Chem. Miner. 39, 455–464.

Schmidt, P., February, E., Bretzke, K., Bellot-Gurlet, L., 2016. Tempering-residue on heat-treated silcrete: an experimental perspective and a potential analytical protocol. Journal of Archaeological Science: Reports. doi:10.1016/j.jasrep.2016.08.014

Schmidt, P., Porraz, G., Bellot-Gurlet, L., February, E., Ligouis, B., Paris, C., Texier, P.-J., Parkington, J.E., Miller, C.E., Nickel, K.G., Conard, N.J., 2015. A previously undescribed organic residue sheds light on heat treatment in the Middle Stone Age. J. Hum. Evol. 85, 22–34.

Schneider, A., 1901. The Probable Function of Calcium Oxalate Crystals in Plants. Bot. Gaz. 32, 142–144.

Schuster, W.S., Mitton, J.B., 2000. Paternity and gene dispersal in limber pine (*Pinus flexilis* James). Heredity 84 (Pt 3), 348–361.

Schwertmann, U., Cornell, R.M., 2000. Iron Oxides in the Laboratory: Preparation and Characterization, 2nd ed. Wiley-VCH, Weinheim.

Seaman, G.V.F., 1975. Electrokinetic behavior of red cells, in: Surgenor, D.M.N. (Ed.), The Red Blood Cell. Academic Press, Harcourt Brace Jovanovich, New York, pp. 1136–1230.

Seeman, M.F., Nilsson, N.E., Summers, G.L., Morris, L.L., Barans, P.J., Dowd, E., Newman, M.E., 2008. Evaluating protein residues on Gainey phase Paleoindian stone tools. Journal of Archaeological Science 35, 2742–2750.

Semenov, S.A., 1964. Prehistoric technology: an experimental study of the oldest tools and artefacts from traces of manufacture and wear. Adams & Dart, Bath.

Semenov, S.A., 1957. Pervobitnoya Tekhnika. Materialy i Issledovania po Archeologii SSSR 54. Nauka, Moskva-Leningrad.

Sendova, M., Zhelyaskov, V., Scalera, M., Ramsey, M., 2005. Micro-Raman spectroscopic study of pottery fragments from the Lapatsa tomb, Cyprus, ca 2500 BC. J. Raman Spectrosc. 36, 829–833.

Shafer, H.J., Holloway, R.G., 1979. Organic Residue Analysis in Determining Stone Tool Function, in: Hayden, B. (Ed.), Lithic Use-Wear Analysis. Academic Press, New York, pp. 385–299.

Shanks, O.C., Bonnichsen, R., Vella, A.T., Ream, W., 2001. Recovery of Protein and DNA Trapped in Stone Tool Microcracks. J. Archaeol. Sci. 28, 965–972.

Shanks, O.C., Hodges, L., Tilley, L., Kornfeld, M., Lou Larson, M., Ream, W., 2005. DNA from ancient stone tools and bones excavated at Bugas-Holding, Wyoming. J. Archaeol. Sci. 32, 27–38.

Shanks, O.C., Kornfeld, M., Ream, W., 2004. DNA and protein recovery from washed experimental stone tools. Archaeometry 46, 663–672.

Shapiro, S.M., O'Shea, D.C., Cummins, H.Z., 1967. Raman Scattering Study of the Alpha-Beta Phase Transition in Quartz. Phys. Rev. Lett. 19, 361–364.

Sharma, S.K., Mammone, J.F., Nicol, M.F., 1981. Raman investigation of ring configurations in vitreous silica. Nature 292, 140–141.

Shendure, J., Ji, H., 2008. Next-generation DNA sequencing. Nat. Biotechnol. 26, 1135–1145.

Shih, W.-Y., Rahardianto, A., Lee, R.-W., Cohen, Y., 2005. Morphometric characterization of calcium sulfate dihydrate (gypsum) scale on reverse osmosis membranes. Journal of Membrane Science 252, 253–263.

Shillito, L.M., Almond, M.J., Wicks, K., Marshall, L.-J.R., Matthews, W., 2009. The use of FT-IR as a screening technique for organic residue analysis of archaeological samples. Spectrochim. Acta A Mol. Biomol. Spectrosc. 72, 120–125.

Siffert, B., 1967. Some reactions of silica in solution: formation of clay. Translation of: Mémoires du Service de la Carte géologique d'Alsace et de Lorraine, no 21 (No. 21). U.S. Department of Agriculture and the National Science Foundation.

Simoneit, B.R.T., 2002. Biomass burning — a review of organic tracers for smoke from incomplete combustion. Appl. Geochem. 17, 129–162.

Simoneit, B.R.T., Rogge, W.F., Lang, Q., Jaffé, R., 2000. Molecular characterization of smoke from campfire burning of pine wood (*Pinus elliottii*). Chemosphere - Global Change Science 2, 107–122.

Singer, P.C., Stumm, W., 1970. Acidic mine drainage: the rate-determining step. Science 167, 1121–1123.

Skoog, D.A., James Holler, F., Crouch, S.R., 2007. Principles of Instrumental Analysis. Thomson Brooks/Cole.

Slack, M.J., Fullagar, R.L.K., Field, J.H., Border, A., 2004. New Pleistocene ages for backed artefact technology in Australia. Archaeology in Oceania 39, 131–137.

Smallwood, A.M., 2015. Building experimental use-wear analogues for Clovis biface functions. Archaeol. Anthropol. Sci. 7, 13–26.

Smith, B.C., 2011. Fundamentals of Fourier Transform Infrared Spectroscopy, Second Edition. CRC Press.

Smith, G.D., Clark, R.J.H., 2004. Raman microscopy in archaeological science. J. Archaeol. Sci. 31, 1137–1160.

Smith, G.D., Clark, R.J.H., 2001. Raman microscopy in art history and conservation science. Stud. Conserv. 46, 92–106.

Smith, P.R., Wilson, M.T., 2001. Handbook of Archaeological Sciences, in: Brothwell, D.R., Pollard, A.M. (Eds.), Blood Residues in Archaeology. Wiley, pp. 313–322.

Smith, P.R., Wilson, M.T., 1992. Blood residues on ancient tool surfaces: A cautionary note. J. Archaeol. Sci. 19, 237–241.

Šmit, Ž., Grime, G.W., Petru, S., Rajta, I., 1999. Microdistribution and composition of usewear polish on prehistoric stone tools. Nucl. Instrum. Methods Phys. Res. B 150, 565–570.

Solazzo, C., Wadsley, M., Dyer, J.M., Clerens, S., Collins, M.J., Plowman, J., 2013. Characterisation of novel α-keratin peptide markers for species identification in keratinous tissues using mass spectrometry. Rapid Commun. Mass Spectrom. 27, 2685–2698.

Solodenko, N., Zupancich, A., Cesaro, S.N., Marder, O., Lemorini, C., Barkai, R., 2015. Fat residue and use-wear found on acheulian biface and scraper associated with butchered elephant remains at the site of revadim, Israel. PLoS One 10, e0118572.

Sorensen, A., Roebroeks, W., van Gijn, A., 2014. Fire production in the deep past? The expedient strike-a-light model. J. Archaeol. Sci. 42, 476–486.

Soressi, M., Hays, M.A., 2003. Manufacture, transport and use of Mousterian bifaces: a case study from the Perigord (France), in: Soressi, M., Dibble, H.L. (Eds.), Multiple Approaches to the Study of Bifacial Technologies. University of Pennsylvania Museum of Archaeology and Anthropology, Philadelphia, pp. 125–148.

Sparkman, O.D., Penton, Z., Kitson, F.G., 2011. Gas Chromatography and Mass Spectrometry: A Practical Guide, 2nd ed. Elsevier Science, Oxford.

Spiteri, C.D., Gillis, R.E., Roffet-Salque, M., Navarro, L.C., Guilaine, J., Manen, C., Muntoni, I.M., Segui, M.S., Urem-Kotsou, D., Whelton, H.L., Others, 2016. Regional asynchronicity in dairy production and processing in early farming communities of the northern Mediterranean. Proceedings of the National Academy of Sciences 113, 13594–13599.

Stapert, D., 1976. Some natural surface modifications on flint in the Netherlands. Palaeohistoria 18, 7–41.

Stefanova, M., Markova, K., Marinov, S., Simoneit, B.R.T., 2005. Biomarkers in the fossils from the Miocene-aged Chukurovo lignite, Bulgaria: sesqui-and diterpenoids. Bull. Geosci. 80, 93–97.

Stemp, W.J., Childs, B.E., Vionnet, S., Brown, C.A., 2009. Quantification and discrimination of lithic use-wear: surface profile measurements and length-scale fractal analysis. Archaeometry 51, 366–382.

Stemp, W.J., Morozov, M., Key, A.J.M., 2015. Quantifying lithic microwear with load variation on experimental basalt flakes using LSCM and area-scale fractal complexity (Asfc). Surface Topography: Metrology and Properties 3, 1–20.

Stephenson, B., 2015. A modified Picro-Sirius Red (PSR) staining procedure with polarization microscopy for identifying collagen in archaeological residues. J. Archaeol. Sci. 61, 235–243.

Stevenson, F.J., Cole, M.A., 1999. Cycles of Soils: Carbon, Nitrogen, Phosphorus, Sulfur, Micronutrients, 2nd ed. Wiley, New York.

Stewart, J.R.M., Allen, R.B., Jones, A.K.G., Penkman, K.E.H., Collins, M.J., 2013. ZooMS: making eggshell visible in the archaeological record. J. Archaeol. Sci. 40, 1797–1804.

Stocum, D.L., 2012. Regenerative Biology and Medicine, 2nd ed. Academic Press, London.

Stuart, B.H., Craft, L., Forbes, S.L., Dent, B.B., 2005. Studies of adipocere using attenuated total reflectance infrared spectroscopy. Forensic Sci. Med. Pathol. 1, 197–201.

Stuart, B.H., Thomas, P.S., 2017. Pigment characterisation in Australian rock art: a review of modern instrumental methods of analysis. Herit Sci 5, 10.

Sullivan, L.A., 1990. Micromorphology and genesis of some calcite pseudomorphs after lenticular gypsum. Soil Res. 28, 483–485.

Sullivan, L.A., Koppi, A.J., 1993. Barite pseudomorphs after lenticular gypsum in a buried soil from central Australia. Soil Res. 31, 393–396.

Summerhayes, G.R., Leavesley, M., Fairbairn, A., Mandui, H., Field, J., Ford, A., Fullagar, R., 2010. Human adaptation and plant use in highland New Guinea 49,000 to 44,000 years ago. Science 330, 78–81.

Super, C., 2017. Ancient DNA Extraction from Stone Tools (BA). University of Montana.

Sutikna, T., Tocheri, M.W., Morwood, M.J., Saptomo, E.W., Jatmiko, Awe, R.D., Wasisto, S., Westaway, K.E., Aubert, M., Li, B., Zhao, J.-X., Storey, M., Alloway, B.V., Morley, M.W., Meijer, H.J.M., van den Bergh, G.D., Grün, R., Dosseto, A., Brumm, A., Jungers, W.L., Roberts, R.G., 2016. Revised stratigraphy and chronology for Homo floresiensis at Liang Bua in Indonesia. Nature 532, 366–369.

Symens, N., 1986. A Functional Analysis of Selected Stone Artifacts from the Magdalenian Site at Verberie, France. Journal of Field Archaeology 13, 213–222.

Takahata, M., Maher, J.R., Juneja, S.C., Inzana, J., Xing, L., Schwarz, E.M., Berger, A.J., Awad, H.A., 2012. Mechanisms of bone fragility in a mouse model of glucocorticoid-treated rheumatoid arthritis: Implications for insufficiency fracture risk. Arthritis & Rheumatism 64, 3649–3659.

Tarnowski, C.P., Ignelzi, M.A., Jr, Morris, M.D., 2002. Mineralization of developing mouse calvaria as revealed by Raman microspectroscopy. Journal of Bone and Mineral Research 17, 1118–1126.

Taylor, B., 2014. Star Carr: Environmental Archaeology, in: Encyclopedia of Global Archaeology. Springer New York, pp. 7009–7025.

Taylor, B., 2011. Early Mesolithic Activity in the Wetlands of the Lake Flixton Basin. Journal of Wetland Archaeology 11, 63–84.

Taylor, B., Milner, N., Conneller, C., in press. Dryland structures, in: Milner, N., Conneller, C., Taylor, B. (Eds.), Star Carr Monograph. White Rose Press, York.

Taylor, M., 1998. Identification of the wood and evidence for human working, in: Mellars, P.A., Dark, P. (Eds.), Star Carr in Context: New Archaeological and Palaeoecological Investigations at the Early Mesolithic Site of Star Carr, North Yorkshire. McDonald Institute Monographs, Cambridge, pp. 52–61.

Taylor, P., 1995. Interactions of Silica with Iron Oxides: Effects on Oxide Transformations and Sorption Properties. Whiteshell Laboratories, Pinawa, Manitoba.

Teerink, B.J., 1991. Hair of West European Mammals: Atlas and Identification Key. Cambridge University Press, Cambridge.

Tekippe, V.J., Ramdas, A.K., Rodriguez, S., 1973. Piezospectroscopic Study of the Raman Spectrum of alpha-Quartz. Phys. Rev. B Condens. Matter 8, 706–717.

Telen, M.J., 2009. The mature erythrocyte, in: Greer, J.P., Foerster, J., Rodgers, G.M., Paraskevas, F., Glader, B., Arber, D.A., Means, R.T. (Eds.), Wintrobe's Clinical Hematology, Clinical Hematology. Wolters Kluwer Health/Lippincott Williams & Wilkins, Philadelphia, pp. 126–155.

Therin, M., 1998. The movement of starch grains in sediments, in: Fullagar, R. (Ed.), A Closer Look: Recent Studies of Stone Tools, 5. Sydney University, Sydney, pp. 61–72.

Thiry, M., Fernandes, P., Milnes, A., Raynal, J.-P., 2014/9. Driving forces for the weathering and alteration of silica in the regolith: Implications for studies of prehistoric flint tools. Earth-Science Reviews 136, 141–154.

Titus, L.W., 1980. Hair Identification for the Archaeologist, A Yukon Sample. Simon Fraser University, Burnaby.

Tobin, D.J., 2005. The Human Hair Fibre, in: Tobin, D.J. (Ed.), Hair in Toxicology: An Important Bio-Monitor, Issues in Toxicology. Royal Society of Chemistry, Cambridge, UK, pp. 34–56.

Toft, P.A., Brinch Petersen, E., 2013. Five Thousand Years of Decorated Amber Pendants from the Danish Mesolithic. Die Kunde: Zeitschrift für niedersächsische Archäologie 64, 197–217.

Tomasini, E.P., Halac, E.B., Reinoso, M., Di Liscia, E.J., Maier, M.S., 2012. Micro-Raman spectroscopy of carbon-based black pigments. J. Raman Spectrosc. 43, 1671–1675.

Torrence, R., Barton, H., 2006. Ancient Starch Research. Left Coast Press, Walnut Creek, California.

Torres, J.M., 2014. Hematite, in: Reid, B.A., Gilmore, R.G. (Eds.), Encyclopedia of Caribbean Archaeology. University Press of Florida, Florida, p. 177.

Trapp, S., Croteau, R., 2001. Defensive resin biosynthesis in conifers. Annu. Rev. Plant Physiol. Plant Mol. Biol. 52, 689–724.

Trigger, B.G., 2006. A History of Archaeological Thought, 2nd ed. Cambridge University Press, Cambridge.

Tringham, R., Cooper, G., Odell, G., Voytek, B., Whitman, A., 1974. Experimentation in the Formation of Edge Damage: A New Approach to Lithic Analysis. J. Field Archaeol. 1, 171–196.

Tromp, M., Dudgeon, J.V., 2015. Differentiating dietary and non-dietary microfossils extracted from human dental calculus: the importance of sweet potato to ancient diet on Rapa Nui. J. Archaeol. Sci. 54, 54–63.

Tuinstra, F., Koenig, J.L., 1970. Raman Spectrum of Graphite. J. Chem. Phys. 53, 1126–1130.

Turner, N., 2014. Ancient Pathways, Ancestral Knowledge: Ethnobotany and Ecological Wisdom of Indigenous Peoples of Northwestern North America. McGill-Queen's Press - MQUP.

Turner, N., 1998. Plant Technology of First Peoples in British Columbia, Royal BC Museum Handbooks. UBC Press, Vancouver.

Turner-Walker, G., 2008. The chemical and microbial degradation of bones and teeth, in: Pinhasi, R., Mays, S. (Eds.), Advances in Human Palaeopathology. Wiley, Chichester, pp. 3–30.

Turner-Walker, G., 2007. Degradation pathways and conservation strategies for ancient bone from wet anoxic sites, in: Proceedings of the 10th Triennial Meeting of the ICOM-CC Working Group for Wet Organic Archaeological Materials. pp. 659–675.

Tuross, N., Barnes, I., Potts, R., 1996. Protein Identification of Blood Residues on Experimental Stone Tools. J. Archaeol. Sci. 23, 289–296.

Tuross, N., Dillehay, T.D., 1995. The Mechanism of Organic Preservation at Monte Verde, Chile, and One Use of Biomolecules in Archaeological Interpretation. J. Field Archaeol. 22, 97–110.

Ugent, D., Dillehay, T., Ramirez, C., 1987. Potato remains from a late pleistocene settlement in south central Chile. Economic Botany 41, 17–27.

Ungar, P.S., Evans, A., 2016. Exposing the past: surface topography and texture of paleontological and archaeological remains. Surf. Topogr.: Metrol. Prop. 4, 1–4.

Unger-Hamilton, R., 1984. The formation of use-wear polish on flint: Beyond the "deposit versus abrasion" controversy. J. Archaeol. Sci. 11, 91–98.

Urem-Kotsou, D., Stern, B., Heron, C., Kotsakis, K., 2002. Birch-bark tar at Neolithic Makriyalos, Greece. Antiquity 76, 962–967.

Vahur, S., Kriiska, A., Leito, I., 2011. Investigation of the adhesive residue on the flint insert and the adhesive lump found from the Pulli early Mesolithic settlement site (Estonia) by micro-ATR-FT-IR spectroscopy. Estonian Journal of Archaeology 15, 3–17.

van Breemen, N., Buurman, P., 2002. Soil Formation, 2nd ed. Kluwer Academic Publishers, New York.

van den Berg, K.J., Boon, J.J., Pastorova I, I., Spetter, L.F., 2000. Mass spectrometric methodology for the analysis of highly oxidized diterpenoid acids in Old Master paintings. J. Mass Spectrom. 35, 512–533.

van den Berg, K.J., Van der Horst, J., Boon, J.J., Shibayama, N., de la Rie, E.R., 1998. Mass spectrometry as a tool to study ageing processes of diterpenoid resins in works of art: GC-and LC-MS studies, in: E.J. Karjalainen, A.E. Hesso, J.E. Jalonen and U.P. Karjalainen (Ed.), Advances in Mass Spectrometry: Proceedings of the 14th International Mass Spectrometry Conference Held in Tampere 25-29 August 1997. Elsevier, Amsterdam, pp. 563–573.

van der Doelen, G.A., Boon, J.J., 1995. Mass spectrometry of resinous compounds from paintings: characterisation of dammar and naturally aged dammar varnish by DTMS and HPLC/GCMS, in: Wright, M.M., Townsend, J.H. (Eds.), Resins Ancient and Modern. Presented at the SSCR 2nd Resins Conference, Department of Zoology, University of Aberdeen, Edinburgh, pp. 70–75.

van Driessche, A.E.S., Benning, L.G., Rodriguez-Blanco, J.D., Ossorio, M., Bots, P., García-Ruiz, J.M., 2012. The role and implications of bassanite as a stable precursor phase to gypsum precipitation. Science 336, 69–72.

van Gijn, A., 2010. Flint in Focus: Lithic Biographies in the Neolithic and Bronze Age. Sidestone Press, Leiden.

van Gijn, A.L., 2007. Goldcliff lithic artefacts: A functional analysis of some lithic implements from sites A and J, in: Bell, M. (Ed.), Prehistoric Coastal Communities: The Mesolithic in Western Britain. Council for British Archaeology, York, pp. 117–121.

van Gijn, A.L., 1998. A closer look: a realistic attempt to "squeeze blood from stones," in: Fullagar, R. (Ed.), A Closer Look: Recent Australian Studies of Stone Tools, Sydney University Archaeological Methods Series. Archaeological Computing Laboratory, School of Archaeology, Sydney, pp. 189–194.

van Gijn, A.L., 1990. The wear and tear of flint : principles of functional analysis applied to Dutch Neolithic assemblages, in: Analecta Praehistorica Leidensia, 1-182. Institute of Prehistory Leiden, Leiden.

van Gijn, A.L., 1990. The Wear and Tear of Flint: Principles of Functional Analysis Applied to Dutch Neolithic Assemblages (PhD). Leiden University.

van Gijn, A.L., 1984. Fish Polish, Fact and Fiction, in: Owen, L.R., Unrath, G. (Eds.), Technical Aspects of Microwear Studies on Stone Tools. Tübingen, pp. 13–28.

van Gijn, A.L., Boon, J., 2006. Birch bark tar, in: Louwe Kooijmans, L.P., Jongste, P.F.B. (Eds.), Schipluiden – Harnaschpolder. A Middle Neolithic Site on the Dutch Coast (3800-3500 BC). Analecta Praehistorica Leidensia, Leiden, pp. 261–266.

van Gijn, A.L., Houkes, R., 2001. Natursteen, in: Louwe Kooijmans, L.P. (Ed.), Archeologie in de Betuweroute: Hardinxveld-Giessendam De Bruin: Een Woonplaats Uit Het Laat-Mesolithicum En de Vroege Swifterbantcultuur in de Rijn/Maasdelta (5500-4450 v. Chr.), 7. Rapportage Archeologische Monumentenzorg, Amersfoort, pp. 193–208.

van Gijn, A.L., Kooijmans, L.P.L., Zandstra, J.G., 2001. Natursteen, in: Louwe Kooijmans, L.P. (Ed.), Archeologie in de Betuweroute: Hardinxveld-Giessendam Polderweg: Een Mesolithisch Jachtkamp in Het Rivierengebied (5500-5000 v. Chr.), 7. Rapportage Archeologische Monumentenzorg, Amersfoort, pp. 163–180.

van Gijn, A., Wentink, K., 2013. The role of flint in mediating identities: The microscopic evidence, in: Hahn, H.P., Weis, H. (Eds.), Mobility, Meaning and Transformations of Things: Shifting Contexts of Material Culture through Time and Space, 9. Oxbow Books, Oxford, pp. 120–132.

van Peer, P., Fullagar, R., Stokes, S., Bailey, R.M., Moeyersons, J., Steenhoudt, F., Geerts, A., Vanderbeken, T., De Dapper, M., Geus, F., 2003. The Early to Middle Stone Age Transition and the Emergence of Modern Human Behaviour at site 8-B-11, Sai Island, Sudan. J. Hum. Evol. 45, 187–193.

Vasse, J.M., Truchet, G.L., 1984. The Rhizobium - legume symbiosis: observation of root infection by bright-field microscopy after staining with methylene blue. Planta 161, 487–489.

Vaughan, P.C., 1985. Use-wear analysis of flaked stone tools. University of Arizona Press, Tucson.

Veall, M.-A., Matheson, C.D., 2014. Improved molecular and biochemical approaches to residue analysis, in: Lemorini, C., Cesaro, S.N. (Eds.), An Integration of the Use-Wear and Residue Analysis for the Identification of the Function of Archaeological Stone Tools. Proceedings of the International Workshop, Rome, March 5th-7th, 2012. Archaeopress, Oxford, pp. 9–26.

Verma, H.R., 2007. Atomic and Nuclear Analytical Methods: XRF, Mössbauer, XPS, NAA and Ion-Beam Spectroscopic Techniques. Springer, Berlin.

Versteegh, G.J.M., Riboulleau, A., 2010. An organic geochemical perspective on terrestrialization, in: Vecoli, M., Clément, G., Meyer-Berthaud, B. (Eds.), The Terrestrialization Process: Modelling Complex Interactions at the Biosphere-Geosphere Interface, Geological Society Special Publication 339. The Geological Society, London, pp. 11–36.

Vilanova, C., Marín, M., Baixeras, J., Latorre, A., Porcar, M., 2014. Selecting microbial strains from pine tree resin: biotechnological applications from a terpene world. PLoS One 9, e100740.

Villa, P., Roebroeks, W., 2014. Neandertal demise: an archaeological analysis of the modern human superiority complex. PLoS One 9, e96424.

Wadley, L., Hodgskiss, T., Grant, M., 2009. Implications for complex cognition from the hafting of tools with compound adhesives in the Middle Stone Age, South Africa. Proceedings of the National Academy of Sciences 106, 9590–9594.

Wadley, L., Langejans, G., 2014. Preliminary study of scrapers around combustion features in layer SS, Sibudu, 58 000 years ago. South African Archaeological Bulletin 69, 19–33.

Wadley, L., Lombard, M., 2007/6. Small things in perspective: the contribution of our blind tests to micro-residue studies on archaeological stone tools. J. Archaeol. Sci. 34, 1001–1010.

Wadley, L., Lombard, M., Williamson, B., 2004. The first residue analysis blind tests: results and lessons learnt. Journal of Archaeological Science 31, 1491–1501.

Walker, D., Godwin, H., 1954. Lake-Stratigraphy, Pollen-Analysis and Vegetational History, in: Clark, J.G.D. (Ed.), Excavations at Star Carr: An Early Mesolithic Site at Seamer near Scarborough, Yorkshire. Cambridge University Press, Cambridge, pp. 25–69.

Wang, J., Liu, L., Georgescu, A., Le, V.V., Ota, M.H., Tang, S., Vanderbilt, M., 2017. Identifying ancient beer brewing through starch analysis: A methodology. Journal of Archaeological Science: Reports 15, 150–160.

Warinner, C., Rodrigues, J.F.M., Vyas, R., Trachsel, C., Shved, N., Grossmann, J., Radini, A., Hancock, Y., Tito, R.Y., Fiddyment, S., Speller, C., Hendy, J., Charlton, S., Luder, H.U., Salazar-García, D.C., Eppler, E., Seiler, R., Hansen, L.H., Castruita, J.A.S., Barkow-Oesterreicher, S., Teoh, K.Y., Kelstrup, C.D., Olsen, J.V., Nanni, P., Kawai, T., Willerslev, E., von Mering, C., Lewis, C.M., Jr, Collins, M.J., Gilbert, M.T.P., Rühli, F., Cappellini, E., 2014. Pathogens and host immunity in the ancient human oral cavity. Nat. Genet. 46, 336–344.

Warren, J.K., 2006. Evaporites: Sediments, Resources and Hydrocarbons. Springer, Berlin.

Watanabe, T., 2002. Pictorial Atlas of Soil and Seed Fungi: Morphologies of Cultured Fungi and Key to Species, 2nd ed. CRC Press, Boca Raton, Florida.

Wayne, R.O., 2009. Plant Cell Biology: From Astronomy to Zoology. Elsevier Science, Amsterdam.

Weiner, S., 2010. Microarchaeology: Beyond the Visible Archaeological Record. Cambridge University Press.

Weisler, M.I., Haslam, M., 2005. Determining the function of Polynesian volcanic glass artifacts: Results of a residue study. Hawaiian Archaeology 10, 1–17.

Weiss, A., Reiff, G., Weiss, A., 1961. Zur Kenntnis wasserbeständiger Kieselsäureester. Z. Anorg. Allg. Chem. 311, 151–179.

Weng, Y.-M., Weng, R.-H., Tzeng, C.-Y., Chen, W., 2003. Structural analysis of triacylglycerols and edible oils by near-infrared Fourier transform Raman spectroscopy. Appl. Spectrosc. 57, 413–418.

Wenk, H.-R., Bulakh, A., 2016. Minerals: Their Constitution and Origin, 2nd ed. Cambridge University Press, Cambridge .

Weyrich, L.S., Duchene, S., Soubrier, J., Arriola, L., Llamas, B., Breen, J., Morris, A.G., Alt, K.W., Caramelli, D., Dresely, V., Farrell, M., Farrer, A.G., Francken, M., Gully, N., Haak, W., Hardy, K., Harvati, K., Held, P., Holmes, E.C., Kaidonis, J., Lalueza-Fox, C., de la Rasilla, M., Rosas, A., Semal, P., Soltysiak, A., Townsend, G., Usai, D., Wahl, J., Huson, D.H., Dobney, K., Cooper, A., 2017. Neanderthal behaviour, diet, and disease inferred from ancient DNA in dental calculus. Nature 544, 357–361.

White, S.N., 2009. Laser Raman spectroscopy as a technique for identification of seafloor hydrothermal and cold seep minerals. Chem. Geol. 259, 240–252.

White, T.D., Folkens, P.A., 2005. The Human Bone Manual. Elsevier Academic Press, London.

Wilkins, J., Schoville, B.J., Brown, K.S., Chazan, M., 2012. Evidence for early hafted hunting technology. Science 338, 942–946.

Williamson, B.S., 2000. Direct Testing of Rock Painting Pigments for Traces of Haemoglobin at Rose Cottage Cave, South Africa. J. Archaeol. Sci. 27, 755–762.

Williams, S.B., 1992. Results of blood residue analysis for NWP's system expansion project, Oregon, Phase 2. Appendix in Fagan, J.L. et al., Northern Pipeline System expansion project, cultural resources assessment report: Oregon segments. Phase 2: Testing, site evaluation, and impact assessment (No. 23). Archaeological Investigations Northwest, Inc., Report no. 23, Portland, Oregon. Submitted to Northwest Pipeline Company, Salt Lake City.

Wilson, K., White, D.J.B., 1986. The anatomy of wood: its diversity and variability. Stobart & Son Ltd., London.

Winkler, M.M., Monaghan, P., Gilbert, J.L., Lautenschlager, E.P., 1998. Comparison of four techniques for monitoring the setting kinetics of gypsum. J. Prosthet. Dent. 79, 532–536.

Wood, J.R., Rawlence, N.J., Rogers, G.M., Austin, J.J., Worthy, T.H., Cooper, A., 2008. Coprolite deposits reveal the diet and ecology of the extinct New Zealand megaherbivore moa (Aves, Dinornithiformes). Quat. Sci. Rev. 27, 2593–2602.

Wouters, J., Gancedo, G., Peckstadt, A., Watteeuw, L., 1992. THE CONSERVATION OF THE CODEX EYCKENSIS: The evolution of the project and the assessment of materials and adhesives for the repair of parchment. Pap. Conserv. 16, 67–77.

Wu, H., Volponi, J.V., Oliver, A.E., Parikh, A.N., Simmons, B.A., Singh, S., 2011. In vivo lipidomics using single-cell Raman spectroscopy. Proc. Natl. Acad. Sci. U. S. A. 108, 3809–3814.

Wylie, A., 2000. Questions of Evidence, Legitimacy, and the (Dis)Unity of Science. American Antiquity 65, 227–237.

Wylie, A., 1989. Archaeological Cables and Tacking: The Implications of Practice for Bernstein's "Options Beyond Objectivism and Relativism." Philosophy of the Social Sciences 19, 1–18.

Wylie, A., 1985. The reaction against analogy. Advances in Archaeological Method and Theory, 3 8, 63–111.

Wylie, A., 1982. An analogy by any other name is just as analogical a commentary on the Gould-Watson dialogue. Journal of Anthropological Archaeology 1, 382–401.

Xhauflair, H., Pawlik, A., Forestier, H., Saos, T., Dizon, E., Gaillard, C., 2017. Use-related or contamination? Residue and use-wear mapping on stone tools used for experimental processing of plants from Southeast Asia. Quat. Int. 427, Part B, 80–93.

Xu, L.-J., Lei, Z.-C., Li, J., Zong, C., Yang, C.J., Ren, B., 2015. Label-free surface-enhanced Raman spectroscopy detection of DNA with single-base sensitivity. J. Am. Chem. Soc. 137, 5149–5154.

Yalow, R.S., 2012. Radioimmunoassay: historical aspects and general considerations, in: Patrono, C., Peskar, B.A. (Eds.), Radioimmunoassay in Basic and Clinical Pharmacology. Springer-Verlag, Berlin.

Yalow, R.S., Berson, S.A., 1959. Assay of plasma insulin in human subjects by immunological methods. Nature 184 (Suppl 21), 1648–1649.

Yaroshevich, A., Nadel, D., Tsatskin, A., 2013. Composite projectiles and hafting technologies at Ohalo II (23 ka, Israel): analyses of impact fractures, morphometric characteristics and adhesive remains on microlithic tools. J. Archaeol. Sci. 40, 4009–4023.

Yohe, R.M., Bamforth, D.B., 2013. Late Pleistocene protein residues from the Mahaffy cache, Colorado. J. Archaeol. Sci. 40, 2337–2343.

Yohe, R.M., II, Newman, M.E., Schneider, J.S., 1991. Immunological Identification of Small-Mammal Proteins on Aboriginal Milling Equipment. Am. Antiq. 56, 659–666.

Young, A., 1976. Tropical Soils and Soil Survey. Cambridge University Press, Cambridge.

Zarrillo, S., Kooyman, B.P., 2006. Evidence for Berry and Maize Processing on the Canadian Plains from Starch Grain Analysis. American Antiquity 71, 473–499.

Zboril, R., Mashlan, D., Petridis, D., Krausova, D., Pikal, P., 2002. Role of intermediates in the process of red ferric pigment manufacture from $FeSO_4 \cdot 7H_2O$, in: Cook, D.C., Hoy, G.R. (Eds.), Industrial Applications of the Mössbauer Effect. Presented at the ISIAME 2000, Springer, Dordrecht, pp. 437–445.

Zboril, R., Mashlan, M., Machala, L., Bezdicka, P., 2003. Iron (III) oxides formed during thermal conversion of rhombohedral iron (III) sulfate, in: Mashlan, M., Miglierini, M., Schaaf, P. (Eds.), Material Research in Atomic Scale by Mössbauer Spectroscopy, NATO Science Series. Presented at the NATO Advanced Research Workshop on Material Research in Atomic Scale by Mössbauer Spectroscopy, Springer, Dordrecht, pp. 21–30.

Zilhão, J., Angelucci, D.E., Badal-García, E., d'Errico, F., Daniel, F., Dayet, L., Douka, K., Higham, T.F.G., Martínez-Sánchez, M.J., Montes-Bernárdez, R., Murcia-Mascarós, S., Pérez-Sirvent, C., Roldán-García, C., Vanhaeren, M., Villaverde, V., Wood, R., Zapata, J., 2010. Symbolic use of marine shells and mineral pigments by Iberian Neandertals. Proc. Natl. Acad. Sci. U. S. A. 107, 1023–1028.

Zimmerman, M.R., 1973. Blood Cells Preserved in a Mummy 2000 Years Old. Science 180, 303–304.

Zinkel, D.F., Zank, L.C., Wesolowski, M.F., 1971. Diterpene resin acids: a compilation of infrared, mass, nuclear magnetic resonance, ultraviolet spectra and gas chromatographic retention data. U.S. Department of Agriculture, Forest Products Labratory, Madison.

Životić, D., Stojanović, K., Gržetić, I., Jovančićević, B., Cvetković, O., Šajnović, A., Simić, V., Stojaković, R., Scheeder, G., 2013. Petrological and geochemical composition of lignite from the D field, Kolubara basin (Serbia). Int. J. Coal Geol. 111, 5–22.

Zupancich, A., Nunziante-Cesaro, S., Blasco, R., Rosell, J., Cristiani, E., Venditti, F., Lemorini, C., Barkai, R., Gopher, A., 2016. Early evidence of stone tool use in bone working activities at Qesem Cave, Israel. Sci. Rep. 6, 37686.